UNIVERSIDAD AUTÓNOMA DE MADRID

FACULTAD DE CIENCIAS

DEPARTAMENTO DE BIOLOGÍA MOLECULAR

TESIS DOCTORAL

African Swine Fever Virus-mediated regulation of RNA metabolism: g5Rp, a putative viral decapping enzyme

ANA QUINTAS GOROZARRI

MADRID, 2015

Memoria de Investigación presentada por

Ana Quintas Gorozarri

Para optar al grado de

Doctor

por la Universidad Autónoma de Madrid

Trabajo dirigido por la

Dra. Yolanda Revilla Novella

Investigador Científico Titular del

Consejo Superior de Investigaciones Científicas

La presente tesis ha sido realizada en el

Centro de Biología Molecular “Severo Ochoa” (UAM-CSIC).

Ana Quintas Gorozarri ha recibido financiación del Ministerio de Ciencia e Innovación dentro del Subprograma de Formación de Personal Investigador (BFU2007-63110/BFU2010-1779-1). El trabajo del laboratorio ha sido financiado en parte a través del proyecto europeo "TARGETED RESEARCH EFFORT ON AFRICAN SWINE FEVER" (ASFORCE), con número de acuerdo 311931.

A mis padres y a Edu

Hay una fuerza motriz más poderosa que el vapor,
la electricidad y la energía atómica:
la voluntad.

Albert Einstein

Content Index

Content Index

Figures and Tables Index

Figures Index

Tables Index

Abbreviations

4E-BP	eIF4E - binding protein
4-SU	4-thiouridine
AdV	Adenovirus
ARNm	Ácido ribonucleico mensajero
ASF	African Swine Fever
ASFV	African Swine Fever Virus
Ba71V	Badajoz 71 ASFV strain addapted to grown on Vero cells
cCL	Conventional Crosslinking
CFP	Cyan Fluorescent Protein
CHX	Ciclohemide
CI	Chloroform : isoamil alochol solution
CLSM	Confocal Laser Screening Microscopy
CLSM	Confocal Laser Scanner Microscopy
CMV	Cytomegalovirus
D.S	standard deviation
Dcp1	Decapping enzyme 1
Dcp2	Decapping enzyme 2
DcpS	Scavenger decapping enzyme
Dhh1/DDX6	DEAD box Helicase Homolog
DMEM	Dulbecco´s Modified Eagle´s Medium
DNA	Deoxyribonucleic Acid
dsRNA	double-stranded RNA
DTT	Dithiothreitol
E	glutamic acid
E70	African Swine Fever virus España 70 strain
E75	African Swine Fever Virus España 75 strain
EBV	Epstein-Barr virus
Edc1	Enhancer of decapping protein 1
Edc2	Enhancer of decapping protein 2
Edc3	Enhancer of decapping protein 3
Edc4	Enhancer of decapping protein 4
EDTA	Ethylenediaminetetraacetic acid
eIF4A	Eukaryotic translation initiation Factor 4A
eIF4E	Eukaryotic translation initiation factor 4E
eIF4F	Eukaryotic translation initiation factor 4F
eIF4G	Eukaryotic translation initiation factor 4G
eIFs	Eukaryotic translation initiation factors
ELISA	Enzime-linked ImunoSorbent Assay
EMCV	encephalomyocarditis virus
EMSA	Electrophoretic mobility shift assay
ERS	Enzyme Restriction Site
F	farads, electrical capacitance unit
FACS	Fluorescence-Activated Cell Sorting
FBS	Fetal Bovine Serum
FRT	Flp Recombination site
FW	forward sequence
G	glicine

g.o.i	gene of interest
GAPDH	Glyceraldehyde 3-phosphate dehydrogenase
GFP	Green Fluorescente Protein
HA	Human influenza hemagglutinin
HCV	hepatitis C virus
hpi	hours post infection
HSV-1	herpes simplex virus
IgG	Immunoglobulin G
IRES	internal ribosome entry site
J	joules, energy unit
KDa	Kilodalton
KSHV	Kaposi´s sarcoma-associated herpesvirus
Lsm1-7	SM-like proteins 1-7
M.O.I	Multiplicity of infection
m^7GDP	7-methyl guanosine diphosphate
m^7GMP	7-methyl guanosine monophosphate
m^7GpppG	cap analog
Malawi LIL/21	African Swine Fever Virus Malawi strain
MFI	mean fluorescence intensity
Mg^{2+}	magnesium
Mn^{2+}	manganese
mRNA	messenger RNA
mTOR	mammalian Target of Rapamycin
MW	molecular weight
NCLDV	Nucleocytoplasmic Large DNA Viruses
nm	nanometers
nsp1	nonstructural protein 1
nt	nucleotides
Nudix domain	Nucleoside diphosphate linked moiety X domain
O/N	Overnight
ORF	Open Reading Frame
P0 / P1 / P2	Eukaryotic acidic ribosomal P proteins
PABP	Poly (A) Binding Proteins
PABPC1	cytoplasmic Poly (A) Binding Protein
PAR-CL	Photoactivatable-ribonucleoside-enhanced Crosslinking
Pat1	Protein Associated with Topoisomerase II
PA-X	Viral RNA-dependent RNA polymerase complex-X
P-Bodies	Processing Bodies
PBS	Phosphate Buffered Saline Solution
PCI	Phenol : chloroform : isoamil alochol solution
PCR	Polimerase Chain reaction
pfu	plate former unit
PKR	double stranded RNA-activated kinase
PMSF	phenylmethylsulfonyl fluoride
PP1	protein phosphatase 1
PPIA	peptidylprolyl isomerase A
Q	glutamines

qPCR	quantitative PCR
R	arginine
RBP7	RNA-polymerase II subunit 7
RIG-1	retinoic acid-inducible gene 1
RNA	Ribonucleic Acid
RPL0	Ribosomal Protein LO
rpm	revolutions per minute
RV	reverse sequence
S.E.M	standard error mean
SARS-CoV	severe acute respiratory syndrome coronavirus
SDS	sodium dodecyl sulfate
SDS-PAGE	sodium dodecyl sulfate polyacrylamide gel electrophoresis
SG	Stress Granules
siRNA	small interfering RNA
TAE	Tris Acetic EDTA solution
TBS	Tris Buffered Solution
tet	teracycline
U	enzymatic Units
U.V	Ultraviolet Light
UTR	Untranslated region
V	volts
VACV	vaccinia virus
vhs	virion host shutoff protein
VSV	vesicular stomatitis virus
WB	Western Blot
wt	wild type
Xrn1	eXoRiboNuclease
YFP	Yellow Fluorescent Protein
β-Gal	Beta-galactosidase
µCi	microCuries, radioactivity unit
Ω	ohm, electric resistance unit

Presentación

El Virus de la Peste Porcina Africana (VPPA) es un virus ADN de gran tamaño que infecta distintas especies de suidos, y cuyas cepas virulentas causan una enfermedad altamente patógena y letal, que cursa con hemorragias generalizadas y para la cual no existe vacuna. La Peste Porcina Africana es endémica en África y Cerdeña, pero desde el 2007, un nuevo brote en la región del Cáucaso se ha extendido por Rusia, poniendo en peligro la cabaña porcina europea. El VPPA, único miembro de la familia *Asfaviridae,* es un virus icosaédrico con envuelta formado por varias capas concéntricas. En el interior se encuentra el nucleoide, que contiene el material genético del virus, una molécula de ADN de doble cadena que codifica para más de 150 secuencias codificantes. La infección del VPPA se caracteriza por una progresiva disminución de la síntesis de proteínas celulares a la vez que se produce la síntesis de las proteínas virales. El mecanismo por el cual el virus logra éste fenómeno es aún desconocido, y ha sido el objeto de estudio de la presente Tesis Doctoral.

Durante la infección por VPPA, hemos observado que se produce una degradación masiva de los ARN mensajeros celulares en el citoplasma de las células infectadas, lo que sugiere que la inhibición de las proteínas celulares es debida a la activa degradación de dichos mensajeros. A este respecto, el genoma del VPPA codifica para una proteína, g5Rp (pD250R en Ba71V), que posee un dominio Núdix hidrolasa y actividad decapping *in vitro*. En esta Tesis, hemos demostrado que g5Rp es capaz de interaccionar con el ARN poliadenilado en células que expresan establemente la proteína. Ésta interacción está mediada principalmente por el dominio N-terminal de g5Rp, y los amino ácidos conservados del dominio Núdix no son necesarios para dicha interacción. Ésta proteína viral también interacciona con los ARN mensajeros virales y celulares en el contexto de la infección, y la sobreexpresión de la misma en células infectadas provoca una disminución de ambas especies de mensajeros, así como de los niveles de ciertas proteínas virales tardías. g5R es un gen temprano e importante para la adecuada progresión de la infección. A tiempos tempranos de la infección, g5Rp presenta una localización subcelular típica de retículo endoplasmático y es capaz de interaccionar con los ribosomas y con PABPC, mientras que a tiempos tardíos, la proteína se acumula alrededor de la factoría viral, donde co-localiza con la estructura cap de los ARN mensajeros y con Dcp1, e interacciona tanto con los ribosomas como con las proteínas virales pp220, p10 y p72. Además, la infección por VPPA provoca la dispersión de los cuerpos citoplasmáticos o P-Bodies, así como la redistribución de los factores de iniciación de la traducción y los ribosomas a los sitios de replicación viral, donde también se localizan los ARN mensajeros virales tardíos.

En conclusión, nuestro estudio indica que g5Rp es un factor viral implicado en la degradación del ARN celular y en la regulación temporal de la expresión génica del virus. Sin embargo, el VPPA utiliza más de un mecanismo para lograr la inhibición de la síntesis de proteínas celulares a la vez que lleva a cabo la síntesis de sus proteínas, como la relocalización de los factores de iniciación de la traducción o de los ribosomas a la factoría viral.

Summary

African Swine Fever Virus (ASFV) is a large DNA virus that infects different species of pig. ASFV virulent strains cause a highly infectious and deadly disease that produces generalized bleeding and for which there is no vaccine. African swine fever is endemic in Africa and Sardinia, but since 2007, a new outbreak in the Caucasus region has spread to Russia, jeopardizing the European pig population. ASFV, the only member of the *Asfaviridae* family, is an enveloped icosahedral virus formed by several concentric layers. The viral genetic material is a double-stranded DNA molecule located inside the nucleoid, which contain more than 150 coding sequences. ASFV infection is characterized by a progressive decrease in the cellular protein synthesis, concomitantly with an increase in the viral protein synthesis. The mechanism by which the virus achieves this phenomenon is still unknown, and has been the object of study of this Thesis.

During ASFV infection, we observed that a massive degradation of cellular mRNA in the cytoplasm of infected cells occurs; suggesting that inhibition of cellular proteins is due to active degradation of mRNA. In this regard, ASFV genome encodes a protein, g5Rp (pD250R in Ba71V), which has a Nudix hydrolase domain and decapping activity *in vitro*. In this Thesis, we have shown that g5Rp is capable of interacting with poly(A) RNA in cells stably expressing the protein. We have determined that this interaction is mediated primarily by the g5Rp N-terminal domain, and that conserved amino acids of the Nudix domain are not required for this interaction. This viral protein also interacts with viral and cellular RNA in the context of infection, and its overexpression in infected cells results in decreased levels of both species of transcripts and of late viral protein levels. g5R is an early gene, which also play an important role in the proper progression of the infection. At early stages of infection, g5Rp presents subcellular localization typical of the endoplasmic reticulum and is able to interact with ribosomes and PABPC, while at later times, the protein accumulates around the viral factories, where it co-localizes with the mRNA cap structure and Dcp1, and interacts with ribosomes and with pp220, p10 and p72 viral proteins. Furthermore, ASFV infection causes scattering of the P-Bodies and a redistribution of translation initiation factors and ribosomes to the viral replication sites, where late viral mRNAs are also located.

In conclusion, our study indicates that g5R protein is a factor involved in the cellular RNA degradation and in the temporal regulation of viral gene expression. Interestingly, ASFV uses more than one mechanism for the inhibition of cellular protein synthesis, as relocation of translation initiation factors and the ribosomes to the viral factories.

Introduction

1.1 AFRICAN SWINE FEVER VIRUS (ASFV)

1.1.1 General aspects of ASFV infection

African Swine Fever Virus (ASFV) is a large, cytoplasmic, double-stranded DNA virus that infects different species of swine, including domestic pigs and wild suids (Costard *et al.*, 2013; Vinuela, 1985). In wild suids, African Swine Fever (ASF) pathogenesis is usually subclinical (Montogomery, 1921), although in some cases the disease can be lethal. Warthogs are asymptomatic carriers of the disease and are considered the most important ASFV vertebrate reservoir in Africa (Costard *et al.*, 2013; Kleiboeker and Scoles, 2001). In domestic pigs, ASF is characterized by an increase of vascular permeability, thrombocytopenia, petechial bleeding and haemorrhagic lesions, which normally lead the animal to death. However, clinical signs of ASF can vary depending on the virulence of the viral strain, being possible to distinguish among different forms of the disease: hyperacute, acute, subacute, chronic and subchronic (Blome *et al.*, 2013).

ASFV is the only member of the Asfaviridae family (Dixon *et al.*, 2004; Dixon *et al.*, 2012) and the single virus able to replicate in arthropods (ticks of the Ornithodoros genus), which act as biological vectors (Burrage, 2013; Kleiboeker and Scoles, 2001). In vertebrates, ASFV replicates in cells of the mononuclear phagocyte system, mainly monocytes and macrophages, although other cellular types can be infected, especially later during the infection. In fact, the activation of the secretory activity in macrophages by ASFV replication plays a key role on ASFV infection, being a modulating element of the pathogenesis (Carrasco *et al.*, 1996a; Carrasco *et al.*, 1996b; Gomez-Villamandos *et al.*, 2013; Vinuela, 1985). The mechanism used by ASFV to entry in host cells has been a considerably discussed topic. Preliminary studies described it as a temperature, energy, cholesterol and low-pH dependent process, which requires receptor-mediate endocytosis (Alcami *et al.*, 1989a; Alcami *et al.*, 1989b; Carrascosa *et al.*, 1999; Geraldes and Valdeira, 1985; Valdeira *et al.*, 1998). Other studies described that ASFV entry requires dynamin and is a clathrin-dependent process (Galindo *et al.*, 2015; Hernaez and Alonso, 2010). This subject has been widely studied on our laboratory. Combining pharmacological inhibitors, specific dominant-negative constructions and confocal and electron microscopy assays, we have demonstrated that ASFV entry in Vero and IPAM cells is predominantly taking place by micropinocytosis, in a process that requires sodium/proton exchangers (Na+/H+), activation of the epidermal growth factor receptor (EGFR) and the phosphatidylinositol-3-kinases (PI3K), phosphorylation of the Serine/threonine-protein kinase (Pak1) together with the activation of Rho-GTPase Rac 1; and that relies on actin-dependent blebbing/ruffling formation (Sanchez *et al.*, 2012).

Traditionally, ASFV is widespread in Africa and in Sardinia, where it is endemic. However, in June 2007, an outbreak in the Caucasus region of Georgia was confirmed (Rowlands *et al.*, 2008). The virus rapidly spread to other neighbourhood regions of East Europe, as Russia, where it has not been controlled, to date. As there is no vaccine or treatment that effectively protect against ASFV infection, this outbreak supposes a real hazard for the world pig population. In this regard, several studies have been directed to decipher the

possible protection mechanism against ASFV infection (Escribano *et al.*, 2013; King *et al.*, 2011; Mulumba-Mfumu *et al.*, 2015; Wardley *et al.*, 1985). First attempts used inactivated viral particles and irradiated lysates of infected cells, but they were unsuccessful (Escribano *et al.*, 2013). Other studies have focused on studying the role of both cellular and humoral immune responses to generate a protective response to ASFV infection. Infection of pigs with the ASFV non-virulent strain OUR/T88/3 confers protection against challenge with the homologous virulent strain OUR/T88/1. However, infected pigs with OUR/T88/3 and then depleted of CD8+T leucocytes are no longer fully protect to the challenge, indicating that cellular immune response is essential to an effective protection against ASFV (Oura *et al.*, 2005). On the other hand, the humoral immune response is also important and it has been deeply studied (Escribano *et al.*, 2013). Passive transfer experiments in swine demonstrated that 85% of pigs inoculated with serum obtained from convalescent pigs previously immunized with the E75CV1-4 E75 strain (Spanish strain E75 adopt to grow in CV1 culture cells) were protected against ASFV isolate E75 infection (Onisk *et al.*, 1994). Moreover, serum from pigs immunized with viral proteins p72, p30 and p54 neutralizes ASFV infection *in vitro*, although it does not protect against virulent strains infection *in vivo* (Gomez-Puertas *et al.*, 1998; Gomez-Puertas *et al.*, 1996). Further approaches have been directed to the use of DNA vaccines to enhance the immune response against ASFV in infected pigs. However, only a partial protection has been achieved using this technique, thus far (Argilaguet *et al.*, 2011).

1.1.2 ASFV virion structure

ASFV virions are icosahedral structures of approximately 200 nm, which are constituted by different concentric layers: the internal core, the core shell, the inner membrane, the capsid and, in the extracellular virions, the external envelope (Andres *et al.*, 1997; Breese and DeBoer, 1966; Carrascosa *et al.*, 1984) (Figure 1).

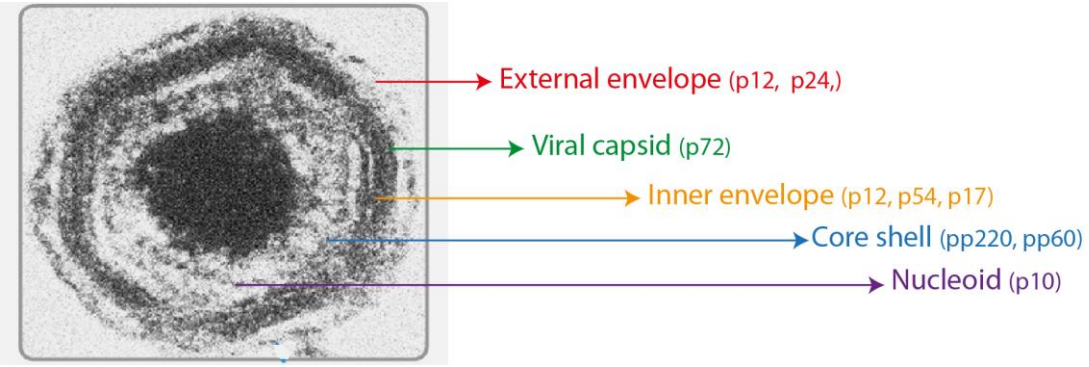

Figure 1. Structure of the extracellular ASFV virion.
Electron microscopy image of the extracellular ASFV particle. ASFV virion is composed by different concentric layers: the external envelope (red), the viral capsid (green), the inner envelope (yellow), the core shell (blue) and the nucleoid (purple). Examples of proteins present in each layer are shown in brackets (reviewed on (Salas and Andres, 2013))

The internal core is formed by the nucleoid, and contains the viral genome and certain nucleoproteins such as the DNA-binding protein p10 (Andres *et al.*, 2002b; Munoz *et al.*, 1993). This layer is also supposed to encompass all the elements required to the synthesis of the early messenger RNAs (mRNAs): the transcriptional machinery, the poly(A) polymerase and the capping enzyme(Salas and Andres, 2013). The core shell is a thick protein layer which surrounds the core and is mainly composed by the polyproteins pp220 and pp62. Both polyproteins are successively processed by a viral protease (S273R gene) and, together, they constitute 32 % of the total mass of the virion (Andres *et al.*, 2002a; Andres *et al.*, 2002b; Andres *et al.*, 1997). The inner envelope is adjacent to the core shell and looks like a single lipid membrane by conventional electron microscopy (Salas and Andres, 2013). This membrane is derived from the endoplasmic reticulum (ER) (Andres *et al.*, 1998) and viral proteins p54, p17 and p12 are constituents of this structure (Rodriguez *et al.*, 2004; Salas and Andres, 2013; Suarez *et al.*, 2010). The capsid is the outermost layer of the intracellular virions, and is composed by approximately 2000 hexagonal capsomers. p72 protein is the major module of the capsomers and constitutes one third of the total mass of the virion (Carrascosa *et al.*, 1984; Garcia-Escudero *et al.*, 1998). The external membrane or outer envelope of the extracellular viral particles is similar to the cellular plasma membrane, and is acquired during the budding process used by ASFV to exit from the cell (Breese and DeBoer, 1966; Carrascosa *et al.*, 1984). This structure contains the viral protein p12, which has been identified as the viral factor needed for the attachment to the host cell (Carrascosa *et al.*, 1991). Other protein suggested to be in the outer membrane is the virus homologue of cellular CD2 protein (CD2v), which mediates the hemadsorption of infected cells (Borca *et al.*, 1994; Rodriguez *et al.*, 1993).

ASFV morphogenesis takes place in specialized areas of the cytoplasm, called viral factories, which are located near to the nucleus and the microtubule organization centre (MTOC). These structures essentially exclude host proteins, but are surrounded by ER membranes and enclosed in vimentin cages (Heath *et al.*, 2001). In addition to ER membranes, mitochondria are also recruited to the periphery of viral factories (Rojo *et al.*, 1998).

1.1.3 ASFV replication and transcription

1.1.3.1 ASFV replication

ASFV genome is a linear double-stranded DNA molecule with variable length (from 170 to 193 kbp) among different viral strains (Dixon *et al.*, 2013; Yanez *et al.*, 1995). This variability is due to the gain and loss of Open Reading Frames (ORFs) in the multigene families and to the deviation of short tandem repeats in genes and intergenic regions (Dixon *et al.*, 1990; Lubisi *et al.*, 2007). ASFV genes are closely distributed, codified in both DNA strands and they do not present introns. Genome termini are hairpin-loops covalently cross-linked, being present in two possible forms inverted and complementary to each other (Dixon *et al.*, 2013).

ASFV replication predominantly takes place in the cytoplasm of infected cell, in the viral factories, and requires viral enzymes expressed immediately after virus entry. Due to this fact, and because of genome similarities, ASFV has been included in the nucleocytoplasmic large DNA viruses (NCLDV) superfamily (Dixon *et al.*, 2013). However, an initial nuclear replication phase has also been described at early times post infection (Rojo *et al.*, 1999). The exact function of this nuclear stage is not clear, but it has been described that nuclear organization is damaged as a consequence of ASFV infection, which includes nucleoli and nuclear envelope disorganization (Ballester *et al.*, 2011). Both nucleoporin p62, a marker of the nuclear envelope; and B-23, a marker of the nucleolus, are found in the cytoplasm of ASFV infected cells at late times post infection, suggesting an important damage in nuclear functions.

ASFV codifies for between 150 and 170 ORFs that express proteins with multiple functions: structural proteins, enzymes, transcription and replication factors, and proteins involved in modulation of ASFV-host cell interaction (Dixon *et al.*, 2013). In this regard, ASFV encodes for several proteins that interfere with host defences, such as A179L, a viral homologous of the anti-apoptotic proteins of the Bcl-2 family (Revilla *et al.*, 1997); EP153R, a homologous of the C-type lectin proteins (Hurtado *et al.*, 2004), or A224L, a homologous of the IAP family of apoptosis inhibitors (Nogal *et al.*, 2001). The viral protein A238L, a homologous of the IkB family that suppresses transcriptional activation of immunomodulatory genes, is especially important. Our laboratory has described that during ASFV infection, A238L protein reaches the nucleus and interacts with the transcriptional co-activator p300, preventing its phosphorylation by PKC-Θ. p300 phosphorylation is essential for the activation of the transcriptional factors NFAT, NFkB and c-jun. Using this mechanism, A238L inhibits the expression of the inflammatory regulator cyclooxygenase-2 (COX-2), the tumour necrosis factor alpha (TNF-alpha) and the inducible nitric-oxide synthase (iNOS) (Granja *et al.*, 2006a; Granja *et al.*, 2004; Granja *et al.*, 2008; Granja *et al.*, 2006b; Granja *et al.*, 2009; Sanchez *et al.*, 2013).

1.1.3.2 ASFV transcription

ASFV mRNAs are structurally similar to their cellular counterparts. *In vitro* transcribed viral mRNAs display no internal methylation, and possess a cap structure in its 5´UTR and a poly(A) tail of 33 nucleotides (nt) in average in its 3 ´UTR (Salas *et al.*, 1981). The cap structure is predominantly the type m^7G (5´) $pppA_m$, which suggests that an enzymatic activity for RNA capping is required to occur. In this regard, ASFV encodes a guanylyltransferase (NP868R) able to exert triphosphatase and guanylyltransferase activities (Pena *et al.*, 1993; Yanez *et al.*, 1995). In addition to the capping enzyme, ASFV genome codifies for a gene (C475L) that shares moderate similarity with the poly(A) polymerase of other NCLDV (Dixon *et al.*, 2013; Rodriguez and Salas, 2013; Yutin *et al.*, 2009), suggesting that the virus also possesses its own viral poly(A) polymerase.

ASFV exhibits a notable independence from its host to carry out the transcriptional process. The virus uses approximately 20 % of its genome to encode 20 genes considered to be related to translation and mRNA modification (Rodriguez and Salas, 2013). Indeed, ASFV virion contains a DNA-dependent RNA

polymerase (Kuznar *et al.*, 1980). In the presence of inhibitors of the cellular Pol II, the viral replication still takes place, indicating that all viral transcripts are transcribed by this viral polymerase (Salas *et al.*, 1988). In addition to the RNA polymerase, ASFV genome also codifies for genes similar to the TFIIB and TFIIS RNA polymerase II transcription factors, and for genes analogous to early, intermediate and late poxvirus transcription factors. Due to the fact that ASFV genome encodes for its own complete transcription system, the virus is able to accurately control the expression of its genes, which occurs in a time-dependent manner. Genes expressed before the onset of viral DNA replication have been designated as prereplicative genes, while genes that are expressed after viral replication are referred as postreplicative genes (Rodriguez and Salas, 2013).

Prereplicative genes have been described by their expression in ASFV-infected cells in the presence of DNA replication and/or protein synthesis inhibitors (Salas *et al.*, 1986). Two classes of transcripts are expressed in the prereplicative stage of the infection, which exhibit different kinetics of accumulation at different times post infection in the presence of these inhibitors (Almazan *et al.*, 1992). Early transcripts are easily detected by primer extension and nuclease S1 assays in the presence of both inhibitors, while immediately early transcripts accumulate in the presence of protein synthesis inhibitors, but are hardly detected when DNA replication inhibitors are present (Almazan *et al.*, 1992). Both transcripts are expressed immediately after of virus entry: in the case of immediately early transcripts, expression is repressed before the onset of viral replication (4 - 5 hours post infection, hpi), while early transcripts expression is maintained until the initiation of viral replication, and rapidly decreases thereafter (8 - 10 hpi). Interestingly, a small amount of immediately early and early mRNAs are observed at late times post infection, due to a reactivation of its expression that takes place late during the infection (20 hpi). This phenomenon has been also observed in vaccinia infection (Masternak and Wittek, 1996) and it has been attributed to the presence of all the components of the transcription machinery and the DNA template during the viral morphogenesis (Rodriguez and Salas, 2013). The multigene family 110, which comprises a set of paralogous genes that are present in multiple copies at the left end of the genome, is expressed immediately after the virus entry (Almendral *et al.*, 1990). For that reason, this family has been selected for the study of ASFV early transcription (Almazan *et al.*, 1992). Transcriptional mapping of the multigene family 110 by primer extension show that early mRNAs possess a defined length. These mRNAs present a short sequence of nucleotides (8-70 nt) upstream of the translation initiation site, and terminate at one or more sites downstream of the termination codon. A conserved sequence motif of seven or more thymidylate residues (7T signal) is located at the 3 ´UTR region of these mRNAs, which has been described as the translational termination signal (Almazan *et al.*, 1992). The majority of immediate early and early genes belong to the multigene families, which are believed to be involved in the control of host responses to the infection (Afonso *et al.*, 2004) and in the viral DNA replication (Rodriguez and Salas, 2013).

Transcription of postreplicative genes takes place after viral replication and is dependent on this process: no postreplicative mRNAs are detectable in ASFV infected cells in the presence of inhibitors of the DNA replication (Almazan *et al.*, 1993; Rodriguez *et al.*, 1996). Two classes of transcripts are expressed on the postreplicative stage of the infection: the intermediate and the late mRNAs. Intermediate genes are differentiated of late genes because the first required transcription factors that are expressed before viral replication, thus they can be expressed ectopically in ASFV-infected cells in the presence of inhibitors of the DNA replication, and the exogenous mRNA can be detected by primer extension (Rodriguez *et al.*, 1996). Expression of the intermediate genes directs the expression of the late genes. Both transcripts also present different kinetics of accumulation: intermediate mRNAs are expressed immediately after viral replication and are rapidly degraded before the accumulation of late transcripts, while the late mRNAs are expressed after the intermediate, accumulate approximately at 12 hpi and are slowly degraded thereafter (Rodriguez *et al.*, 1996). In contrast to poxvirus, which possesses heterogeneous late transcripts with imprecise termination sites and a poly(A) leader sequence on its 5´UTR region (Yang *et al.*, 2012), ASFV intermediate and late mRNAs retain an exact length (they initiate and terminate at fixed sites) and do not present poly(A) sequence at the 5´UTR. Indeed, their structure is similar to early transcripts, and they also present the T7 termination signal at the 3 ´UTR sequence. In fact, the T7 motif is considered to be the termination signal for all the viral temporal transcripts, because a strong correlation between the presence of these motif and the transcript termination site in all the mapped ASFV transcripts has been observed (Garcia *et al.*, 1995; Rodriguez and Salas, 2013).

Despite these differences, the mechanism used by ASFV to temporally express its genes has been proposed to be similar to the cascade mechanism displayed by poxvirus (Broyles, 2003) : transcription factors necessary for the expression of the intermediate genes are codified by the early genes; transcription factors necessary for the expression of late genes are codified by the intermediate genes, and the transcriptional factors necessary for early gene expression are expressed at late times post infection and packaged into the viral particles (Rodriguez and Salas, 2013) (Figure 2).

Few experimental analyses have been performed regarding ASFV promoter sequences. Alignment of the 50 nt sequence upstream of the initiation codon of mapped prereplicative genes shows that these regions are rich in A-T residues, but they do not present similarity of sequence (Rodriguez and Salas, 2013). Alignment of the upstream sequences from the initiation codon of both intermediate genes I226R and I243L revealed that these sequences are highly conserved at positions -25 to -15 and -9 to +9 (Rodriguez *et al.*, 1996). Regarding late *cis-acting* sequences, only the one that regulates the B646L gene (which encodes for the capsid protein, p72) has been characterized in detail (Garcia-Escudero and Vinuela, 2000). This promoter sequence covers 41 nt upstream of the ORF and presents two conserved regions: the first is located between the position -18 and -14 (TATTT), and the second is closer to the transcription start point, and it is located at position -4 to +2 (TATATA). Only the latter is moderately conserved among other intermediate and late

genes (Rodriguez and Salas, 2013). Mutational analysis of the TATATA region in the p72 promoter revealed that the -1 position is essential for the activity of the promoter, while changes in +1 and +2 positions considerably reduced its activity, but are not essential. Activity of other late promoters elements is also reduced when the TATA sequence is mutated, suggesting that this region can be a late promoter motif (Garcia-Escudero and Vinuela, 2000).

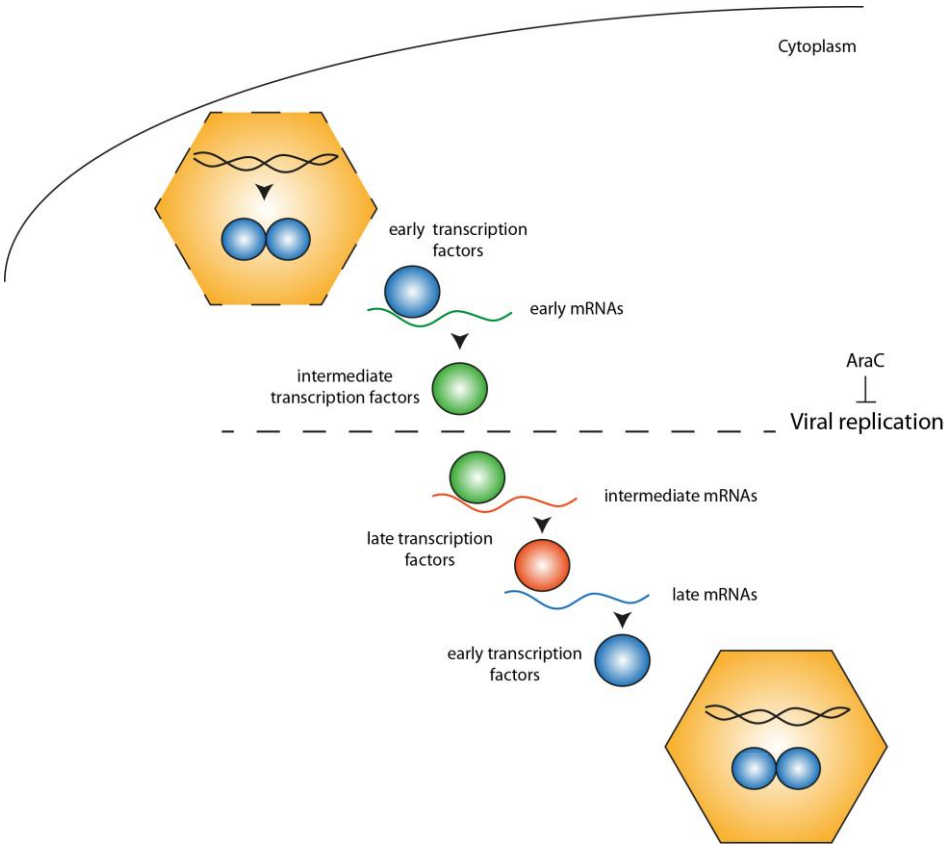

Figure 2. Schematic representation of the transcriptional cascade mechanism proposed to ASFV.
ASFV exerts a tight control of viral genes transcription. After viral entry and until the onset of the viral replication, immediate early and early genes are expressed, while after viral replication intermediate and late genes synthesis takes place. The mechanism used by ASFV to achieve this goal involves sequential expression of the different viral transcription factors: immediate and early transcription require transcriptional factors expressed at late times post infection and packaged into the viral particles, intermediate transcription needs the expression of the transcriptional factors encoded in early genes, and late transcription require transcription factors encoded in intermediate genes. AraC is an inhibitor of viral replication.

1.1.4 Translational regulation by ASFV

As commented on the previous section, ASFV mRNAs are structurally similar to the cellular mRNAs, and the fact that ASFV mRNAs are capped suggests that they are translated by a canonical cap-dependent mechanism, as it happens with most of cellular mRNAs.

The initiation of translation consists in the recruitment of the ribosome to the mRNA and it is one of most regulated steps in gene expression. The eukaryotic translation initiation factors (eIFs) play a central role in this process and are usually targets for fine viral regulation. The phosphorylation of eIF2 represents one of the most important steps in the regulation of the cellular translation since it allows rapid and reversible modulation of translation initiation. The phosphorylation of the α subunit inhibits eIF2 activity and is performed by several cellular protein kinases (Donnelly *et al.*, 2013; Proud, 2005; Wek *et al.*, 2006), and

among them, the double stranded RNA-activated kinase (PKR), the PKR-like endoplasmic reticulum (ER) kinase (PERK) and general control non-derepressible-2 (GCN2) play a major role in response to viral infections (Barber *et al.*, 1993; Berlanga *et al.*, 2006; Cheng *et al.*, 2005; Garcia *et al.*, 2007).

Similarly to vaccinia virus (VACV) infection, during ASFV infection P-eIF2α levels decrease at early times post infection, and remain undetectable throughout the infection (Castello *et al.*, 2009b). ASFV genome encodes a protein (DP71L) which possesses a characteristic binding protein phosphatase 1 motif (VxF) (Cohen, 2002) and that is able to interact with protein phosphatase 1 (PP1) *in vitro* and *in vivo. In vitro*, recombinant 6xHis-PP1 protein directly interacts with the recombinant protein GST-Dp71L, as demonstrated by pulldown assays (Rivera *et al.*, 2007). *In vivo*, co-immunoprecipitation assays in cells transduced with a lentiviral vector expressing DP71L-V5 protein demonstrate that this viral protein can be detected in complex with the three forms of PP1. This result was further confirmed by yeast two-hybrid interaction assays (Zhang *et al.*, 2010). Individual expression of DP71L induces a decrease of phosphorylated eIF2α and enhances the expression of co-transfected reporter genes. In these experiments, an increase in Beta-galactosidase (β-Gal) activity can be observed in cells transduced with the lentiviral vector expressing DP171L and cotransfected with the β-Gal reporter plasmid (Zhang *et al.*, 2010). These results suggest that DP71L plays a role keeping the translation machinery active to allow viral protein synthesis. A schematic representation of this process is shown in Figure 3 A. However, the depletion of DP71L in the viral strains Malawi Lil 20/1 and E70 does not lead to an increase in the levels of P-eIF2α, suggesting that as VACV, ASFV possesses alternative mechanisms to avoid eIF2α phosphorylation (Zhang *et al.*, 2010).

The other key viral regulation point involves the recruitment of ribosomes and the eukaryotic translation initiation factor 4F (eIF4F) formation. eIF4F, as key component of the cap-dependent translation machinery, is accurately regulated in response to extracellular stimuli, stress and viral infections. eIF4F is a complex composed by three proteins: eukaryotic translation initiation factor 4A (eIF4A), eukaryotic translation initiation factor 4E (eIF4E) and eukaryotic translation initiation factor 4G (eIF4G) (Prevot *et al.*, 2003). eIF4A is a RNA helicase implicated in unwinding the secondary structure of the 5´end of the mRNA together with eIF4B; eIF4E binds the cap structure at the mRNA 5´terminus, and eIF4G is a scaffolding protein that forms a molecular bridge between the mRNA and the small ribosomal subunit 40 S. eIF4G coordinates the initiation of translation via protein-protein interactions: the N-terminus domain is involved in the recruitment of the mRNA by its interaction with the cap-binding factor eIF4E and the cytoplasmic Poly(A) Binding Protein (PABPC); and at the same time, the C-terminal domain recruits the small ribosomal subunit by its interaction with eIF3 (Jackson *et al.*, 2010) (Figure 3 B).

eIF4G has been reported to be a substrate for caspase-3 (Bushell *et al.*, 1999; Prevot *et al.*, 2003), being its proteolytic cleavage a potential cause of the shutoff during apoptosis (Marissen and Lloyd, 1998). At late times post infection, ASFV induces apoptotic response (Ramiro-Ibanez *et al.*, 1996) and, consequently, caspase-3 activation (Granja *et al.*, 2004). However, eIF4G is not affected by caspase-3

cleavage in ASFV-infected cells (Castello *et al.*, 2009b) indicating some possibilities: that the cleavage sites are not accessible to the protease (perhaps protected by protein-protein interactions); that eIF4G is not at the same location than caspase-3; or that caspase-3 activity is abrogated. Regarding the last possibility, ASFV encodes for an inhibitor of the apoptosis (IAP)-like protein (A224L), which has been reported to be an inhibitor of caspase 3 (Nogal *et al.*, 2001). The possibility that this factor protects translation machinery from caspase 3-mediated degradation has been not further studied, to date. On the other hand, ASVF induces mammalian target of rapamycin (mTOR)-mediated phosphorylation of eIF4G at Ser1108 (Castello *et al.*, 2009b), which has been associated to "translational activation" (Kimball *et al.*, 2000; Raught *et al.*, 2000), and in parallel, ASFV triggers the phosphorylation of eIF4E at Ser209 by Mnk-1 (Figure 3 B). Although the biological relevance of the eIF4E phosphorylation is controversial (Morley and Naegele, 2002), its importance for some viral infections has been demonstrated. In the case of influenza virus, vesicular stomatitis virus (VSV) and adenovirus (AdV), the dephosphorylation of eIF4E correlates with the inhibition of the cellular protein synthesis (Connor and Lyles, 2002; Cuesta *et al.*, 2004; Feigenblum and Schneider, 1993). Whereas, for hepatitis C virus (HCV) or murine norovirus 1 eIF4E phosphorylation is important for virus translation and for the progression of the infection, respectively (Panda *et al.*, 2014; Royall *et al.*, 2015). During ASFV infection, eIF4E phosphorylation is related to an enhancement of the viral replication and protein synthesis (Castello *et al.*, 2009b). eIF4E phosphorylation takes place after 8 hours post ASFV infection and reaches its maximum levels at 14 - 18 hpi. This phosphorylation in infected cells is avoided in the presence of the Mnk-1 inhibitor CGP57380, and correlates with the phosphorylation of this kinase, suggesting that it relies in Mnk1 activation, as reported before (Pyronnet, 2000; Pyronnet *et al.*, 1999) (Figure 3 B).

The eIF4E-binding proteins (4E-BPs) are well-known negative regulators of the cap-dependent translation (Sonenberg and Hinnebusch, 2009). In its hypo-phosphorylated state, 4E-BPs are able to associate with eIF4E and compete with eIF4G, impairing eIF4F assembly. On the other hand, 4E-BPs are inactivated by mTOR-mediated hyperphosphorylation, allowing cap-dependent translation (Bhandari *et al.*, 2001; Richter and Sonenberg, 2005). Similarly to VACV and other DNA viruses (Buchkovich *et al.*, 2008), we have described that ASFV infection promotes 4E-BP1 phosphorylation at early times post infection, but in this case it is progressively hypo-phosphorylated at later times (from 14 hpi). eIF4G, eIF4E and 4E-BP1 phosphorylations are concomitant with an increase of eIF4F assembly (Castello *et al.*, 2009b). The hypo-phosphorylation observed at late times post infection may be due to a viral mechanism to stop the viral protein synthesis when late morphogenesis stage is taking place (Figure 3B).

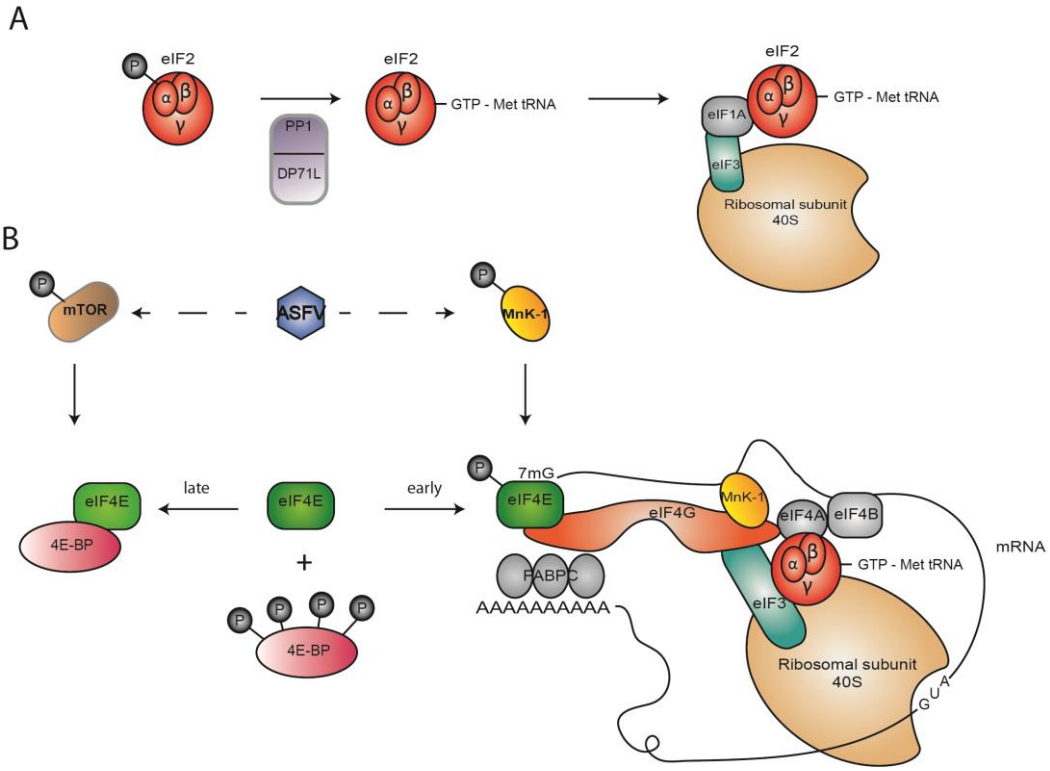

Figure 3. Regulation of translation in ASFV infection.
A) ASFV infection prevents eIF2α phosphorylation. During ASFV infection, viral protein DP71L is able to interact with PP1 and promotes its activation, which leads to the dephosphorylation of eIF2α and allows cap-dependent translation. B) ASFV infection stimulates eIF4F assembly. During ASFV infection, eIF4E and eIF4G are phosphorylated by mTOR and Mnk1, respectively, which promote their interaction and the formation of eIF4F. Additionally, at early times post infection 4E-BP is hyper-phosphorylated, which inhibits 4E-BP and eIF4E interaction. At late times post infection, 4E-BP is hypo-phosphorylated, which leads to its interaction with eIF4E and to an inhibition of the translation. The phenomenon observed at late times post infection may be due to a viral mechanism to stop the viral protein synthesis when late morphogenesis stage is going on.

Nevertheless, phosphorylation of eIF4G, eIF4E and 4E-BP1 is important but not essential to the ASFV infection in cultured Vero cells, since the presence of inhibitors of Mnk-1 (CGP57380) and mTOR (rapamycin) affects moderately the viral protein synthesis and virus production. However, the activities of eIF4G and eIF4E *per se* are essential for ASFV, because depletion of those factors by specific small interfering RNAs (siRNAs) strongly abrogates viral protein synthesis, viral factory formation and virus production. In the case of the depletion of eIF4E, the viral factories detected in the cytoplasm of the infected cells are aberrant, while depletion of eIF4G promotes a reduction in size and number of the factories (Castello *et al.*, 2009b).

1.1.5 mRNA metabolism regulation by ASFV

ASFV genome also encodes for proteins involved in mRNA metabolism. In this regard, ASFV D250R gene encodes a protein, g5Rp or pD250R (depending on the viral strain), that harbours a Nudix hydrolase motif, which is comparable to other Nudix hydrolases, such as the host decapping enzyme 2 (Dcp2) or the viral proteins D9 and D10 of VACV (McLennan, 2007). In viruses, presence of Nudix Hydrolases is almost exclusive of the members of the NCLDV (Rodriguez and Salas, 2013). It has been described that g5Rp exerts decapping activity *in vitro* (Parrish *et al.*, 2009), although this protein can also degrade other substrates as

diphosphoinositol polyphosphates under these conditions (Cartwright *et al.*, 2002). This protein, one of the targets of the present Thesis, is widely described in section 1.3.2.1.2.

Additionally, ASFV genome encodes a protein called pD339L that contains a protein-protein interaction SHS2 domain similar to the SHS2 domain found in the RNA-polymerase II subunit 7 (RBP7) (Rodriguez and Salas, 2013). RBP7 is involved in numerous functions, including mediating both transcription and cytoplasmic mRNA decay pathways. In yeast, RBP7 travels from nucleus to cytoplasm, where stimulates the deadenylation process. RBP7 is a component of the Processing Bodies (P-Bodies) that interacts with the decapping activator protein associated with topoisomerase II (Pat1) and also stimulates 3´-5´ decay route (Lotan *et al.*, 2007). Due to its similarity with this protein, pD339L could be embracing a similar role on ASFV infection.

1.2 CELLULAR RNA DECAY

RNA decay mechanisms play a key role on mRNA physiology: not only control gene expression by determining RNA levels available for translation, but also is implicated in mRNA surveillance by removal of aberrant mRNAs (Garneau *et al.*, 2007; Miller and Pearce, 2014). In eukaryotes, mRNAs are protected from degradation by two constructions: the cap structure at the 5´ end of the mRNA and the poly(A) tail at the 3´end (Ross, 1995). Both structures have an essential function on RNA fate: depending on their interaction with different proteins, RNAs can be translated, repressed or degraded (Decker and Parker, 2012; Schwartz and Parker, 1999). For initiation of translation, the cap binding protein eIF4E and PABPC have to interact with both components. Through eIF4G, both proteins generate a closed mRNA loop that promotes translation and efficiently protects RNA from nucleases (Wells *et al.*, 1998).

In eukaryotic major decay pathways, the poly(A) tail interacts with the deadenylation complex, which shortens it targeting RNAs for degradation (Chen and Shyu, 2011; Decker and Parker, 1993). Deadenylation is a common rate-limiting step on RNA decay. Three major deadenylases have been described in eukaryotes: the Pan2-Pan3 complex, the CCR4-NOT complex, and the poly(A) ribonulease (PARN) (Parker and Song, 2004). After deadenylation, mRNAs could be eliminated by two general pathways depending on the degradation direction. In the 3´-5´decay pathway, RNAs are targeted by the exosome, a multi-protein complex of 3´-5´exonucleases that degrade RNA body. Resultant products are then decapped by the scavenger decapping enzyme, DcpS (Wang and Kiledjian, 2001). In the 5´-3 decay route, after deadenylation mRNAs are decapped by the decapping enzymes Dcp1 and Dcp2, leaving a 5´- monophosphate RNA (5´-P-RNA) available for the action of the 5´-3´exonuclease Xrn1 (Garneau *et al.*, 2007) (Figure 4).

Additionally to the two major pathways, mRNA could also be degraded by other specific routes. In *S. cerevisiae* it has been described that certain mRNAs, as RPS28B and EDC1, can be degraded by a deadenylation-independent mechanism that does not require previous deadenylation process and directly decaps the mRNAs (Garneau *et al.*, 2007). mRNAs could also be degraded by specialized endonucleolytic

pathways, which are initiated by the endonucleolytic cleavage of the RNA body. Resultant RNA fragments are then eliminated by Xrn1 and the exosome complex. These pathways are activated in response to certain physiological stimuli such as stress, viral infections or aberrant sequence and structural RNAs .This is the case of the RNA interference pathway (Eulalio *et al.*, 2007). Other examples of endonucleolytic decay are the Nonsense-mediated decay (NMD) and the No-go decay (NGD). Both routes are cellular mRNA surveillance pathways that control the quality of the newly synthesise mRNA and avoid the accumulation of the potentially toxic aberrant proteins (Siwaszek *et al.*, 2014).

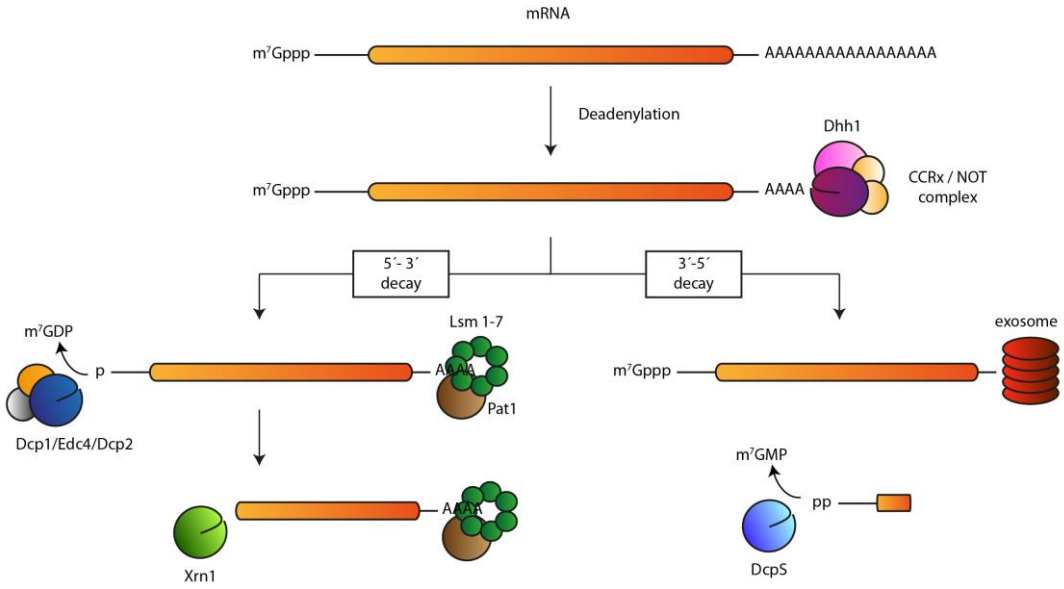

Figure 4. Major cellular mRNA decay pathways.
The majority of the mRNAs are degraded by the deadenylation-dependent decay routes. Deadenylation is carried out by the CCRX/NOT complex of deadenylases that shorten the poly(A) tail at the 3'end of the mRNAs. After deadenylation, mRNAs can be targeted to decapping by the decapping activators Pat1-Lsm1 and Dhh1 and decapped by the Dcp2, entering in the 5´-3' RNA decay route. Decapped mRNAs are degraded in 5´-3´orientation by the exonuclease Xrn1. Alternatively, after deadenylation mRNAs can be degraded by the 3´-5' endonuclease complex, the exosome. The resultant cap structure is removed by DcpS.

1.2.1 Decapping 5´–3´decay pathway

Decapping is an essential step in the 5´-3´RNA decay route because it induces RNAs to 5´-3´ degradation. In eukaryotes, this process is carried out by the decapping enzyme Dcp2, and it is a highly regulated phenomenon: numerous proteins, among which Dcp1 is described at the major activator, have been described to act as enhancers or inhibitors of decapping (Arribas-Layton *et al.*, 2013; Ling *et al.*, 2011; Meyer *et al.*, 2004).

The cap structure is an inverted 7-methylguanosine (m^7G) bound by a 5´-5´triphosphate bridge to the first nucleotide of eukaryotic mRNAs. Different types of cap structure exist in nature. Cap 0 structure contains the guanosine methylated at the N7 position. Formation of the Cap 1 structure occurs by 2´O methylation on the ribose residue on the first adjacent nucleotide to the m^7Gcap. Cap 1 structure can be converted to a Cap 2 by further 2´O methylation on the following nucleotide (Ghosh and Lima, 2010) (Figure

5). Capping is a process that mainly occurs at nucleus concomitant to transcription. In these conditions, it is carried out by three enzymes: a triphosphatase, a RNA guanylyltransferase and a methyltransferase (Ghosh and Lima, 2010). However, it also has been described to occur post-transcriptionally at cytoplasm by a capping enzyme complex that phosphorylates 5´-monophospahte RNA, which can function as a substrate for recapping (Otsuka *et al.*, 2009). As commented above, the cap structure plays a critical role on mRNA stability and regulation. Due to its unique chemical properties, it is resistant to exonuclease activity and additionally, it can interact with multiple proteins, called cap binding proteins, which possess a determining role on mRNA fate. In the nucleus, cap interacts with the Cap Binding Complex (CBP), which stimulates splicing and export of RNA. In the cytoplasm, cap is recognised by eIF4E, which is essential for translation initiation (Topisirovic *et al.*, 2011).

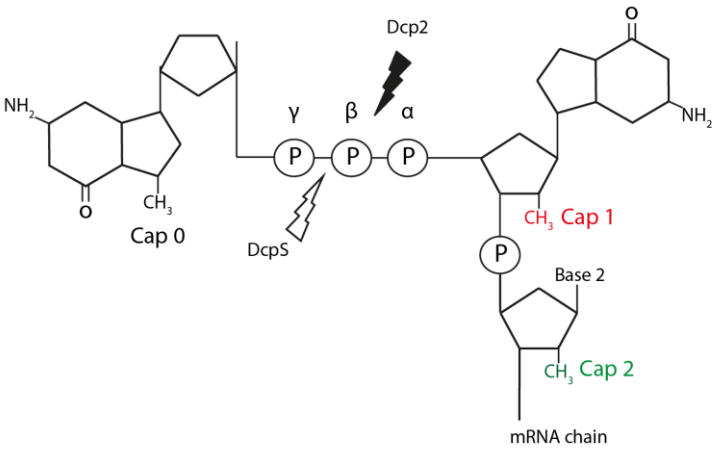

Figure 5. Schematic representation of the cap structure.
Capping of mRNAs is a common feature of all the RNA Polymerase II transcripts. Capping is a process that mainly occurs at the nucleus and consist in the addition of a methylated guanine by an inverse 5´-5´phosphate bridge at the 5'end of the mRNA. This structure is known as Cap 0 (black) and can undergo further methylation at the 2'O position on the ribose residue on the first adjacent nucleotide. This structure is termed Cap 1 (red). Cap 1 structure can be converted to a Cap 2 (green) by further 2´O methylation on the following nucleotide. Dcp2 catalyse the hydrolysis of the cap structure between γ and β phosphates, giving m^7GDP and 5´monophosphate as products. On the other hand, Dcp3 catalyse the hydrolysis of the cap structure between β and α phosphate, in a reaction that release m^7GMP.

1.2.1.1 Nudix hydrolases as decapping enzymes

Dcp2, the best characterized decapping enzyme in eukaryotes (Arribas-Layton *et al.*, 2013), belongs to the Nudix (nucleoside diphosphate linked moiety X) hydrolases superfamily (McLennan, 2006). These enzymes are highly conserved among species, being present on bacteria, yeast, archea, eukaryotes and viruses (Bessman *et al.*, 1996). Nudix hydrolases are able to catalyse the hydrolysis of nucleoside diphosphates bound to another moiety X, which could be a wide range of substrates: di and tri-phosphates, canonical and oxidised nucleotide di-phosphates, dinucleoside polyphosphates, dinucleotide coenzymes and capped RNAs (McLennan, 2006). Catalytic activity of these enzymes relies on the Nudix motif or Nudix box, a 23 amino acidic sequence highly conserved that presents the consensus sequence $Gx_5Ex_5[UA]xREx_2EExGU$, where X could be any amino acid, and U is an hydrophobic residue. The structure of this motif is a loop-α helix-loop which is able to bind divalent cations (commonly Mg^{2+}or Mn^{2+}) and to act as the catalytic site. Glutamic residues of Nudix motif have been demonstrated to play an important role on divalent cation

binding and to be essential for the catalysis activity, although these enzymes hold a wide variation regarding the individual residues implicated in the attack and the number of cations involved on the reaction. Nudix motif forms part of the Nudix fold, an α/β/α sandwich which contains supplementary regions not conserved along all the members and that defines enzymes specificity (Gabelli *et al.*, 2001; Mildvan *et al.*, 2005). Indeed, the members of this huge family possess substrate multispecificy and ambiguity, meaning that the same Nudix hydrolase is able to act over different related or non-related substrates with same or different specificity (McLennan, 2013).

Nudix hydrolases with decapping activity play an important role on mRNA metabolism, and they are also conserved from bacteria to mammals (McLennan, 2013; Song *et al.*, 2013). In eukaryotes, Nudix hydrolases with decapping activity are able to hydrolyse the cap structure, releasing 7-methylguanosine monophosphate (m^7GMP) or 7-methylguanosine diphosphate (m^7GDP) and 5´-monophosphate mRNA (Figure 5) (Mildvan *et al.*, 2005). In these enzymes, the conserved glutamic residues of the Nudix motif are essential for the decapping activity, because mutation of these amino acids in several Nudix decapping enzymes causes a loss of the decapping activity *in vitro* (Lin *et al.*, 1996; Steiger *et al.*, 2003; Wang *et al.*, 2002).

1.2.1.1.1 Dcp2

Dcp2 enzyme was firstly described as a decapping coactivator in *S. Cerevisiae* (Dunckley and Parker, 1999). Subsequent studies demonstrated that purified Dcp2 proteins from different species, as yeast, plant or human, were able to decapp mRNAs *in vitro*, releasing m^7GDP and 5´-monophosphorylated mRNAs as products (Iwasaki *et al.*, 2007; Piccirillo *et al.*, 2003; Steiger *et al.*, 2003). In the case of yeast Dcp2, decapping reaction (measured as product release) is more efficient on large mRNAs (at least 29 nt)(Steiger *et al.*, 2003), and is specific for the 5´UTR sequence: substitution of RNA sequence by DNA is not hydrolysed by Dcp2 (Dunckley and Parker, 1999).

Together with the Nudix motif, Dcp2 proteins present another two conserved motifs: Box A and Box B. Box B is situated down-stream the Nudix motif and it has been linked to the ability of Dcp2 to interact with the RNA body. RNA binding is essential to the catalysis by Dcp2, because this enzyme is not able to hydrolyze cap analogous which do not possess a RNA body, such as m^7GpppG. Moreover, Dcp2 decapping activity is subrogated by uncapped mRNAs but not by cap analogous; and truncated Dcp2 proteins, which do not possess Box B and are not thus able to bind RNA, do not present decapping activity *in vitro* (Piccirillo *et al.*, 2003). Dcp2 possesses a bipartite surface that creates a basic channel among Nudix motif and Box B sequences. This channel acts as a platform for RNA interaction and is important for the catalysis: single mutations of amino acids in the channel cause a loss on efficiency of decapping. Although cavity is present in other Nudix hydrolases, the basic channel is characteristic of Dcp2 (Deshmukh *et al.*, 2008; She *et al.*, 2008).

Kinetic assays demonstrated that Dcp2 binds RNA with high affinity, but low specificity; while cap structure is bound with high specificity but low affinity (Deshmukh *et al.*, 2008).

Dcp2 Box A is localised up-stream of Nudix box, in the highly conserved N-terminal regulatory domain (NRD). This motif has been related with fidelity of the hydrolysis process, because truncated proteins without Box A generate both m^7GDP and m^7GMP products (Piccirillo *et al.*, 2003). The N-terminal domain of the protein is non-essential for the catalysis *in vitro*, although highly stimulates the decapping reaction. On the contrary, the N-terminal domain is essential for this activity *in vivo* (She *et al.*, 2006). Moreover, it has been demonstrated that N-terminal domain directly interacts with the decapping co-activator Dcp1 (Dunckley and Parker, 1999; She *et al.*, 2006). The N-terminal domain and the Nudix domain of Dcp2 are linked by a flexible hinge region, allowing Dcp2 to adopt two conformations: one open and less efficient, and other closed and most active (She *et al.*, 2008). Cap analogues and Dcp1 stimulate the closed conformation of Dcp2 (She *et al.*, 2008). On the other hand, the C-terminal domain of Dcp2 is not conserved among eukaryotes. However, in both yeast and humans, this domain is implicated in the interaction with other decapping activators, such as Edc3 or Edc4 (Fromm *et al.*, 2012; Jonas and Izaurralde, 2013).

Dcp2 is a RNA-binding protein that displays substrate specificity: Dcp2 binds with more affinity mRNAs that possess a 5´ stem-loop structure. This structure was firstly described for the mRNA encoding for the exosome subunit Rrp41 (Li *et al.*, 2008), but has been identified in several mRNAs, indicating that it could play a more general role in enhancing decapping (Li *et al.*, 2009). The regulatory effect of the loop-structure relies on its structural integrity, and not on its primary sequence. Position of the loop is also important: RNA-Dcp2 interaction is reduced when the loop-structure is located further than 10 nt from the cap structure (Li *et al.*, 2009).

1.2.1.1.2 Other Nudix decapping enzymes

In mammalian cells, 24 Nudix hydrolase genes and at least 5 pseudogenes have been described (McLennan, 2006), being Dcp2 and Nudix-type motif 16 (Nutd16) the best known decapping enzymes. Nutd16 possess decapping activity *in vitro* (Taylor and Peculis, 2008), and was firstly discovered on *Xenopus* (Ghosh *et al.*, 2004). Nutd16 has been pointed to act as an additional decapping enzyme together with Dcp2 (Li *et al.*, 2011; Song *et al.*, 2010). In addition to Dcp2 and Nudt16, six additional mouse Nudix enzymes have been described to possess decapping activity *in vitro*: Nudt2, Nudt3, Nudt12, Nudt15, Nudt17 and Nudt19 (Song *et al.*, 2013).

1.2.1.2 Decapping activators

Dcp1 is the main activator of Dcp2. In yeast, Dcp1 directly interacts with Dcp2, stimulating Dcp2 activity *in vitro* and being essential for this process *in vivo* (Beelman *et al.*, 1996; Dunckley and Parker, 1999; Steiger *et al.*, 2003). In mammalian cells, this interaction is more fragile and requires the presence of the enhancer of decapping Edc4 (Chang *et al.*, 2014; Fenger-Gron *et al.*, 2005). Dcp1 from yeast possesses an α-

helix structure that is not conserved in other eukaryotic Dcp1 enzymes (α1 and α2) and that is the main domain involved in Dcp2 interaction, which could explain why other co-factors are needed to stabilize that interaction in higher eukaryotes (She *et al.*, 2004; She *et al.*, 2008). Dcp1 stimulates Dcp2 decapping activity by promoting the Dcp2 closed conformation (She *et al.*, 2008). Indeed, Dcp1 not only activates by itself Dcp2 activity, but also stimulates decapping by recruiting other decapping activators, as the enhancers of decapping proteins 1 and 2 (Edc1 and Edc2) or the enhancer of decapping protein 3 (Edc3) (Borja *et al.*, 2011; Tritschler *et al.*, 2007).

Edc4 is also known as human enhancer of decapping large subunit (Hedls) and as Ge-1 in *Drosophila melanogaster*. This decapping activator has no yeast homologs; it is only conserved in metazoans (Arribas-Layton *et al.*, 2013). Edc4 stimulates hDcp2 decapping activity *in vitro* (Fenger-Gron *et al.*, 2005) and acts as a scaffold protein of the decapping complex, directly interacting with hDcp1, hDcp2 and Xrn1. Moreover, the association between these proteins is essential for decapping *in vivo* (Chang *et al.*, 2014).

Other important decapping activators are Edc1 and Edc2, Edc3, Pat 1, the Sm-like proteins 1-7 (Lsm1-7) complex and the DEAD box helicase homolog Dhh1 (also known as Rck/p54 or DDX6 in humans and Me31B in Drosophila). All of them are present in the P-Bodies structures (reviewed on (Eulalio *et al.*, 2007)), and stimulate the decapping activity of Dcp1:Dcp2 enzymes by several mechanism (Coller and Parker, 2005; Fischer and Weis, 2002; Fromm *et al.*, 2012; Nissan *et al.*, 2010; Schwartz *et al.*, 2003; Tharun and Parker, 2001; Tritschler *et al.*, 2007). Pat1 and Dhh1 are also able to inhibit translation (Coller and Parker, 2005; Nissan *et al.*, 2010). Due to this fact, both Dhh1 and Pat1 have been described as the effectors of a general mechanism that targets mRNAs from an active translation state to a repressed mRNP, which could end in decapping and 5´-3´RNA degradation.

1.2.1.3 Decapping inhibitors

Several evidences suggest that decapping and translation are mainly competitive process. It means that initiation translation factors might be removed from cap before decapping takes place (Schwartz and Parker, 2000). Translation initiation factors in fact inhibit decapping: mutations of several eIFs as eIF4E, eIF4G or eIF4A promote an increase of deadenylation and decapping rates (Schwartz and Parker, 1999).In yeast, eIF4E inhibits decapping *in vitro* (an effect that depends on eIF4E ability to bind the cap structure (Schwartz and Parker, 2000)) and *in vivo,* although in this case accessibility of the cap by decapping enzymes does not seem to be merely controlled by competition with eIF4E (Schwartz and Parker, 1999). Poly(A) tail and poly(A) binding proteins (Pab1 in yeast, PABP in mammals) are also inhibitors of decapping. In yeast, Pab1p is able to inhibit deadenylation and decapping in *in vitro* (Wilusz *et al.*, 2001) and *in vivo* (Caponigro and Parker, 1995). PABP also interacts with the 5´cap structure *in vitro*. This interaction can occur concomitantly with PABP-poly(A) tail interaction (Khanna and Kiledjian, 2004), which suggest that PABP protects both 5´and 3´RNA ends of the exonucleases action.

1.3 MANIPULATION OF CELLULAR mRNA METABOLISM BY VIRUSES

mRNA turnover is not only important in cellular gene expression regulation, but it also plays an essential role on antiviral defence (Abernathy and Glaunsinger, 2015; Pichlmair *et al.*, 2006; Rigby and Rehwinkel, 2015; Waterhouse *et al.*, 2001). Uncapped 5´triphosphate viral mRNAs can be recognised by the host immune system and trigger antiviral responses, such as PKR or retinoic acid-inducible gene-1 (RIG-1) activation (Nallagatla *et al.*, 2008; Pichlmair *et al.*, 2006). In this regard, viruses have developed several strategies in order to protect their mRNAs from the cellular-induced mRNA decay routes and to avoid detection of viral mRNAs by the host innate immunity (Narayanan and Makino, 2013). Some viruses synthesise a cap structure similar to the one found in cellular mRNAs. Retroviridae and bornaviridae use both the cellular RNA polymerase II and the cellular capping machinery to synthesise their viral mRNAs; a strategy that makes viral transcripts exert the same cap structure that cellular mRNAs (Koonin and Moss, 2010). Double-stranded DNA viruses, like vaccinia and ASFV, encode for their own capping enzymes which also produced viral mRNA with a cap structure that resembles the cellular one (Decroly *et al.*, 2012; Pena *et al.*, 1993). On the other hand, some viruses, such us influenza viruses, arenaviruses and hantiviruses, acquire the cap structure from cellular mRNAs, using a technique called “cap-snatching”. This technique consists in stealing the cap structure of the cellular mRNA through the activity of endonucleases, which cut the host transcript several nucleotides downstream of the 5´cap structure. After the cleavage, the resultant short capped mRNA is used as primer for the synthesis of the viral mRNA (Decroly *et al.*, 2012; Koonin and Moss, 2010). The yeast L-A double stranded RNA virus also uses cap-snatching (Fujimura and Esteban, 2011), but it displays a different cap-snatching mechanism to the one described above. Through the decapping activity of the viral capsid Gag protein, L-A viruses transfer only the m^7Gp from cellular mRNAs to viral mRNAs. Many viruses also protect their mRNAs at the 3´end. This is the case of alphaviruses, picornaviruses, coronaviruses and ASFV, which polyadenylate their transcripts, adding a poly(A) tail similar to the one found in their eukaryotic counterparts (Narayanan and Makino, 2013; Salas *et al.*, 1981). In addition to these *cis-acting* elements, other viruses use *trans-acting* elements to protect their mRNAs, as picornaviruses, calciviruses and astroviruses, which protect their 5´UTR by covalent interaction with viral proteins. In the case of picornaviruses, their viral mRNAs possess an internal ribosome entry site (IRES), which allows translation of viral mRNAs in a cap-independent manner and also acts as a barrier to the action of endonucleases (Narayanan and Makino, 2013).

1.3.1 Viral mechanism to regulate mRNA decay pathways

Viruses not only protect their mRNAs to avoid cellular mRNA decay routes, but also strongly alter RNA metabolism in order to block or subvert stress responses to facilitate viral replication (Reineke and Lloyd, 2013; Sanchez *et al.*, 2013).

1.3.1.1 P-Bodies and viral infection

Processing Bodies, or P-Bodies, are cytoplasmic messenger ribonucleoproteins (mRNPs) granules, which contain non-translating mRNAs and that are enriched for RNA decay machinery components (Decker and Parker, 2012). P-bodies are dynamic complexes constitutively present in cells, although their size and number can increase under stress stimuli or in circumstances when translational repression is augmented (Kedersha *et al.*, 2005; Teixeira *et al.*, 2005). Components of P-Bodies include the decapping enzymes Dcp1 and Dcp2, the decapping activators Edc3 and Edc4, the Lsm1-7 complex and the translation repressors Dhh1 and Pat1, among others (reviewed on (Eulalio *et al.*, 2007)). In yeast and mammals, P-Bodies are structures where active RNA decay can take place (Cougot *et al.*, 2004; Sheth and Parker, 2003), although formation of P-Bodies is not necessary for mRNA decapping or for translation repression (Buchan *et al.*, 2008; Decker *et al.*, 2007), indicating that mRNA decay can occur outside of this structures. Stress conditions, such as heat shock, oxidative stress or viral infections, can also trigger the formation of other cytoplasmic RNA granules, called stress granules (SGs). These structures share several features with P-Bodies: both of them contain non-translating mRNAs and RNA decay machinery components, such as Xrn1. However, stress granules present proteins that cannot be found in P-Bodies, such as eukaryotic initiation factors (eIF4G or eIF3), Ras GTPase-activating protein-binding protein 1 (G3BP) or the 40S ribosomal subunit (Eulalio *et al.*, 2007). P-Bodies and stress granules are dynamically linked and it is believed that mRNA can move between polysomes, P-Bodies and stress granules in a working model known as mRNA cycle. In this model, mRNA is translated until it is targeted by proteins that repress translation, such as Dhh1 or Pat1, in response to a defect on translation or through specific recruitment. After that, ribosomes can be removed and the rest of the decapping machinery can be recruited. Therefore, decapping and RNA degradation can take place. Alternatively, mRNAs can remain stalled in translation repression and accumulate in stress granules or they can re-enter in translation if degradation machinery is replaced by translation initiation factors (Decker and Parker, 2012).

P-Bodies and stress granules are also involved in host defences (Beckham and Parker, 2008; Li *et al.*, 2015). In this regard, some mRNA decay pathways, such as micro RNAs (miRNAs) or siRNAs, contribute to antiviral defence in mammals and plants (Dykxhoorn, 2007). This decay routes stimulate the recruitment of P-Bodies components into targeted mRNAs, which enter into translation repression and mRNA degradation (Valencia-Sanchez *et al.*, 2006). In addition, proteins that contribute to antiviral defence, like protein kinase R (PKR) and the apolipoprotein B mRNA editing enzyme, catalytic polypeptide-like 3G and 3F (APOBEC3G and APOBEC3F), are also accumulated in P bodies (Beckham and Parker, 2008; Hebner *et al.*, 2006; Wichroski *et al.*, 2006). It is not surprising that viruses have developed multiple mechanisms to interfere with these structures in order to promote efficient translation of viral mRNAs (Figure 6). Some viral strategies are focused on the disruption of the cellular mRNA decay machinery by inactivation of P-Body components. This is the case of the West Nile Virus, which causes a progressive decrease in P-Bodies number

and a relocalization of many of its components (such as DDX6, Lsm1, or Xrn1) into the viral replication sites, while neither Dcp1 nor Edc4 are recruited to the viral factories. Interestingly, the recruited P-Body components are important to West Nile Virus replication, as silencing of these proteins reduce percentage of infected cells and viral RNA (Chahar *et al.*, 2013). Adenoviruses also promote a decrease in P-Bodies, and their components are also redistributed, but in this case to aggresomes, where they are probably inactivated or degraded (Greer *et al.*, 2011). Polioviruses completely eliminate P-Bodies, and also degrade Xrn1, Pan3 and Dcp1a proteins in a process that requires viral replication and the expression of the viral proteinases. Interestingly, other P-Body components like Edc3 or Edc4 are unaffected by poliovirus infection (Dougherty *et al.*, 2011).

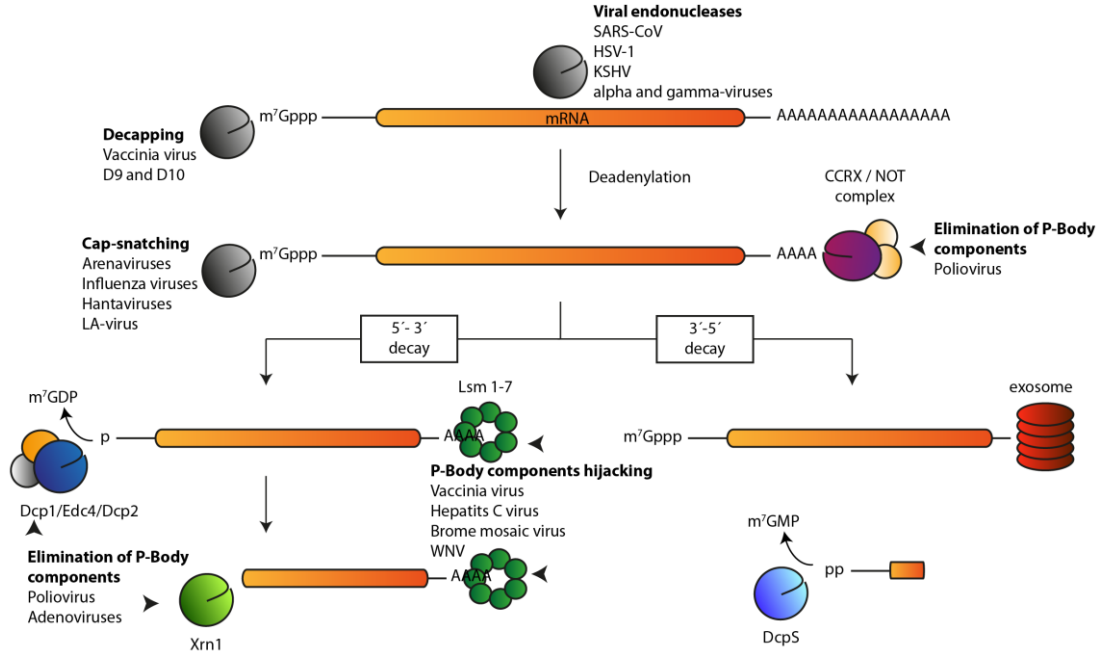

Figure 6. Viruses manipulate cellular mRNA decay pathways.
In order to successfully translate the viral mRNAs and avoid its degradation by the host immune defences, viruses have developed multiple mechanisms to subvert cellular RNA decay components. Poliovirus and adenovirus eliminates P-body components by the action of viral proteases or in by distributing them to agressomes, respectively. Vaccinia virus, West Nile virus, brome mosaic virus and hepatitis C virus use P-body components to their own benefit. Kaposi´s sarcoma-associated herpesvirus (KSHV), Epstein-Barr virus (EBV), severe acute respiratory syndrome coronavirus (SARS-CoV) and Herpes simplex virus (HSV-1) directly degrade host mRNA by the action of endonucleases. Vaccinia virus also target cellular mRNAs using decapping enzymes. Arenaviruses, influenza viruses, hantaviruses and LA-viruses use the cap-snatching technique as a mechanism for capping viral mRNAs and for eliminate cellular mRNAs.

Viruses have also developed mechanisms to use the mRNA decay components to their own benefit. Brome mosaic virus, vaccinia virus and hepatitis C virus (HCV) employ this strategy, and use the Lsm1-7 complex to promote viral RNA replication and translation. (Mas *et al.*, 2006; Narayanan and Makino, 2013; Scheller *et al.*, 2009).Brome mosaic virus uses Lsm1-7 complex together with the decapping activators Pat1p and Dhh1 (DDX6) to recruit the viral RNA to the replication complex (Mas *et al.*, 2006). Vaccinia intermediate and late mRNAs are characterized by the presence of a poly(A) track localized at the 5´ UTR of the viral mRNAs, and the Lsm1-7 complex is able to interact with this 5´ poly(A) sequence. This interaction leads to a stabilization of the mRNAs due to the inhibition of both the decapping and the exosome degradation routes,

and it has been proposed as a mechanism employed by vaccinia to protect late viral mRNAs from D9 and D10 decapping activity (Bergman *et al.*, 2007). HCV hijacks the P-Body and stress granules components DDX6, Lsm1, Xrn1, G3BP and PABP1, and redistributes them to the HCV production factory around lipid droplets. DDX6, Lsm1 and PABP1 are essential to HCV replication, since the inhibition of their expression by both specific shRNAs and siRNAs causes a reduction on HCV RNA levels (Ariumi *et al.*, 2011). Recently, it has been described that Lsm1 contributes to the activation of HCV IRES-mediated translation, but it is not required to stimulate viral replication (Roberts *et al.*, 2014) (Figure 6).

1.3.2 Viral mechanisms to promote mRNA decay

Additionally to the strategies mentioned above, during infection viruses can alter the distribution and quantity of cellular mRNAs by modifying cellular RNA metabolism functions. In the case of herpes simplex virus-1 (HSV-1), the splicing machinery is inhibited leading to an accumulation of cellular mRNAs at the nucleus of infected cells (Sandri-Goldin, 2011), while in the case of AdV, VSV, poliovirus or influenza virus host mRNAs export from the nucleus to the cytoplasm is impaired by targeting the nuclear pore complex (Blanchette *et al.*, 2008; Castello *et al.*, 2009a; Park *et al.*, 2008; Satterly *et al.*, 2007; von Kobbe *et al.*, 2000). In this regard, adenovirus early proteins E4orf6 and E1B55K perform several functions, and, among them, they stimulate nuclear export of late viral mRNAs and block nuclear export of the majority of cellular mRNAs (Blanchette *et al.*, 2008). VSV genome encodes for the matrix protein M, which directly interacts with the nucleoporin Nup98 and the mRNA export factor 1 (Rae1) and blocks mRNA nuclear export. M viral protein localizes at the nuclear envelope or rim, and it is dependent on Nup98 to carry out the inhibition of the nuclear transport, as demonstrated by VSV infection in $Nup98^{-/-}$ mouse cells (Quan *et al.*, 2014; von Kobbe *et al.*, 2000). Poliovirus infection also impairs mRNA nucleus-cytoplasm transport. The viral 2A protease interferes with the RNA transport from the nucleus to the cytoplasm, causing an accumulation of poly(A) RNA at the nucleus. This process is concomitant with the proteolysis and redistribution of the components of the nuclear pore complex Nup98, Nup153 and Nup62 (Castello *et al.*, 2009a). Influenza virus also hijacks nuclear mRNA export. Viral NS1 protein interacts with several components of the nuclear pore complex, and its expression in cells causes nuclear retention of poly(A) RNAs (Satterly *et al.*, 2007). In other cases, viruses stimulate directly mRNA degradation as occurs in alpha- and gamma-herpesvirus, severe acute respiratory syndrome coronavirus (SARS-CoV) and influenza virus, which encode to viral ribonucleases that induce cellular host shutoff by promoting mRNA degradation (Covarrubias *et al.*, 2011; Feng *et al.*, 2005; Huang *et al.*, 2011; Jagger *et al.*, 2012; Richner *et al.*, 2011). Alpha-herpesviruses, such as HSV-1, encode for an endonuclease termed virion host shutoff protein (vhs), which cleavages mRNAs preferentially at an unstructured region of the capped mRNAs (Shiflett and Read, 2013). Vhs degrades both host mRNAs and viral mRNAs in order to eliminate the first and to ensure the temporal expression of the latter (Feng *et al.*, 2005; Taddeo *et al.*, 2013). Gamma-herpesviruses genome also encodes for a viral endonuclease, known as host shutoff factor SOX in Kaposi´s sarcoma-associated herpesvirus (KSHV), muSOX in murine gamma-

herpesvirus 68 and BGLF5 in Epstein-Barr virus (EBV). This endonuclease cleavages cellular and viral mRNAs anywhere along the RNA body, which subsequently undergoes degradation by the cellular exonuclease Xrn1 (Covarrubias *et al.*, 2011; Richner *et al.*, 2011). SARS coronavirus non-structural protein 1 (nsp1) protein also promotes cellular mRNA degradation, but using a novel mechanism that inhibits translation initiation and promotes the endonucleolytic cut of cellular mRNAs by recruitment of a cellular endonuclease, which has not been identified, so far. Interestingly, SARS-CoV mRNAs possess a 5´leader sequence that makes them resilient to nsp1 activity (Huang *et al.*, 2011). Viral RNA-dependent RNA polymerase complex-X (PA-X) protein of influenza virus is another mRNA endonuclease that increases cellular mRNAs degradation, but seems not to affect viral protein synthesis (Jagger *et al.*, 2012). On the other hand, cap-snatching is also a mechanism used by some viruses to promote cellular mRNAs degradation, since uncapped cellular mRNAs can enter in the cellular 5´-3´degradation pathway (Figure 6).

1.3.2.1 Viral decapping enzymes

Only two families of viruses have been described to use direct decapping as part of their strategy to inhibit cellular translation and to promote viral protein synthesis: vaccinia virus, which possesses two viral decapping enzymes D9 and D10, and the yeast double-stranded L-A virus, which uses a specific mechanism of decapping related to cap-snatching that has been described previously in this section (Abernathy and Glaunsinger, 2015).

1.3.2.1.1 D9 and D10 decapping enzymes of vaccinia virus

As commented in previous sections, vaccinia genome encodes for two decapping enzymes, D9 and D10, which present approximately 25% of sequence similarity. Both proteins possess a Nudix motif, which, as we have described in section 1.2.1.1, is related to RNA decapping (Parrish and Moss, 2007; Parrish *et al.*, 2007).

In vitro assays demonstrated that both D9 and D10 recombinant proteins exhibit decapping activity, being able to hydrolase the 5´RNA cap structure and release m^7GDP and 5´-monophosphate RNA as products. In both cases, single site mutations of the conserved glutamic residues (E125Q, E129Q, and E130Q in D9 and E141Q, E144Q and E1145Q in D10) in the Nudix motif cause a loss of the decapping activity, indicating that the Nudix motif is essential for the catalysis (Parrish and Moss, 2007; Parrish *et al.*, 2007). Although closely related, D9 and D10 present some differences between them. Both proteins require a RNA body attached to the cap structure to carry out the hydrolysis reaction. However, D9 needs longer capped RNAs for optimal activity: D10 efficiently decapps RNAs of 24 nt, while D9 requires at least a 39 nt RNA body displaying better decapping activity in longer RNAs. Moreover, D9 has stronger sensitivity to uncapped RNAs than D10. On the other hand, D10 is intensely inhibited by methylated cap analogues, showing more affinity for m^7GpppG than for m^7GpppA; while D9 is only weakly inhibited by this kind of substrates. Neither D9 nor

D10 are inhibited by non-methylated cap analogues (Parrish and Moss, 2007; Parrish *et al.*, 2007). Additionally, D9 possesses an early promoter, while D10 possesses a late promoter (Shors *et al.*, 1999).

By using cotransfection assays, *Shors et al*. demonstrated that D9 and D10 endorse repression of *lacZ* reporter gene expression under control of both intermediate and late viral promoters (Shors *et al.*, 1999). Moreover, both D9 and D10 proteins cause a repression of *lacZ* expression when it was under control of the T7 promoter, but not when it was under control of the encephalomyocarditis virus (ECMV) leader sequence. These results indicate that D9 and D10 effect is not specific for viral promoters, and also that only capped mRNAs are targeted by these proteins (Shors *et al.*, 1999). Vaccinia virus strains that possess an extra copy of D9 or D10 cause a decrease in viral protein synthesis at late times post infection (12 hpi to D10 and 20 hpi to D9), and a reduction on the late F17 viral mRNA levels. Moreover, overexpression of D10 causes a severe decrease on vaccinia viral production (Shors *et al.*, 1999).

Further analysis of D10 and D9 function has been performed by generation of D10 and D9 vaccinia deletion mutants (vΔD10 and vΔD9) (Liu *et al.*, 2014; Parrish and Moss, 2006). Infection of vΔD10 on BS-C-1 cells causes a delay in both early and late viral transcription initiation (Parrish and Moss, 2006) Furthermore, viral early and late mRNAs, together with cellular actin mRNA, persist longer in vΔD10 infected cells, a phenomenon which is concomitant to a prolonged synthesis of cellular and viral early proteins (Parrish and Moss, 2006). Additional characterization of these proteins has been achieved by generation of two alternative inactive D10 viruses: the first possesses site mutations in the catalytic Nudix domain (vD10mu), while the second one harbours STOP codons that prevent D10 expression (vD10stop). Infections with both viruses have a similar but less pronounced effect in cellular and viral mRNA levels compared to ΔD10 infection (Liu *et al.*, 2014). Despite this moderate effect on *in vitro* experiments, both vD10mu and vD10stop viruses cause a more attenuated infection in *in vivo*, suggesting that this decapping enzyme may help to limit antiviral responses by accelerating host mRNA degradation during poxvirus infection (Liu *et al.*, 2014). Due to the evidences mentioned above, it has been described that both D9 and D10 enzymes are involved both in the degradation of cellular mRNA and in the temporal expression of viral mRNA (Parrish and Moss, 2007).

Recently, vaccinia D9 and D10 double catalytic mutant has been successfully achieved (Liu *et al.*, 2015). This double mutant (vD9muD10mu) is not able to replicate in human and monkey cell lines, but effectively replicates in mouse cells. The infection of this double mutant virus in the non-permissive cell lines is characterised by a pronounced decrease in the amount of cellular and late viral mRNAs and in the protein synthesis, concomitantly with an increase in the double-stranded RNA (dsRNA) levels. dsRNA production is a common feature among RNA and DNA viruses, and a its accumulation triggers the activation of the host anti-viral defences, such as protein kinase R (PKR) and the RNaseL (Onomoto *et al.*, 2014; Perdiguero and Esteban, 2009). Activation of PKR causes the phosphorylation of eIF2α and translation repression, while the activation of RNaseL promotes RNA degradation. Both processes explain the decreased levels of mRNA in vD9muD10mu infected cells. These results indicate that vaccinia decapping enzymes are not only involved in

decay of host and viral mRNAs, but also in the degradation of dsRNAs to avoid cellular anti-viral defences (Liu *et al.*, 2015).

1.3.2.1.2 ASFV *in vitro* decapping enzyme: g5Rp

As commented on section 1.1.5, ASFV genome encodes for an enzyme that possesses a Nudix hydrolase motif, g5Rp (or pD250R, depending on the viral strain). *Cartwright et al.* demonstrated that purified histidine-tagged g5Rp from *E.coli* hydrolases *in vitro* a wide range of guanine and adenine nucleoside 5´-triphosphates (GTP and ATP) and dinucleoside polyphosphates (Gp3G, Gp4G, Gp5G and Ap3A, Ap4A and Ap5A), exhibiting higher substrate efficiency with diphosphoinositol pentakisphosphate (PP-InsP5). In these conditions, g5Rp was not able to hydrolyse cap analogues such as m^7GpppG, m^7GpppC, m^7GpppA, m^7GppGm^7G or m^7GpppGm^7G (Cartwright *et al.*, 2002). On a second study, *Parrish et al* analysed g5R mRNA decapping activity *in vitro,* and demonstrated that recombinant MBP-g5Rp is able to hydrolyse cap analogues when they are attached to a RNA body, releasing m^7GDP as a product (Parrish *et al.*, 2009). The Nudix motif of the protein is essential for the catalysis, because single site mutation of the conserved residues E147, E150 and E151 causes a loss of decapping activity. As demonstrated by electrophoretic mobility shift assay (EMSA), g5Rp is able to directly interact with the RNA body. Moreover, g5Rp activity is strongly inhibited by uncapped RNAs, but is not affected by cap analogues or methylated nucleotides, suggesting that g5Rp preferentially recognise the RNA moiety on the substrate.

Nevertheless, the role of this protein *in vivo* is still unknown. g5Rp high homology (at least for the Nudix domain) with Dcp2 and the fact that this protein possesses decapping activity *in vitro* suggest its involvement in mRNA regulation. Therefore, this viral enzyme represents a good candidate to be the viral factor involved in the degradation of the cellular mRNAs (contributing in the cellular shutoff), and in the temporal regulation of viral mRNAs.

In this Thesis, we have worked in deciphering the role of g5R in vivo. Both Ba71V D250R and Malawi g5R ORFs has been approached. However, by the time this Thesis started, only the protein form Malawi strain was characterized *in vitro*. Due to this fact, we adopted Malawi nomenclature, although in the experiments in which Ba71V-pD250R was studied, this last nomenclature should be used.

Objectives

The main objective of this Thesis is to study the mechanism displayed by African Swine Fever Virus to manipulate RNA metabolism and cellular translation resources, in order to decipher how the virus impairs cellular protein synthesis while promotes temporal viral gene expression.

To achieve this goal, we set the following specific objectives:

1. To analyse mRNA status in ASFV infection. To achieve this, we focus, firstly, on the analysis of mRNA levels, and, secondly, on the study of the distribution of mRNA in ASFV-infected cells.
2. To characterize the putative ASFV decapping enzyme g5Rp (also known as pD250R in Ba71V strain), due to the fact that it is a good candidate to function as an mRNA regulator during the infection.
3. To study the role of g5R protein in the cellular shutoff and in the viral temporal gene expression in the context of the infection. In this regard, we have analysed both the g5Rp effect on ASFV infection, but also the proteins interacting with g5Rp to accomplish or modulate its function.
4. To explore cellular components involved in the regulation of both cellular and viral protein synthesis during ASFV infection. We have focused on the analysis of the components of the cellular decapping machinery, specially P-Bodies and the cap structure, and on the study of ASFV-mediated control of the factors of the translational cellular machinery and of the cellular organelles as ribosomes.

Materials and Methods

3.1 CELL LINES

Vero (CCL 81), COS-7 (CLR 1650) (epithelial and fibroblast kidney cells from African green monkey, respectively) and HeLa (ATTC CCL-2, epithelial cells of human cervix) cells were obtained from the *American Type Culture Collection* (ATTC). HeLa GFP stable cell lines were obtained, as detailed below, from HeLa cell line. All the three lines were cultivated in Dulbecco's Modified Eagle's medium (DMEM) (Dulbecco and Freeman, 1959) supplemented with 5% of fetal bovine serum (FBS) and maintained at 37ºC under a controlled 7% CO_2 atmosphere saturated with water vapour. Medium was supplemented with 2 mM L-glutamine, 0.4 mM nonessential amino acids and 0.05 mg/ml gentamicin for Vero and COS-7 cells and 0.1mg/ml penicillin plus 10^2 U streptavidin for HeLa cells.

3.2 VIRUS STRAINS

Infections were carried out with the African Swine Fever Virus (ASFV) strain Ba71V (Vero adapted Ba71 strain) (Enjuanes *et al.*, 1976). Virus preparations were obtained from cells cultured in bottles infected with BA71V with multiplicity of infection (M.O.I) 0.2 plaque former units (pfu) per cell. 72 hour post infection (hpi), cells were harvested and centrifuged at 3000 rpm for 15 minutes to eliminate cellular debris. Supernatant was clarified by overnight (16 hours) 7000 rpm centrifugation at 4º C and finally pellets were resuspended in 2% FBS complete medium, sonicated and viral particle were stored at -80º C. Ba71V was titrated by plaque assay in Vero cells as described before (Enjuanes *et al.*, 1976).

3.3 REACTIVES

3.3.1 Buffers and reactives

The following solutions were used: Phosphate buffered saline (PBS), Tris buffered solution (TBS), Tris Acetate EDTA Solution (2 M Tris base, 5.7 % glacial acetic acid and EDTA (pH 8) (TAE 50X)), ethylenediaminetetraacetic acid (EDTA), sodium dodecyl sulfate (SDS), Phenol: Chloroform: Isoamil Alcohol pH 8 (PCI) produced by the mixture of phenol pH 8 (Sigma) Chloroform (Merck) and Isoamil Alcohol (Merck) in 25:24:1 rate; Chloroform : Isoamil Alcohol (CI 24:1). Cytosine arabinose (AraC) was used a final concentration of 40µg/ml, and Cicloheximide(CHX) was used at 100 µg/ml.

3.3.2 Antibodies and Oligonucleotide probes

Antibodies used in this project are detailed in Table 1

Antigen	Antibody	Specie	Technique	Working Dilution	Origin
Human influenza hemagglutinin	HA	mouse	FACS Immunofluorescence	1/100 1/500	Roche 11867423001
Green Fluorescent Protein	GFP	mouse	Western blot	1/1000	Roche 1181460001
Dcp1A (C-terminal)	Dcp1	rabbit	Western Blot Immunoprecipitation Immunofluorescence	1/ 1000 1/200 1/100	Sigma Aldrich D5444
Edc4 (S-15)	Edc4	goat	Immunoprecipitation	1/100	Santa Cruz sc- 137444
USP10 (156-170)	USP10	rabbit	Western blot Immunofluorescence	1/1000 1/100	Sigma Aldrich U7384
C-terminus of eukaryotic acidic ribosomal P-proteins P0, P1 and P2	3BH5	mouse	Western blot	1/10	(Vilella *et al.*, 1991)
C-terminus of calnexin	calnexin	rabbit	Immunofluorescence	1/200	StressMarq SPC-108B
β-actin	β-actin	goat	Western blot	1/1000	Santa Cruz Biotechnology sc-1616
Tubulin	Tubulin	mouse	Western blot	1/250	Sigma-Aldrich T9026-100UL
Cap structure of mRNA (clon H-20)	Cap	mouse	Immunofluorescence Immunoprecipitation	1/100	Synaptic Systems 201 001
Viral protein g5R	g5Rp	rabbit	Western blot	1/1000	Generated in this thesis
Viral protein p32	p32	mouse	Western blot FACS Immunofluorescence	1/1000 1/500 1/3000	(Prados *et al.*, 1993)
Viral protein p72	p72	rabbit	Western blot	1/1000	Generated at our laboratory
Viral protein p72	p72 17LD3	mouse	FACS Immunofluorescence	1/100 1/300	Ingenasa (Sanz *et al.*, 1985)
Viral protein CD2v	CD2v	rabbit	Immunofluorescence	1/750	(Galindo *et al.*, 2000)
Inducible proteins of ASFV	ASFV	rabbit	Western blot	1/4000	Generated at our laboratory (del Val and Vinuela, 1987)
Rat IgG	Alexa fluor-488	donkey	FACS Immunofluorescence	1/500 1/500	Invitrogen A-21208
Mouse IgG	Alexa fluor-488	donkey	FACS Immunofluorescence	1/500 1/500	Invitrogen A-21202
Mouse IgG	Alexa fluor-555	donkey	Immunofluorescence	1/500	Invitrogen A-31570
Mouse IgG	Alexa fluor-647	donkey	FACS Immunofluorescence	1/500 1/500	Invitrogen A-31571
Rabbit IgG	Alexa fluor-555	donkey	Immunofluorescence	1/500	Invitrogen A-31572
Rabbit IgG	Alexa fluor-647	donkey	FACS Immunofluorescence	1/500 1/500	Invitrogen A-31573
Goat IgG	Alexa fluor-555	donkey	Immunofluorescence	1/500	Invitrogen A-21432
Goat IgG	Alexa fluor-647	donkey	Immunofluorescence	1/500	Invitrogen A-21447
Mouse IgG	Mouse peroxidase		Western blot	1/10000	Amersham Biosciences
Rabbit IgG	Rabbit peroxidase		Western blot	1/4000	Amersham Biosciences
Goat IgG	Goat peroxidase		Western blot	1/20000	Sigma Aldrich

Table 1. Antibodies used in this Thesis.
Dcp1A: Decapping enzyme 1A; Edc4: Enhancer of decapping-4; ASFV: African Swine Fever Virus; IgG: Immunoglobulin G

Oligonucleotide probes used are detailed in Table 2

Target	Probe	Sequence	Working concentration	Technique	Origin
Poly(A) tail	Oligo d(T)	TTTTT(n=50)TT-FitC	2.5 mM	RT	BioNova
Poly(A) tail	Oligo d(T) - FITC	TTTTT(n=50)TT-FitC	1 µM	FISH	Sigma Aldrich
Poly(A) tail	Oligo d(T) - Texas Red	TTTTT(n=50)TT-Texas Red	1 µM	FISH Dual fluorescence method	Invitrogen
Viral A224L mRNA	A224L mRNA	GCTTTGATTTCGTGCATCTATGGAGC	1 µM	FISH	Invitrogen

Table 2. Oligonucleotide probes used in this Thesis.
FISH: Fluorescence *In Situ* Hybridization; RT: Retrotranscription

3.4 CLONING PROCESS

During this study, several genes have been cloned in different plasmids to express both wild type (wt) and mutated proteins in eukaryotic or bacterial systems, to generate stable cell lines and to obtain viral mutated strains. In general, the gene of interest was amplified by PCR using specific probes (Table 2) and viral ASFV genome or certain vectors as DNA template. The cloning process of these products required the usage of the following techniques:

3.4.1 Electrophoretic separation of DNA products

PCR products were isolated with 0.7%-1% agarose gels. Gels were made in 1 x TAE buffer and percentage of agarose varied depending on amplicon size. For separation, PCR products were mixed with loading buffer (0.25 % Bromophenol Blue, 50 % glycerol and 1 mM EDTA) and electrophoreticaly separated in agarose gels for 1 hour (80 – 100 V).

3.4.2 DNA purification from agarose gels

Products of interest were sliced from agarose gel using an U.V transiluminator and a scalpel. In order to extract the products from the matrix, we used the *Wizard SV gel and PCR Clean-UP System* (Promega) following manufacturer's instructions. After purification, products were quantified in a Nanodrop ND-1000 (Thermo Scientific).

3.4.3 Enzyme digestion

After purification, amplicon and vector were digested with specific restriction enzymes following manufacturer´s instructions to each enzyme (NEB). Digestion time was modified depending on product size and DNA ends.

3.4.4 Ligation

Purified vector and insert were ligated overnight at 16º C with T4 ligase (Roche) following manufacturer's protocol. Ligation rate varied depending on quantity and size products. In general, we used plasmid: insert rate of 1: 3 or 1: 10.

3.5 PRIMERS

Primers used this thesis are detailed in Table 3

Name	Sequence	Description	Application
g5R FW g5R RV	ATGCAGCTTAAAACGTCTATTGG CTAGTGCTTATATCGTAAATAGT	g5R mRNA detection primers	PCR
p32 FW p32 RV	CCGAGCCCTCATCAGAGGAACC GGGGTTCCATGAATGGTTTGG	p32 mRNA detection primers	PCR
p72 FW p72 RV	CGCGGATCCATGGCATCAGGAGGAG CGCGAGATCTAGCTGACCATGGGCC	p72 mRNA detection primers	PCR
β actin FW β actin RV	GAGAAGATGACCCAGATCATG TCAGGAGGAGCAATGATCTTG	β actin mRNA detection primers	PCR
qA238L FW qA238L RV	GCAGATCCGACTCAAAAAGACT ACTCCATATTTCCTGTAAAGACTGC	A238L mRNA detection primers	quantitaive PCR
q p32 FW q p32 RV	CCGAGCCCTCATCAGAGGAACC GGGGTTCCATGAATGGTTTGG	p32 mRNA detection primers	quantitaive PCR
qA224L FW qA224L RV	AAGCACCCTTTACAGGTGCATGGC TCCTATAATGCCCAAGGTTGCACGG	A224L mRNA detection primers	quantitaive PCR
q p72 FW q p72 RV	CCCGAGAACTCTCACAATATCC CGTTGCGTCCGTAATAGGAG	p72 mRNA detection primers	quantitaive PCR
q g5R FW q g5R RV	AATACCAAAAATTTAGGAAAAATTGG GCCCTTTGCTTGGTTGATTA	g5R mRNA detection primers	quantitaive PCR
qBIRC2 FW qBIRC2 RV	GCTGACCCACCAATTATTCATTTTGG CACACACGTCAACTGTTGAAAGAGAGC	BIRC2 mRNA detection primers	quantitaive PCR
q eIF4A1 FW q eIF4A1 RV	AATCCGCATCTTGGTGAAAC CCCTCTCCACTGCCACAA	eIF4A1 mRNA detection primers	quantitaive PCR
q eIF4E FW q eIF4E RV	CAGCAGAGACGAAGTGACCTT ACATTAACAACAGCGCCACA	eIF4E mRNA detection primers	quantitaive PCR
q β actin FW q β actin RV	AGGTCATCACCATTGGCAAC CGTGGATGCCACAGGACT	β actin mRNA detection primers	quantitaive PCR
18S M.m FW 18S M. m RV	GGAGAGGGAGCCTGAGAAAC TCGGGAGTGGGTAATTTGC	Macaca mulata 18S rRNA detection primers	quantitaive PCR
18S H.S FW 18S H.S RV	GCAATTATTCCCCATGAACG GGGACTTAATCAACGCAAGC	Hommo sapiens 18S rRNA detection primers	quantitaive PCR
BamHI g5R FW EcoRI g5R RV	GGGGGATCCATGGATACTGCCATGCAGCTT GGGGAATTC**CTACTA**GTGCTTATATCGTAA	g5R cloning in pGEX-2T	GST-g5R production
EcoRI g5R FW BamHI g5R RV	GGGGAATTCATGGATACTGCCATGCAGCTT GGGGGGGGATCC**CTACTA**GTGCTTATATCGTAA	g5R cloning in pEGFP-C2	GFP-5R production
KpnI GFP FW	GGGGGTAACATGGTGAGCAAGGGCGAGGAG	GFP-g5R cloning in pCDANFRT/TO	Stable cell line generation
g5RmutREEGG FW g5RmutREEGG RV	TCGGACCTTACCTGTGCCATAGGGGGGTTTGAAGAAGAAACCGGGATT AATCCCGGTTTCTTCTTCAAACCCCCCTATGGCACAGGTAAGGTCCGA	mutation R146G/E147G (REGG) g5R Nudix domain	Punctual mutation
g5RmutEEQQ FW g5RmutEEQQ RV	TGTGCCATACGGGAGTTTGAACAACAAACCGGGATTACCCGCGAATAT ATATTCGCGGGTAATCCCGGTTTGTTGTTCAAACTCCCGTATGGCACA	mutation E150Q/E151Q (EEQQ) g5R Nudix doma	Punctual mutation
F1 KpnI FW F1 SmaI RV	GGGGGGGGTAACAGGTGGTCAAATTTGCTATTA GGGCCCGGGCTGTAACGTTTTTGAACCAGA	up stream flanking g5R sequence	g5R ASFV deletion mutant
F2 PstI FW F2 HindIII RV	GGGCTGCAGGCTGTACGTTTTATTAGCAAA GGGAAGCTTCAGATGTTGAGTGAAGAGGAA	down stream flanking g5R sequence	g5R ASFV deletion mutant

Name	Sequence	Description	Application
Nexo GFP g5R FW	TCGAGCTCAAGCTTCGAATTCATGGATACTGCCATGC AGCTT	pEGFP / g5R	Stable cell line generation
Nexo GFP g5R RV	AAGCTGCATGGCAGTATCCATGAATTCGAAGCTTGA GCTCGA		
BamHI g5R Nterm RV	GGGGGATCC**CTACTA**AATTTCCCATAGAAGTGT	BamH1/ **STOP codons** / g5R upstream Nudix	Stable cell line generation
Nexo GFP g5R Cterm FW	AGCTCAAGCTTCGAATTCACCCGCGAATATTACCAG	pEGFP / g5R down stream Nudix	Stable cell line generation
Nexo GFP g5R Cterm RV	AATCTGGTAATATTCGCGGGTGAATTCGAAGCTTGA GCTCGA		
Nexo g5R N term C term FW	TCAGAAACACTTCTATGGGAAATTACCCGCGAATATT ACCAGATTCTC	g5R upstream Nudix / g5R down stream Nudix	Stable cell line generation
Nexo g5R N term C term RV	AATCTGGTAATATTCGCGGGTAATTTCCCATAGAAGT GTTTCC	g5R down stream Nudix / g5R up stream Nudix	
KpnI prom_g5R FW	GCGGGTACCTGAATATCTTGTGAACACAGC	g5R up stream sequence containing viral promoter	cloning promoter and g5R in pHA-2
BamHI noSTOP_g5R RV	GCGGGATCCGTGCTTATATCGTAAATAGTTTTTAATA AA	g5R 3´sequence without stop codons	

Table 3. Primers used in this Thesis
FW: Forward sequence, RV: reverse sequence. All primer sequences are shown on its 5´- 3´orientation.

3.6 PLASMIDS

Plasmids generated and used, except these mentioned as gift, in this study are:

- **pHA-2**: eukaryotic expression plasmid designed to produce protein of interest tagged to HA epitope at its C-terminal domain. This vector was obtained after cloning HA protein into pCDNA 3.1 vector and was a kind gift from Dr. Ricardo Madrid (BioAssays, Madrid, Spain).
- **promg5R-HA**: eukaryotic expression vector that contains Ba71V g5R gene (D250R) fused to HA sequence. Expression of g5R-HA protein is controlled by g5R viral promoter, so this vector allows g5R-HA protein expression only in infected ASFV cells. To generate this vector, g5R sequence was amplified by PCR with ASFV genome as template using KpnI_promg5R FW and BamHI_noSTOP_g5R RV primers (Table 3). g5R sequence was digested with *KpnI/BamHI* and ligated to pHA-2.
- **pCDNAg5R:** eukaryotic expression vector that contains g5R gene from Malawi Lil 20/1 strain. This plasmid was a kind gift of Dr. Linda Dixon (The Pirbright Institute, Pirbright, United Kingdom).
- **pEGFP-C2**: eukaryotic expression plasmid that express the enhanced Green Fluorescent Protein (eGFP) under the Cytomegalovirus (CMV) promoter (Invitrogen). This vector contains a polylinker at GFP C-teminal domain, which makes possible to generate GFP recombinant proteins. It has been used as template to generate GFP-gene of interest amplicons and as a transfection control.
- **pCFP-C2**: eukaryotic expression plasmid that express the Cyan Fluorescent Protein (CFP) under the CMV promoter. This vector contains a polylinker at CFP C-teminal domain, which makes possible to generate CFP recombinant proteins.

- **pCFP g5R wt, pCFP g5R EEQQ and pCFP g5R REGG:** Ba71V g5R gene (D250R) was cloned into pCFP-C2 vector to generate pCFP-g5R wild type (wt) construction using EcoRI g5R FW and BamHI g5R RV primers (Table 3) and ASFV genome as DNA template. Product and vector were digested with *BamHI/EcoRI* enzymes and ligated overnight (O/N). To generate the two punctual mutants of the g5R catalytic domain (pCFP g5R EEQQ and pCFP g5R REGG) we used g5RmutREGG (FW and RV) and g5RmutEEQQ (FW and RV) primers and *Pfu turbo* (Agilent Technologies) and *Dpn1* (Stratagen). Single-site mutation method is described in detail in section 3.8.
- **pOG44**: vector that expresses Flp recombinase protein, an enzyme that enables specific gene insertion on Flp Recombination Target (FRT) sites. When co- transfected with pCDNA5 FRT/TO vector containing the gene of interest, mediates integration of this gene on Flp in TREx cell lines genome (Invitrogen). This plasmid was used to generate HeLa GFP stable cell lines and was kindly gifted from Dr. Fernando Rodriguez Pascual (Centro de Biología Molecular "Severo Ochoa", Madrid, Spain).
- **pCDNA5/FRT/TO**: Inducible expression vector aimed for use with the Flp-In T-REx System (Invitrogen). When cotransfected with pOG44 plasmid into Flp-In-TREx mammalian host cell line, the pCDNA5/FRT/TO containing the gene of interest is integrated in the cellular genome in an Flp recombinase dependent manner. The plasmid contains CMV promoter fussed to TetO2 promoter, allowing the expression of the protein of interest only in presence of tetracycline. pCDNA5/FRT/TO was kindly gifted by Dr. Fernando Rodriguez Pascual (Centro de Biología Molecular "Severo Ochoa", Madrid, Spain).
- **pCDNA5/FRT/TO GFP-g5R wt**: pCDNA5/FRT/TO containing GFP-g5R wt sequence. The GFP-g5R insert was obtained by fusion PCR using KpnI GFP FW, nexo GFPg5R FW and RV and BamHI g5R RV as primers; and pEGFP-C2 and pCFP g5R wt as DNA templates for eGFP and g5R wt sequences, respectively (Figure 7).
- **pCDNA5/FRT/TO GFP-g5R EEQQ and pCDNA5/FRT/TO GFP-g5R REGG**: pCDNA5/FRT/TO containing GFP-g5R EEQQ and REGG catalytic site mutant sequences. These mutations affect the conserved amino acids at g5R catalytic domain (Nudix motif): in REGG mutation arginine 146 and glutamic acid 147 were substituted by glycine (R146G/E147G); EEQQ mutation is a substitution of glutamic acids 150 and 151 by two glutamines (E150Q/E151Q). Both mutations have been described to produce a loss of catalytic activity (Parrish *et al.*, 2009). GFP-g5R EEQQ and REGG inserts were obtained by fusion PCR using KpnI GFP FW, nexo GFPg5R FW and RV, and BamHI g5R RV primers and pEGFP-C2 and pCFP g5R EEQQ or REGG as DNA templates (Figure 7).

- **pCDNA5/FRT/TO GFP-g5R N-terminal**: pCDNA5/FRT/TO containing GFP fused to g5R N-terminal sequence, defined as the sequence up-stream of Nudix domain. GFP-g5R N-terminal insert was obtained by fusion PCR using KpnI GFP FW, nexo GFPg5R FW and RV, and BamHI g5R N-term RV primers and pEGFP-C2 and pCFP g5R wt as DNA templates (Figure 7).
- **pCDNA5/FRT/TO GFP-g5R C-terminal:** pCDNA5/FRT/TO containing GFP fused to g5R C-terminal sequence, defined as the sequence down-stream of Nudix domain. GFP-g5R C-terminal insert was obtained by fusion PCR using KpnI GFP FW, nexo GFPg5RCterm FW and RV, and BamHI g5R RV primers and pEGFP-C2 and pCFP g5R wt as DNA templates (Figure 7).
- **pCDNA5/FRT/TO GFP-g5R ΔNudix**: pcDNA5/FR/TO containing GFP sequence tagged to a g5R version that completely lacks Nudix domain (ΔNudix). GFP-g5R ΔNudix insert was obtained by two fusion PCR: Inserts needed were obtained with KpnI GFP FW, nexo GFPg5R Fw and RV, g5RNtermCterm FW and RV and BamHI g5R RV primers. pEGFP-C2 and pCFP g5Rwt were used as DNA templates. First fusion PCR generated GFP g5R N-terminal insert; and second fusion PCR produced GFP-g5R ΔNudix (Figure 7).
- **pGEX-2T**: bacterial GST expression vector. This vector contains a polylinker at GST 3´end which make possible generate GST recombinant proteins (GE Healthcare).
- **pGEX-g5R wt**. bacterial expression plasmid that contain GST-g5R wt sequence. This plasmid was obtained by cloning g5R gene (Malawi Lil 20/1) in the pGEX-2T vector. For that, BamHI g5Rwt FW and EcoRI g5Rwt RV primers were used to amplify g5R gene from pCDNAg5R. After digestion with *BamHI/EcoRI*, g5R sequence was inserted in pGEX-2T plasmid. pGEX-g5R wt was transformed in *E.coli*.to produce GST-g5R wt protein, which was used to generate specific anti g5R serum and to perform pulldown assays.
- **p72GAL10T:** plasmid used to obtain deletion ASFV mutants. This vector was generated by cloning *LacZ* operon under viral p72 promoter into pUC118 plasmid (Garcia *et al.*, 1995). 10T termination ASFV signal was added at the end of LacZ to ensure the end of transcription. At both sides of the operon, enzyme restriction sites were included to clone the sequences that flank the deletion gene (F1 and F2).
- **p72Δg5RGAL10T:** p72GAL10T plasmid that contains the Ba71V g5R flanking sequences F1 and F2. Both sequences were amplified from ASFV genome using F1 KpnI FW, F1 SmaI RV, F2 PstI FW and F2 HindIII RV primers, respectively. After digestion with *KpnI/SmaI* or *PstI/HindIII*, Fi and F2 inserts were successively cloned into p72GAL10T plasmid. We used this vector to the generation of ASFV g5R deletion mutant, process detailed in following sections.

- **p72ΔEP153RGAL10T:** p72GAL10T plasmid which contains Ba71V EP153R F1 and F2 sequences. This plasmid was generated as described previously (Galindo *et al.*, 2000). p72ΔEP153R GAL10T was used as positive control in ASFV g5R deletion mutant assays.
- **p71ΔCD2vGUS10T:** p72GUS10T plasmid which contains Ba71V EP402R (CD2v gene) F1 and F2 sequences. This plasmid was generated in our laboratory as described on section 3.13 but using p72BetaGUS10T as vector. In this case, *gusA* is the reporter gene. p72ΔCD2vGUS10T was used as positive control in ASFV g5R deletion mutant assays.
- **pZAB 11/7 42:** p72Gal10T plasmid containing eGFP-g5R wt fused protein under control of g5R viral promoter (Ba71V). This vector allows the expression of GFP-g5Rp wt only under ASFV infection and was generated by BioAssays.

3.7 POLIMERASE CHAIN REACTION (PCR)

3.7.1 Conventional PCR (PCR)

Conventional reactions of PCR were used to obtain inserts in cloning processes, to check ligation after the cloning and to determine levels of some genes during infection and after different treatments. PCR reactions were performed in a final volume of 25 or 50 µl, depending on the desired quantity of amplicon. For each reaction, we added 1x PCR reaction buffer for Taq DNA polymerase (10 mM Tris-HCl, 50 mM KCl, pH 8.3) supplied by the manufacturer (Roche), 2 mM $MgCL_2$, 0.2 mM of each dNTP´s, 250 ng of each primer, 0.5-1 ng template DNA and 1 U of Taq polimerase (Roche). Thermocycler programme differed depending on the product size and the melting Temperature of primers. When needed, PCR products were isolated in agarose gels and purified as described in section 3.4.2.

3.7.2 Fusion PCR

In order to obtain fused sequences of two genes, we performed fusion PCR. This technique was used to produce the GFP-g5R sequences for generating HeLa stable cell lines. Fusion PCR is performed in two steps that allow us to generate, in the first step, the two products that are going to be fused and, in the second step, the fused product (full length sequence). Along with the 5´ and 3´primers that amplify the full product and included the enzyme restriction sites, it is needed 5´and 3´ "nexo primers" that contain the 3´end of the first sequence and the 5´end of the second one (Figure 7).

In the first stage, we performed two separately PCRs: one using the 5´primer with the restriction site, the 3´nexo primer and the DNA template of the gene that is going to be in the 5´end of the final product; and another reaction with the 5´nexo primer, the 3´primer with the restriction site and the DNA template that encodes the protein that is going to be fused in the 3´end of the final product. Once both products have been amplified and purified by agarose gel, we performed the fusion PCR. In this case, we mixed products to be fused with all PCR reaction components except primers, and programmed

thermocycler with the following conditions: 1 cycle of 30 sec at 98ºC and 5 cycles with 3 temperatures (30 sec at 98º C, 30 sec at 56ºC, 45 sec at 72º C).

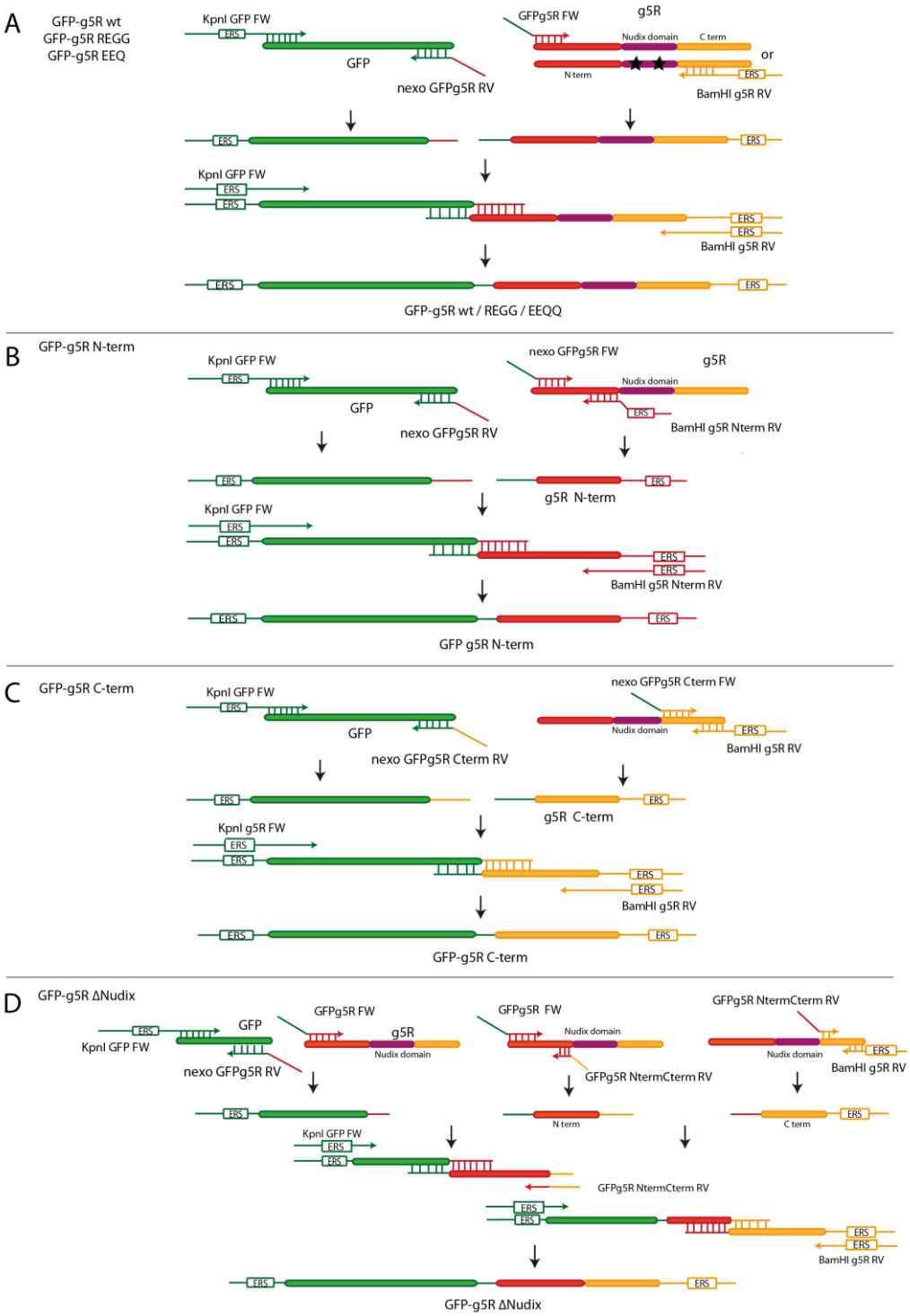

Figure 7. Schematic representation of generation of GFP-g5R products by fusion PCR

To generate the GFP-g5R sequences, fusion PCR was carried out, since it permits to fuse two sequences in a unique product by two PCR steps. In this case, we used pEGFP-C2 and pCFP g5R wt, EEQQ or REGG as templates for GFP gene and g5R wt, g5R EEQQ, g5R REGG, g5R N-terminal, C-terminal or ΔNudix sequences, respectively. Primers used in each case are detailed on Table 3. In general, FW and RV primers containing an enzyme restriction site (ERS) bind the 5´end of GFP and the 3´end of g5R wt, g5R REQQ or g5R REGG in **A)**, or the N-terminal or C-terminal domains of g5R in **B), C)** and **D)**. On the other hand, Nexo primers are designed to contain 21 nt of both the 3´and 5´sequences of the genes to be fuse, and hybridize with the 3´end of GFP sequence and the 5´end of the g5R sequences (g5R wt, g5R catalytic mutants or g5R domains). First PCR adds the ERS and the complementary 21 nt to each sequence, while second PCR permits fusion of both sequences by hybridization of complementary nucleotides and amplification of full product with FW and RV primers. Final product is directly cloned into the vector of interest after enzyme digestion. eGFP sequence is represented in green, g5R N-terminal in red, Nudix domain in purple and g5R C-terminal domain in yellow. FW: forward sequence; RV: reverse sequence; ERS: enzyme restriction site.

This PCR allows both products to merge and generate the full product. After that, we added to the reaction 5´and 3´primers containing the enzyme restriction sites, and performed a PCR to amplify full length product. After amplification, products were purified by agarose gel and cloned into pCDNA5/FRT/TO vector (Figure 7).

3.7.3 Quantitative PCR (qPCR)

To analyse and quantify the expression of different genes in the infection context and to determine which mRNA´s were bound to g5R protein, we achieved qPCR assays. We used MicroAmp® Optical 384-Well Reaction Plate with Barcode and Fast Syber Green Master Mix (Life Technologies) in all cases. To quantify expression of genes from cells extracts, we used 5 ng per reaction of cDNA as template (3 technical replicates for each sample); to quantify and analyse RNA bound to g5R proteins (detailed in further sections), we amplified all cDNA obtained after the IP. Total reaction volume was 10 µl in both cases. For each gene, we prepared a Master Mix with 1x Syber Green Master Mix and 0.25 mM forward and reverse primers. After preparing each reaction, plates were covered with MicroAmp Optical adhesive films (Life Technologies) and qPCR was run with the following conditions: 1 cycle of 20 sec at 95º and 40 cycles with two temperatures (10 sec at 95º C and 20 sec at 60ºC) in a ABI PRISM 7900HT SDS thermocycler (Applied Biosystems). The amplification cycles were followed by a dissociation cycle, which was used to determine the specificity of each product. Results were analysed with SDS program. In the case of RNA extracted from cells, values were normalized to 18S gene, while in RNA extracted from immunoprecipitated proteins, values were normalized to starting quantity of RNA (Input RNA). Experimental values are expressed as mean +/- standard deviation (S.D) or standard error of the mean (S.E.M), as indicated. Statistical analysis was performed by Student´s *t* test and statistical significance was set at $p<0.05$.

3.8 SINGLE SITE-MUTATION

With the purpose of generating two mutants of the catalytic domain of g5R (Parrish *et al.*, 2009), we used *Pfu turbo* (Agilent Technologies) and *DpnI* (Stratagen) enzymes. In general, 210 ng of vector containing the gen to be mutated were mixed with 1x Pfu reaction buffer (supplied by manufacturer), 10 mM dNTP´s mix and 5 U of *Pfu Turbo enzyme*. This master mix was split in three tubes: we added 1 µl of 5´primer containing the single mutation to first tube; 1 µl of 3´primer containing the single mutation to second tube, and 1 µl of H_2O as negative control in the last tube. These samples were subjected to 3 PCR cycles with following conditions: 1 min at 95º C, 1 min at 55º C and 8 min at 68º C. This process will ensure copy of 5´and 3´chains of vector using mutated primers as initiators. After that, we mixed tube 1 and 2 and prepared a second PCR: 1 cycle of 1 min at 95º C, 18 cycles with 1 min at 95º C, 1 min at 55º C and 8 min at 68º C, and a final cycle of 10 min at 68ºC. This PCR reaction amplifies both chains of vector containing mutation. Final product was treated with 10 U of *Dpn1 enzyme* for 2h at 37º C, which eliminates the original methylated

non-mutated plasmid. Resultant construction was transformed by electroporation into BL21 cells and amplified to DNA extraction. Mutations were validated by sequencing.

3.9 BACTERIAL MANIPULATION

3.9.1 Bacterial strains

In this Thesis, the following *E.coli* strains were used:

- **DH5α**: [F-, RecA1, hsdR17, (rK-, mK-), LacZY, argF, U169, supE44, thil, gyrA96, relA1]. This strain (Hanahan, 1983) was used for amplification and purification of all vectors except pCDNA5/FRT/TO plasmids, that were maintained in TOP10 cells and pCFP g5R EEQQ and pCFP g5R REGG, which were maintained in BL21 (DE3) cells.
- **TOP10 Chemically Competent cells**: [F- mcrA Δ(mrr-hsdRMS-mcrBC) Φ80lacZΔM15 Δ lacX74 recA1 araD139 Δ(araleu)7697 galU galK rpsL (StrR) endA1 nupG] This strain was used for propagation of pCDNA5/FRT/TO vectors (Invitrogen).
- **BL21 (DE3)**: [F- ompT hsdS(r_B- m_B-) gal dcm(DE3)]. Derived from BL21, this strain contains the RNA polymerase gene of T7 bacteriophage (Studier and Moffatt, 1986). Protein expression is induced by IPTG. This strain was used for expression and purification of recombinant GST-g5R protein and for amplification of pCDNA g5R EEQQ and pCDNA g5R REGG.

3.9.2 Bacteria culture and maintenance

All *E.coli* strains were cultivated in Luria-Bertani medium (LB) supplemented with Ampicillin or Kanamycin (both 100 µg/ml) depending on plasmid resistance gene. For amplification in solid phase, bacteria were seeded on the same medium supplemented with 1.5 % bacto – agar and 100 µg/ml of corresponding antibiotic. For preservation, bacteria were conserved in the same media with 50 % of glycerol at -70º C.

3.9.3 Bacteria transformation and plasmid DNA extraction

Bacteria were transformed by different methods reliant on bacterial strain:

- Heat shock transformation of DH5α strains: 100 µl of competent cells were mixed with 100-250 ng DNA and maintained for 30 min at 4º C , then 1 min at 42º C and finally at 4º C. After transformation, bacteria were recovered in SOC media (2% tryptone, 0.5% yeast extract, 10 mM NaCl, 2.5 mM KCl, 10 mM MgCl2, 10 mM MgSO4, and 20 mM glucose) at 37ºC with gentle shaking for 1 hour. After recovery, bacteria were cultivated O/N at 37º C in LB-agar supplemented with selection antibiotic.

- Heat shock transformation of TOP10 cells: 50 µl of TOP10 cells were mixed with 10 µl of DNA and put on ice for 5 min. After that, mixture was resuspended in 200 µl of SOC medium and cultivated O/N at 37º C in LB-agar supplemented with selection antibiotic.
- Electroporation of BL21 strains: 30 µl of BL21 cells were mixed with 1.5 µl of vector an kept at 4º C for 1 min. After that, cells + DNA were placed in an electroporation cuvette (0.2 cm electrode) previously cooled on ice, ensuring that mixture displayed a continuous phase in the bottom of the cuvette. Cells were pulsed using following conditions: 2.5 kV, 200 Ω, and 25 µF. After transformation, bacteria were recovered in SOC media at 37ºC with shaking during 1 hour. After recovery, bacteria were cultivated O/N at 37º C in LB-agar supplemented with selection antibiotic.

For DNA plasmid rescue, we used two kits: for recovering low quantity of DNA we used *Wizard Plus SV Miniprep DNA purification Systems* (Promega), and for recovering high quantity of DNA we used *Qiagen Plasmid Maxi Kit* (Qiagen). In both cases, we followed manufacturer's protocols.

3.10 VIRUS MANIPULATION

All the viral infections of this work were done with the viral strain BA71V (Enjuanes *et al.*, 1976). HeLa and Vero cells infections were done in DMEM 2% FBS, while COS-7 cells were infected in DMEM 5 % FBS. Depending on the requirements of the experiment, from 1 - 5 M.O.I was used. In general, viruses were inoculated in ¼ of total volume of the plate to allow viral adsorption with gentle shaking. After 90 min at 37º C, virus inoculum was removed and infection progressed until indicated times post infection for each assay. Recovery was made in DMEM 2% FBS for HeLa and Vero cells, and in DMEM 5 % FBS for COS-7 cells. Cells not infected were called Mock, and were currently used as controls.

3.11 TRANSIENT TRANSFECTION

Transient transfections were carried out with LipofectAMINE PLUS reagent system (Invitrogen) following manufacturer's instructions. In general, 1 µg of DNA was transfected per 1 x 10^6 cells. DNA : LipofectAMINE : PLUS reagent rate was 1 : 10 : 2.5, respectively. DNA and PLUS reagent were mixed at room temperature for 15 min. After that, LipofectAMINE reagent was added over DNA – Plus complexes and allowed to mix for 20 min at RT. DMEM medium was removed and transfection inoculum was added to cells in a free FBS and antibiotic medium for 4.5 - 5 hours. Cells were recovered with DMEM 5 % FBS O/N. After 16 - 24 hours, cells were infected and analysed at indicated times post infection or directly analysed by CLSM.

3.12 GENERATION OF STABLE HELA CELL LINES

In order to study g5R function, 6 inducible HeLa cell lines were established expressing GFP tagged g5R proteins: HeLa GFP-g5R wt expresses GFP fused to g5Rp wild type form, HeLa GFP-g5R REGG and HeLa GFP-g5R EEQQ cell lines expresses GFP tagged to two punctual mutants of g5Rp catalytic Nudix domain (R146G/E147G and E150Q/E151Q) which lack the decapping activity *in vitro* (Parrish *et al.*, 2009); HeLa GFP-g5R N-term and HeLa GFP-g5R C-term produce GFP fused to the N-terminus and the C-terminus domains of g5Rp, respectively, and HeLa GFP g5R ΔNudix synthetize GFP tagged to a variant of g5Rp that lacks the catalytic Nudix motif.

To obtain this stable cell lines, HeLa Flp-in TREx cell lines (a kind gift from Dr. Matthias Hentze, European Molecular Biology Laboratory, Heidelberg, Germany) were required (Flp-In TREx Core Kit, Invitrogen). HeLa Flp-In TRex are HeLa stable host cell line previously transfected and selected to integrate into its genome a Flp Recombination Target (FRT) site and a copy of Tet repressor (Strein *et al.*, 2014). The FRT sites allows integration of gene of interest in a specific genomic location, while the presence of Tet repressor ensures protein synthesis only in presence of tetracycline. To generate the HeLa Flp in TREx GFP-g5R cell lines, pOG44 plasmid must be co-transfected with each pCDNA5/FRT/TO GFP-g5R constructions. While these vectors contain the gene of interest, pOG44 codifies to Flp recombinase, needed to insert this gene in the FRT genomic site. Co-transfections were realized using the Effectene Transfection Reagent System (Qiagen) following manufacturer´s protocol. Briefly, 300 ng pCDNA5/FRT/TO vectors were mixed with 500 ng pOG44 plasmid and the Enhancer reagent in a DNA: enhancer rate of 1 µg : 8 µL (V_f = 100 µl). After vortexing 1 min, 10 µl of Effectene reagent was added to the mixture. Resultant solution was incubated 5 - 10 min at RT and diluted in 500 µl medium before added to cells (40 - 50 % confluent). Next day, antibiotics for selection were added: 1/1000 Blasticidin S (InvivoGen) and 1/500 Hygomycin B (Invitrogen). Blasticidin was added to selection of cells that contain pCDNA5/FRT/TO vectors, while Hygromicyn ensured selection of cells with Tet Repressor. When cells reached 90 - 100 % confluence (normally one day after antibiotics addition), they were split into 15 cm^2 dishes without antibiotics, and allowed to grow until colonies reach confluence. Antibiotics for selection were added one day after. Colonies grew for 5 days, and then were seeded into a 6 well plate without antibiotics. This protocol will completely separate cells and make them accessible for antibiotics, so most of them died at this stage. Antibiotics were added next day. When some colonies grew over each other (approx. 3 week after transfection) cells were transferred to 10 cm^2 dishes and successively sub-cultured into these plates until all non-transfected cells died. Finally, positive cells were enriched by FACS sorting (approx. 4-5 weeks after transfection). FACS was done in the Flow Cytometry Core Facility of the European Molecular Biology Laboratory. Proteins of interest were induced adding 1/4000 Tetracycline (5 mg/ml) for 16 - 20 hours. HeLa eGFP and HeLa MOV10-YFP stable cell lines were used as negative and positive controls for RNA-proteins assays, and were a kind gift of Dr. Matthias Hentze (European Molecular Biology Laboratory, Heidelberg, Germany).

3.13 GENERATION OF ASFV DELETION VIRUS

For generation of g5R Ba71V deletion mutant, p72Δg5RGAL10 T plasmid was transfected in COS-7 cells with LipofectAMINE PLUs Reagent System as detailed before. 24 hours post transfection, cells were infected with 0.2 M.O.I of BA71V strain to permit homologous recombination between plasmid and viral genome. Infection was allowed to progress until 72 hours, and supernatant containing recombinant particles was recovered. These particles were used to infect new COS-7 cells in presence of 0.7 % agar - 2 x DMEM (8 mM L-glutamine, 0.1 mg/ml gentamicine, 0.8 mM nonessential amino acids, 160 µg/ml DEAE dextran sulfate, 4 % FBS). 48 - 72 hours after infection, positive colonies were selected by adding X-Gal (75 mg/ml) Cells infected with recombinant virus expressed β-Galactosidase, which produces a blue product in presence of its substrate (X-Gal). Blue colonies were extracted from agar by aspiration and amplified in a new round of infection, being this successive round-process repeated until only blue colonies appeared in the infected plates.

3.14 SILENCING g5R mRNA

With the purpose of studying g5Rp function in ASFV infection, we first tried to silence expression of g5R gene using small interference RNAs (siRNAs). siRNAs used in this study are listened below:

Target	Probe	Sequence	Working concentration	Technique	Origin
g5R mRNA	sig5R-1 sense	GACCGCAUGUGGUAUCAUATT	40 mM	Silencing	BioNova
	sig5R-1 anti sense	UAUGAUACCACAUGCGGUCTT			
g5R mRNA	sig5R-2 sense	CAGAUUCUCCCAGAGUUUATT	40 mM	Silencing	BioNova
	sig5R-2 anti sense	UAAACUCUGGGAGAAUCUGTT			
g5R mRNA	sig5R-3 sense	UCCUUGCAAUGUUAUGUAATT	40 mM	silencing	BioNova
	sig5R-3 anti sense	UUACAUAACAUUGCAAGGATT			

Table 4. siRNA used to silence g5R gene expression

To transfect siRNAs we used the LipofectAMINE 2000 Reagent system, following manufacturer´s instructions. Briefly, 40 or 100 nM siRNA against g5R mRNA were transfected per $2x10^6$ Vero cells 24 hours before ASFV infection. Previous to transfection, cells were cultivated 24 hours FBS free. Adsorption was done without siRNA, which was added after this process. siRNA transfection mix was left until samples were recovered. To corroborate the efficiency of silencing process, g5R mRNA levels were analysed by PCR or qPCR. Effect of g5Rp suppression on ASFV infection was studied by qPCR of representative viral and cellular mRNAs. GAPDH (Glyceraldehyde 3-phosphate dehydrogenase) and RPL0 genes were used as calibrators, and Mock infected cells were used as normalizer. Experimental values are expressed as mean +/- standard deviation (S.D). Statistical analysis was performed by Student´s *t* test and statistical significance was set at $p<0.05$.

3.15 RNA EXTRACTION AND RETROTRANSCRIPTION TO CDNA

Related to their origin, RNA samples were extracted by two methods:

3.15.1 Total RNA extraction

Total RNA was extracted from cells with *RNeasy Plus Mini Kit* (Qiagen) following manufacturer´s instructions, and quantified with a Nanodrop NP-1000.

3.15.2 RNA extraction from RNA–protein complexes

After immunoprecipitation or GFP pull down (see sections below), RNA bound to proteins was extracted using phenol : chloroform : isoamil alcohol (PCI). In general, 1 vol. of PCI was added to the precipitated samples, vortexed 31 sec and centrifuged at maximum speed for 5 min (RT). Upper phase was recovered after centrifugation and combined with 1 vol. of chloroform : isoamil alcohol (CI), mixed and centrifuged in the same conditions. New upper phase is transferred to a clean eppendorf and incubated with 2 µg glycogen, 1/ 10 from total volume of NaCl and 2.5 vol. 100 % cold ethanol O/N at -20º C. Next day, samples were centrifuged at 14,000 rpm for 20 min. Supernatant was discarded and pellet washed with 70 % cold Et-OH. Precipitated RNA is let to dry and resuspended in RNAses free water. Quantification was made by Nanodrop ND-1000.

Isolated RNA was retrotranscribed to cDNA using *Retrotranscriptase enzyme* (Roche) following manufacturer´s instructions. In general, we retrotrancribed 1µg of RNA when it was extracted from cell lysate, and all available RNA when it was extracted from immunoprecipitated samples (IP). Purified RNA was incubated with 2.5 mM Oligo $d(T)_{50}$ and 2 mM random primers at 65ºC for 10 min in order to eliminate secondary RNA structure and facilitate retrotranscription. Immediately after that, samples were mixed with 10 mM dNTP´s mix, 1x retrotranscription buffer, RNAses inhibitors (RNAsin Plus, Roche) and 1 U Retrotranscriptase enzyme. Samples were incubated 30 - 40 min at 55º C and finally enzyme was inactivated 5 min at 85º C. cDNAs were analysed by PCR or qPCR, depending on assays requirements.

3.16 GENERATION OF A SPECIFIC ANTIBODY AGAINST g5R PROTEIN

In order to determinate g5Rp expression and localization, we generated a specific anti-g5Rp serum. With this purpose, g5R gene was cloned in pGEX vector to generate pGEX-g5R wt, which was transformed in BL21 cells. To induce GST-g5R protein synthesis, BL21 were grown in low oxygen conditions O/N at 37º C. After 16 hours, samples were recovered and lysate in Buffer 6 (50 mM Tris HCL ph7.5; 0.5 M ClNa; 1mM EDTA; 7 mM β-2-Mercatptoethanol; 5 % glycerol). GST-g5R protein was purified using glutathione columns and eluted with Eluting Buffer (50 mM Tris HCl pH 8; 100 mM ClNa; 10 mM glutathione). Correct expression, solubility and purification of GST-g5Rp wt was analysed by Coomassie blue stain and Western blot using anti-GST antibody.

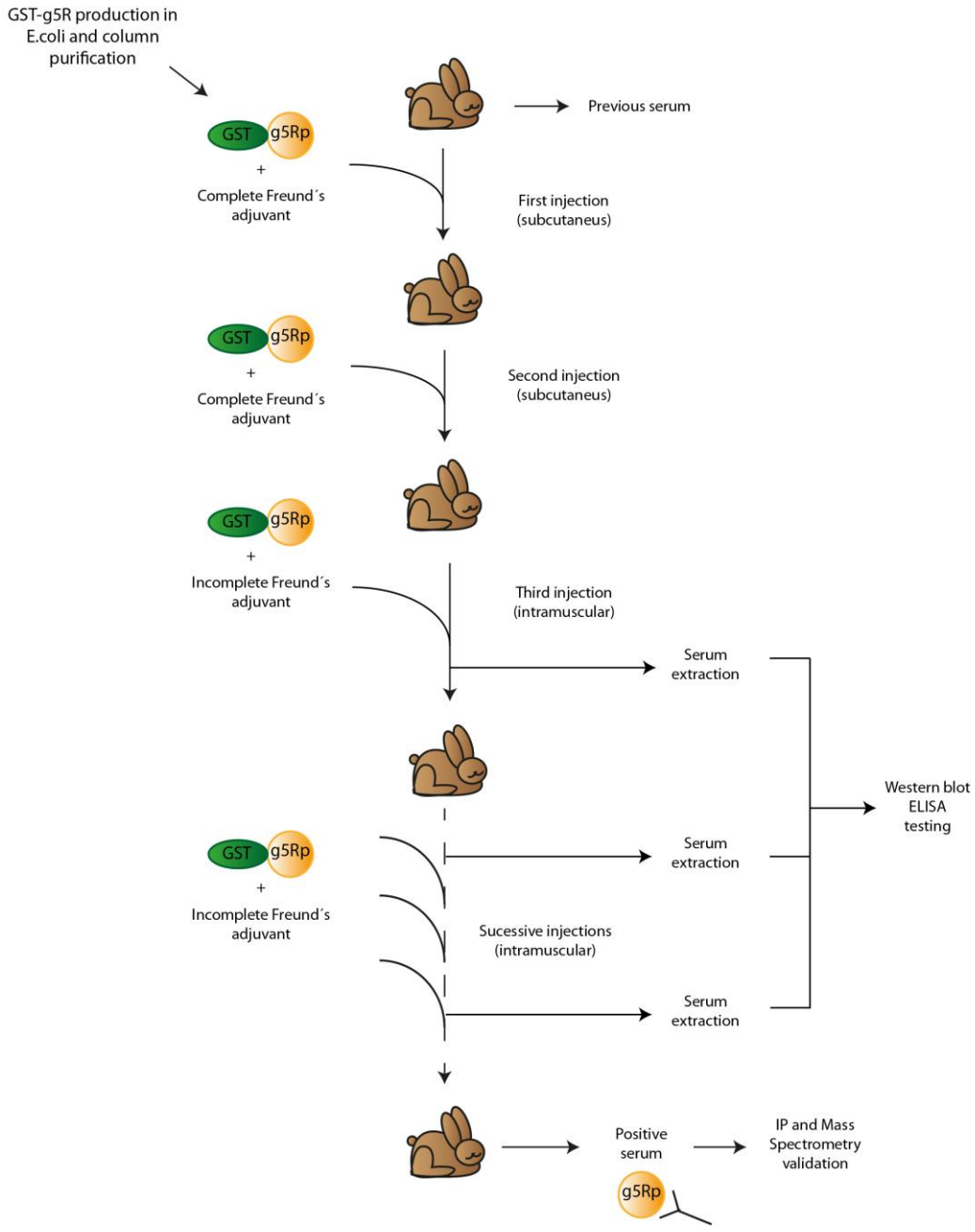

Figure 8. Schematic representation of generation of specific anti-g5R antibody.
GST-g5R wt protein was produced in *Escherichia coli*, purified by glutathione sepharose columns and mixed with Freund´s adjuvant to be successively injected into rabbits. Prior to first injection, rabbit serum was extracted as negative control (previous serum). Specific anti-g5Rp serum was tested by Western blot and ELISA assays after third, fifth and seventh injections. Once serum was determinate as positive, further validation was carried out with immunoprecipitation (IP) and Mass Spectrometry assays.

Once GST-g5Rp wt was purified, we proceed to generate the specific antibody: 500 µg of GST-g5Rp wt were complemented with 50 % complete Freund's adjuvant (Sigma), sonicated (6 x 10 sec at 4º C) and subcutaneously injected to each of rabbit (1232 and 1233 rabbits). Previously to first injection, rabbit sera were extracted as negative control (previous serum 1232 or 1233). 15 days after first immunization, rabbits were subcutaneously re-injected with 250 µg each of GST-g5Rp wt and 50 % complete Freund´s adjuvant. Next injections were inoculated intramuscularly (250 µg of protein and 50 % incomplete Freund´s adjuvant) once per month until anti-g5Rp was generated (7 injections). To check anti-g5Rp reactivity, serum samples

were recovered from both animals after third, fifth and seventh boost, and tested by Western blot and ELISA (Figure 8). To further confirmation, g5Rp antibody was used on immunoprecipitation assays and the gel band obtained was sequenced by LC-MS/MS (Ion Trap). This analysis was carried out in the CBMSO Protein Chemistry Facility, a member of the ProteoRed network.

3.17 ENZYME-LINKED IMMUNOSORBENT ASSAY (ELISA)

In order to determine sensitivity of g5Rp antibody, ELISA was completed in a Linbro 96 (Nunc). In general, 50 ng of GST (positive control) or GST-g5R wt protein (antigen) were attached to wells surface and incubated O/N at 4º C. Plates were washed 4 times with PBS 1x - 0.05 % Tween 20 and incubated with consecutive dilutions (1/100) of previous serum (negative control), anti-GST (positive control) or anti-g5Rp serum for 1h at 37ºC. After 4 washes with PBS 1x - 0.05 % Tween 20, plates were incubated with anti-rabbit or anti-mouse peroxidase antibodies (1h, 37º C). To eliminate excess of secondary antibodies, plates were washed 3 times with same solution. After final wash, plate was developed adding OPD reaction buffer: 2 mg/ml OPD, citrate buffer (20 mM acetic acid,50 mM sodium phosphate, pH 5) and 30% H_2O_2. Reaction was stopped with 3 N SO_4H_2 when colour appeared, and absorbance values were measured in an EL 340 Biokinetics Microplate Reader (BIO-TEK Instruments). Optimum working antibody concentration was then calculated.

3.18 PROTEIN EXTRACTION AND ELECTROPHORESIS ASSAYS

Total protein extracts were obtained from infected and non-infected cells as follows: seeded cells were harvested using a piston and then washed twice with cold PBS. Samples were lysate in modified RIPA buffer (mRIPA) containing 50 mM Tris-HCl pH 7.5; 1 % Nonidet NP-40; 0.25 % sodium deoxycholate; 150 mM NaCl, 1mM EDTA and 1x proteases inhibitors (c0mplete Mini, EDTA free protease inhibitor cocktail tablets, Roche) and 1 x phosphatases inhibitors (PhosSTOP EASY pack, Roche). To facilitate lysis, after mRIPA addition extracts were incubated at 4ºC for 5 min. Samples were processed or stored at -20 ºC, depending on the assay. For analysis, samples were centrifuged 5 min at 14.000 rpm to eliminate cellular DNA. Quantification of total protein was done using the Bicinchoninic acid *(BCA) Protein Assay Kit* (Pierce) following manufacturer´s protocol. For protein electrophoretic separation assays, 10 - 60 µg total proteins were mixed with Laemmli buffer (ref) and boiled at 95º C for 5 min. After centrifugation, extracts were separated by electrophoretic mobility in sodium dodecyl sulfate polyacrylamide gels (SDS-PAGE) in reductive conditions. Percentage of acrylamide varied between assays depending on proteins molecular weights.

3.18.1 Coomassie brilliant blue gel staining

After electrophoretic resolution, proteins were non-specifically dyed with Coomassie brilliant blue. Gels were incubated for 20 min with Coomassie solution (10 % acetic acid, 25 % isopropanol and 0.1 % Coomassie Blue R250) to protein staining. For distaining, gels were washed with 10 % acetic acid - 20 %

ethanol solution until bands were distinguished. For storage and analysis, gels were dried in a DryGelSr (Hoefer Scientific Instruments).

3.18.2 Silver staining of polyacrylamide gels

Alternatively to the Coomassie staining, polyacrylamide gels were dyed with silver staining solution. After electrophoretic resolution, gels were fixed with 30 % ethanol and 10% acetic acid during 15 min and thus, incubated with Sensitizing Solution (30 % ethanol, 5 % sodium thiosulfate, 7 % p/v sodium acetate, 0.125 % glutaraldehyde) during 30 min. After sensitization, gels were washed three times for 1 min with distilled H_2O and incubated with Staining solution (2.5 % p/v silver nitrate, 0.15 % formaldehyde), and, after that, gels were washed twice for 1 min with distilled water and the Developer solution was added (0.04% Formaldehyde, 2% Sodium Carbonate). The reaction was stopped with Termination solution (1 % acetic acid) when protein bands were detected.

3.18.3 Immunodetection by Western blot

Following separation, proteins were electrophoretically transferred to *Inmobilon-P* membranes (Millipore). Blocking was made incubating membranes with methanol and letting them dried (30 min). Membranes were then incubated with primary antibodies diluted in blocking solution (1 % non-fat-dry-milk in TBS) at 4º C O/N. After washing 5 min with TBS 1x, peroxidase secondary antibodies were added in blocking solution 1h at room temperature. Antibodies dilutions are indicated in Table 1. For detection of band of interest, we used the chemiluminescent *ECL Western blotting Analysis System* (Amersham Pharmacia), following manufacturer´s instructions. Light was captured by photographic films (Agfa) and signal was analysed by densitometry when required.

3.19 ^{35}S METABOLIC LABELLING

In order to study protein synthesis, we performed ^{35}S metabolic labeling assays. Vero cells were infected or non-infected with ASFV (M.O.I = 5 pfu/cell) and harvested at indicated times post infection. 2 hour prior to recovering samples, monolayer was incubated with 200 µCi ^{35}S-methionine, which was incorporated to proteins synthetize *de novo*. Samples were resuspended on mRIPA buffer and labeled protein levels were analysed by SDS-PAGE. Gels were dried in a DryGelSr and radioactivity signal was captured by direct contact of gels with photographic films at -80º C.

3.20 CONVENTIONAL CROSSLINKING (CCL) AND PHOTOACTIVATABLE-RIBONUCLEOSIDE-ENHANCED CROSSLINKING (PAR-CL)

With the purpose to study RNA-protein interactions we used cCl and PAR-CL techniques, two UV light irradiation methods which fix these interactions only when contact is direct and do not cause protein-protein connections (Pashev *et al.*, 1991). Crosslinking methods used in this project are detailed below:

3.20.1 Conventional crosslinking

Conventional crosslinking triggers covalent bound of natural photo-reactive nucleotide bases to specific amino acids (Phe, Trp, Tyr, Cys, and Lys) when samples are irradiated with 254 nm ultraviolet (U.V) light (Brimacombe *et al.*, 1988). For cCL, cell monolayer was washed twice with RT PBS and then U.V irradiated at 256 nm (0.15 J/cm^2) on ice and in absence of PBS. It is especially important no trace of medium or PBS remain at the dish when irradiated as it could interfere with crosslinking. Immediately after crosslinking, cold PBS was added to cells, which are maintained at 4º C until collection. Crosslinking was made in a SpectroLinker XL-1000 or XL-1500 (Spectronics Corporations).

3.20.2 Photoactivatable-ribonucleoside-enhanced crosslinking (PAR-CL)

PAR-CL requires incorporation of the photoactivatable analogue nucleotide 4-thiouridine (4-SU, Santa Cruz) into nascent RNA, which is coupled to amino acids when excited at 365 nm UV (Hafner *et al.*, 2010). PAR-CL has been made following previous described protocols (Castello *et al.*, 2012; Strein *et al.*, 2014): 100 µM 4-SU was added to plates for 2 to 16 hours. Incubation time varied related to experimental procedure (see section 1.20.1). After PAR-CL, samples were recovered following same protocol as for cCL: cells were washed with pre-warmed PBS, 365 nm UV irradiated with 0.15 J/cm^2 (SpectroLinker XL-1000 or XL-1500, Spectronics Corporations) and maintained in cold PBS at 4º C until processing.

3.21 IMMUNOPRECIPITATION (IP)

With the aim of studying protein-protein and RNA-protein interactions, different immunoprecipitations assays were carried out. We used different techniques that we have classified by beads type.

3.21.1 GFP-Trap_A beads Immunoprecipitation

Two methods were developed to studying RNA-protein interaction based on the use of GFP_Trap_A beads (Chromotek) (Rothbauer *et al.*, 2008). These beads are covalently bound to a small GFP-binding protein that allows an efficient in one step purification of GFP-fused proteins.

3.21.1.1 Dual fluorescence method

We used the protocol previously described in (Strein *et al.*, 2014). 12 x 10^6 - 25 x 10^6 HeLa stable cell lines were induced with 1 µg/mL tetracycline (tet) for 20 hours before harvesting. Samples were conventional or PAR crosslinked (as described before) and resuspended in 300 µL of GBP lysis buffer (100 mM KCl, 5 mM $MgCl_2$, 10 mM Tris pH 7.5, 1% NP40, 1 mM DTT, 100 units/mL RNAsin [Roche], 1× phenylmethylsulfonyl fluoride (PMSF, Roche), and 200 µM ribonucleoside vanadyl complex [NEB]). Samples were incubated 5 min at 4º C, subjected to a frozen cycle to favoured lysis, centrifuged 10 min at 10.000 rpm to eliminate cellular debris and distributed to three tubes for technical replicates. As negative control, ½ of

total sample was treated with RNAses A and T1 before immunoprecipitation. In order to avoid unspecific binding to beads, each replicate was mixed with dilution buffer (500 mM NaCl, 1 mM Mg2Cl, 0.05% SDS, 0.05% NP-40, 50 mM Tris-HCl pH 7.5, 100 units/mL RNAsin, 1× PMSF, and 200 µM ribonucleoside vanadyl complex) and incubated with 10 µL of GFP-Trap_A beads for 4 h at 4º C with rotation. After incubation, samples were washed with medium salt wash buffer (250 mM NaCl, 1 mM Mg2Cl, 0.025% SDS, 0.05% NP-40, 20 mM Tris-HCl pH7.5) and treated with blocking buffer (200 mM LiCl, 20 mM Tris pH 7.5, 1 mM EDTA, 0.01% NP40, 100 µg/mL *Escherichia coli* tRNA, 100 µg/mL BSA) for 15 min at 4º C with rotation. After blocking, beads were incubated for 1h at 4 º C with Hybridization buffer (500 mM LiCl, 20 mM Tris pH 7.5, 0.05% LiDS, 1 mM EDTA, 5 mM DTT, 0.01% NP40, 100 units/mL RNaseOUT) supplemented with 40 nM of Oligo $d(T)_{25}$-Tred (Sigma). To remove unspecific bound probe, samples were washed as described below:

- Once (2 min) with High salt wash buffer (500 mM LiCl, 20 mM Tris pH 7.5, 0.01% LiDS, 0.01% NP40, 1 mM EDTA, 5 mM DTT).
- Twice (2 x 2 min) with Medium wash salt buffer (200 mM LiCl, 20 mM Tris pH 7.5, 0.01% LiDS, 0.01% NP40, 1 mM EDTA, 5 mM DTT).

All buffers described before were supplemented with RNAsin (1/500) and 1 x PSMF. After final wash, beads were transferred to a 96-well optical plate (CBG Thermo scientific, NUNC) and GFP an Texas-Red signals were measured in a TECAN Safire II microplate reader following these parameters: for GFP, excitation was made at 490 nm and emission was recovered at 515 nm; and for Texas Red, excitation was made at 590 nm and emission was recovered at 616 nm. Experimental values are expressed as mean +/- standard deviation (S.D). Statistical analysis was performed by Student´s *t* test and statistical significance was set at $p<0.05$. Data shown proceed from at least three replicates.

As commented in section 3.20, crosslinking is a useful and specific method to fixed RNA-protein interactions, but it has been described that, due to its chemical differences, cCL and PAR-CL could affect efficiency of protein capture process, being some proteins more effectively captured by cCL or PAR-CL (Castello *et al.*, 2012). For this reason and in order to achieve the best results in the GFP-g5Rp immunoprecipitation assays here described, we optimised both crosslinking techniques. HeLa MOV10-YFP was used as positive control, as MOV10 is a well-known RNA binding protein (Gregersen *et al.*, 2014). HeLa GFP-g5R wt, HeLa MOV10-YFP and GFP g5R EEQQ were induced O/N with tetracycline and subjected to cCL or PAR-CL as indicated in Figure 9. Cells were recovered and treated to dual fluorescence analysis as described in this section. We observed that both GFP-g5R proteins were more efficiently immunoprecipitated by PAR-CL, and consistently more RNA was detected bound with PAR-CL technique. Due to these results, we decided to carry out all dual fluorescence experiments with PAR-crosslinking (Figure 9).

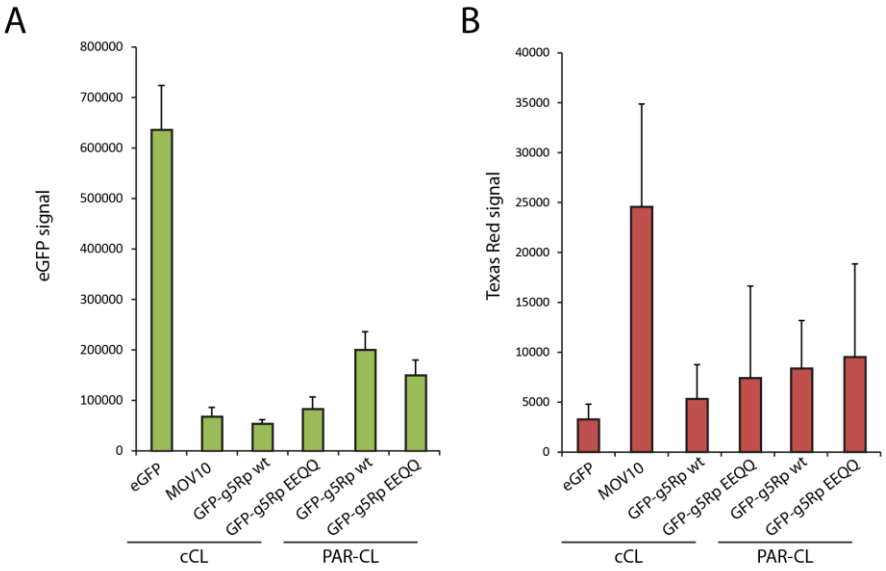

Figure 9. Optimization of the immunoprecipitation of GFP-g5R complexes.
PAR-Crosslinking and conventional Crosslinking techniques were tested in order to determine which method was more optimum for the immunoprecipitation of GFP-g5Rp complexes. HeLa GFP-g5R wt and GFP-g5R EEQQ lines were induced and RNA-protein interaction were fixed by PAR CL and cCL respectively. GFP fusion proteins were immunoprecipitated using GFP_Tap_A beads and both GFP **(A)** and Texas Red signals **(B)** were measured in a TECAN Safire microplate reader. Data is represented in arbitrary units. Error bars: mean +/- S.D. (n = 3).

3.21.1.2 Immunoprecipitation and RT-qPCR analysis

In order to analyse g5Rp-RNA interaction in the context of infection, we optimised the GFP Trap_A beads immunoprecipitation protocol: after immunoprecipitation, RNA was extracted from the protein complexes and analysed by RT-qPCR. As explained before, 4-SU is a ribonucleoside analogue that incorporates to nascent RNA, having a possible undesirable effect on some cellular processes (Burger *et al.*, 2013). To assess this possibility, Hela GFP g5R wt cells were subjected to two different 4SU treatments: first, 4SU was added 2 hour prior tet induction, and second, 4-SU was added after viral adsorption (Figure 10 A). In both cases, HeLa GFP-g5R wt cells were induced O/N with tet and Mock infected or ASFV infected M.O.I of 5 pfu/cell. Cells were PAR-crosslinked and samples were collected at 6 and 14 hpi to analyse the viral proteins level by Western blot. By using the anti - tASFV serum, ASFV proteins were detected, showing that some late viral proteins expression (as p17 or p24) was affected by 4SU presence at 14 hpi (Figure 10 B). To further validate these results, we also tested ASFV infection in 4-SU presence or absence in Vero cells by Western blot. In this case we checked viral infection by detecting the early viral protein p32 and the late viral protein p72. We observed that 4-SU had an effect on synthesis of the late viral protein similar to that detected on HeLa cells (p72) (Figure 10 C). Due to this undesirable effect of 4SU, we decided to carry out the cross linking experiments in ASFV infection by using the conventional cross linking method.

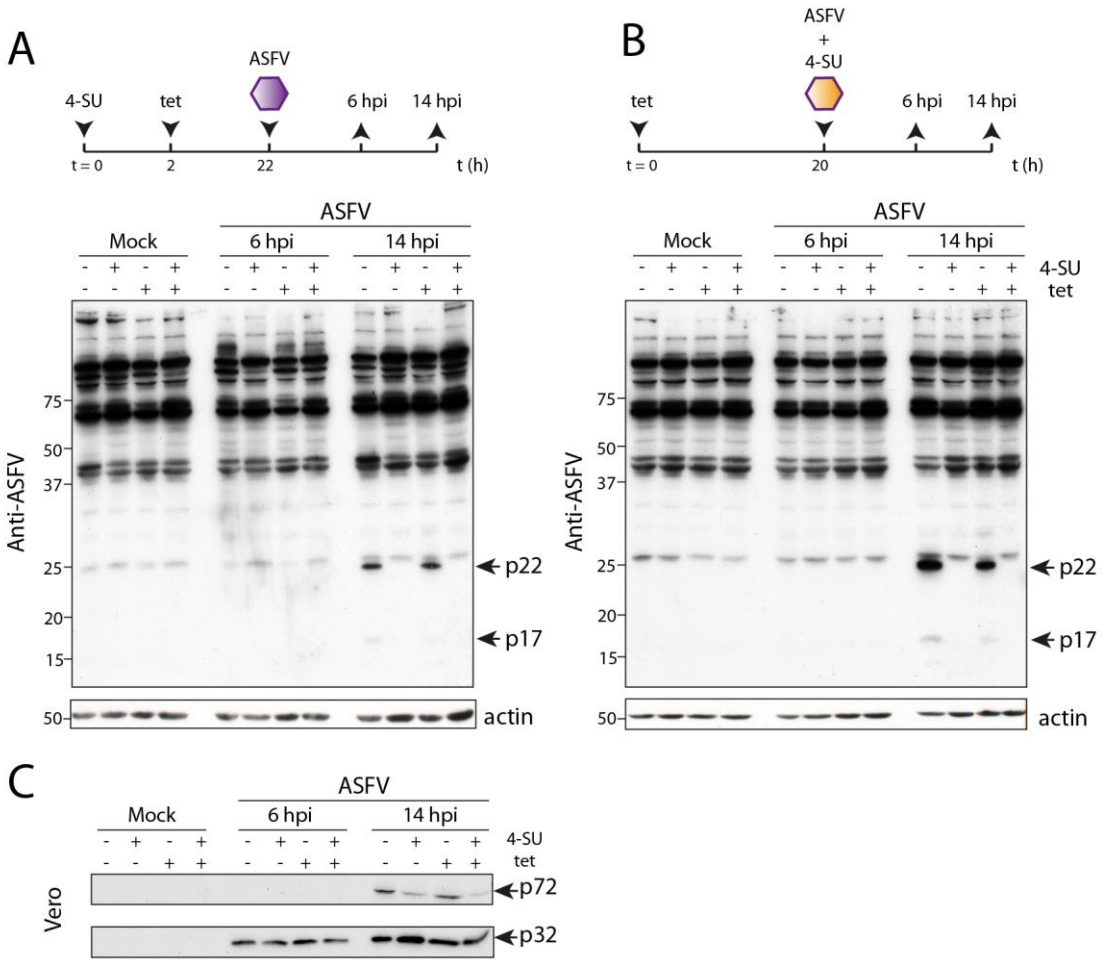

Figure 10. Effect of 4 -SU in ASFV infection.
In order to test the side effects of the 4-SU presence in ASFV infection, two different experimental procedures were carried out. In the first **(A)** HeLa GFP-g5R wt stable cell line was treated with 4-SU 2 hours prior to induction of the recombinant GFP-g5R wt protein with tetracycline (tet), and samples were recovered at the indicated times post infection. A schematic representation of the experimental procedure is shown in the upper panel. ASFV protein levels were analysed by Western blot using a specific serum able to recognise viral proteins induced with the infection (anti-ASFV) (bottom panel). In the second approach **(B)** 4-SU was added to HeLa GFP-g5R wt expressing cells together with the viral inoculum (18 hours after the induction with tetracycline). A schematic representation of the experimental procedure is shown in the upper panel. ASFV protein levels were analysed by Western blot using the serum anti-ASFV (bottom panel). In both cases, actin was used as loading control .**C)** In order to validate the previous results, COS-7 cells were Mock-infected or ASFV-infected in the presence or the absence of tetracycline and 4-SU. ASFV p72 and p32 protein levels were analysed with specific anti-p72 and anti-p32 antibodies, respectively. 4-SU: 4-thiouridine.

12 x 10^6 HeLa eGFP, 24 x 10^6 HeLa MOV10-YFP and 48 x 10^6 HeLa GFP g5R wt cells were induced for protein expression with tetracycline (0.6 µg/ml and 1.2 µg/ml, respectively) for 20 h, conventional crosslinked and harvested as described before. In this case, cells were resuspended in 0.3 - 1.2 ml of lysis buffer (100 mM KCl, 5 mM $MgCl_2$, 10 mM Tris pH 7.5, 0.5 % NP40, 1 mM DTT, 100 units/mL RNAsin, 1× PMSF and 200 µM ribonucleoside vanadyl complex). After mixing with dilution buffer (500 mM NaCl, 1 mM Mg2Cl, 0.05% SDS, 0.025% NP-40, 50 mM Tris-HCl pH 7.5, 1/500 RNAsin, 1× PMSF, and 200 µM ribonucleoside vanadyl complex), 10% of sample was removed as Input and stored at 4º C until RNA extraction. Samples were incubated with 20 µl of GFP-Trap_A beads for 4 h at 4º C with rotation, and washed as follows:

- Once (2 x 2 min) with Wash buffer 1 (500 mM NaCl, 1 mM $MgCL_2$,20 mM pH 7.5 Tris -HCl, 0.025% NP-40, 1 / 500 RNasin and PMSF).

- Twice (2 x 2 min) with Wash Buffer 2 (250 mM NaCl, 1 mM $MgCL_2$, 20 mM pH 7.5 Tris HCl, 0.025% NP-40, 1 / 500 RNasin and PMSF).
- Twice (2 x 2 min) with Wash Buffer 3 (150 mM NaCl, 1 mM $MgCL_2$, 20 mM pH 7.5 Tris HCl, 0.025% NP-40, 1 / 500 RNasin and PMSF).

After final wash, 3 µl of sample were removed to check immunoprecipitation efficiency by Western blot. To elute immunoprecipitated proteins, beads were mixed with 2x Laemmli buffer and boiled 5 min at 95º C. After centrifugation, supernatant was recovered and the process was repeated to ensure all proteins were extracted from beads. Samples were analysed by Western blot using anti-GFP as detector. Elution of RNA-protein complexes was made by direct treatment of beads with proteinase K: beads were incubated with 1 x Proteinase K buffer (50 mM Tris HCl pH 7.5, 750 mM NaCl, 1 % SDS, 50 mM EDTA, 2.5 mM DTT and 25 mM $CaCl_2$) and 10 µg Proteinase K in a final volume of 100 µl for 1h at 37º C with strong shaking. RNA was extracted from immunoprecipitates with phenol:chroloform:isoamil alcohol (See section 3.15.2) and analysed by qPCR as described in 3.7.3 section. In general, immunoprecipitated eGFP was used as calibrator, and samples were normalized to total RNA (Input). Experimental values are expressed as mean +/- standard error of the mean (S.E.M) and proceeded from three independent experiments. Statistical analysis was performed by Student´s *t* test and statistical significance was set at $p<0.05$.

3.21.2 Agarose beads Immunoprecipitation

Agarose beads immunoprecipitations were used to study protein - protein interactions. 10^6 Vero cells were infected or non-infected (Mock) with ASFV (M.O.I = 5 pfu/cell) and lysate at indicated times post infection with mRIPA buffer containing 5 - 10 µg of specific antibody. For immunoprecipitation, each sample was incubated with 20 µl of equilibrated A/G or G agarose beads O/N at 4º C with gentle shaking. Next, samples were 6 times washed with PBS 1x - 0.05 % NP-40 and proteins were eluted by adding 2 x Laemmli buffer. Eluted proteins were then boiled 5 min at 95º C and centrifuged. Supernatant was removed and process was repeated twice to ensure all proteins were extracted. Finally, protein interactions were analysed by Western blot.

3.22 PULLDOWN ASSAYS

In order to determine proteins that could interact with g5Rp, pulldowns assays were performed. GST or GST-g5R wt proteins were expressed in *E.coli* and purified by glutathione beads. After that, both proteins were incubated with Vero cells Mock-infected or ASFV-infected at 6 hpi or 16 hpi. After intensive washing, GST complexes were resolved by SDS-PAGE electrophoresis and peptides were sequenced by Mass Spectrometry (a work realised by the Proteomics Core Facility of CBMSO). Identification of the peptides were performed comparing sample peptides to UniProt ASFV-Ba71V data base (in order to identify viral proteins) or to UniProt Primates data base (in order to identify cellular proteins).

3.23 FLUORESCENCE-ACTIVATED CELL SORTING (FACS)

FACS technique was carried out with the purpose of studying protein expression in the context of ASFV infection. Cells were harvested and centrifuged at 2000 rpm at 4ºC for 5 min, washed twice with cold 1x PBS and fixed for 30 min in 2 % paraformaldehyde (PFA) at 4º C. After that, cells were washed again 3 times with PBS and permeabilized with Staining buffer (0.2 % saponin; 5 % BSA; 1 x PBS) for 15 min at RT. Primary antibodies were added to cells diluted (Table 1) in Staining buffer and incubated for 30 min at RT in absence of light. After one wash with staining buffer, cells were incubated at the specific dilution (Table 1) with secondary antibodies in same conditions settle for primary antibodies. Finally, samples were washed twice and protein presence was analysed in 2 x 10^6 cells in a FACSCalibur (BD Science). Experimental values are expressed as mean +/- standard deviation (S.D) or standard error of the mean (S.E.M), as indicated. Statistical analysis was performed by Student´s *t* test and statistical significance was set at $p<0.05$.

3.24 FLUORESCENCE ANALYSIS

In order to check GFP fusion proteins induction after tetracycline addition in HeLa stable cells lines or to corroborate transient transfections with eGFP constructions, cells were analysed in a Nikon microscope, which possess a fluorescence lamp. Photos were taken with a Nikon DSQ1 Mc camera attached to microscope and analysed with NIS-Elements F 3.2 program.

3.25 IMMUNOFLUORESCENCE ASSAYS

To study protein interactions, expression and localization, we used immunofluorescence techniques. Cells were seeded on cover glasses, and either induced or transient transfected, or infected at indicated MOI and harvested at corresponding times post infection. Cell monolayer was washed 3 times with cold 1 x PBS, fixed with 4 % paraformaldehyde for 20 min at RT and washed again to eliminate PFA residues. Cells were permeabilized for 30 min with 0.2 % Triton X-100 PBS and blocked with 1 % BSA - PBS for 30 min to avoid unspecific interactions. Primary antibody was added diluted in 5 % BSA in PBS (Table 1) and incubated for 1h in absence of light at RT. Cells were washed 3 times with PBS and treated with fluorescent secondary antibodies. These antibodies were selected by its reactivity to primary antibodies specie. After successive washes with distilled water and ethanol, cover glasses were fixed to microscope slides with Prolong Gold (Invitrogen) or DAPI-fluoromount-G (SouthernBiotech) and analysed by CLSM.

3.26 FLUORESCENCE *IN SITU* HYBRIDIZATION (FISH)

To analyse RNA expression, localization and RNA-protein interactions, we performed FISH technique. Cells were fixed with 4 % PFA and permeabilized with 0.2 % Triton-X 100 as described to Immunofluorescence and then washed with 1 x PBs to eliminate any detergent residues. Instead to blocking buffer, cells were washed once with 1 x SSC buffer (150 mM NaCl; 15 M sodium citrate pH 7.0) and once

with 2x SSC buffer. Cells were then incubated with Pre-Hybridization buffer (2x SSC, 20 % formamide; 0.2 % BSA, 1mg/ml yeast tRNA) for 15 min at37º C and next treated with Hybridization buffer, (Pre-Hybridization buffer plus 10 % dextran sulphate) and 1 µM fluorescein tagged probe for 4 h at 37º C. Once probe hybridized, samples were washed successively for 5 min at 42º C with 2x SCC - 20 % formamide, 2 x SSC, 1x SSC and finally with PBS. When protein detection was required, we proceeded to incubation of primary antibodies. We followed protocol for Immunofluorescence (described in section 3.25) but antibody incubations were made only in 1 x PBS. After primary and secondary antibodies incubations, cells were washed with PBS, fixed to microscope slides as describe before and analysed by CSLM.

3.27 CONFOCAL LASER SCANNING MICROSCOPY (CLSM)

In this Thesis, two confocal systems were used: Zeiss LSM 710 Confocal Laser Scanning Microscope System coupled to a vertical AxioImagerM2 microscope (vertical LSM710) and Zeiss LSM510 META Confocal Laser Scanning Microscope System coupled to an inverted Axiovert200 microscope (LSM 710). Election of confocal microscope system was made in relation to the number of signal channels we needed to use (3 to LSM510 META and 4 to vertical LSM710). In general, laser conditions were adjusted using Mock cells as negative control and images were taken in a single plane with a 63 x objective and processed with *ImageJ* software. When required, quantification of intensity of signal was also analysed using *ImageJ* software. Experimental values are expressed as mean +/- standard deviation (S.D) or standard error of the mean (S.E.M), as indicated. Statistical analysis was performed by Student´s *t* test and statistical significance was set at $p<0.05$.

3.28 POLYSOME PROFILE

With the aim of analyse the translation stage of infected and non-infected cells, polysome profile was performed. Protocol has been previously described in (Martinez-Azorin *et al.*, 2008): 1 x 10^6 Vero cells were infected or non-infected with ASFV and samples were collected at indicated times post infection. Cell monolayer was removed with a scraper, centrifuged at 2,000 rpm for 5 min, washed with PBS supplemented with 100 µg/ml of cicloheximide (CHX) and resuspended in lysis buffer (15 mM Tris-HCl pH 7.5, 80 mM KCl, 5 mM MgCL, 1 % Triton X-100, 1 % NP-40, 100 µg/ml CHX, 40 U/ml RNAsin and 1 x protease inhibitors cocktail). For polysome profile, 10 % to 50 % sacarose gradients were made by mixing 10 % and 50 % sacarose solutions in a gradient former. Both sacarose solutions were made by solving 10 mg or 50 mg of sacarose in buffer A (10 mM Tris HCl pH 7.4, 80 mM KCl, 10 mM $MgCl_2$). Before gradient generation, these solutions were autoclaved and supplemented with 100 µg/ml CHX. Samples were loaded on top of sucrose gradients and centrifuged for polysome separation at 39,000 rpm for 2.5h at 4º C in a SW40 Ti rotor (Beckman Coultier). Gradients were fractionated in an ISCO density-gradient fractionator and polysome profile was obtained by continuous measurement of 260 nm absorbance in a ISCO UA-5 UV monitor. Data was collected by *PicoLog* software.

3.29 *IN SILICO* ANALISIS OF g5R

To study g5Rp homology sequence, we used *Clustal Omega* software, from EMBL-EBI platform (European Bioinformatics Institute). We analysed g5R amino acidic sequence comparing it with other described eukaryotic and viral decapping enzymes: human Dcp2, *S.pombe* Dcp2, *S cerevisiae* Dcp2 and D9 and D10 from vaccinia virus.

For tri-dimensional structural prediction and electrostatic surface representation of g5Rp, we used *PyMol* software (Schrödinger). Structural prediction was made based on *S.pombe* Dcp2 crystal structure (She *et al.*, 2006).

Results

4.1 ASFV PROMOTES SHUTOFF ON INFECTED CELLS

As explained in Introduction section, the majority of viruses manipulate host gene expression in order to efficiently synthetize viral proteins, while impair cellular protein synthesis (Bushell and Sarnow, 2002; Narayanan and Makino, 2013; Reineke and Lloyd, 2013; Schneider and Mohr, 2003). This phenomenon is called cellular shutoff. Viruses accomplish this singularity by numerous mechanisms: from viral endonucleases that eliminate cellular mRNAs (alpha-herpesviruses, gamma-herpesviruses, influenza viruses or SAR coronavirus (Abernathy and Glaunsinger, 2015)), to proteases that cleave eukaryotic initiation factors to difficult cellular protein synthesis while facilitate viral protein expression (picornaviruses, calciviruses or retroviruses (Castello *et al.*, 2006; Lloyd, 2006)).

4.1.1 Cellular protein synthesis is impaired in ASFV infection

It has been previously demonstrated that ASFV induces a strong cellular shutoff (Castello *et al.*, 2009b; Rodriguez *et al.*, 2001), but the molecular mechanisms by which this important regulatory step is achieved remain elusive. In order to study that process, we analysed protein synthesis by incorporation of ^{35}S-methionine in ASFV-infected Vero cells.^{35}S-methionine was added to cells 2 hours prior to sample collection at 8, 18, 24 and 40 hpi. Samples were lysed in modified RIPA buffer and protein levels were analysed by SDS-PAGE. We observed that, during ASFV infection, cellular protein synthesis was inhibited from 8 hpi and completely abolished at 24 hpi, concomitantly with an increment of viral protein synthesis (Figure 11 A). To determine if the previous result was due to a defect in translation rate, we analysed the polysome profile of Mock-infected and ASFV-infected Vero cells. Polysomes are mRNAs interacting with two or more ribosomes, and, in this kind of analysis, de novo protein synthesis is represented by the number and amount of ribosomes found within the polysomal mRNA fraction (Figure 11 B and (Martinez-Azorin *et al.*, 2008)). Mock-infected and 14 hpi ASFV-infected Vero cells (M.O.I = 5 pfu/cell) were washed and lysate in presence of 100 µg/ml cycloheximide (CHX), an inhibitor of proteins synthesis which blocks the elongation step of the translation process and causes ribosomes stall into mRNA (Schneider-Poetsch *et al.*, 2010). This treatment allows polysome analysis in sacarose gradients (Martinez-Azorin *et al.*, 2008). After high speed centrifugation, these gradients were examined in a polygraph and densitometry values were read at 260 nm. We observed that ASFV infection promoted a reduction in the total amount of polysomes (calculated as the area under the polysome fraction) but not in the polysomes number (calculated as the number of peaks in this fraction), which suggests that ASFV infection triggers a decrease on the rate of translation initiation (Figure 11 B). Indeed, when we calculated translation efficient rate in Mock-infected and ASFV-infected cells, we observed a slightly reduction induced by the infection (Figure 11 C). These results point to a decrement in protein synthesis as responsible of the cellular shutoff observed during ASFV infection.

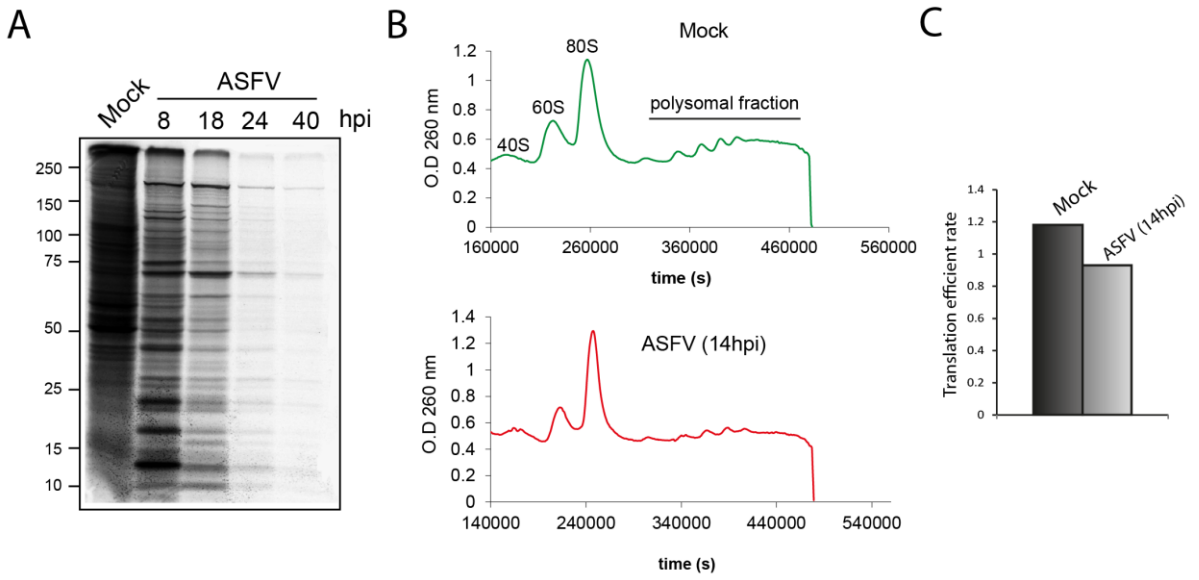

Figure 11. ASFV infection promotes cellular shutoff and a decrease on the initiation translation rate.
A) Analysis of cellular protein synthesis during ASFV infection by metabolic assay. Vero cells were Mock-infected or ASFV infected with M.O.I of 5 pfu/cell and ^{35}S-methionine was added to cells 2 hours prior to sample collection at 8, 18, 24 and 40 hpi. Samples were lysed in modified RIPA buffer and protein levels were analysed by SDS-PAGE. **B)** Polysome profile analysis. Vero cells were Mock-infected or ASFV-infected (M.O.I 5 pfu/cell) and samples were recovered at 14 hpi in presence of cyclohemide (100 µg/mL). Polysomes were fractionated in sucrose gradients and examined in a polygraph. Densitometry values were read at 260 nm and represented as a function of time (seconds,s). **C)** Translation efficient rate of samples described in B). Translation efficient rate was calculated as the ratio between the polysome fraction area and the 80S fraction area.

4.1.2 ASFV infection regulates poly(A) mRNA levels in cytoplasm of infected cells

After the previous results, we decided to analyse in deeply the cause of the cellular shutoff induced by ASFV. To explore this, we first analysed poly(A) RNA levels in infected cells by FISH. Vero cells were Mock-infected or ASFV-infected with M.O.I of 5 pfu/cell and fixed at 8 and 16 hpi, then poly(A) RNA was detected with a fluorescein Oligo d(T) probe that specifically binds poly(A) RNA tails. To-Pro-3 was used to stain DNA and localize nucleus and viral factories (Figure 12 A). Poly(A) RNAs exhibited a diffuse pattern in the cytoplasm and a punctuated distribution in the nucleus of Mock-infected cells, whereas in infected cells, the Oligo d(T) signal was progressively clustered around the viral factory and increased in the nucleus (Figure 12 A). These results could indicate that during ASFV infection poly(A) RNAs are being degraded in the cytoplasm and gathered in the nucleus. This nuclear increase is probably due to an impairment of nuclear export, in line with previously reported experiments showing that ASFV infection causes nuclear changes and partially supporting the idea of altered nucleus-cytoplasmic RNA carriage in ASFV infected cells (Ballester *et al.*, 2011). However, it could be also a consequence of the enhanced cytoplasmic RNA degradation rate triggered by ASFV, as occurs in other viral systems such as alpha- and gamma- herpesviruses or influenza viruses (Abernathy and Glaunsinger, 2015).

In order to validate and quantify the decrease of poly(A) RNAs reported above, we further analysed some representative cellular mRNAs by RT-qPCR. Vero cells were Mock-infected or ASFV-infected (M.O.I = 5 pfu/cell) and samples were analysed at the indicated times post infection (Figure 12 B). We observed a

significant decrease of all the analysed cellular mRNAs. Furthermore, at 14 hpi, mRNA levels were strongly reduced; correlating with the protein shutoff observed at 18 hpi in the ^{35}S metabolic assays (Figure 12 B).

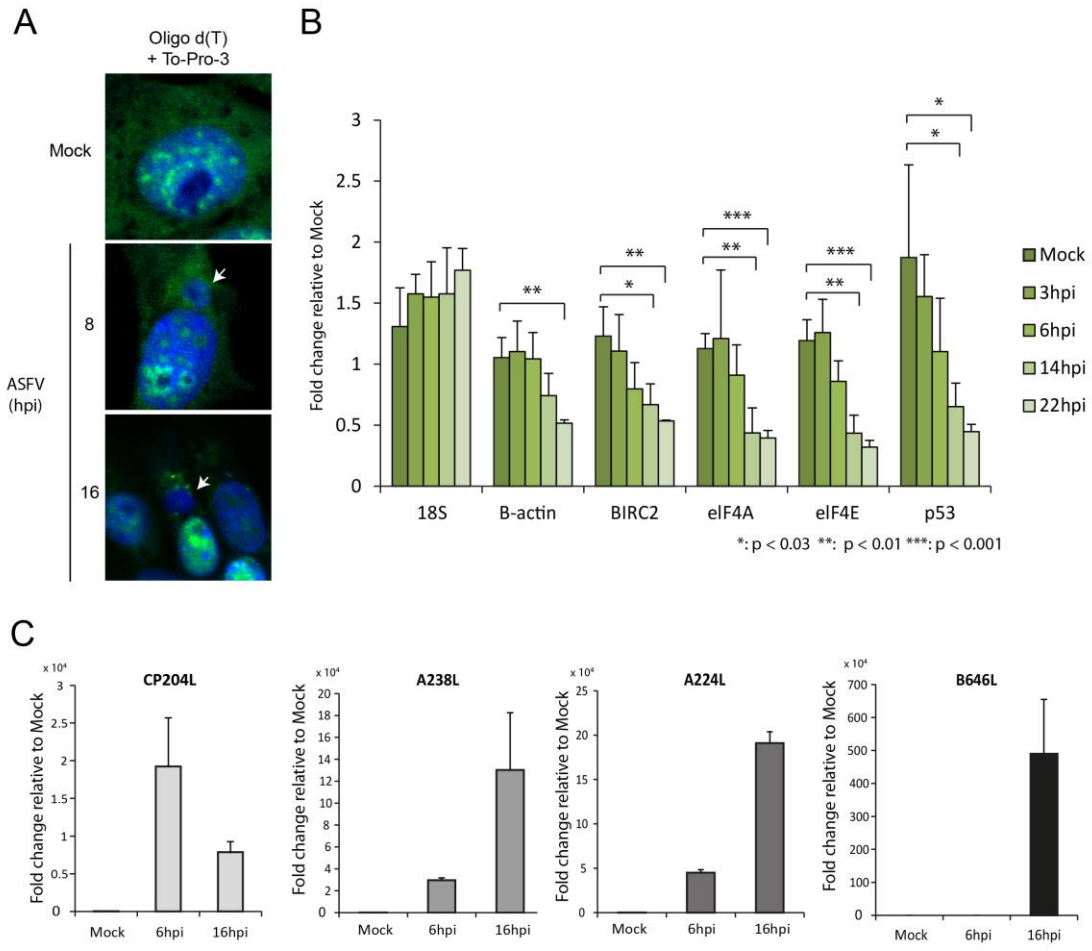

Figure 12. Effect of ASFV infection on cellular and viral mRNAs.
A) Analysis of poly(A) mRNA distribution during ASFV infection. Vero cells were infected with ASFV (M.O.I = 5 pfu/cell) and fixed to glass coverslip at indicated hours post infection (hpi). Poly(A) mRNAs were localized using a specific Oligo d(T) fluorescein tagged probe (green) and To-Pro-3 (blue) was used to stain viral and cellular DNA. Arrows show the viral factories. **B)** Quantification of the cellular mRNA levels during ASFV infection. Vero cells were infected with 5 pfu/cell and samples were recovered at different times post infection. After RNA extraction, cellular mRNA levels of representative genes were measured by RT-qPCR. RNA values (mean+/-S.D) were referred to Mock (n=3) *: $p < 0.03$ **: $p < 0.01$ ***: $p < 0.001$. **C)** Quantification of the viral mRNA levels during ASFV infection. Vero cells were infected with 1 pfu/cell and samples were recovered at different times post infection. After RNA extraction, mRNA levels of viral representative genes (CP204L, A238L, A224L and B646L) were measured by qRT-PCR. RNA values (mean+/-S.D) were referred to Mock (n=2).

Next we analysed representative early, early-late and late viral mRNA levels during ASFV infection. On the contrary to cellular mRNAs, viral mRNAs importantly increased during the infection. In this respect, mRNA from the early protein p32 (CP204L gene (Prados *et al.*, 1993)) displayed its maximum expression at 6hpi (Figure 12 C, left panel), mRNA from the viral protein A238L began its expression at early times post infection but raised its maximum at later times post infection (Figure 12 C, middle-left panel (Granja *et al.*, 2006a)), and late viral genes such as A224L (Chacon *et al.*, 1995) and B604L (p72 protein (Garcia-Escudero and Vinuela, 2000)) were expressed after viral replication (approximately 6-8 hpi) and raised its maximum at late times post infection (Figure 12 C, right panels).

Taken together, these results corroborate the previous data obtained in section 4.1.2, indicating that, during ASFV infection, degradation of cellular mRNA is activated, which produces a decrease of cellular protein synthesis at late times post infection. On the other hand, viral mRNAs are fully expressed and somehow excluded from this degradation by a still not fully understood mechanism.

4.1.3 ASFV late mRNAs are localized surrounding the viral factories

We demonstrated in previous section that despite mRNA levels decrease during the infection, a bulk of poly(A) mRNAs remains and is clustered around the viral factories (Figure 12). It has been previously described that in vaccinia infection, viral mRNAs are recruited to replication sites in order to promote and facilitate viral protein synthesis (Katsafanas and Moss, 2007). We hypothesise that ASFV could be using a similar strategy, and in order to explain the experimental observation described in 4.1.2, we analyse the location of viral mRNAs by FISH using FITC fluorescein probes that specifically recognise viral p72 and A224L mRNAs. Signals corresponding to p72 and A224L probes were mainly detected surrounding viral factories, while, as expected, no cytoplasmic signal in Mock-infected cells was detected (Figure 13). Considering that viral factory is a compartment in some way separated from the cytoplasm of the cell (Salas and Andres, 2013), these images could indicate that viral mRNAs corresponding to late viral proteins are clustered close to viral replication sites, where they would be protected from cellular and viral mechanisms of degradation.

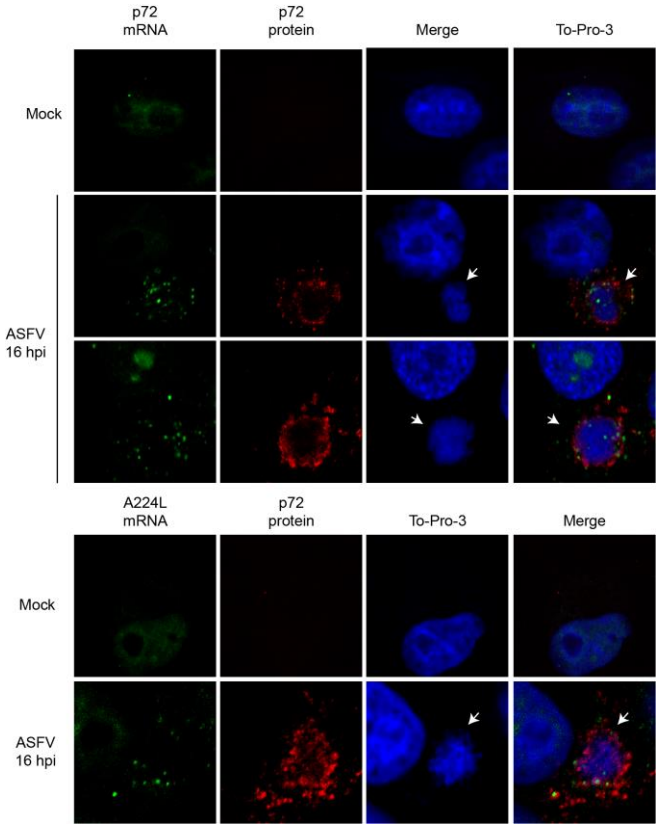

Figure 13. Late viral mRNAs localize at the periphery of the viral factories.
Vero cells were Mock-infected or ASFV-infected (M.O.I = 5 pfu/cell) and fixed at 16 hours post infection (hpi).Viral mRNAs were detected using specific fluorescein probes (green) against both viral p72 mRNA (upper panels) and A224L mRNA (bottom panels).Infection progress was tested in both cases using a specific antibody against the viral protein p72 (red). Cellular nucleus and viral factories were stained with To-Pro-3 (blue). Arrows show the viral factories.

4.2 ASFV g5R PROTEIN

After the findings presented above and due to the fact of ASFV encodes for a protein (g5Rp) that has been shown to display decapping activity in vitro (Parrish *et al.*, 2009) we conjectured whether g5Rp could act as a viral decapping enzyme *in vivo* implicated in both the temporal regulation of viral genes and in the degradation of cellular mRNAs.

4.2.1 ASFV g5R protein possesses a Nudix motif

ASFV Ba71V genome contains 150 ORFs encoding for numerous proteins (Dixon *et al.*, 2013). One of them is g5Rp (D250R gene in Ba71V isolate), which possesses a canonical Nudix motif sequence (Cartwright *et al.*, 2002; Parrish *et al.*, 2009). In order to analyse the homology of Ba71V g5Rp Nudix motif with other well-known decapping enzymes, we aligned g5Rp Nudix amino acidic sequence with the corresponding Nudix motif of the human Dcp2 (hDcp2) and Nudt16 enzymes, yeast *S.cerevisiae* and *S.pombe* Dcp2 enzymes (SpDcp2 and ScDcp2) and the viral proteins D9 and D10 from vaccinia. We observed that g5Rp shares a minimum of 17% of identity with all the analysed sequences, sharing most similarities with Dcp2 from *S.pombe* (21.46 % of homology, Table 5 and Figure 14 A). Indeed, g5Rp not only possesses all the amino acids highly conserved among all these enzymes, but also shares structural homology with them: g5Rp structure could be predicted based on SpDcp2 crystal structure (Figure 14 B). Maximum structural similarities between both enzymes were found in the helix structure of the catalytic Nudix motif, while N-terminal and C-terminal domains share lower similarities. These side domains of the Nudix motif are commonly implicated in regulation of the decapping activity and are less conserved in this kind of viral enzymes (McLennan, 2007). These results indicate that g5Rp possesses a conserved Nudix domain, signalling it as a possible ASFV decapping enzyme.

Protein	VACV D10	VACV D9	Human Nutd16	**ASFV g5Rp**	S.cerevisiae Dcp2	human Dcp2	S.pombe Dcp2
VACV D10	100	23.79	15.44	16.49	18.81	12.87	18,81
VACV D9	23.79	100	17.12	19.19	18.82	14.62	19,77
Human Nutd16	15.44	17.12	100	17.61	16.77	16.35	18,87
ASFV g5Rp	16.49	19.19	17.61	100	19.63	16.44	21,46
S.cerevisiae Dcp2	18.81	18.82	16.77	19.63	100	26.96	29,86
human Dcp2	12.87	14.62	16.35	16.44	26.96	100	37,5
S.cerevisiae Dcp2	18.81	19.77	18.87	21.46	29.86	37,5	100

Table 5. Percent identity matrix of ASFV g5R protein.
The Nudix sequence of different decapping enzymes and ASFV g5R protein were aligned in order to determine g5Rp homology. Percentage of identity was extracted from the alignment using Clustal-Ω software.

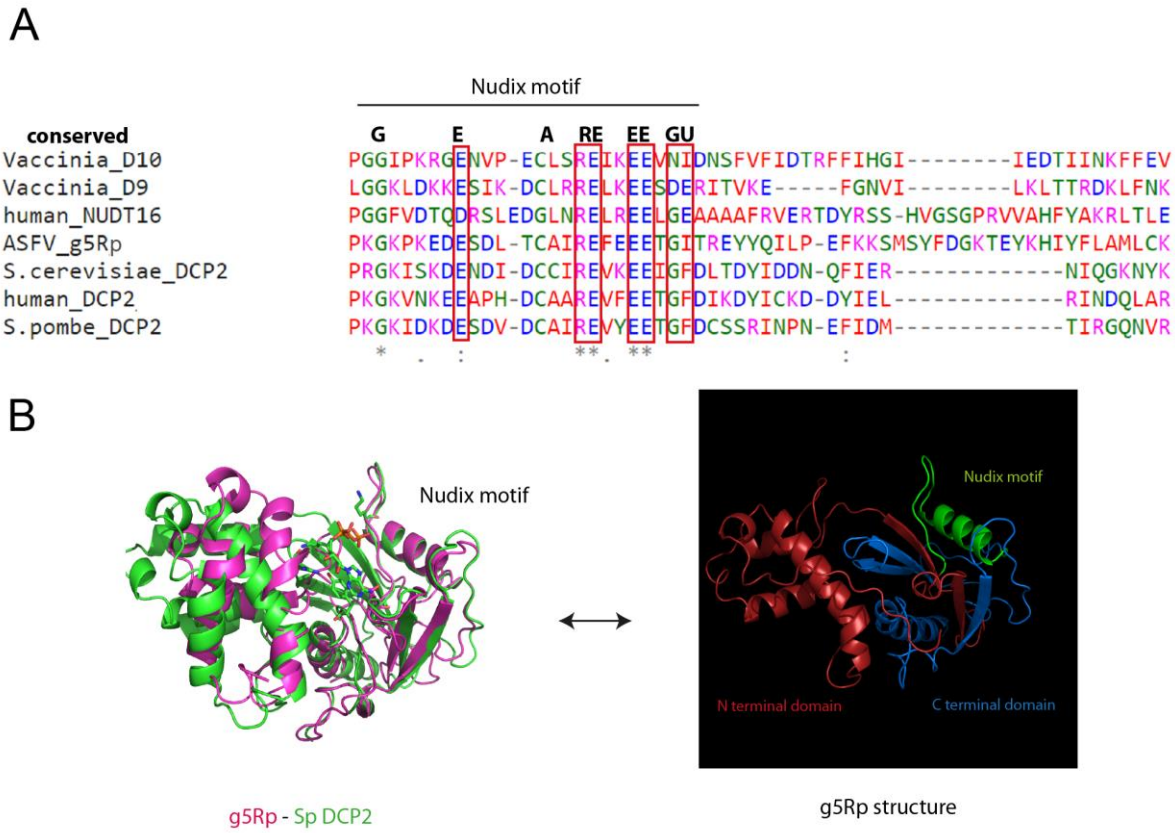

Figure 14. ASFV g5R protein possesses a Nudix domain.
A) Alignment of g5Rp Nudix motif sequence with other viral and eukaryotic conserved Nudix amino acidic sequences. Alignments were done with the Clustal-Ω software (EMBL). Colours represent the different characteristics of the amino acids: small and hydrophobic (red), acidic (blue), basic (magenta), Hydroxyl, sulfhydryl, amine or G residues (green) and others (grey). *: (asterisk) positions which have a single, fully conserved residue; : (colon) conservation between groups of strongly similar properties; . (period) conservation between groups of weakly similar properties. **B)** Structural prediction of g5R protein based in Dcp2 (Decapping Enzyme 2) of *S. pombe*. g5Rp structure is shown in pink and SpDcp2 structure is shown in green (left panel). g5Rp structure is represented alone in the right panel. The N-terminal domain, the C-terminal domain and the Nudix motif of the protein are shown in red, blue and green, respectively.

4.2.2 g5R protein is expressed at early times post ASFV infection

In order to investigate the function of this protein, we first studied g5Rp expression in ASFV infected cells. With that purpose, we generated a specific anti-g5Rp serum by successive injection of purified GST-g5Rp wt recombinant protein obtained from *E.coli* in two rabbits (1232 and 1233). Resulting serums were tested by Western Blot and ELISA (Figure 15 A), and its specificity validated by IP and Mass Spectrometry sequencing (data not shown). Both specific g5Rp serums recognized a protein with the expected size (30 kDa) that was exclusively detected in ASFV-infected cells (Figure 15 B). To analyse the kinetic of expression of g5Rp during the infection, Vero cells were Mock-infected or ASFV-infected with M.O.I 5 pfu/cell and harvested at indicated times post infection. g5Rp levels were analysed by Western blot using the specific anti-g5Rp serum. Tubulin was used as loading control. We observed that g5R protein is expressed as early as 4 hour post infection (hpi) and accumulates until late times post infection (24 hpi) (Figure 15 B).

ASFV infection is characterized by a tune temporal regulation of viral gene expression, which allows transcripts to be classified as immediate early, early, intermediate or late depending on its distinctive

accumulation kinetics and on its expression in the presence of inhibitors of viral replication (reviewed on (Rodriguez and Salas, 2013). AraC is a cytosine analogue that possesses arabinose instead of the ribose motif. When added to cells, AraC incorporates to DNA and blocks replication, while in ASFV infected cells, AraC has been shown to impair viral replication, thus producing a loss of intermediate and late gene expression (Figure 15 C middle panels, Figure 15 D bottom panels and (Almazan *et al.*, 1993; Rodriguez *et al.*, 1996)). Therefore, g5R mRNA and protein expression were tested in Mock-infected or ASFV-infected cells in the presence or absence of AraC. g5R protein and mRNA levels were analysed by Western Blot and RT-PCR, respectively. In these conditions, both g5R mRNA and protein were detected in the presence of AraC, indicating that g5Rp expression does not require viral replication and/or viral late protein expression (Figure 15 C and D, upper panels). However, AraC presence also produced a slightly decrease in both protein and mRNA g5Rp levels, suggesting that g5R mRNA could be synthetized at two different times during ASFV infection. This is, in fact, a common feature of some early and immediate early ASFV genes (Rodriguez and Salas, 2013).

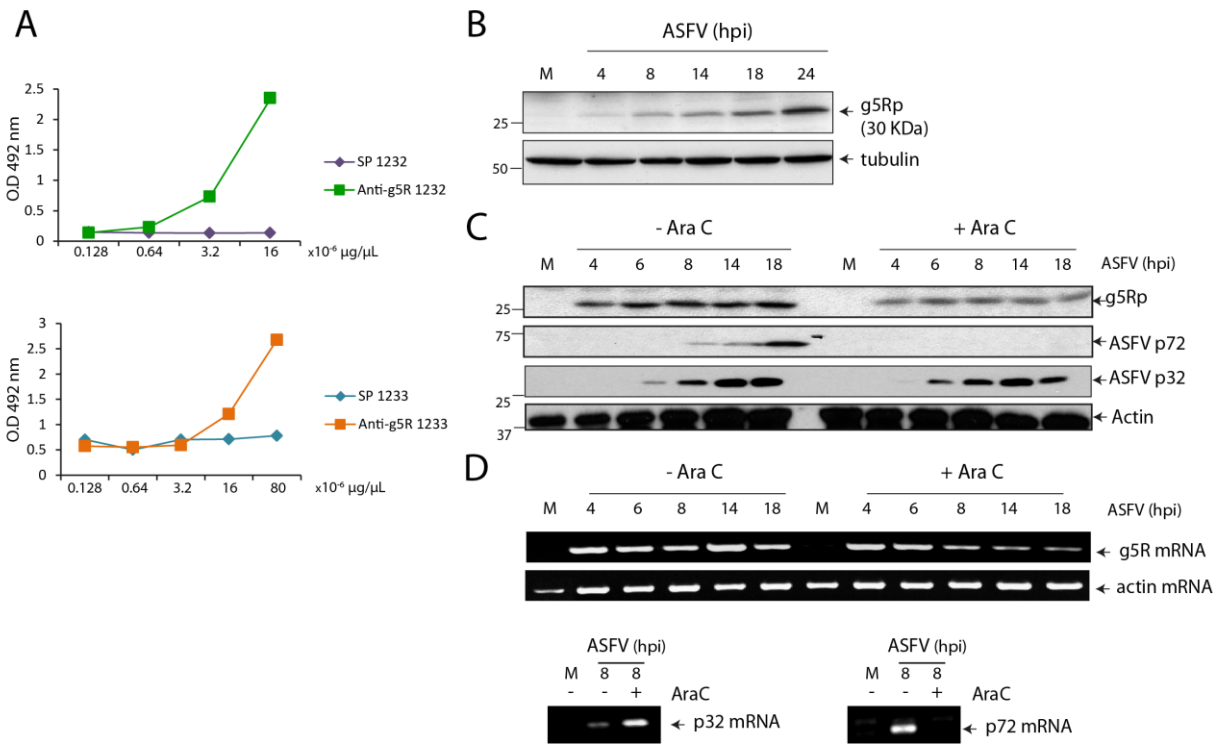

Figure 15. g5Rp expression during ASFV infection.
A) Specific serums raised against g5R protein were obtained by successive injection of the recombinant GST-g5R protein in two different rabbits (1232 and 1233) and titrated by ELISA. Previous serums from both rabbits (SP 1232 and SP 1233) were used as negative control (purple and blue). Specific anti-g5Rp serums form rabbits 1232 and 1233 are represented in green and orange, respectively. **B)** g5Rp is expressed at early time post infection and accumulates until late times post infection. At indicated times after infection, Mock-infected and ASFV-infected Vero cells (M.O.I = 5 pfu/cell) were lysate in sample buffer and g5R protein levels were analysed by Western Blot (WB) using the specific anti-g5Rp serum (1233). Tubulin was used as loading control. **C)** and **D)**. Vero cells were Mock-infected or ASFV-infected in the presence or the absence of the inhibitor of the viral replication, AraC (40 µg/mL). Samples were recovered at indicated times post infection to analyse g5R protein or mRNA levels by Western blot (C) or RT-PCR (D), respectively. In both cases, p32 (an early viral gene) and p72 (a late viral gene) protein or mRNA were used to confirm the effect of AraC, and actin was used as loading control. C) g5R protein levels were measured by WB using the specific anti-g5Rp serum, while p72 and p32 levels were analysed using specific antibodies. D) mRNA levels of g5Rp, p32 and p72 were measure by RT-PCR using specific probes. Data are representative images from two separate experiments.

4.2.3 g5R protein location during ASFV infection

Once we determined the kinetic of expression of g5Rp, we elucidate the subcellular distribution of the protein, to further study its role during the infection. *Cartwright et al*. previously suggested that g5Rp exhibits an endoplasmic reticulum (ER) pattern. To localize the protein, the authors used a construction that expresses g5Rp from Malawi ASFV strain tagged to the HA epitope under control of its own viral promoter (Cartwright *et al.*, 2002). With the purpose of validate that suggestion in our conditions, we generated a similar construction to that mentioned above, which contains Ba71V g5R protein tagged to HA epitope under the control of viral g5Rp promoter (promg5Rp-HA), in such a way that ASFV infection is required to express the cloned g5Rp-HA. A schematic representation of this vector is shown in Figure 16 A. After transfection in COS-7 cells followed by infection with ASFV Ba71V (M.O.I = 5 pfu/cell) this construction allowed us to locate g5Rp in the context of the infection. We used a specific antibody that recognise the well-known ER protein calnexin (Tjoelker *et al.*, 1994) to detect ER, and anti-HA antibody to localize g5Rp. At the indicated times post infection, cells were fixed and protein localization was analysed by immunofluorescence and CLSM. Mock cells were used as negative control. Progression of viral infection was assessed by the presence of the viral factories, which, together with cellular DNA, were stained with DAPI. We detected that g5Rp presented a similar distribution pattern to that displayed by calnexin during all the viral cycle, indicating that g5Rp exhibits ER localization, a fact possibly related to its function (Figure 16 B). Interestingly, g5Rp was accumulated to the periphery of the viral factories at late times post infection. ASFV infection leads to the collapse of ER (Andres *et al.*, 1998; Windsor *et al.*, 2012). Indeed, it has been previously described that viral membranes precursors are derived from the ER cisternae, which are recruited to the viral factory and later modified (Salas and Andres, 2013). This fact explains the presence of both calnexin and g5Rp at the periphery of the viral replication sites at late times post infection. To confirm our results, we further studied g5Rp location by analysing the distribution of g5Rp compared with the ASFV major capsid protein p72, which localizes at the viral factories (Epifano *et al.*, 2006; Garcia-Escudero *et al.*, 1998). We used the anti-g5Rp serum (1233) and a specific monoclonal anti p72 antibody to localize both proteins. As it is shown in Figure 16 C, at 16 hpi p72 was found within the viral factories, while g5Rp was located at the surroundings of these structures. Additionally, and in order to discard possible side effects of HA epitope, we analysed g5Rp-HA location using both anti HA and anti g5Rp specific antibodies by CSLM in ASFV-infected COS-7 cells (16 hpi). Both products co-localized precisely (Figure 16 D), indicating that HA flag did not interfere in g5Rp distribution.

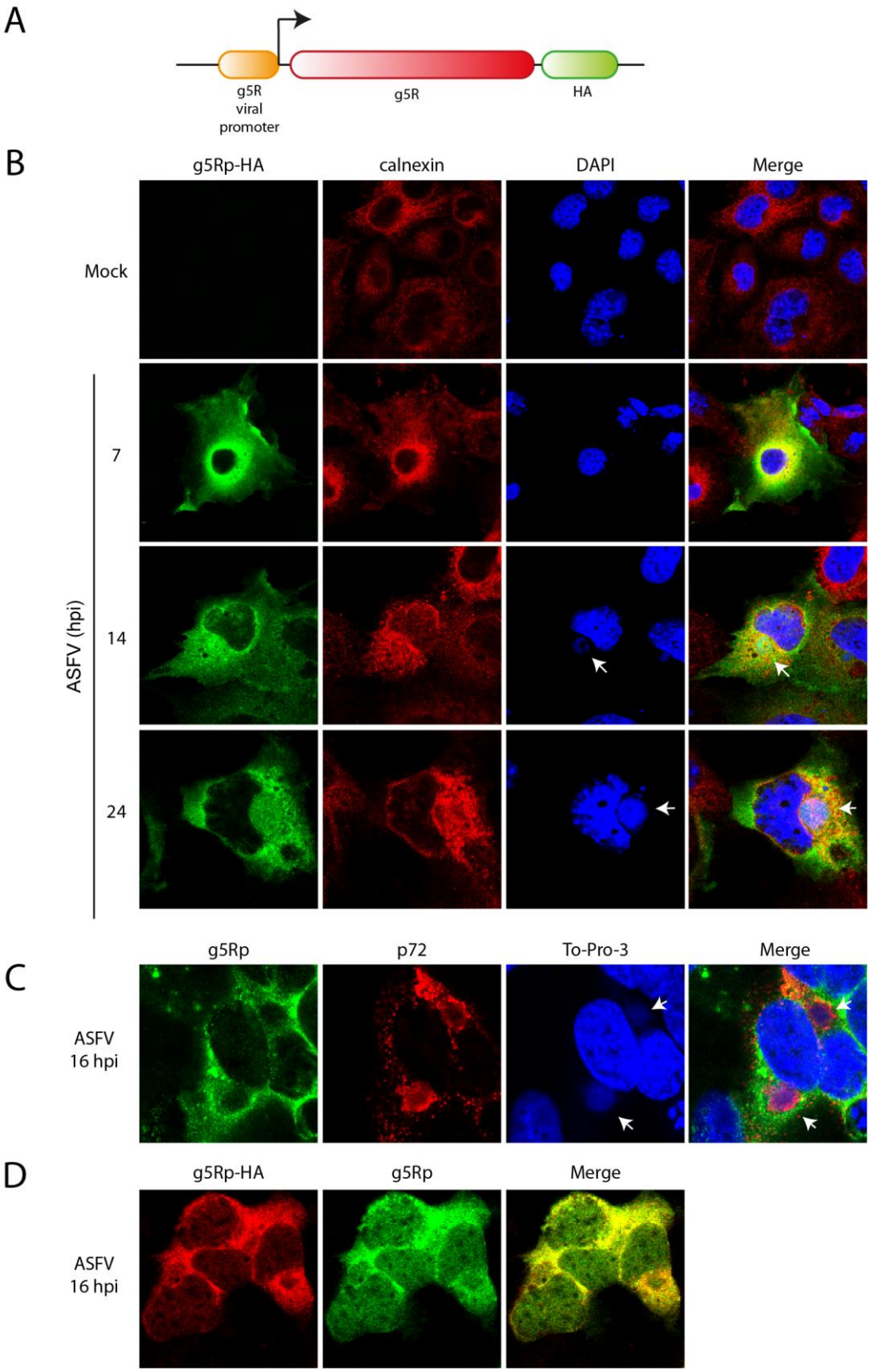

Figure 16. Localization of g5R protein during ASFV infection.

A) Schematic representation of the promg5R-HA plasmid used to localize g5Rp during ASFV infection. g5R sequence was cloned in frame with the Hemaglutinin (HA) epitope under the control of the g5R viral promoter. **B)** and **D)** COS-7 cells were transfected with promg5R-HA vector, infected with ASFV (M.O.I = 5pfu/cell) and fixed at indicated times post infection. B) Calnexin and g5Rp were localised using specific anti-HA (green) and anti-calnexin (red) antibodies. The progress of the infection was checked by detecting the presence of the viral factories. Cellular and viral DNA was stained with DAPI (blue). **C)** g5R protein localizes on the surroundings of the viral factories in ASFV-infected COS-7 cells at late times post infection (16 hpi). g5Rp and p72 locations were detected using anti-g5Rp (1233) and anti-p72 specific serums (green and red, respectively). D) HA epitope does not affect g5Rp distribution. g5Rp-HA location was analysed in ASFV-infected COS-7 cells (16 hpi) using both ant-HA antibody and the specific anti-g5Rp serum (1233). Arrows show the viral factories. Data are representative images from two separate experiments.

4.2.4 g5Rp binds cellular poly(A) RNA in cultured cells

In order to analyse g5Rp function *in vivo*, we generated six stable HeLa Flip TREx cell lines that express GFP tagged to g5Rp wt form or different GFP-g5Rp variants. GFP-g5Rp REGG and GFP-g5Rp EEQQ possess single-site mutations in two different conserved glutamate residues of the g5Rp Nudix motif that make them unable to decapp *in vitro* (Parrish *et al.*, 2009). With the aim of mapping the g5Rp functional domains, three additional variants of the protein were constructed. The constructions named GFP-g5R N-term and GFP-g5R C-term contain only the g5Rp N-terminal or C-terminal domains, respectively. (We stablished both domains taking Nudix sequence as reference: N-terminal domain protein contains the sequence of g5Rp upstream of the Nudix conserved motif, while C-terminal domain protein covers the sequence downstream of the Nudix). The GFP-g5Rp ΔNudix is a fusion protein that possesses both N-terminal and C-terminal domains but lacks the g5Rp Nudix motif. A schematic representation of all generated constructions is showed in Figure 17 A and a more detailed description of the constructions can be found in Material and Methods section.

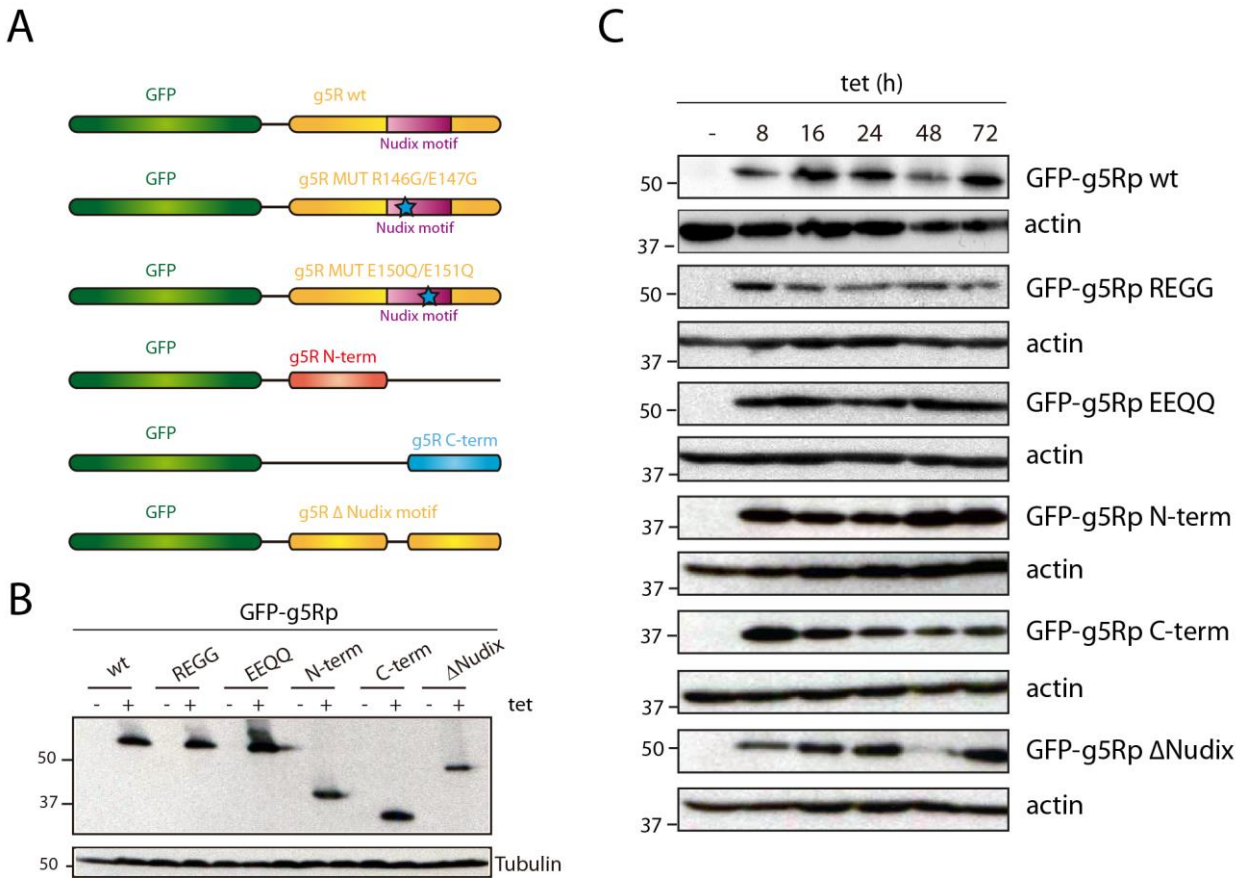

Figure 17. Generation of stable HeLa cell lines GFP-g5Rp.
A) Schematic representation of the six vectors constructed containing GFP tagged to i) g5R wild type (wt), ii) two punctual mutants of the Nudix domain of g5R (GFP-g5R R146G/E147G or REGG and E150Q/E151Q or EEQQ),iii) the N-terminal domain of g5R (GFP-g5R N-term), iv) the C-terminal domain (GFP-g5R C-term), and v) a deletion mutant that lack the Nudix domain (GFP-g5R ΔNudix motif). These vectors were used to generate 6 stable HeLa cell lines able to express the recombinant proteins after the addition of tetracycline (tet). **B)** and **C)** Analysis of the size (B) and the kinetics of expression (C) of the recombinant proteins by Western Blot. Specific anti-GFP antibody was used to analyse the expression of the GFP-g5Rp fusion proteins and tubulin (B) and actin (C) were used as loading control. Data are representative images from two separate experiments. h:hours

HeLa Flip TREx cell lines (Invitrogen) are characterized by containing a unique genomic site for integration of the gene of interest (Flp site) and by holding a copy of the Tet Repressor. Co-transfection of pCDNA5/FRT/TO (enclosing the gene of interest) and pOG44 (codifying for Flp recombinase) allowed us to generate stable cells lines with one copy of the gene of interest integrated on its genome that express the fusion protein only in the presence of tetracycline. Size and expression of the different GFP-g5R proteins were analysed by fluorescent microscopy (data not shown) and by Western blot (Figure 17 B and C). As expected, GFP-g5Rp fusion proteins were only expressed in tetracycline presence (indicating that there was no unspecific protein synthesis) and all of them showed the expected sizes (Figure 17 B). Furthermore, and in respect to the kinetic of expression of the constructs, all of the fusion proteins tested were expressed from 8 until 72 hours in constant presence of tetracycline (Figure 17 C).

In order to determine the possible role of g5Rp in mRNA metabolism in cultured cells, after screening the level of expression of the different GFP-g5Rp constructs, we next analysed RNA binding ability of the recombinant proteins. We used a dual fluorescence method, which has been described as a useful technique to measure RNA-protein interactions (Strein *et al.*, 2014). In this system, HeLa eGFP is used as negative control (as GFP is a well-known non RNA-binding protein) (Strein *et al.*, 2014). Figure 18 shows a schematic representation of the experimental procedure.

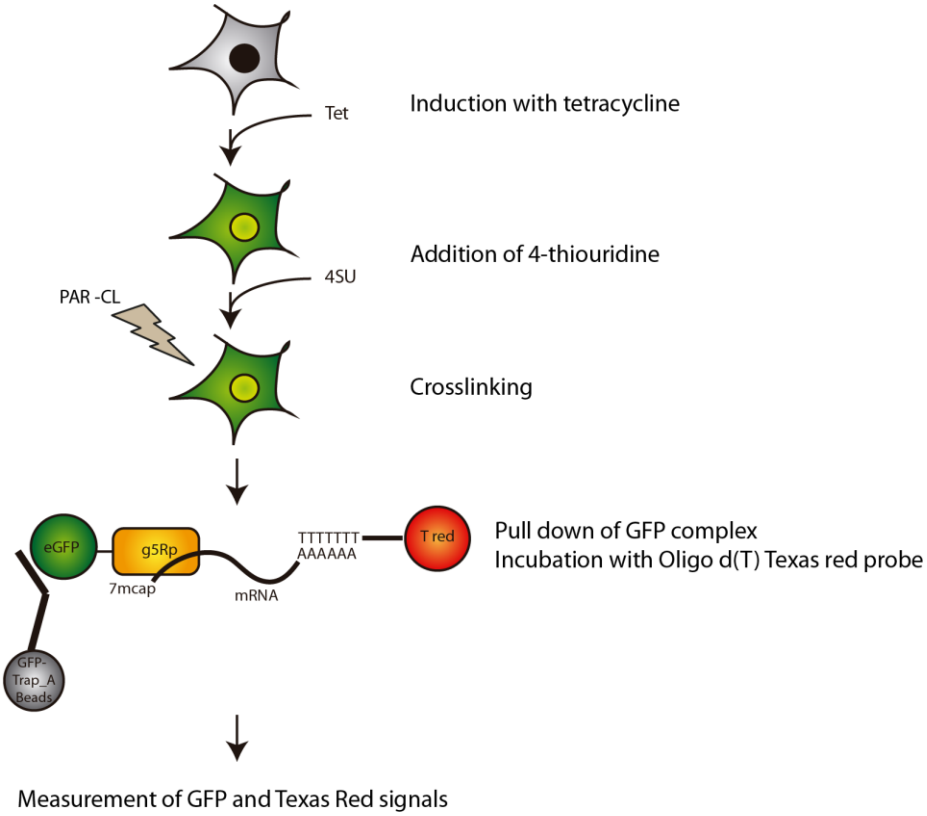

Figure 18. Schematic representation of the dual fluorescence method.
HeLa cells were treated with tetracycline during 18 hours (O/N) in order to induce the expression of GFP-g5Rp recombinant proteins. RNA-protein interaction was fixed by PAR-Crosslinking (PAR-CL), and the fusion proteins were immunoprecipitated using an antibody anti-GFP covalently coupled to the surface of agarose beads (GFP-Trap_A). The immunoprecipitated complexes were then incubated with Oligo d(T) Texas Red probe (T Red). Quantification of the RNA bound to the different proteins was carried out by measuring the GFP and the Texas red signal in a TECAN Safire II microplate reader.

Briefly, the different HeLa cell lines expressing GFP-g5Rp wt, GFP-g5Rp constructs or eGFP were induced with tetracycline (tet) and incubated with 4-thiouridine (4-SU) O/N (18 hours), which was added 2 hours prior the induction in order to be incorporated into nascent RNA and to fix the RNA-protein interactions by PAR-crosslinking. GFP fusion proteins were then immunoprecipitated using GFP-Trap_A beads and resulting complexes were incubated with Oligo d(T)-Texas Red probe. Specificity of immunoprecipitation process was tested by SDS-PAGE and silver staining (data not shown), while the specificity of the RNA binding was demonstrated by treatment with RNases A and T1. GFP and Texas red fluorescent signals were measured and Texas Red signal/eGFP signal rate was used as a method to quantify the RNA bound per complex. As Figure 19 shows, GFP-g5Rp wt protein was able to bind around 25 folds more RNA compared to eGFP, demonstrating that g5Rp is acting as a RNA-binding protein in this system. In addition, the level of RNAs bound to the g5Rp catalytic mutants showed no significant differences in relation to GFP-g5Rp wt, suggesting that these mutations, although reported to be important for the catalytic process *in vitro* (Parrish *et al.*, 2009), are not implicated in RNA binding.

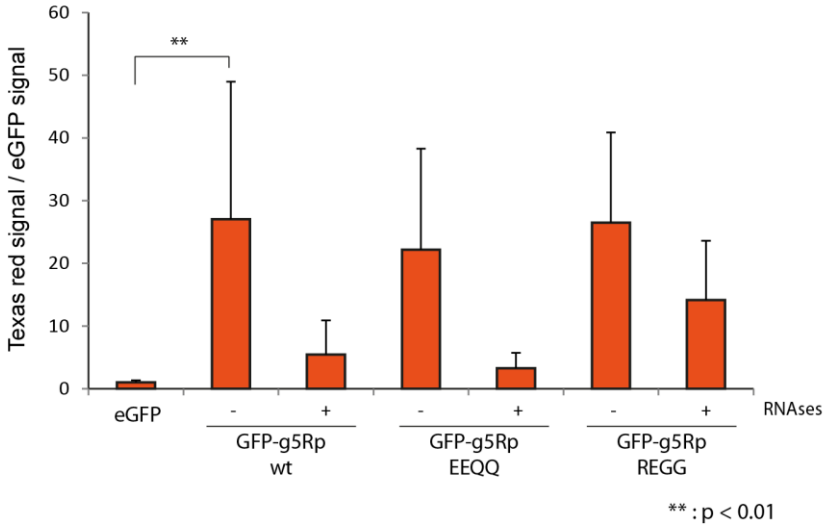

Figure 19. g5R protein binds poly(A) RNA in cultured HeLa cell lines.
HeLa cells were induced with tetracycline O/N for the expression of eGFP, GFP-g5Rp wt and GFP-g5Rp catalytic mutants (REGG and EEQQ). RNA levels bound to the different fusion proteins were analysed by the dual fluorescence method. RNAses A and T1 treatment was carried out as specificity control. +/– symbols indicates presence or absence of this treatment. RNA values (mean+/-S.D) were expressed at the ratio of the Texas Red signal/eGFP signal and referred to eGFP. **: p < 0,01 (n=3).

4.2.5 N–terminal domain of g5Rp is mainly involved in RNA interaction

Interestingly, when we analysed the RNA bound to the different g5Rp domains (described in Figure 17), we observed that GFP-g5Rp N-terminal was able to bind 10 folds more RNA than either GFP-g5Rp wt or GFP-g5Rp C-terminal domain, while the ΔNudix construction bound considerably less than the N-terminal domain but more than the wt form (Figure 20 A).These results point to the N-terminal domain as a main player in g5Rp-RNA interaction, while the C-terminal domain seems not to be directly implicated in this function. On the other hand, the Nudix domain, although indispensable for the decapping activity *in vitro* (Dunckley and Parker, 1999; Parrish *et al.*, 2009; Parrish *et al.*, 2007; Song *et al.*, 2013) is not essential for the

RNA binding. Furthermore, and interestingly, the absence of the Nudix domain contributed to the stability of the RNA binding, probably due to the fact of no degradation of the bound RNA, as no decapping activity in this mutant can be expected. In order to further study the difference among RNA levels bound to the different domains of the viral protein, we have accomplished g5Rp surface electrostatic representation using *PyMol* software. According with the charge, protein surface is represented in red (negative) or blue (positive) (Figure 20 B and C). We observed that the N-terminal domain of the protein presents a basic channel, which could act as a RNA-binding platform (Figure 20 B). This structure is characteristic and exclusive of this domain, as we did not find it when the C-terminal domain was explored (Figure 20 C). These results correlate with the experimental data obtained from dual fluorescence analysis and support the hypothesis that g5Rp N-terminal domain is the main responsible for the g5Rp-RNA interaction. This data also draw a parallel with the data reported in the literature, conferring importance to this channel in the RNA-binding activity (Deshmukh *et al.*, 2008; She *et al.*, 2008).

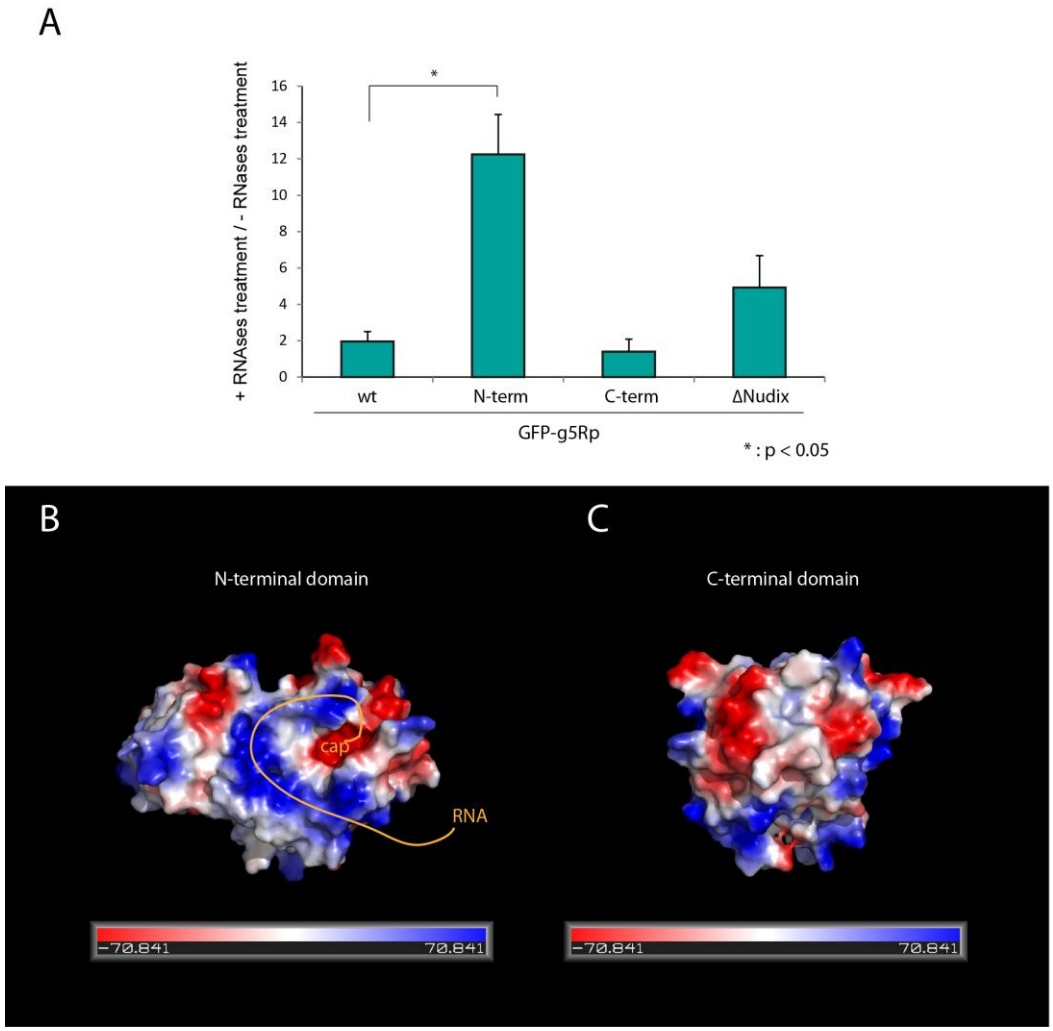

Figure 20. The N-Terminal domain of g5Rp is mainly involved in the RNA-g5Rp interaction.
A) RNA levels bound to the recombinant proteins GFP-g5Rp wt, GFP-g5Rp N-terminal, GFP-g5Rp C-terminal and GFP-g5Rp ΔNudix were measured after its induction in HeLa cell lines using the dual fluorescence method. In this case, RNA values (mean+/-S.D) were expressed at the ratio of the RNAses treatment/no RNAses treatment and referred to eGFP. *: $p < 0,01$. (n=3) **B)** and **C)** Electrostatic surface representation of g5R protein. According with the charge, protein surface is represented in red (negative) or blue (positive). B) Electrostatic surface representation of the g5Rp N-terminal domain and the Nudix motif. The hypothetical interaction site of cap structure and mRNA is shown in orange. C) Electrostatic surface representation of the g5Rp C-terminal domain.

4.3 g5Rp EFFECT ON ASFV INFECTION

4.3.1 g5Rp overexpression affects viral protein levels

Our previous results indicate that g5Rp is able to bind RNA *in vivo*, which point to g5Rp to be implicated in RNA regulation during the infection, which probably affects to the synthesis of the viral proteins overall. To test this possibility we studied ASFV infection on HeLa cells ectopically expressing different constructions of g5Rp, after induction with tetracycline (tet). First, and in order to elucidate possible side-effects of tet on ASFV infection, we tested viral protein synthesis in the presence of the antibiotic in COS-7 cells by using Ba71V (M.O.I = 2 pfu/cell) to infect cells. The ASFV protein levels were analysed by Western blot using a specific antibody developed against ASFV-infected Vero cells (kindly gifted by Dr. A.L. Carrascosa) (anti-ASFV). We confirmed that the presence of tet did not affect the viral protein synthesis (Figure 21 A). Next, and in order to analyse the effect of the GFP-g5Rp wt protein on ASFV infection, we induced the expression of eGFP or GFP-g5Rp wt in HeLa cells and then infected the cultures with ASFV (M.O.I = 2 pfu/cell). Viral protein levels were analyzed by Western blot with anti-ASFV antibody.

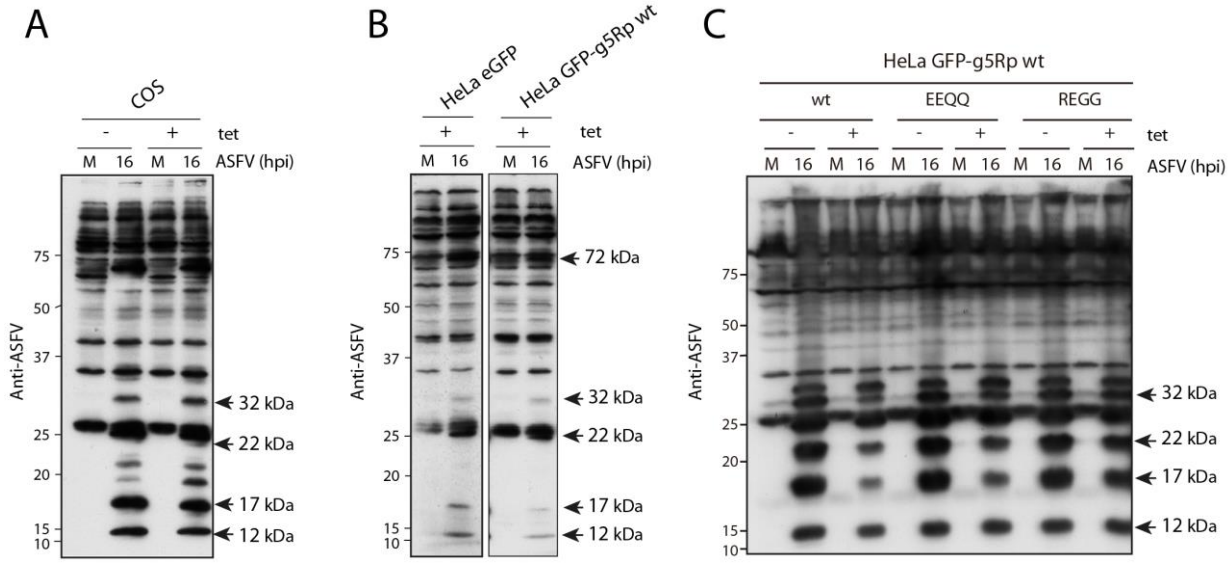

Figure 21. Expression of GFP-g5Rp wt causes a slightly decrease on several ASFV viral proteins on infected HeLa cells.
A) Effect of tetracycline in ASFV infection. COS-7 cells were Mock-infected or ASFV-infected (M.O.I = 2 pfu/cell) in the absence or presence of tetracycline (tet), and samples were recovered at 16 hours post infection (hpi). ASFV protein levels were analysed by SDS-PAGE and immunoblotting with a specific antibody that recognises ASFV induced proteins (anti-ASFV).**B)** and **C)** Effect of GFP-g5Rp wt overexpression on ASFV infection. HeLa cells were treated with tetracycline (tet) O/N to induce eGFP and GFP-g5Rp wt proteins (B) or GFP-g5Rp wt, REGG, and EEQQ proteins (C) and then Mock infected or ASFV-infected with M.O.I of 2 or 5 pfu/cell, respectively. ASFV protein levels were analysed by Western blot using anti-ASFV serum in both cases. Data are representative images from two separate experiments.

As Figure 21 B shows, a slightly decrease on the level of several late ASFV proteins, like p17 and p12, was observed in extracts from GFP-g5Rp wt-expressing cells, compared to GFP. Finally, we induced and infected HeLa cells stably expressing GFP-g5Rp wt, GFP-g5Rp REGG and GFP-g5Rp EEQQ and analysed ASFV protein levels by Western blot in the presence or the absence of tet. Again, we observed a slightly decrease in the level of ASFV-proteins corresponding to molecular weight (MW) 32, 22, 17 and 12 KDa when HeLa

GFP-g5Rp wt cells were analysed, a reduction that was less significant in HeLa GFP-REGG-or EEQQ expressing cells (Figure 21 C). These results suggested that g5Rp expression under the control of the stable pCMV promoter from the beginning of the viral cycle could affect viral protein synthesis due to the putative decapping activity of g5Rp, reinforced by the fact of minor effect was observed in the Nudix-mutants expressing cells.

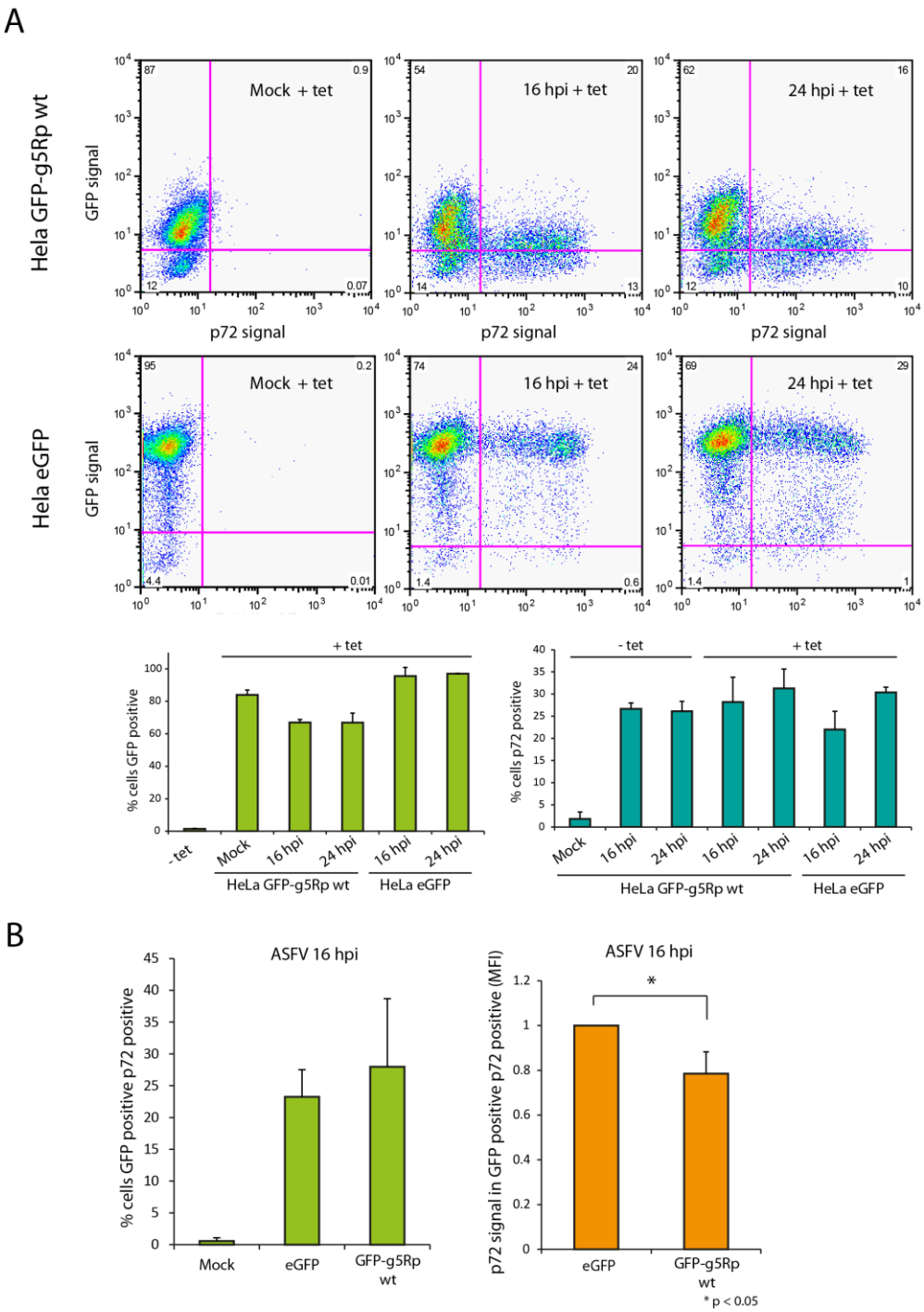

Figure 22. ASFV-infected HeLa cells expressing GFP-g5Rp wt display reduced levels of the viral protein p72.
HeLa cells were Mock-infected or ASFV-infected (M.O.I = 5 pfu/cell) after O/N induction with tetracycline (tet) to express eGFP or GFP-g5Rp wt. At 16 and 24 hours post infection (hpi) eGFP, GFP-g5Rp wt and p72 levels were analysed by FACS. p72 protein was detected using a specific monoclonal antibody. **A)** Representative images of the population of HeLa cells expressing GFP-g5Rp wt (upper panels) or eGFP (middle panels) and p72 (x axis). Quantification of the percentage of GFP positive or p72 positive cells at 16 and 24 hpi are showed at the bottom (percentage of cells +/- S.D, n=2). **B)** Percentage of GFP positive and p72positive cells at 16 hpi in eGFP or GFP-g5Rp wt expressing cells (right graphic bars, percentage +/- S.EM, n=5) and quantification of the p72 mean signal in these populations of cells (mean fluorescence intensity, MFI +/- S.E.M; n=5).

Since the results mentioned above are important in terms of defining g5Rp as a decapping enzyme during ASFV infection, we further validated the effect of g5Rp expression on the level of viral p72 protein by FACS. To achieve this, HeLa eGFP and HeLa GFP-g5Rp wt cells were induced with tetracycline, Mock-infected or ASFV-infected (M.O.I = 5 pfu/cell), and p72 levels were analysed by using an anti p72 monoclonal antibody at 16 and 24 hpi. As shown in Figure 22 A, both HeLa GFP-g5Rp wt (upper panel) and HeLa eGFP (lower panel) cells were successfully infected and able to synthetized viral p72 protein. Percentage of GFP positive or p72 positive cells in the presence of the absence of tet were represented as bars graphics in Figure 22 A bottom panels (histograms). Both eGFP and GFP-g5Rp wt expression was maintained during the infection (left histogram), and, on the other hand, percentage of p72 positive cells was similar in both stable cell lines and in the presence or absence of tetracycline (right histogram). Interestingly, when the p72 mean fluorescent signal was analysed in GFP positive and p72 positive populations at 16 hpi, a significant decrease in GFP-g5Rp wt cells vs GFP was observed (Figure 22 B). These data indicated that overexpression of GFP-g5Rp wt causes a reduction on p72 levels and that this reduction was not due to a minor infection rate but a specific effect of g5Rp activity on p72 viral protein expression. Taken together, these results suggest a role of ASFV g5Rp as a putative viral decapping enzyme, which seems to function regulating the synthesis of several viral products during the viral cycle.

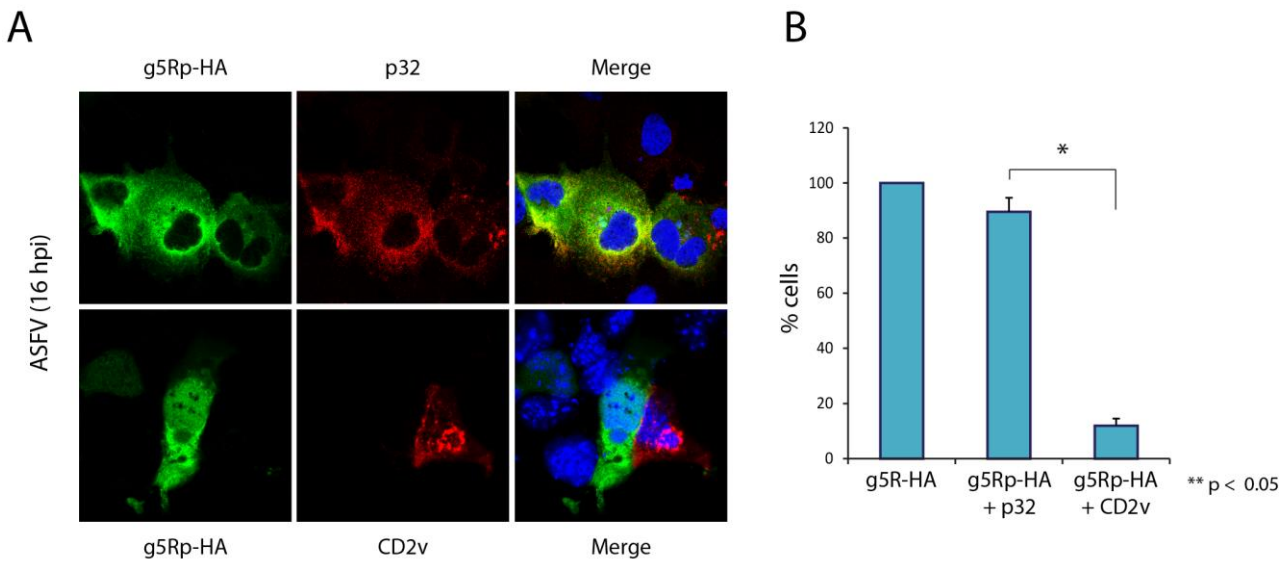

Figure 23. Ectopically expression of g5Rp affects late viral protein CD2v expression.
A) Analysis of cells co-expressing g5Rp-HA and p32 or CD2v viral proteins by CSLM. COS-7 cells were transfected with promg5R-HA vector and ASFV-infected with M.O.I of 5 pfu/cell. At 16 hpi, monolayer was fixed and g5Rp-HA, p32 and CD2v distribution was analysed using specific antibodies. g5Rp-HA is shown in green while p32 and CD2v are shown in red (upper and bottom panels, respectively). **B)** Quantification of cells co-expresing g5Rp-HA and p32 or Cd2v. Data was obtained by counting 339 and 130 transfected cells per condition and is represented referred to total g5Rp-HA expressing cells (mean +/- S.E.M, n = 2). *: $p < 0.05$. Data are representative images from two separate experiments.

Interestingly, we have also observed by CLSM that the number of cells co-expressing g5Rp-HA and p32 (an early, abundant ASFV protein (Prados *et al.*, 1993)) was significantly higher than the number of cells co-expressing g5Rp-HA and CD2v, a late viral protein (Rodriguez *et al.*, 1993) (Figure 23 A).

Quantification of co-expressing cells (g5Rp-HA and p32 or g5Rp-HA and CD2v) was made counting at least 120 g5Rp-HA cells per condition. Percentage was calculated related to total g5Rp-HA transfected cells. (Figure 23 B).

In summary, these results not only corroborated the result explained above, since indicate that g5Rp regulates the expression of ASFV proteins, but also added information about the specific regulation g5Rp-dependent of ASFV late proteins, since it is likely that when g5Rp is overexpressed, a significant lower number of cells expressing both g5Rp and CD2v late protein were detected.

4.3.2 ASFV g5Rp effect on mRNAs

During this Thesis we have demonstrated that g5Rp *perse* is able to bind cellular mRNA when ectopically transfected in HeLa cells (section 4.2.4); furthermore, when overexpressed in the context of the infection, g5Rp produced a decrease in late viral protein levels. Next, we further explore whether this RNA-binding ability also occurs during the viral infection to reinforce the putative role of the protein in binding specific mRNAs.

4.3.2.1 g5Rp is able to bind both viral and cellular mRNAs in the context of ASFV infection

We have analysed g5Rp-RNA interaction by GFP immunoprecipitation and RT-qPCR during the infection. A schematic representation of the experimental procedure is shown in Figure 24 A. HeLa cells stably expressing eGFP and GFP-g5Rp wt were induced with tetracycline and ASFV-infected (M.O.I = 5 pfu/cell) during 7 or 14 hours. RNA-protein interaction was fixed by conventional crosslinking (cCL) and GFP complexes were immunoprecipitated with GFP Trap_A beads. We performed Western blot analysis using anti-GFP antibody to detect fused proteins and to check immunoprecipitation process; and MOV10-YFP expressing cells were used as a positive control of protein-RNA binding (Figure 24 B). After immunoprecipitation, we extracted the RNA bound to the complexes, which was analysed by RT-qPCR amplifying representative cellular (eIF4E and B-actin) and viral (A238L as early-late gene and A224L and p72 as late genes) mRNAs. We observed that GFP-g5Rp wt protein was able to bound both viral and cellular mRNAs in the context of ASFV infection (14 hpi), while eGFP control was not able to bind mRNA at all. Hence, the binding is likely to be specific, as mRNA corresponding to actin, despite the high amount present in the cells, is only weakly bound, compared to eIF4E which is, interestingly, efficiently bound by g5Rp (Figure 24 C).

Furthermore, the fact that g5Rp was able to bind both cellular and viral RNAs, partially supported the hypothesis that the viral protein could be involved in both cellular shutoff and in the regulation of temporal viral RNAs expression.

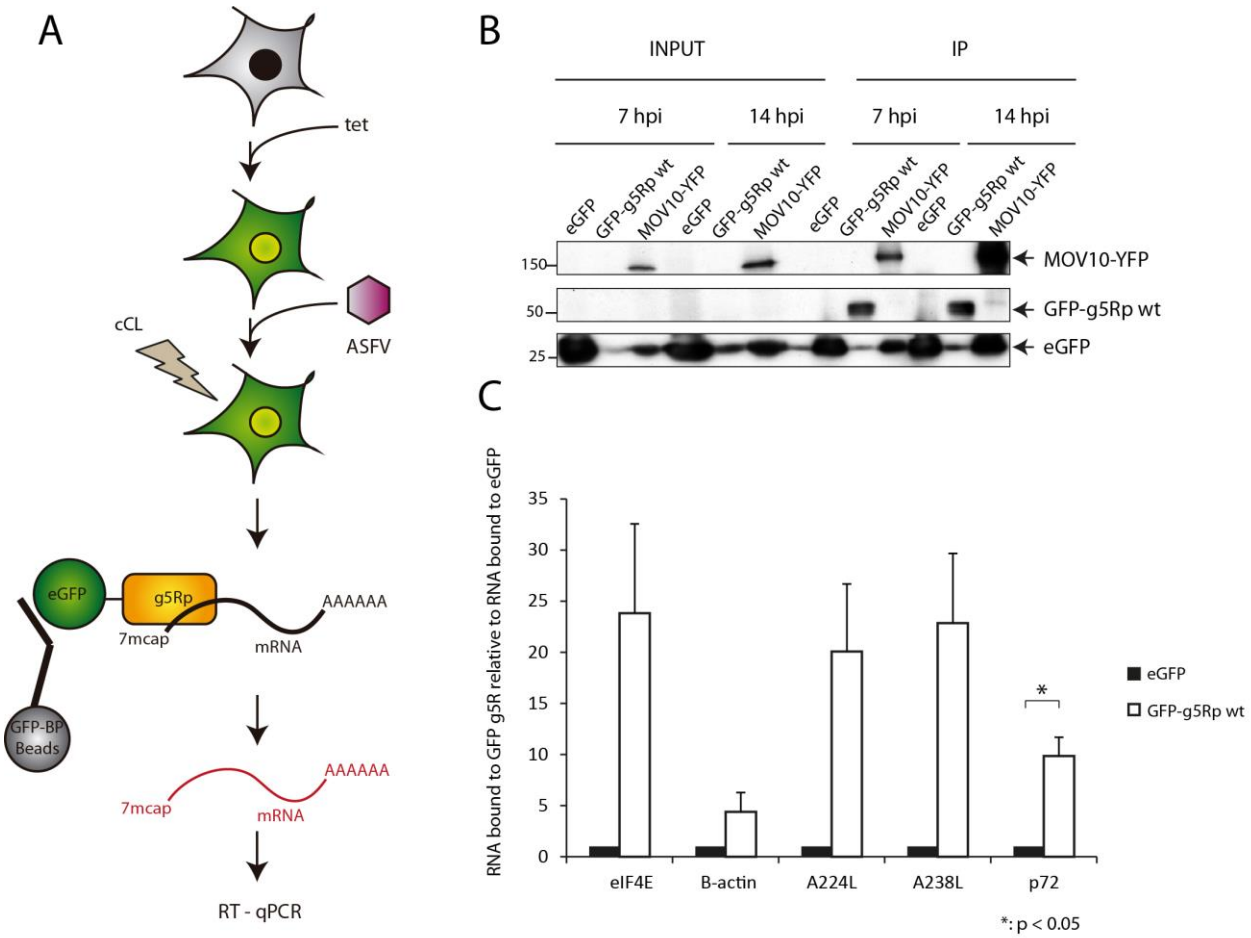

Figure 24. GFP-g5Rp wt is able to bind both viral and cellular mRNAs in the context of ASFV infection.
A) Schematic representation of the experimental procedure. After induction of the recombinant proteins with tetracycline (tet), HeLa cells were ASFV infected (M.O.I = 5 pfu/cell) and crosslinked at 7 or 14 hour post infection (hpi). eGFP and GFP g5Rp wt were immunoprecipitated with GFP_Trap_A beads and RNA bound to them were extracted using phenol:chlorofom:isoamil alcohol (25:24:1) and analysed by RT-qPCR. HeLa stable cells expressing MOV10-YFP were used as positive control. **B)** Immunoprecipitation of all the fusion proteins was checked by Western blot prior to RNA extraction. Complexes were detected using a specific anti-GFP antibody. **C)** Quantification of representative cellular (eIF4E and B-actin) and viral (A224L, A238L and p72) mRNAs extracted from the immunoprecipitated fusion proteins by RT-qPCR at 14 hpi. Values are represented as the RNA bound to GFP-g5R protein relative to the RNA bound to eGFP (mean +/- S.E.M) n=3. * $p < 0.05$.

4.3.2.2 Effect of g5Rp on viral mRNAs expression

After demonstration that g5Rp binds viral mRNAs and in order to clarify the consequence of this role on the expression of specific ASFV mRNAs, we analysed by CSLM the level of A224L mRNA in infected cells overexpressing g5Rp-HA. 24 hours post transfection, COS-7 cells were Mock-infected or ASFV-infected with M.O.I = 5 pfu/cell, fixed at 7 hpi and 24 hpi post infection, and viral A224L mRNA level was analysed using an specific Texas red tagged probe (Figure 25). As expected, no signal of A224L mRNA probe was detected in Mock cells. At 7 hpi, A224L mRNA was clearly detected in eGPF cells (Figure 25 upper pannels), while in cells expressing g5Rp-HA a lower signal was perceived (Figure 25 lower panels), indicating that overexpressed g5Rp enhances degradation of the A224L mRNA. At 24 hpi, A224L mRNA was detected in both eGFP and GFP-g5Rp cells, although the signal was again reduced in overexpressing g5Rp-HA cells, supporting a discriminatory expression of g5Rp together with late viral proteins. It is also important to highlight that

ectopic g5Rp expression in these experiments is regulated by the viral promoter, and it should behave in the infected cells as an “extra copy” expression of the g5R gene.

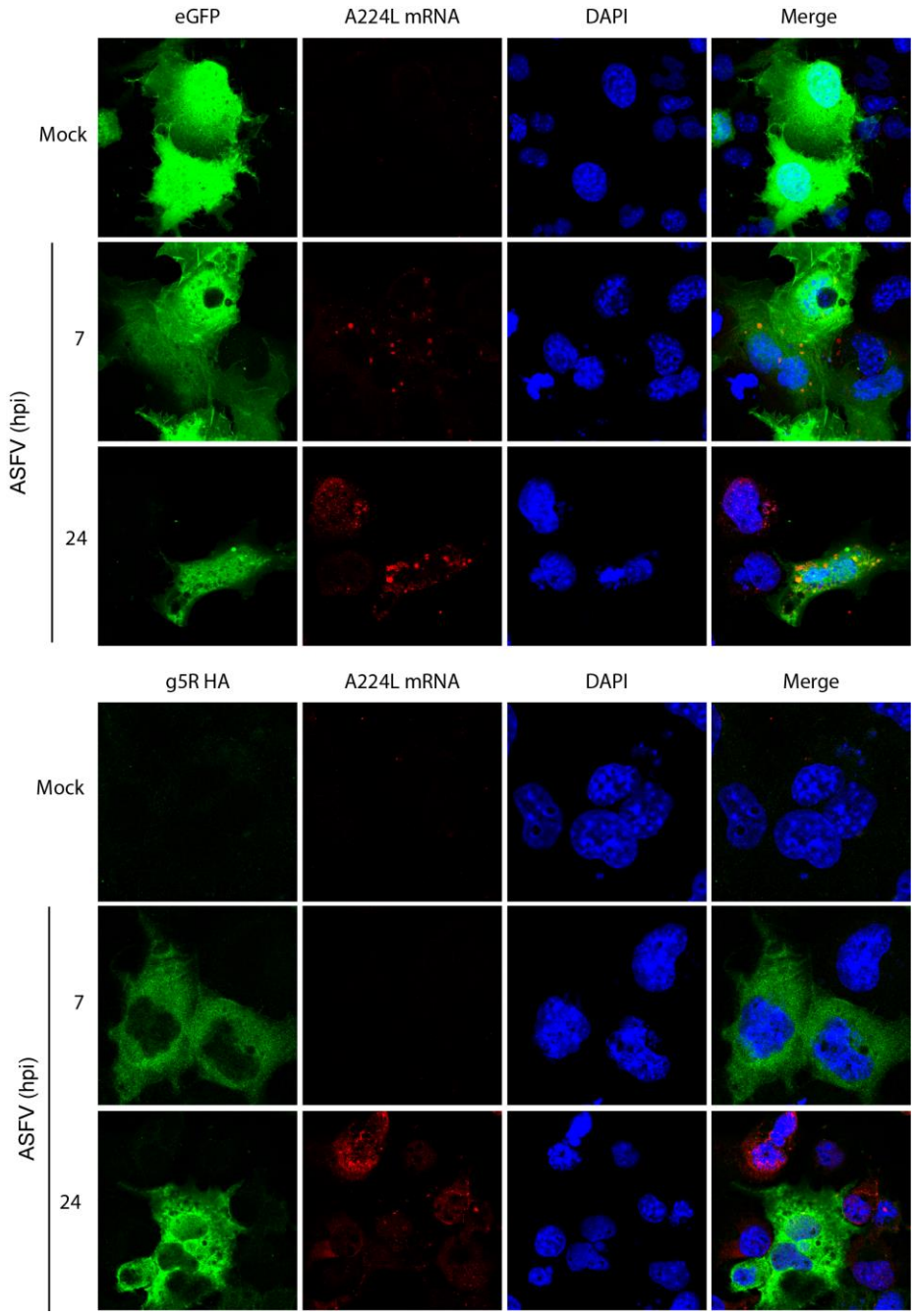

Figure 25. Localization of A224L viral mRNA in ASFV-infected COS-7 cells overexpressing g5Rp-HA protein.
COS-7 cells were transfected with eGFP (upper panles) or promg5R-HA (bottom panels) and Mock-infected or ASFV-infected with M.O.I = 5pfu/cell. At 7 and 24 hpi, monolayer was fixed and viral A224L mRNA was detected using a specific probed tagged to Texas Red (red). g5Rp-HA was detected using a specific anti-HA antibody (green). Viral factories and cellular nucleus were stained with DAPI (blue).

In order to further study the effect of g5R protein over viral mRNAs, we analysed A238L, A224L and p72 mRNA levels by RT-qPCR in HeLa cells, after ASFV-infection (16 hpi, M.O.I = 5 pfu/cell) and expression of eGFP or GFP-g5Rp wt. We observed that in HeLa cells expressing GFP-g5Rp wt, all the viral mRNAs studied were decreased compared to eGFP expressing cells (Figure 26). This data corroborated CSLM results showed

above, and indicated that g5Rp overexpression causes a reduction of at least two late viral mRNAs, which also support the decrease observed in the protein levels in section 4.3.1.

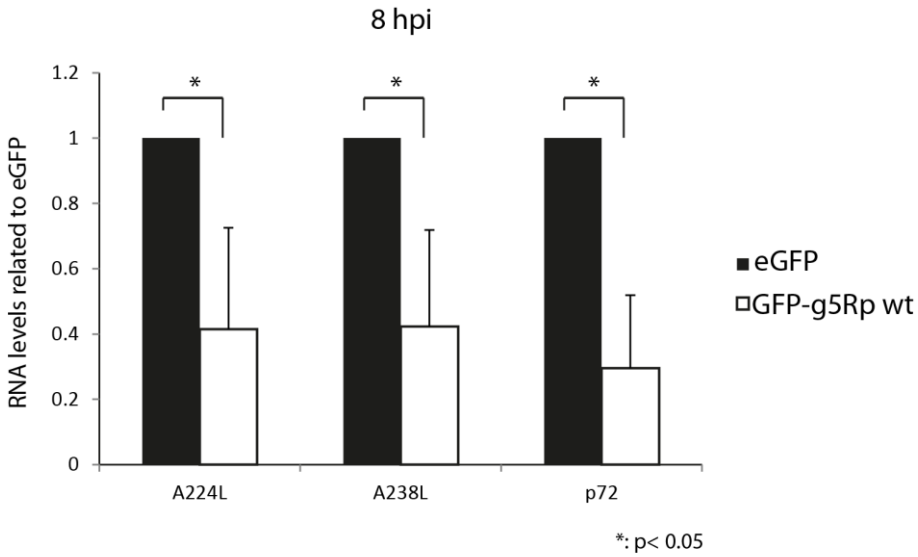

Figure 26. Expression of GFP-g5Rp wt protein in ASFV infected cells causes a decrease of late viral mRNA levels.
HeLa cells were induced to express eGFP and GFP-g5Rp with tetracycline 18 hours prior to ASFV-infection (M.O.I = 5 pfu/cell). At 8 hpi, cells were harvested and total mRNA was extracted. Viral A224L, A238L and p72 mRNA levels were analysed by RT-qPCR using specific primers. Values represent RNA levels present in GFP-g5Rp wt expressing cells related to eGFP expressing cells and are normalized to 18S RNA (media +/- S.D, n=3)
*: $p < 0.05$.

4.3.2.3 Effect of g5Rp on cellular mRNAs

The results showed above indicate that g5Rp overexpression affects viral mRNA levels. On the other hand and in order to clarify the possible role of the protein in the cellular shutoff, we also study the effect of g5Rp overexpression on cellular mRNAs. We analysed eIF4E and β-actin mRNA levels by RT-qPCR in ASFV-infected (16 hpi, M.O.I = 5 pfu/cell) stably HeLa cells, which were previously induced with tetracycline to express eGFP or GFP-g5Rp wt, respectively. As Figure 27 shows, levels of both RNAs were decreased in ASFV-infected HeLa cells expressing GFP-g5Rp wt compared to cells expressing eGFP alone. This result indicates that g5Rp is not only able to promote viral mRNA decay, but also cellular mRNA degradation in the context of the infection. Moreover, this degradation appears to be a selective process, because g5Rp effect is more patent in eIF4E mRNA than in B-actin mRNA levels.

In summary, these results point to g5Rp as a new viral decapping enzyme, functioning as a regulator of both viral and cellular protein synthesis by specifically modulating mRNA levels.

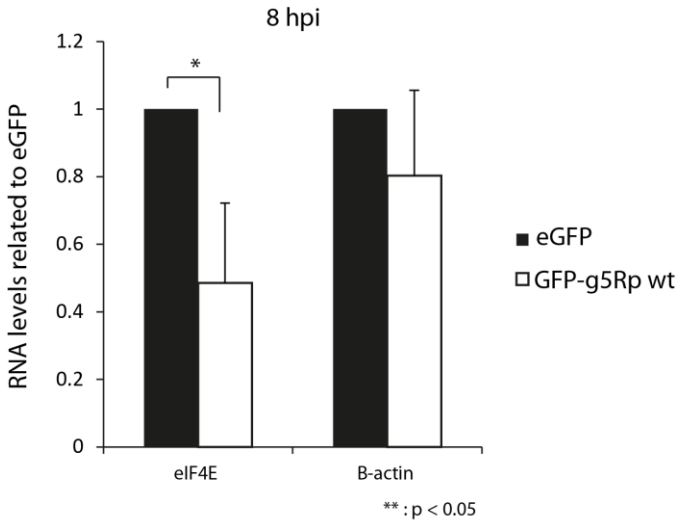

Figure 27. Expression of GFP-g5Rp wt protein causes a decrease of cellular mRNA levels in ASFV-infected HeLa cells.
HeLa cells were induced to express eGFP and GFP-g5Rp with tetracycline (O/N), and then ASFV-infected with M.O.I = 5 pfu/cell. At 8 hpi, cells were harvested and total mRNA was extracted. eIF4E and B-actin mRNA levels were analysed by RT-qPCR using specific primers. Values represent RNA levels present in GFP-g5Rp wt expressing cells related to eGFP expressing cells and are normalized to 18S RNA (media +/- S.D, n=3) **: $p < 0.05$.

4.3.3 g5Rp is an important gene in ASFV infection

The results explained above showed that g5Rp binds both viral and cellular mRNAs *in vivo*, thus suggesting that the role of the viral protein during the infection could be related to the regulation of the temporal expression of the viral mRNAs during the viral cycle and also in the degradation of cellular mRNAs. To further study g5Rp function during ASFV infection and to characterize the molecular mechanism employed by the protein, we set up two types of strategies.

1.3.3.1. Silencing g5R expression by using specific siRNA

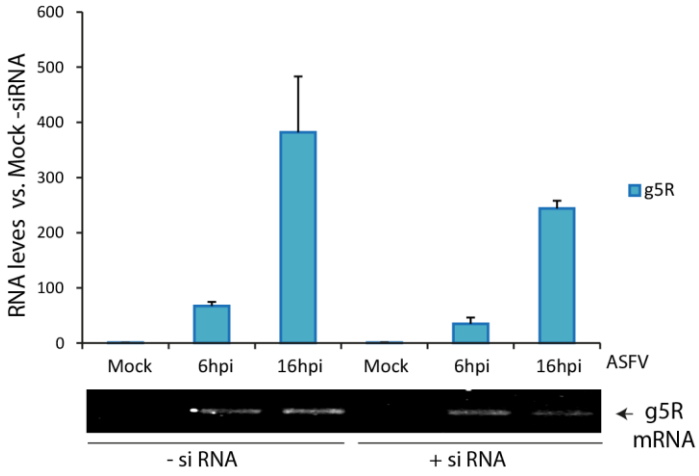

Figure 28. Partial depletion of g5R gene.
Vero cells were serum deprived for 24 hours and transfected or non-transfected with 40 nM of a specific g5R siRNA . 24 h after transfection, Vero cells were Mock or ASFV-infected (M. O. I = 1 pfu/cell). Samples were recovered at 6 and 16 hours post infection and total RNA was extracted and retrotranscribed. mRNA levels of g5R mRNA were analysed by PCR and qPCR. Graphic bars show RNA levels referred to non-silenced Mock and normalized to ribosomal protein P0 (PRLP) and peptidylprolyl isomerase A (PPIA) mRNAs (mean +/- S.D, n=2).

Three specific g5Rp-siRNAs were used under different conditions to optimize silencing reactions. However, for all the conditions tested, we only achieved approximately a 40% of silencing rate (Figure 28). This limited result prevented us from observing significant differences between silenced and non-silenced samples in terms of levels of mRNAs corresponding either to viral or cellular transcripts (data not shown). Thus, clear conclusions from these experiments could not be extracted.

1.3.3.2. Generation of a deletion ASFV mutant lacking of the g5R gene.

As a second approach to study the specific role of the viral protein, we tried to generate an ASFV g5Rp deletion mutant (ASFVΔg5R, Ba71V strain) following a protocol that has been widely used in our lab to generate ASFV recombinant mutants.

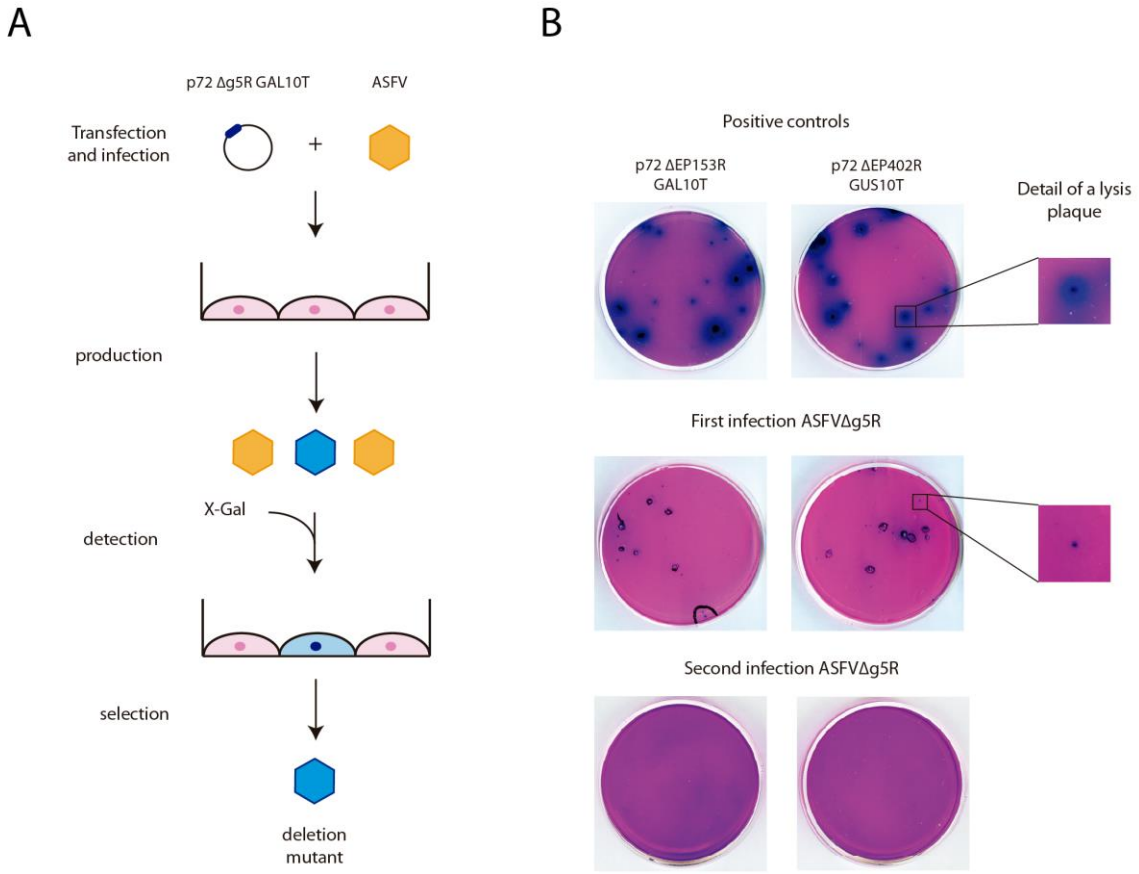

Figure 29. g5R gene is important to effective viral production.
Generation of ASFV g5R deletion mutant (ASFVΔg5R). **A)** Schematic representation of the experimental procedure. The gene of interest (in this case g5R) and its flanking sequences were cloned in the p72BetaGAL10T vector (p72Δg5RGAL10T). Vero cells were transfected with this construction and ASFV-infected to allow homologous recombination between the vector and the viral genome. Positive recombinant viral particles should carry a copy of the Beta galactosidase gene instead of the gene of interest, which allowed its selection by titration in presence of X-gal. **B)** g5R is an important gene for ASFV infection cycle. p72ΔEP153R Gal 10 T and p72ΔEP402R Gal 10 T, which are constructions that had been successfully used to generate ASFV deletion mutants previously in our lab, were used as positive controls (upper panels). First round of transfection and infection with p72Δg5RpGAL10T generate small positive clones (middle panels), but disappear in the following infection steps (bottom panels). Data are representative images from two separate experiments.

To achieve this, we constructed a vector containing g5R gene flanking sequences (F1 and F2, see Materials and Methods) at both sides of β-Gal gene (p72Δg5RGAL10T) and then transfected this plasmid in Vero cells. Followed by ASFV infection, this procedure should allow recombination between homologous

regions of the construction and the viral genome, in such a way that resultant viral particles containing β-Gal gene instead of g5R can be routinely selected by titration in agarose plates and in X-Gal presence (Garcia *et al.*, 1995).Figure 29 A shows a representation of the experimental process. As an internal control of the transfection-infection procedure, reflecting the somatic recombination we used two vectors generated in our group, p72ΔEP153RGAL10T (Hurtado *et al.*, 2004) and p72ΔEP402RGUS10T (Rodriguez *et al.*, 1993), which have been previously used to successfully obtain the corresponding ASFV deletion mutants: Ba71VΔEP153R and Ba71VΔEP402R (ΔCD2v). Using similar conditions, we intended to generate the virus ASFVΔg5R.

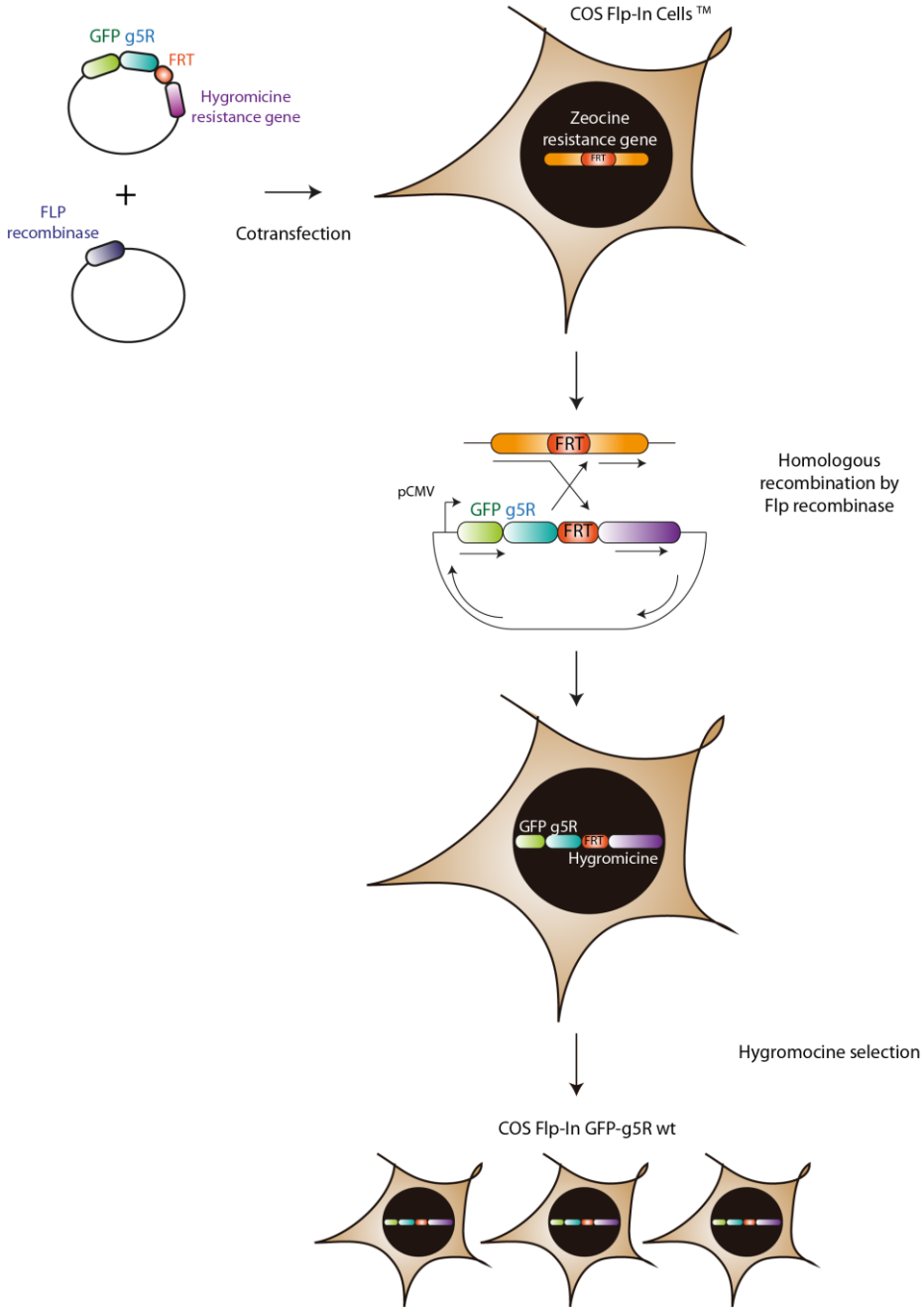

Figure 30. Experimental approximation to obtain a helper cell line that supports ASFVΔg5R infection.
COS Flip in cell line possess a Flip Recombination Site (FRT) integrated at its genome. Cotransfection of pCDNA5/FRT/TO GFP-g5R wt and pOG44 vector (that encodes for the FLP recombinase) will allow the integration of GFP-g5Rp wt and Hygromicine resistance sequences into the cellular genome. Positive clones will be selected by their resistance to Hygromicine.

However, after different trials, and although we were able to obtain blue viral particles after the first transfection/infection steps, these positive clones presented a smaller size comparing to the positive controls (Figure 29 B, upper and middle panels), and were lost in the successive rounds of infection (Figure 29 B bottom panels). This procedure was repeated unsuccessfully several times in separated experiments, thus suggesting an important role for g5Rp in the viral infection, which explains that viral particles lacking this protein cannot productively grow. In parallel, a similar protocol was developed to delete another non-related ASFV gene, A238L, which was successfully achieved, thus guarantying the efficiency of the experimental procedure (data not shown).

Since this conventional method failed to generate the ASFV g5R deletion mutant virus, we are currently working on the development of a helper cell line which constitutively expressed g5Rp and might be able to support ASFVΔg5R growth since ectopically provides the essential g5R protein. To generate this helper cell line we will use COS Flip in cells, a kind gift of Dr. Carlos Martins (Facultad Técnica de Veterinaria, Lisboa, Portugal), that are further transfected with pCDNA5/FRT/TO GFP-g5Rp wt vector, and selected with hygromicine. Resultant COS GFP-g5Rp wt cells will be sorted by FACS and next used to generate ASFV Δg5R. A schematic representation of the experimental procedure is shown on Figure 30.

4.4 EFFECT OF ASFV INFECTION ON CELLULAR DECAPPING MACHINERY

In this Thesis, we observed that g5Rp played a role on decay of both viral and cellular mRNAs. To further deciphering the molecular mechanism performed by g5Rp during ASFV infection, we analysed the cellular machinery of decapping during ASFV infection and when g5Rp is overexpressed.

As mentioned in the Introduction section, in the 5´- 3´ RNA degradation route the cellular decapping Dcp2 subunit has been described as the catalytic enzyme, in charge of hydrolyse the cap structure from the 5´end of RNAs. However, RNA degradation is a tightly controlled process that is modulated by numerous regulators. Among these, cellular Dcp1 has a determinant role, but other proteins as Edc3, Edc4, Lsm1-7 complex, Pat1 or Dhh1 have been described to be also implicated (Arribas-Layton *et al.*, 2013; Garneau *et al.*, 2007; Ling *et al.*, 2011). All these proteins have been described to localize in cytoplasmic foci (known as Processing Bodies or P-Bodies) in normal cells (Eulalio *et al.*, 2007). The number and size of these RNA granules rise in conditions that trigger an increase in non-translating RNAs, such as stress stimuli or viral infections (Decker and Parker, 2012). Indeed, some host viral defence proteins accumulate at these structures (Beckham and Parker, 2008) and, for this reason, viruses have developed several mechanisms to subrogate P-Bodies formation. In some cases, viruses are also able to use P-body components to their own benefit (Narayanan and Makino, 2013; Reineke and Lloyd, 2013). In order to determinate if ASFV infection is modulating the decapping machinery and in some way affecting the P-bodies structure and/or size, we decided to analyse the levels and subcellular distribution of Dcp1 and Edc4 during the infection.

4.4.1 Effect of ASFV infection on the P-Body components Dcp1 and Edc4

To analyze DCP1 and Edc4 localization during ASFV infection, COS-7 cells were Mock-infected or ASFV-infected with M.O.I = 2 pfu/cell. At 16 hpi, cells were fixed and both proteins were detected with specific antibodies by CSLM, whereas ASFV infection was assessed by the presence of viral factories (Figure 31 A) or p72 protein expression (Figure 31 B).

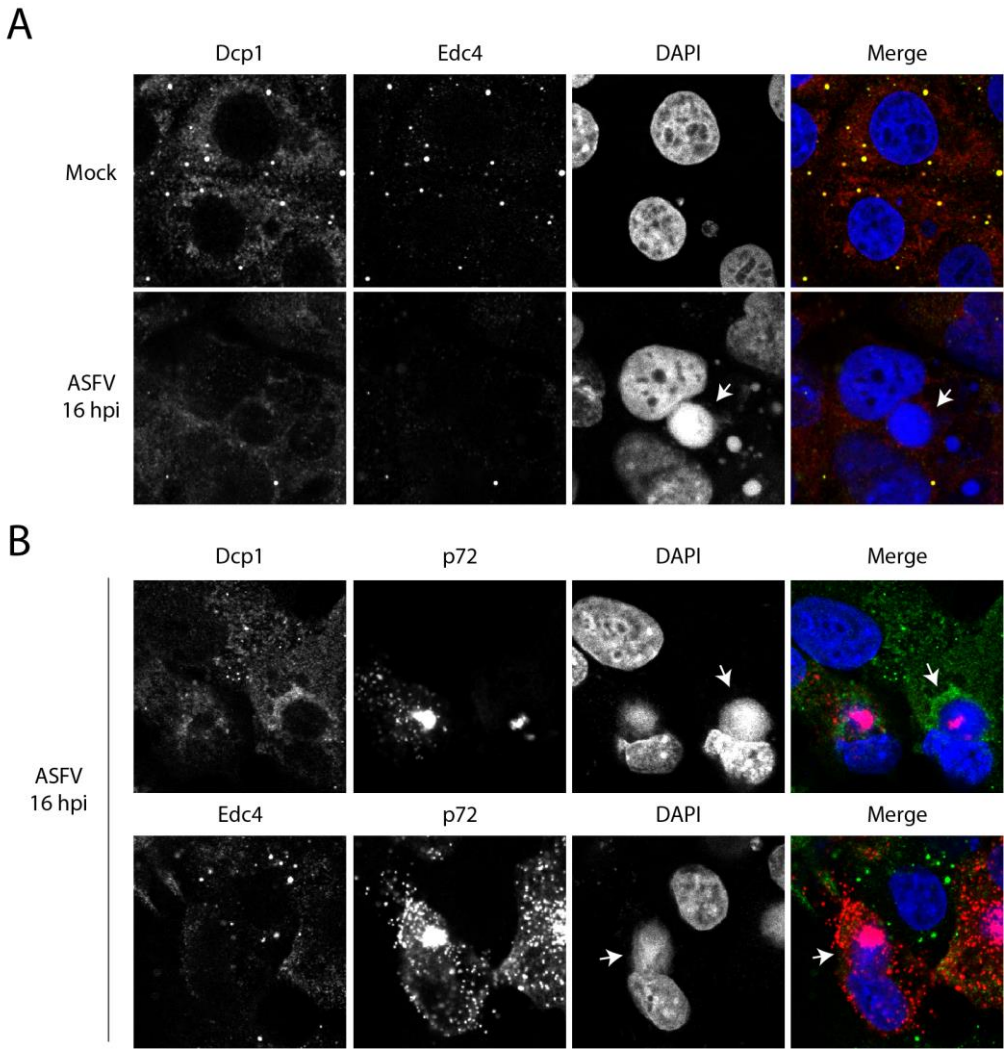

Figure 31. Localization of Dcp1 and Edc4 in ASFV infected cells.
A) COS-7 cells were Mock-infected or ASFV-infected with M.O.I of 5 pfu/cell. At 16 hpi, monolayer was fixed and Dcp1 and Edc4 were detected by CLSM using specific antibodies. Edc4 and Dcp1 distributions are shown in gray at the individual panels and in green and red, respectively, in the Merge panels. Infection progress was checked by the presence of viral factories (blue in the merge panels). **B)** COS-7 cells were ASFV-infected (M.O.I of 5 pfu/cell) and Dcp1 and Edc4 were localized using specific antibodies by CSLM at 16 hpi. Edc4 and Dcp1 distributions are shown in gray at the individual panels and in green in the Merge panels. Infection progress was checked by the presence of the viral protein p72 (red, in the merge panels). Arrows show the viral factories. Data are representative images from two separate experiments.

As expected, we observed that in Mock-infected cells, Dcp1 and Edc4 co-localized and presented a punctuated pattern (Figure 31 A, upper panels). However, in ASFV infected cells, this pattern was missing, and both Dcp1 and Edc4 proteins showed a more heterogeneous distribution, that was, furthermore, less intense (Figure 31 A bottom panels) probably due either to the general shutoff induced by the infection or, alternatively, to a specific virus-induced down regulation mechanism. Furthermore, Dcp1 signal was

distributed around the viral factories, indicating that Dcp1 should play a virus-regulated role (Figure 31 B, upper panels). On the other hand, Edc4 signal was clearly excluded from the viral factories (Figure 31 B, bottom panels). In the merge panel, the difference on Edc4 pattern between un-infected and infected cells can be clearly appreciated, as in the cell positive for p72 (red), almost any green mark corresponding to Edc4 was observed, and, on the contrary, in the cell aside, no red mark corresponding to infection appeared, but green granules corresponding to Edc4 are very patent. This change on localization and structure of the P-Bodies components is very common among viruses, which are able to interact with these cellular anti-viral defence mechanisms in order to facilitate viral replication.

4.4.2 g5Rp partially co-localizes with Dcp1 on the periphery of the viral factories

Further the effect of ASFV overall on distribution of P-Body components, we focused our attention on studying the potential interaction between g5Rp and Dcp1 or Edc4. Taking into consideration the possible role of g5Rp as a decapping enzyme, we hypothesised that the protein could be using these decapping activators to perform its function in a similar manner to Dcp2.

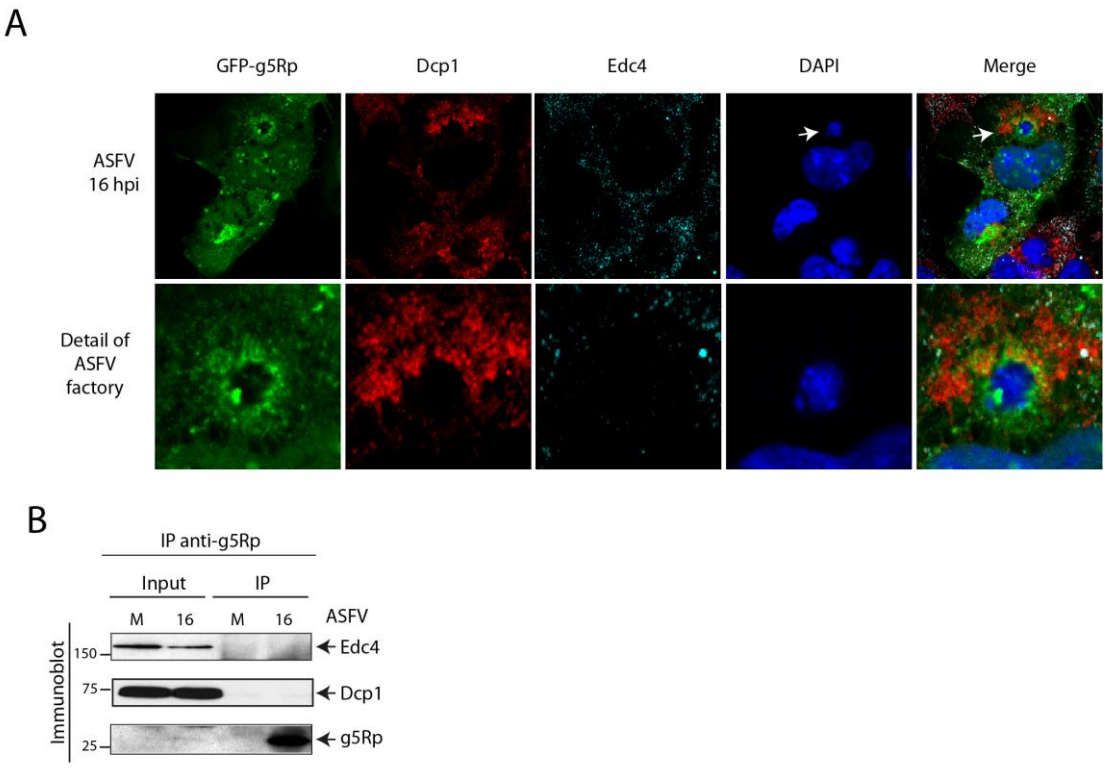

Figure 32. g5Rp co-localizes, but not directly interacts, with Dcp1 at the periphery of the viral factories.
A) COS-7 cells were transfected with pZAB 11/7 42 vector, which contains GFP-g5R sequence under control of g5R viral promoter. After transfection, cells were ASFV-infected and GFP-g5Rp (green), Dcp1 (red) and Edc4 (cyan) location was analysed by CLSM. Dcp1 and Edc4 were detected using specific antibodies. DAPI was used to stain cellular nucleus and viral factories (blue). Bottom panels represent a detail of the viral factories. Arrows show the viral factories. **B)** Coimmunoprecipitation assays using specific anti-g5Rp serum. Vero cells were Mock-infected or ASFV-infected at 16 hpi and samples were collected in presence of anti-g5Rp serum. Thus, samples were incubated with agarose beads O/N, and after intensive washing Dcp1, Edc4 y g5Rp levels were analysed by Western blot. Protein detection was carried out using specific anti Dcp1 and anti-Edc4 antibodies, while g5Rp was detected with anti-g5Rp serum. Data are representative images from two separate experiments..

With this objective, we analysed g5Rp location in relation to Dcp1 or Edc4 during ASFV infection by CSLM. COS-7 cells were transfected with pZAB 11/7 42 vector, a construction that contains the GFP-g5Rp fused protein under control of the g5Rp viral promoter, and then infected with a M.O.I of 5 pfu/cell. At 16 hpi, cells were fixed and GFP-g5Rp, Dcp1 and Edc4 distribution was analysed. As it is shown Figure 32 A, the pattern of distribution of GFP-g5Rp was different from the one corresponding to Edc4, suggesting that both proteins do not mainly co-localize. On the other hand, both GFP-g5Rp and Dcp1 accumulated at the surroundings of the viral factories, where they partially co-localized (Figure 32 A).

To further study the possible interaction between g5Rp and Dcp1 or Edc4, we performed coimmunoprecipitation assays. Vero cells were Mock-infected or ASFV-infected with M.O.I of 5 pfu/cell and samples were recovered at 16 hpi in presence of the specific anti-g5Rp serum. After immunoprecipitation with this antibody, possible g5Rp-protein interactions were analysed by Western Blot using specific antibodies against Dcp1 or Edc4 (Figure 32 B). Results demonstrated that g5Rp is not directly interacting neither Dcp1 nor Edc4. Furthermore, and as we will show later, Dcp1 did not appear as a protein binding GST-g5R in pull-down assays. However, the fact of Dcp1 accumulates at the surroundings of the viral factories suggest that Dcp1 could be playing a role on ASFV infection and maybe in viral-induced mRNA decay.

4.4.3 Cap distribution in ASFV infected cells

Due to the fact that the cap is a key player of the decapping process and that g5Rp is a putative viral decapping enzyme, we examined the distribution of this structure in the context of ASFV infection and its possible localization *versus* g5R protein. To achieve this, we used a specific antibody able to recognise both m^7G and m_3G structures by CSLM. It should be noted that the antibody recognizes both the cap structures attached to the RNA body and the free cap analogous (such as m^7Gp or m^7GpppG), but, however, it does not have affinity to uncapped RNAs (Bochnig *et al.*, 1987). COS cells were Mock-infected or ASFV-infected (M.O.I = 5 pfu/cell) and fixed at 16 hpi. g5R protein was detected using our specific serum and nucleus and viral factories were stained with DAPI. In Mock-infected cells, the cap structure was localized both at the cytoplasm and, strongly, at the nucleus (Figure 33 A, upper panels), suggesting that the capped RNAs are present in both compartments. The observed increase at the nucleus is not surprising, given that RNA capping is a process that mainly occurs at this organelle. On the contrary, in ASFV-infected cells cap signal was augmented in the cytoplasm, especially at the periphery of the viral factories, where it partially co-localized with g5Rp (Figure 33 A, bottom panels). The reduction of the cap signal in the nucleus of infected cells may be due to an impairment of both nuclear transport and functions, as we commented in section 4.1.2. Conversely, the increase of the cap signal at the viral replication sites may corresponds to capped viral mRNAs, which, as described in (Castello *et al.*, 2009b) and as we demonstrated in section 4.1.3, are surrounding these structures. The fact that the cap co-localize with g5Rp at these sites indicates that both

factors could be interacting, which would corroborate the role of g5Rp as a decapping enzyme. Interestingly, when we analysed cap signal intensity, we observed it was slightly increased in ASFV-infected cells when compared to Mock-infected cells (Figure 33 B). Given that ASFV infection causes a decrease in the Oligo d (T) signal and in the mRNA levels (section 4.1.2), we could expect a similar phenomenon regarding the cap levels. However, it should be noticed that the antibody not only recognise capped mRNAs, but also free cap structures, which may rise due to the ASFV-stimulated rates of RNA decapping and degradation.

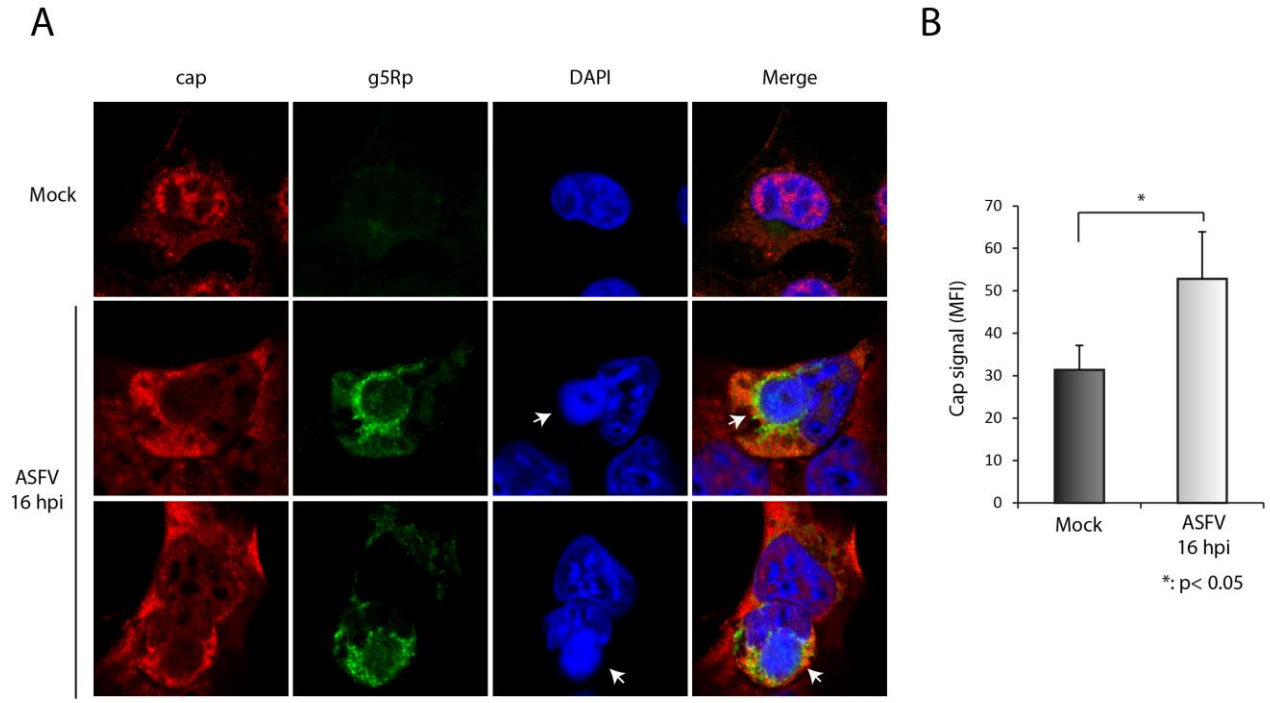

Figure 33. ASFV infection affects the location and levels of the 5´ cap structure.
A) Analysis of the location of the cap structure in ASFV-infected cells. COS-7 cells were infected with M.O.I = 5 pfu/cell and fixed at 16 hpi. Cap structure (red) and g5R protein (green) were detected by using an anti-cap specific antibody and the anti-g5Rp serum, respectively by CSLM. Cellular and viral DNA was stained with DAPI (blue). Arrows show the viral factories **B)** Quantification of the cap signal in Mock-infected and ASFV-infected cells by *ImageJ* software (mean fluorescence intensity, MFI +/- S.D, n = 2). *: p < 0.05. Data are representative images from two separate experiments.

Data presented in this section corroborates our previous findings with the specific viral mRNAs probes (section 4.1.3), indicating viral mRNAs are located at viral factories, and also reinforces the clue of g5Rp as a viral decapping enzyme.

4.5 EFFECT OF ASFV INFECTION ON CELLULAR TRANSLATION MACHINERY

Viruses not only manipulate the cellular decapping machinery in order to avoid defence responses, but also manipulate the translation initiation machinery to enhance its own viral protein synthesis and to impair cellular protein synthesis: this is the case of vaccinia infection, where eukaryotic translation initiation factors (eIFs) are redistributed to viral factories (Katsafanas and Moss, 2007; Walsh *et al.*, 2008)). Once that we have demonstrated that viral mRNAs are located at the periphery of viral factories in previous sections (section 4.1.3), we then hypothesised that translation could also take place at these sites, and that eIFs could

be recruited to ASFV viral factories, as happens in vaccinia infection. This is an important point to explore in the virus biology, since it was not previously described the regulation of eIFs during ASFV infection, a topic that was further studied in (Castello *et al.*, 2009b). In this work, we previously demonstrated that ASFV translation relies on the host cap-dependent translation machinery. Indeed, both eIF4E and eIF4G are essential for the progression of the infection, since deletion of both factors triggers a decrease in the number and size of viral factories and a reduction of the viral titre. Moreover, during ASFV infection formation of the translation initiation complex is stimulated by phosphorylation of eIF4G, eIF4E and 4E-BP, while eIF2α is maintained unphosphorylated to avoid translational repression.

4.5.1 ASFV infection triggers a redistribution of eIF4E and eIF4G

To analyse eukaryotic translation initiation factors distribution, Vero cells were Mock-infected or ASFV-infected (M.O.I = 5 pfu/cell) and fixed at 16 hpi. Location of eIF4G and eIF4E were then analysed by CSLM (green and red, respectively, in Figure 34 A).To-Pro-3 was used to visualize viral factories (blue). In Mock-infected cells, both initiation translation factors were spread in the cytoplasm (Figure 34, upper panels). However, in ASFV-infected cells both factors are clustered at the viral factories (Figure 34, bottom panels), indicating that, as we expected, ASFV triggers the redistribution of eIFs to the viral factories to its own benefit, facilitating the translation of viral mRNA and thus the viral protein synthesis. Taken together with the data exposed on the above section, these results indicate that viral factories are structures where active translation takes place, but also structures where viral mRNA degradation can occur .

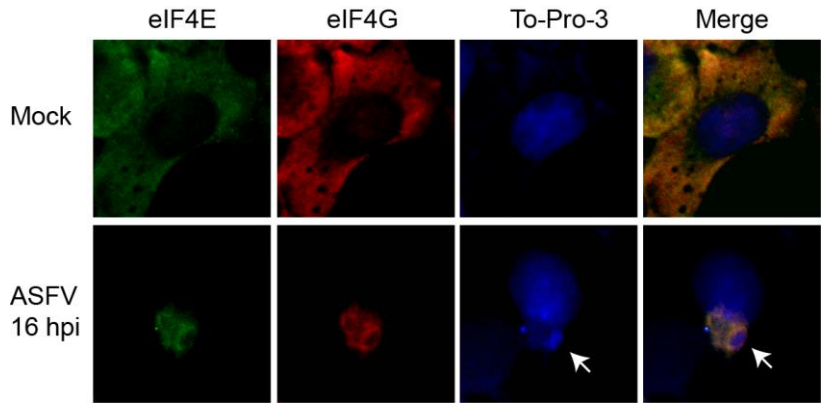

Figure 34. eIF4G and eIF4E are redistributed to the viral factories during ASFV infection.
Vero cells were Mock-infected or ASFV-infected with M.O.I = 5 pfu/cell, and fixed to glass coverslip at 16 hpi. eIF4E (green) and eIF4G (red) location was detected by indirect immunofluorescence by CLSM. Cell nuclei and ASFV viral factories were stained with To-Pro-3 (blue). Arrows show the viral factories. Data are representative images from two separate experiments.

4.5.2 ASFV infection promotes ribosome redistribution

The above findings demonstrated that translation initiation factors are redistributed to viral factories. In order to test if ASFV infection was affecting to other components of the translation process, we studied ribosomes redistribution by CSLM. Ribosomes were detected with a specific antibody that recognises ribosomal P protein (a kind gift of Dr. Juan Pedro García Ballesta, CBMSO, Madrid, Spain (Martinez-Azorin *et al.*, 2008)) and p72 viral protein was used to detect viral factories (Figure 35). Ribosomal

P protein presented a similar pattern of eIFs and localized spread at the cytoplasm of Mock-infected cells. In contrast, in ASFV-infected cells Ribosomal P protein co-localized with p72 protein and is clustered at the periphery of viral factories, suggesting that also ribosomes were mobilized to the viral factories.

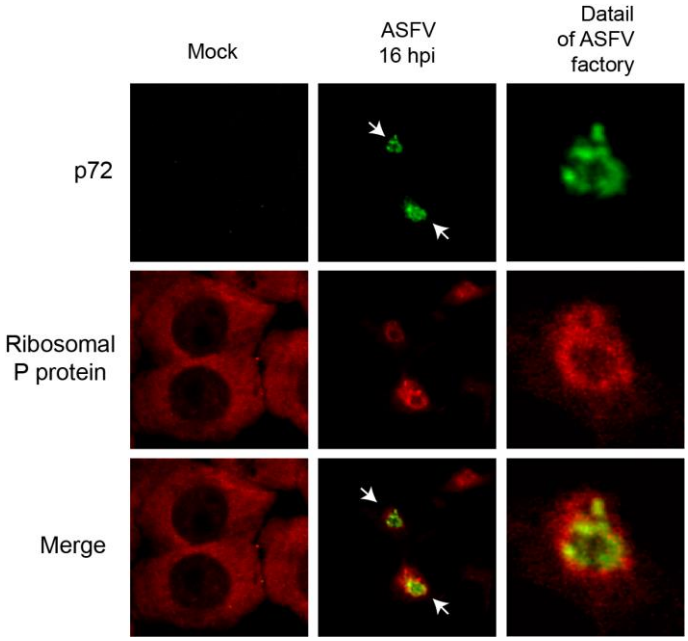

Figure 35. P-ribosomal protein is clustered at the periphery of ASFV viral factories.
Vero cells were Mock-infected or ASFV-infected with 5 pfu/cell and fixed at 16 hpi. Ribosomal P-protein (red) and ASFV p72 protein (green) were detected by immunofluorescence by using specific antisera. Nucleus and viral factories were detected with To-Pro-3 (blue). Arrows show the viral factories. Data are representative images from two separate experiments.

Considering, as we have demonstrated in this work, that ASFV infection promotes a cellular mRNA decay, all together the results presented here suggest that ASFV uses different mechanisms to carry out the cellular shut off: on one hand, ASFV impairs cellular protein synthesis by mRNA degradation, on the other hand, ASFV recruits eIFs and ribosomes to viral factories where are not accessible for cellular mRNAs. Furthermore, it is likely ASFV modulates both translation and mRNA metabolism not only to impair cellular protein synthesis, but also to facilitate viral infection progression, using the components of the translation machinery to that purpose.

4.5.3 g5Rp interacts with several cellular and viral proteins during ASFV infection

Due to the fact that eIFs, ribosomes and g5Rp are clustered at the periphery of viral factories at late times post infection, we decided to analyse if the viral protein could be interacting with any of these translation machinery components in the context of the infection. Additionally, and in order to further analyze the mechanism of g5Rp function as a protein that cleaves viral mRNAs, thus acting as a regulator of viral temporal expression, we also explored whether g5Rp could be interacting with viral proteins. To achieve this, we performed pulldown assays as follows: purified GST and GST-g5R proteins were coupled to

glutathione beads, then incubated with extracts of Mock-infected or ASFV-infected Vero cells recovered at 6 or 18 hpi (M.O.I = 5 pfu/cell), and, after intensive washing, resultant protein complexes were sequenced by Mass Spectrometry. In order to identify the interacting cellular and viral proteins, we analysed the obtained peptides matching them against two different data bases: firstly, we used Uniprot ASFV-Ba71V strain database, which allowed us to identify the viral peptides bound to GST or GST-g5Rp samples (Table 6), and secondly, Uniprot Primates data base allowed us to identify cellular proteins interacting with both GST and GST-g5Rp complexes (Table 3).

Accession number	Protein	Identified sequences	Score
Q08358	Polyprotein pp220 African swine fever virus (strain Badajoz 1971 Vero-adapted) GN=Ba71V-92 PE=1 SV=3 - [PP220_ASFB7]	FSGLVSAENIAEFEK VGGAALTVEELGLSK VAAEIQQGR	9,60
P22776	Major capsid protein p72 African swine fever virus (strain Badajoz 1971 Vero-adapted) GN=Ba71V-081 PE=1 SV=2 - [MCP_ASFB7]	NLVYYCEYPGER IILAQDLLNSR	5,73
Q89769	Structural DNA-binding protein p10 African swine fever virus (strain Badajoz 1971 Vero-adapted)GN=Ba71V-049 PE=1 SV=1 - [P10_ASFB7]	THASSSMHSGMLYK	2,35

Table 6. Identification of viral proteins interacting with g5Rp.
Data found by sequencing the peptides interacting with GST-g5Rp after incubation of the recombinant protein with extracts of ASFV-infected cells (18 hpi). Identification of peptides was carried out using Uniprot ASFV-Ba71 strain data base. The table shows the Uniprot accession number (accession number), the identified protein (protein), the peptide sequences which allowed identification of the protein (identified sequence) and the score.

Regarding viral protein analysis, in samples where GST-g5Rp was incubated with Mock-infected or 6 hpi -infected extracts no viral peptides were found (data not shown). Obviously, Mock sample was used as negative control, as no viral proteins are expected in this sample. These results indicate that, at early times post infection, g5Rp is not interacting with other viral proteins. However, when GST-g5R protein was incubated with extracts from 18 hpi- infected Vero cells, we were able to identify at least three viral proteins interacting with GST-g5Rp: the DNA binding protein p10, the polyprotein pp220 and the major protein of the capsid, p72 (Table 6). All these proteins are packaged into the virion particles, and therefore are recruited to viral factories at late times post infection. The fact that g5Rp is able to interact with these proteins went in parallel with the results obtained by CSLM in section 4.2.3, which showed location of g5Rp at the edge of the viral factories at late times post infection. This result also suggests that g5Rp could be packaged into the virions.

When we analysed cellular peptides in GST-g5Rp samples, we observed that in all the conditions tested (Mock, 6hpi and 18hpi) GST-g5Rp was interacting with several ribosomes components, such as the40S ribosomal protein S14 or the 60S ribosomal protein L8, which are proteins involved in the regulation and in the correct reconstitution of the ribosome. These results support g5Rp presence at the ER and the hypothesis of g5Rp implicated in mRNA metabolism. Not only that, but interestingly, g5Rp is interacting with cytoplasmic Poly(A) binding protein (PABPC) exclusively at early times (6hpi) post infection, as no bound PABPC was detected in the sample corresponding to 16 hpi. This fact reinforces the idea of g5Rp interacting

with the translation complex. In all the cases, GST samples were used to discriminate between specific and unspecific interactions.

Sample	Accesion number	Protein	Indetified sequences	Score
Mock	P62263	40S ribosomal protein S14 OS=Homo sapiens GN=RPS14 PE=1 SV=3 - [RS14_HUMAN]	TPGPGAQSALR ELGITALHIK IEDVTPIPSDSTR	7,29
	E9PKZ0	60S ribosomal protein L8 (Fragment) OS=Homo sapiens GN=RPL8 PE=1 SV=1 - [E9PKZ0_HUMAN]	ASGNYATVISHNPETK AVVGVVAGGGR	6,77
	C9J4Z3	60S ribosomal protein L37a OS=Homo sapiens GN=RPL37A PE=4 SV=1 - [C9J4Z3_HUMAN]	TVAGGAWTYNTTSAVTVK AVGIWHCGSCMK	5,65
ASFV 6 hpi	J3KTJ8	60S ribosomal protein L26 (Fragment) OS=Homo sapiens GN=RPL26 PE=4 SV=4 - [J3KTJ8_HUMAN]	KDDEVQVVR DDEVQVVR YVIYIER FNPFVTSDR	9,01
	A0A024R9E2	Poly(A) binding protein, cytoplasmic 1, isoform CRA_c OS=Homo sapiens GN=PABPC1 PE=4 SV=1 - [A0A024R9E2_HUMAN]	VEIIANDQGNR LLQDFFNGK STAGDTHLGGEDFDNR	8,15
	E9PKZ0	60S ribosomal protein L8 (Fragment) OS=Homo sapiens GN=RPL8 PE=1 SV=1 - [E9PKZ0_HUMAN]	ASGNYATVISHNPETK AVVGVVAGGGR AVDFAER	6,08
	A2A3R7	40S ribosomal protein S6 OS=Homo sapiens GN=RPS6 PE=1 SV=1 - [A2A3R7_HUMAN]	MATEVAADALGEEWK LNISFPATGcQK	6,06
	P62263	40S ribosomal protein S14 OS=Homo sapiens GN=RPS14 PE=1 SV=3 - [RS14_HUMAN]	TPGPGAQSALR IEDVTPIPSDSTR	5,60
	E9PPU1	40S ribosomal protein S3 OS=Homo sapiens GN=RPS3 PE=1 SV=1 - [E9PPU1_HUMAN]	DEILPTTPISEQK TEIIILATR	4,86
ASFV 18 hpi	Q9BS10	Similar to ribosomal protein S8 (Fragment) OS=Homo sapiens PE=2 SV=1 - [Q9BS10_HUMAN]	ISSLLEEQFQQGK ADGYVLEGK	11,66
	B5MCT8	40S ribosomal protein S9 OS=Homo sapiens GN=RPS9 PE=3 SV=1 - [B5MCT8_HUMAN]	LFEGNALLR LIGEYGLR	7,02
	P62263	40S ribosomal protein S14 OS=Homo sapiens GN=RPS14 PE=1 SV=3 - [RS14_HUMAN]	IEDVTPIPSDSTR TPGPGAQSALR	6,36
	K7EMA7	60S ribosomal protein L23a OS=Homo sapiens GN=RPL23A PE=3 SV=1 - [K7EMA7_HUMAN]	VNTLIRPDGEK LAPDYDALDVANK	5,59
	F8W7C6	60S ribosomal protein L10 OS=Homo sapiens GN=RPL10 PE=1 SV=2 - [F8W7C6_HUMAN]	FNADEFEDMVAEK MLSCAGADR	5,59
	V5XJZ0	Ribosomal protein S4, X-linked (Fragment) OS=Macaca fascicularis GN=RPS4X PE=4 SV=1 - [V5XJZ0_MACFA]	VNDTIQIDLETGK LSNIFVIGK	5,55
	C9JXB8	60S ribosomal protein L24 OS=Homo sapiens GN=RPL24 PE=1 SV=1 - [C9JXB8_HUMAN]	AITGASLADIMAK CESAFLSK	5,38
	M0R0P7	60S ribosomal protein L18a OS=Homo sapiens GN=RPL18A PE=1 SV=1 - [M0R0P7_HUMAN]	SSGEIVYCGQVFEK DLTTAGAVTQcYR	4,80

Table 7. Identification of cellular proteins interacting with g5Rp.
Data found by sequencing the peptides interacting with GST-g5Rp after incubation of the recombinant protein with extracts of Mock-infected or ASFV-infected cells and recovered at 6hpi and 18 hpi. Identification of peptides was carried out using Uniprot Primates data base. The table shows the Uniprot accession number (accession number), the identified protein (protein), the peptide sequences which allowed identification of the protein (identified sequence) and the score.

Discussion

5.1 RNA METABOLISM REGULATION IN ASFV INFECTION: g5Rp, A PUTATIVE VIRAL DECAPPING ENZYME

5.1.1 Cellular shutoff in ASFV infection

Due to the limited size of their genomes, viruses rely on the host translation machinery for the efficient synthesis of the viral proteins (Schneider and Mohr, 2003). Therefore, viruses must manipulate cellular mRNA metabolism and translation to impair host protein synthesis and to liberate cellular resources, in order to ensure and facilitate their own viral protein expression. Viruses have developed multiple mechanisms to achieve this goal. In this Thesis, we have demonstrated that ASFV infection causes active cellular mRNA degradation: poly(A) mRNA signal decreases progressively form the cytoplasm of infected cells, being only detectable at the periphery of the viral factories at late times post infection. Moreover, mRNA levels of all the cellular genes tested by RT-qPCR diminish with ASFV infection, a phenomenon concomitant with a progressive reduction on cellular protein synthesis at late times post infection and with a reduction of the translation efficient rate. This inhibition of the cellular protein synthesis, known as cellular shutoff, is accompanied by an increase of viral protein synthesis, suggesting that ASFV infection promotes cellular mRNA degradation in parallel to viral mRNA expression. Thus, viral mRNAs are somehow excluded from this massive mRNA degradation, but the mechanism used by the virus to accomplish this phenomenon is still unknown.

Interestingly, during ASFV infection we also observed an accumulation of the poly(A) mRNA at the nucleus, which could be due to an ASFV-induced impairment of the nuclear-cytoplasm transport. In this regard, a previous study has demonstrated that ASFV activates the disruption of the nuclear organization at early times post infection, causing the disassembling of the nuclear lamina and the redistribution to the cytoplasm of nuclear proteins from 4 hours post infection (Ballester *et al.*, 2011). Additionally, poly(A) mRNAs nuclear accumulation could be a secondary effect of the aberrant accumulation of the cytoplasmic poly(A) binding protein (PABPC) at this organelle, as occurs in other viral infections (Abernathy *et al.*, 2014). PABPC is a protein that binds both the poly(A) tail of the mRNAs and proteins involved in the initiation translation complex in the cytoplasm, contributing to the stability of the mRNA and enhancing translation. PABPC also possesses nuclear localization signals that are only exposed when the protein is not interacting with the poly(A) tail. A rapid decrease of poly(A) mRNA, due to the viral infections, can cause the release of PABPC from poly(A) tails at the cytoplasm, leading to the exposure of PABPC nuclear localization signal that could be then recognised by the nuclear import machinery (Kumar *et al.*, 2011). In this regard, cells expressing the viral endonucleases vhs (alpha-herpesvirus), SOX (gamma-herpesvirus), PA-X (influenza virus) or nsp1 (SARS coronavirus) present an anomalous accumulation of PABPC at the nucleus. This accumulation leads to a hyperadenylation of nascent transcripts and to their retention at nucleus, probably because they are recognise as aberrant by the nuclear mRNA surveillance machinery (Abernathy and Glaunsinger, 2015;

Arias *et al.*, 2009; Khaperskyy *et al.*, 2014; Kumar and Glaunsinger, 2010). Due to the fact that poly(A) RNAs also accumulates at the nucleus and that mRNAs are eliminated at the cytoplasm, we cannot discard that a similar process could be happening in ASFV infection. However, PABPC localization in ASFV-infected cells should be further investigated in order to validate this hypothesis.

Nevertheless and due to the results obtained in this Thesis, it is likely that both strategies (active mRNA degradation at the cytoplasm and accumulation at the nucleus) are used by ASFV to perform the cellular shutoff.

We have also observed that late viral mRNAs are localized in cytoplasmic granules clustered near the viral factories. This fact could be a viral mechanism to protect their mRNAs to the massive RNA degradation. In this regard, a similar mechanism has been proposed to vaccinia infection, as D10 does not localize in viral factory areas (Parrish *et al.*, 2007). This topic will be further discussed in this section.

5.1.2 g5Rp as a putative viral decapping enzyme *in vivo*

5.1.2.1 g5Rp expression and localization

ASFV is able to control accurately the expression of its genes in a time-dependent manner. Immediate early and early viral genes are expressed after viral entry and repressed before or during viral replication, respectively, while intermediate and late genes are expressed after viral replication. Intermediate genes are rapidly degraded before the accumulation of late transcripts, while late mRNAs are slowly degraded after their accumulation (Rodriguez and Salas, 2013). Thus, the temporal expression of ASFV genes involves regulation of both mRNA transcription and degradation. As mentioned above, ASFV displays viral mRNA expression concomitantly with cellular mRNA degradation. In this regard, ASFV genome encodes for a protein called g5Rp (pD250R in Ba71V strain) that harbours a Nudix domain, which is comparable to other Nudix hydrolases such as the host decapping enzyme 2 (Dcp2) or the viral proteins D9 and D10 of VACV (McLennan, 2007). Additionally, g5Rp possesses decapping activity *in vitro* (Parrish *et al.*, 2009). These two features suggest g5Rp involvement in mRNA decapping and make it a candidate to be the viral factor involved in both the viral mRNAs degradation (which may contribute to the viral temporal expression) and the cellular mRNA degradation (which could contribute to the cellular shutoff).

g5Rp Nudix motif is similar to that found in other cellular and viral decapping enzymes, but its sequence presents a higher similarity to the yeast SpDcp2 (McLennan, 2007). Contrary to what happens in vaccinia, ASFV genome contains only this Nudix hydrolase (Parrish *et al.*, 2009). In this Thesis, we have demonstrated that g5R mRNA is expressed since 4 hpi until late times post infection in ASFV-infected Vero cells (MOI of 5 pfu/cell) and that g5R protein accumulates progressively during the infection. Experimentally, ASFV immediate early and early genes are described by their expression in infected cells in the presence of inhibitors of the viral replication, such as cytosine arabinoside (AraC) (Salas *et al.*, 1986). We demonstrated

that g5R mRNA and protein expression takes place in the presence of this compound, indicating that g5R is an early viral gene. However, in the presence of AraC, g5R mRNA levels slightly decrease, suggesting that a second boost of g5R expression takes place after viral replication. In vaccinia, the decapping enzymes D9 and D10 present different times of expression during the infection: D9 is expressed at early times post infection, while D10 is a late viral gene, and it has been suggested that both enzymes act in an overlapping and complementary manner (Parrish and Moss, 2006; Parrish and Moss, 2007). However, and as explained above, g5Rp is the unique enzyme in ASFV genome which harbours a Nudix motif. As a putative viral decapping enzyme implicated in the cellular shut off and/or in the temporal viral gene expression, it can be possible that ASFV carry out two boost of expression to assure the presence of the g5R protein during all the infective cycle, in order to perform both putative functions.

Regarding g5Rp subcellular localization, our results indicate that the protein presents an endoplasmic reticulum (ER) distribution pattern, which was previously suggested by *Cartwright et al*. The authors proposed that, as g5Rp sequence does not harbours any ER peptide signal, it is probably that the protein associates with ER at the cytosolic side and does not translocate into the ER lumen. They also suggested that this localization could be related to a localized activity of the protein (Cartwright *et al.*, 2002). In eukaryotic cells, translation could occur both in ribosomes freely spread on the cytoplasm and in ribosomes bound to the surface of the ER. Traditionally, it was stabilised that mRNAs translated at the ER codify to secretory or membrane proteins, while mRNAs encoding for cytosolic proteins were translated at the cytosolic ribosomes. However, recent findings have demonstrated that a large fraction of mRNAs encoding for cytosolic proteins are also translated at the ER-associated ribosomes (reviewed in (Reid and Nicchitta, 2015)). Given that ER is a site where active translation is concentrated, g5Rp location at this organelle could be related to its possible role in cellular mRNA degradation and protein synthesis impairment. In this regard, pulldown assays in which GST-g5R protein was incubated with lysates of ASFV-infected Vero cells collected at 6 hpi demonstrate that g5Rp is able to interact with the translation machinery component PABPC and with the 40S and 60S ribosomes subunits, supporting g5Rp presence at the ER and at the translation complexes. Interestingly, it has been described that KSVH SOX endonuclease co-sediments with the 40S ribosomal subunit (Covarrubias *et al.*, 2011). The authors suggest that SOX could be recruited to the mRNA by association with the translation initiation machinery. Due to the fact that g5Rp interacts with both 40S and 60S, could be possible that ASFV g5R protein uses a similar mechanism to SOX. On the other hand, pull down assays of GST-g5R protein after incubation with infected extracts collected at 16 hpi show that g5Rp still interacts with ribosomes at late times post infection, but no longer interacts with PABPC. These data is in parallel with the hypothesis of PABPC being relocated to the nucleus during ASFV infection.

Remarkably, g5Rp could be also clearly detected at the periphery of the nucleus during the infection. In this regard, it has been described that the viral matrix protein of VSV localizes at the periphery of the

nucleus, in the nuclear rim (von Kobbe *et al.*, 2000). M protein interacts directly with the nucleoporin Nup98, which is a component of the Nuclear Pore Complex (NPC) involved in the mRNA export process (Powers *et al.*, 1997). This interaction causes a blockade of mRNA transport and leads to the accumulation of poly(A) mRNAs at the nucleus. Due to the fact that g5Rp localization is similar to the M protein, and that during ASFV infection poly(A) mRNAs are clustered to the nucleus, it may be possible that this protein is also involved in some way in targeting mRNA nuclear-cytoplasm transport.

On the other hand, at late times post infection, g5Rp accumulates at the periphery of viral factories. ASFV factories are areas enclosed by ER membranes, which explains the presence of g5Rp and calnexin (a well-known ER protein (Tjoelker *et al.*, 1994)) at these structures at late times post infection. Interestingly, g5Rp is able to interact with the viral proteins pp220, p72 and p10 at late times post infection. All these proteins are packaged into the virion, thus will be located at the viral factories at later times, partially explaining its interaction with g5Rp. Other possibility is that g5Rp could also be packaged into the virion. Further experiments at our laboratory will be conducted to decipher this possibility. The fact that g5Rp is only gathered at this structures late during the infection could be related to its function as a dual regulator of both cellular and viral mRNA metabolism. At early times post infection, g5Rp is associated at the ER of infected cells, maybe to degrade cellular mRNAs and impair cellular protein synthesis. Whereas, at late times post infection, this enzyme accumulates where late mRNAs localize probably to stop late viral transcription and keep the energy resources. These resources could be then used in the viral morphology and viral egress processes.

5.1.2.2 g5Rp function

It has been described that g5Rp holds two enzymatic activities *in vitro*. First description of the protein demonstrated that g5Rp possesses high affinity substrate for PP-InsP5 (diphosphoinositol polyphosphates) and pointed to a possible implication of g5Rp in viral membrane morphogenesis (Cartwright *et al.*, 2002). However, a second study demonstrated that g5Rp is able to hydrolyse cap structures *in vitro* when attached to a RNA body, a common feature of decapping enzymes (McLennan, 2007; Parrish *et al.*, 2009) (Song *et al.*, 2010). High variability of substrates is a shared characteristic among Nudix enzymes (McLennan, 2013). In mammalian cells, six Nudix hydrolases with diverse enzymatic activities have been described to possess also decapping activity *in vitro* (Song *et al.*, 2013). Thus, it is possible that g5Rp be a dual enzyme able to display both activities.

On the subject of g5Rp decapping activity, it has been previously demonstrated that this protein is able to bind RNA *in vitro* by EMSA assays (Parrish *et al.*, 2009). Moreover, its decapping activity is highly inhibited by uncapped mRNAs, suggesting that g5Rp recognises its substrate mainly by the RNA body (Parrish *et al.*, 2009). In this Thesis, we described for the first time that this protein is able to bind RNA *in vivo*. Substitutions of the conserved glutamic residues 147, 150 and 151 impair strongly g5Rp decapping

activity *in vitro* (Parrish *et al.*, 2009). However, we have demonstrated that these mutations do not affect g5Rp RNA-binding capacity. These residues are highly conserved among different Nudix hydrolases, and in yeast and mammals, it has been described that they are involved in coordinating the divalent cation essential for the catalysis (Mildvan *et al.*, 2005; She *et al.*, 2006). Due to its position in the Nudix pocket in comparison with SpDcp2, and after mutational analysis, the VACV D10 homologous residues, glutamics 141, 144 and 145, have been also described to be involved in the catalytic reaction and in the direct contact with the cap structure (Souliere *et al.*, 2009; Souliere *et al.*, 2010). Given that these residues are as well highly conserved in g5Rp and that g5Rp and SpDcp2 Nudix motif are structurally similar, it could be expected that E147, E150 and E151 are playing a similar role on g5Rp catalytic pocket, being mainly involved in the catalytic reaction and/or in the cap recognition, but not in the RNA-interaction.

Dual fluorescent method allowed us to identify the N-terminal domain of g5Rp as the main player of RNA-g5Rp interaction. On the other hand, g5Rp C-terminal domain seems to be not implicated. Electrostatic surface representation confirmed these results and showed that g5Rp N-terminal domain possesses a basic channel that could be acting as a RNA-binding platform. A positively charged channel is also present at the dorsal surface of the Nudix domain of *S.pombe*, *S.cerevisiae* and human Dcp2 enzymes, and it has been described as the RNA-binding region: mutations of residues of this channel drive to a decrease on Dcp2 substrate affinity (Deshmukh *et al.*, 2008; She *et al.*, 2008). Furthermore, in these enzymes, residues from the Box B, which are essential for the RNA-binding activity in biochemical studies (Piccirillo *et al.*, 2003), located directly on this dorsal surface. However, amino acidic sequence of the Box B region is not clearly conserved in the viral decapping enzymes D10 and g5Rp (McLennan, 2007; Souliere *et al.*, 2009). In this regard, and unlike the cap-binding cavity, basic amino acids of the positive channel are only discreetly conserved at the level of primary sequence between SpDcp2 and ScDcp2, while the surface of this region in both enzymes is enriched in positive charged residues (Deshmukh *et al.*, 2008). Indeed, D10 presents a similar number of basic amino acids in this region (McLennan, 2007). These results suggest that only the positive surface is important to the RNA-binding, and support our results of the basic channel of the N-terminal domain of g5Rp as the RNA-binding motif of this enzyme.

RNA-binding plays a critical role on the substrate recognition of eukaryotic decapping enzymes. *In vitro* assays demonstrated that hDcp2 is not able to hydrolyse cap analogues, and only displays decapping activity when the cap is attached to a RNA body (Piccirillo *et al.*, 2003; van Dijk *et al.*, 2002). Moreover, hDcp2 enzymatic activity is not inhibited in cap analogue competition assays and it requires long RNA substrates (at least 23 nt) (Wang *et al.*, 2002). Yeast and *C.elegans* Dcp2 proteins also prefer long RNAs and display tiny activity on cap analogue substrates (Cohen *et al.*, 2005; Steiger *et al.*, 2003). According to these evidences, it has been suggested that eukaryotic Dcp2 enzymes are unable to recognize the cap directly and they require binding to the RNA to detect the cap substrate. On the other hand, viral decapping enzyme D10 is strongly inhibited by uncapped RNA and by methylated cap analogues (Parrish *et al.*, 2007), suggesting

that differences in substrate recognition between this viral enzyme and its eukaryotic counterparts exist. The first seems to recognize its substrate by the interaction of both the RNA and the cap structure, while the latter mainly recognize its substrate by RNA body-interaction. Interestingly, VACV D9 enzyme prefers longer mRNA substrates, is more efficiently inhibited by uncapped mRNAs and is less affected by methylated cap analogous than D10 (Parrish and Moss, 2007). In this regard, D9 behaves in a similar way to eukaryotic decapping enzymes. g5R protein is strongly inhibited by uncapped mRNAs (whose inhibitory effect is higher in this enzyme than in D9 or D10), and its decapping activity is not affected by free methylated cap derivatives (Parrish *et al.*, 2009), suggesting that g5Rp may have higher affinity to mRNA than that VACV enzymes have. These evidences, and also the fact that ASFV enzyme displays more sequence similarity with eukaryotic Dcp2 than with its viral counterparts (McLennan, 2007; Parrish *et al.*, 2009), suggest that the mechanism used by g5Rp for substrate recognition is closer to the one resembled by eukaryotic enzymes. Thus, g5Rp substrate recognition may occur mainly by interaction through the RNA domain, highlighting the importance of the RNA binding in g5Rp catalytic process.

The fact that the g5Rp N-terminal domain was able to bind more RNA than the g5Rp wild type form is surprising. However, it should be taken into consideration that g5Rp is a putative catalytic enzyme, whose function might be to accelerate the hydrolysis of the cap structure. In this regard, g5Rp-RNA interaction should be fast, causing RNA rapidly releases after decapping. This will explain the lower levels of RNA that we are able to detect interacting with the g5Rp wt form when compared to the N-terminal form, which is able to bind RNA but unable to decapp. Our results also indicate that the Nudix motif is not necessary to the RNA-g5Rp interaction, as the g5Rp N-terminal construction does not possess this sequence and fully interacts with the mRNA. This fact suggests that g5Rp RNA-binding capacity is independent to its catalytic activity. This feature has also been shown in Dcp2. Studies carried out *in vitro* to identify the minimal domain with decapping activity in human Dcp2 showed that a construction that harbours incomplete Nudix fold and does not present enzymatic activity is able to bind RNA (Piccirillo *et al.*, 2003). However, further studies mapping different regions of the g5Rp N-terminal domain should be carried out to determine the exact areas and amino acids implicated in the RNA-binding.

Interestingly, g5Rp ΔNudix domain is also able to bind RNA, although in a lesser extent than the N-terminal construction. Given that both proteins only differ on the presence of the C-terminal domain in the g5Rp ΔNudix construction, one possible explanation may be that the C-terminal domain is involved in the destabilization and release of the RNA.

In this Thesis, we have established that g5Rp does not only bind cellular mRNAs in cultured cells, but also host and viral mRNAs in the context of the infection. The fact that this protein interacts with cellular mRNAs suggests that g5Rp is involved in the cellular shutoff observed in ASFV infection, while g5Rp - viral mRNAs interaction may be related to the viral temporal gene expression. This is the mechanism that has been proposed to vaccinia, whose decapping enzymes D9 and D10 eliminates both viral and cellular mRNAs

(Liu *et al.*, 2014; Parrish and Moss, 2006; Shors *et al.*, 1999). In this regard, there are several examples of viruses that display mechanisms to massively degrade host cellular mRNAs and that also affect its own viral mRNAs. This is the case of alpha- and gamma- herpesviruses, which encode to viral endonucleases able to eliminate both cellular and viral mRNAs (Abernathy *et al.*, 2014; Taddeo *et al.*, 2013). Alpha-herpesviruses are characterised by the temporal expression of their genes, and the viral endonuclease , vhs, has been involved in mediating the effective transition between the immediate early, early and late genes (Taddeo *et al.*, 2013) (Abernathy and Glaunsinger, 2015). Gamma-herpesvirues-encoded SOX protein also target viral mRNAs, and its inactivation causes an altered composition of progeny virions, suggesting that during gamma-herpes virus infection regulation of viral mRNAs by degradation plays an important role on gene expression and on viral particle composition (Abernathy *et al.*, 2014).

Regarding cellular mRNA-g5Rp interaction, we have observed that eIF4E mRNA levels attached to GFP-g5Rp wt and related to eGFP are clearly superior than the B-actin mRNA levels bound to GFP-g5Rp wt and referred to eGFP. These results suggest that g5Rp may display more affinity for determinate cellular substrates. Selectivity in host mRNA degradation has been previously described to other viral systems, such us alpha-herpesvirus or vaccinia. Concerning alpha-herpesviruses, it has been described that the endonuclease vhs rapidly degraded stable host mRNAs like β-actin or GAPDH, while mRNAs containing AU-rich sequences are translational repressed and their decay rates are slowed, indicating that vhs discriminates between different classes of cellular mRNAs (Esclatine *et al.*, 2004). Regarding vaccinia infection, microarrays analysis of cDNA from Mock-infected and VACV-infected cells revealed that host mRNAs are differently regulated (Guerra *et al.*, 2003). The vast majority are downregulated during vaccinia infection, and, among this, Guerra et al. differentiate three clusters: the first includes transcripts that are upregulated at 2 hours post infection (hpi) and repressed at 6 and 16 hpi, the second contains transcripts that are repressed at 6 and 16 hpi and the last includes transcripts that are repressed from 2 hpi to 16 hpi (Guerra *et al.*, 2003). Due to this different cellular mRNA degradation patterns, it has been suggested that D9, which presents more affinity to the RNA body than D10, may be able to discern among different mRNA sequences (Parrish and Moss, 2007). In a similar manner, ASFV infection may be discriminating among cellular transcripts, using g5Rp as a mechanism to recognise different cellular mRNAs. This hypothesis is supported by the fact that g5Rp is even more inhibited than D9 by uncapped mRNAs and that it is not affected by methylated cap analogous, as mentioned above. In this regard, *in vitro* RNA-binding assays demonstrated that g5R protein is able to interact with uncapped cellular mRNAs, but the observed shift in the EMSA was not complete (Parrish *et al.*, 2009). *Parrish et al* suggest that this could have two different explanations: first is the requirement of the cap structure to stabilize g5Rp-RNA interaction; and the second is that g5Rp only displays strong affinity for molecules with certain features, as it has been described to Dcp2 (Li *et al.*, 2009; Li *et al.*, 2008). This second hypothesis goes in parallel with our suggestion.

One might infer that g5Rp is also able to differentiate between different viral mRNAs, in order to carry out the temporal regulation of viral gene expression. We have observed that p72 mRNA levels bound to GFP-g5Rp wt and referred to eGFP are lower than the A224L and A238L mRNAs attached to GFP-g5Rp wt and referred to eGFP at 14 hpi, supporting the idea of a specific recognition of the viral substrate. However, a broader study should be conducted in order to determine specific g5Rp interactions with early and late viral mRNAs during all ASFV viral cycle to confirm this hypothesis and to define the exact mechanism used by g5Rp, as well as the possible sequences recognised by this protein. Viral mRNA specificity has been also suggested to D10 decapping enzyme. This enzyme is more effectively inhibited by m^7GpppG than m^7GpppA, thus it has been described that possesses more affinity by the first cap analogue structure (Parrish *et al.*, 2007). Given that cellular mRNAs and vaccinia early mRNAs have both m^7GpppG_m and m^7GpppA_m structures at their 5´ends, and that intermediate and late VACV mRNAs present exclusively m7GpppAm caps, it has been proposed that D10 could be preferentially recognising the host and early viral mRNAs (Parrish *et al.*, 2007). However, and for the reasons mentioned above, we are more inclined to think that the possible mechanism used by g5Rp to differentiate among different viral mRNAs would implicate recognition of the RNA sequence, instead of recognition by the cap structure. A possible explanation to the RNA affinity differences found between ASFV and VACV decapping enzymes could be related to the fact that g5Rp is the only protein encoded by ASFV genome that possesses a Nudix motif. VACV uses two enzymes with different substrate affinity to degrade viral mRNAs in a complementary way, while ASFV may use only one enzyme able to differentiate different substrates by the RNA body.

Regarding g5Rp function, in this work we have demonstrated that infected cells expressing recombinant GFP-g5Rp wt protein present a slightly reduction on some late viral proteins levels when compared to cells expressing eGFP or the catalytic mutant versions of the protein (GFP-g5Rp REGG and EEQQ). Moreover, analysis by FACS proves that p72 levels in cells overexpressing g5Rp are also reduced, and that the percentage of cells co-expressing CD2v and the recombinant protein g5Rp-HA is clearly reduced when compared to percentage of cells co-expressing g5Rp-HA and p32. We have also observed that A224L mRNA signal is decreased in infected cells expressing g5Rp-HA protein and that expression of GFP-g5Rp in the context of the infection leads to a decrease of both cellular and late viral mRNA levels. Although we have not been able to demonstrate the mechanism used in ASFV to eliminate mRNAs, all the evidences presented above indicate that g5Rp is involved in the cellular shutoff and in the temporal viral genes expression processes, as described to other viral systems (Abernathy and Glaunsinger, 2015). In this regard, modified VACV virus that possess and inducible extra copy of D9 and D10 and that consequently overexpress both proteins during vaccinia infection, present a decrease on viral protein synthesis and a reduction of viral late mRNA levels (Shors *et al.*, 1999). That suggests g5Rp could be acting in a similar manner to VACV decapping enzymes and supports the idea that g5Rp function as a regulator of both cellular and viral RNA metabolism.

Additionally, it is probable that ASFV uses different strategies in a complementary manner, and that g5Rp may act synergistically with other viral proteins. Following this further, ASFV genome encodes for a viral AP endonuclease, pE296R, which has been described to be involved in the viral DNA repair system (Redrejo-Rodriguez *et al.*, 2006). However, it could be possible that this enzyme also displays endoribonuclease activity, as it has been described to the human AP endoribonuclease Ape1 (Barnes *et al.*, 2009). Other viral endonucleases with a dual function have been also described in viral systems, such as the gamma-herpesviruses Epstein-Barr virus (EBV) and Kaposi´s sarcoma-associated herpesvirus (KSHV). Both viruses encode for nucleases implicated in viral genome maturation and mRNA degradation processes (Abernathy *et al.*, 2014; Feederle *et al.*, 2009; Glaunsinger *et al.*, 2005; Rowe *et al.*, 2007).

Suppression of the expression of the gene of interest is a common technique used to study gene function. In this regard, deletion of the viral endonuclease vhs in HSV-1 causes a persistence of cellular mRNAs and a delay on the initiation of the expression of early and late viral mRNAs (Taddeo *et al.*, 2013). In a same manner, deletion of D10 in vaccinia virus (ΔD10) causes that viral transcription initiates more slowly. Early viral mRNAs accumulated to higher levels, and, in addition, early, late and cellular mRNAs persist longer on ΔD10-infected cells when compared to VACV wt infection (Liu *et al.*, 2014; Parrish and Moss, 2006). Contrary to what was expected, infection with the double D9 and D10 vaccinia mutant causes a sharp decrease of both cellular and viral mRNA, a stop of late viral protein synthesis and an inhibition of the viral replication in non-permissive cells (Liu *et al.*, 2015).

In order to test the effect of g5R deletion on ASFV infection, we tried to silence g5R mRNA expression by using a specific siRNA. However, silencing achieved was not enough to observe significant difference between silenced and non-silenced cells. We have also tried to obtain ASFVΔg5R mutant by substitution of the g5R gene by a β-gal reporter gene. Unfortunately, after serial passages and rounds of amplification, we were not successful and no g5R-deleted virus was achieved, thus indirectly suggesting that g5Rp is important to ASFV infection. In vaccinia, due to the fact that D9 and D10 function in a complementary manner, *Parrish et. al* succeeded in the collection of each deletion virus (ΔD9 and ΔD10, respectively) (Parrish and Moss, 2006). However, double D9 and D10 mutant has been very hard to obtain, and only recently has been successfully achieved, proving the important function of these genes in vaccinia infection and maybe indicating that vaccinia is able to use the cellular machinery of decapping during the infection (Liu *et al.*, 2015). Importantly, this double D9 and D10 VACV mutant has been generated by point mutations in the conserved amino acids of the catalytic Nudix motif of both enzymes, therefore is not a "canonic" deletion mutant since contains both genes although they are putatively unable to decapp. Indeed, it has been previously described that deletion of D10 gene by its substitution with a GFP reporter gene is more deleterious for the progression of vaccinia infection than D10 point catalytic mutant (muD10), since ΔD10 virus presents smaller lysis plates than muD10 virus (Liu *et al.*, 2014). These results prompted us to develop a similar approach in ASFV generating an ASFV with a catalytic inactive g5Rp, instead to try the ASFV

Δg5Rp. However, it should be taken into consideration that *Liu et all* generated D10 point mutation virus by homologous recombination between the GFP gene inserted in the ΔD10 virus and a D10 mutated gene present in a vector. Due to the fact we have not been able to generate the first Δg5Rp deletion mutant, we had to develop alternative strategies to obtain it. We are currently working on developing a helper cell line that constitutively expresses the g5R protein, providing the g5R copy needed to support ASFVΔg5Rp infection. We have choose COS Flip in cell line because this system allows the integration of a single copy of the gen of interest in a specific genomic location (FLP site), eliminating the risk of random insertion. Additionally, it is possible to integrate in COS Flip in genome a TET Repressor gene, generating COS Flp in TREx cells lines. This procedure allows the generation of stable cell lines with inducible expression of your gene of interest, thus providing an additional approximation to obtain the deletion mutant.

5.1.3 ASFV regulation of cellular mRNA metabolism

In order to ensure viral translation, viruses have to avoid the cellular mRNA degradation pathways. Given that RNA granules play a key role on mRNA translation and decay, most viruses have developed strategies to subvert the components of these structures (Narayanan and Makino, 2013; Reineke and Lloyd, 2013). Two kinds of RNA granules can be found in eukaryotic cells: the Processing-Bodies (P-Bodies) and the Stress Granules (SGs). P-Bodies are constitutively present in cells and enriched in decapping machinery components. Moreover, P-Bodies size and number increase when translation rate decays and their formation depends on the presence of mRNA decay intermediates. Stress granules forms in specific stress conditions, and disappear when the stress stimuli stops. SGs are composed of decapping machinery components, but also of ribosomes and some eukaryotic initiation factors (eIFs) (Reineke and Lloyd, 2013). While P-bodies have been defined as structures where active mRNA degradation can take place, SGs have been defined as sites of translational repression (Decker and Parker, 2012). Due to this fact, we have focused our attention on P-bodies more that in SG.

We have described that ASFV infection causes a reduction of P-bodies, and consequently, a loss of interaction between the P-Body components Dcp1 and Edc4. Furthermore, both Dcp1 and Edc4 signals decrease in ASFV-infected cells when analysed by CSLM. Edc4 is spread at the cytoplasm of ASFV-infected cells, while Dcp1 accumulates at the surroundings of the viral factories. As explained above, disruption of P-bodies and re-localization of the components is a common mechanism used by viruses in order to avoid the cellular mRNA decay routes and facilitate viral infection (Reineke and Lloyd, 2013). And so, for instance, in the case of West Nile Virus, P-Body components (such as Lsm1, Gw182, DDX3, DDX6 and Xrn1) are recruited to the viral factories and needed to viral replication, whereas neither Dcp1 nor Edc4 are recruited (Chahar *et al.*, 2013). Hepatitis C Virus also disrupts P-bodies and hijacks P-Body components (Lsm1,DDX3, DDX6, Xrn1, Pat1 and Ago2, but not Dcp2) to the viral production sites, and silencing of some of these components suppresses HCV RNA accumulation, indicating that these proteins are required for HCV replication (Ariumi *et*

al., 2011). In this regard, it could be interesting in the near future to check if Dcp1 is essential to ASFV viral replication.

We have observed that Dcp1 and g5Rp co-localize at the periphery of the viral factories. Due to the fact that Dcp1 is a decapping activator (She *et al.*, 2008), we speculate that this protein could be stimulating the RNA decay process at these structures. However, and due to the fact that g5Rp is not directly interacting with Dcp1, this activation could be achieved by Dcp1 ability to interact with other decapping activators, such as Edc3 or Xrn1 (Fromm *et al.*, 2012; Jonas and Izaurralde, 2013; Tritschler *et al.*, 2007). Edc3 is a RNA binding protein that could associate with other decapping activators as Pat1, Lsm 1-7, Dhh1 or Xrn1 acting as a scaffold protein in the formation of the P-Bodies (Fenger-Gron *et al.*, 2005; Fromont-Racine *et al.*, 2000; Ling *et al.*, 2011), thus the presence of Dcp1 at these structures could be accompanied to other decapping factors, which together would facilitate the RNA degradation process. Further studies should be conducted in order to clarify if other decapping activators could also be recruited to the viral replication sites and the mechanism displayed by ASFV to achieve this goal.

During ASFV infection, the location of the cap structure is especially interesting, both by itself and in relation with g5Rp distribution. In order to determine its relation to g5Rp, we used a specific antibody that recognizes both m^7G and m_3G structures (monoclonal antibody H-20, Synaptic Systems (Bochnig *et al.*, 1987)), which means that this antibody is able to recognise both m_3G and m^7G-capped mRNAs. The capping process consists in the addition of a 7-methylated-guanosine (m^7G) by an inverted 5´-5´triphophate bridge to the first RNA nucleotide (m^7GpppN, where N is any nucleotide) (Ghosh and Lima, 2010), while m_3G cap structure is a Nuclear Localization Signal (NLS) for the spliceosomal UsnRNPs, whose biogenesis involves a nucleus-cytoplasm cycle. In this regard, ASFV genome encodes by a viral capping enzyme (NP868R), which displays gyanylyltransferase activity (Pena *et al.*, 1993). In Mock-infected cells, cap signal is spread at the cytoplasm and is more intense in the nucleus, while in ASFV-infected cells the nuclear signal decreases and accumulates at the periphery of the viral factories. Nuclear signal of Mock-infected cells could be due to the capping process, which takes place mainly at this structure, and cytoplasmic signal may correspond to the capped mRNAs. In ASFV infected cells, the increased signal accumulates at the periphery of the viral factories could correspond to the viral capped mRNAs, which have been described by our lab (Castello *et al.*, 2009b) and in this Thesis to be located at the viral replication sites. Interestingly, when we measured cap signal mean intensity, we observed an increase in ASFV-infected cells compared to Mock-infected cells. We have proved here that poly(A) mRNA signal decays at the cytoplasm of infected cells, and that cellular mRNA levels also decreased with ASFV infection, thus this cap signal increment was surprising to us. However, as mentioned before, the cap species recognised by the anti-cap antibody should be taken into consideration (Bochnig *et al.*, 1987), since it recognizes not only capped mRNAs, but also the structures m^7Gp (m^7GMP) and m^7GpppA. *In vitro*, g5Rp hydrolyses capped mRNAs releasing m^7GDP and 5´monophosphorylated RNAs as products, thus we speculate that ASFV-infection may trigger an accumulation of m^7GDP, probably due to

g5Rp decapping activity. In mammalian cells, this decapping product elimination involves m^7GMP production (Taverniti and Seraphin, 2015), which could also rise as a consequence of the accumulation of m^7GDP and may be the cause by which the cap signal increases. Another possibility to explain the cap augmented signal in infected cells would be the accumulation of the m_3G capped RNAs at the cytoplasm of infected cells on account of the ASFV-induced impairment of the nucleus-cytoplasm transport.

We have also described that the cap structure together with g5Rp co-localize at the edge of the viral factories. Indeed, localization of g5Rp at the periphery of viral factories at late times post infection was surprising. In vaccinia, viral mRNAs are recruited to the replication sites (Katsafanas and Moss, 2007). However, D10 is not recruited to the viral factories (Parrish and Moss, 2006), thus it has been proposed that this re-localization could be used as a viral tool to avoid late viral mRNAs degradation (McLennan, 2007). The fact that g5Rp co-localizes with the cap structure at these areas suggest that active decapping could be taking place, thus indicating that ASFV uses a different mechanism to vaccinia to this end. In this regard, g5Rp could be regulated by other cellular or viral proteins, as it happens in alpha-herpesvirus infection. Vhs endonuclease is regulated by several viral factors (UL47, VP16 and VP22) and at least one cellular protein. All of them are packaged into the virions, and it has been suggested that they regulate vhs activity in a temporal manner (Abernathy and Glaunsinger, 2015; Shu *et al.*, 2013a; Shu *et al.*, 2013b; Taddeo *et al.*, 2007). In this regard, we have demonstrated that g5Rp is able to interact at late times post infection with at least three different viral proteins: pp220, p10 and p72. pp220 is a polyprotein that is processed by proteolysis during the maturation process of the virion, giving rise to the structural proteins p150, p37, p34 and p14, which are the major components of the core shell layer (Andres *et al.*, 2002b; Andres *et al.*, 1997; Simon-Mateo *et al.*, 1993). p10 is a structural viral protein that is localized at the nucleoid of the virion particles and that exerts DNA binding activity (Nunes-Correia *et al.*, 2008). Finally, p72 is the major component of the viral capsid and it is essential for the formation of this structure (Garcia-Escudero *et al.*, 1998). All these proteins are part of the virion and are localised at the viral factories at late times post infection, probably interacting with g5Rp at these structures. This fact makes them candidates as late regulators of g5Rp function. Furthermore, we cannot exclude the possibility that g5Rp may be regulated by phosphorylation and/or unphosphorylation events. In this regard, ASFV genome encodes for a viral serine-threonine protein kinase (j9L in Malawi strain) that displays phosphorylation activity *in vitro* (Baylis *et al.*, 1993). According to this hypothesis, analysis of g5Rp sequence using *Prosite* Server revealed that the protein possesses two putative phosphorylation sites (data not shown). Interestingly, j9L protein is packaged into virions, which indicates that at late times post infection it is recruited to the viral factories. Although speculative, j9L could be acting as a regulator of g5Rp activity at these structures as a mechanism to ensure late viral translation.

We have previously described that ASFV translation relies on host translation machinery (Castello *et al.*, 2009b). Deletion of eIF4E and eIF4G leads to a decrease in the number of viral factories, in the case of eIF4G elimination, and to the formation of aberrant viral replication sites, when eIF4E is supressed.

Moreover, ASFV infection stimulates the formation of the translation initiation complex by phosphorylation of eIF4E, eIF4G and the eIF4E Binding Protein 4E-BP, which phosphorylated is not able to interact with eIF4E (Castello *et al.*, 2009b). During ASFV infection, eIF2α phosphorylation is avoided in order to ensure translation, a process which seems to involve the viral protein DP71L (Rivera *et al.*, 2007; Zhang *et al.*, 2010). In this regard, we have demonstrated that ASFV infection triggers the re-localization of eIFs and ribosomes to the viral factories. The fact that all these components, together with late viral mRNAs, localize at the same cytoplasmic areas suggests that transcription and translation take place at this foci in close proximity, which maximize the efficiency of both processes. Coupling between replication, transcription and translation has been suggested to many other viruses, such as vaccinia, Sindbis virus or vesicular stomatitis virus (Katsafanas and Moss, 2007; Sanz *et al.*, 2007; Whitlow *et al.*, 2008).

Our laboratory has also described that eIF4G location at the viral factories changes during the infection. At 8-10 hpi, this initiation translation factor is accumulated together with the viral DNA, whereas at late times post-infection (18 hpi), eIF4G is redistributed to the surroundings of the viral factories, probably due to a viral mechanism to compartmentalize translation and morphogenesis (Castello *et al.*, 2009b). Although speculative, this differential location between g5Rp and eIF4G soon after viral replication, but not a later times post infection, could indicate an additional viral mechanism to regulate g5Rp decapping activity. In this hypothesis, translation of late viral mRNAs may take place inside the viral factories, where viral mRNAs are protected from the decapping activity of g5Rp. At later times post infection, when morphogenesis is fully activated, the translation complexes are displaced to the edge of viral factories, where viral mRNAs could be targeted by g5Rp. This will be a mechanism used by the virus to maximize the energy resources, firstly on translation, and once translation is not required, in morphogenesis. eIF4E is a decapping inhibitor able to interact with the cap structure and, consequently, to limit its interaction with the decapping enzymes (Schwartz and Parker, 1999; Schwartz and Parker, 2000). Therefore, presence of eIF4E at the periphery of viral factories could compete with g5Rp to interact with viral late mRNAs, which could explain the slowly decrease of late viral mRNAs.

In conclusion, the results presented in this Thesis indicate that g5Rp is a RNA-binding protein able to interact *in vivo* with both cellular and viral mRNAs in the context of the infection. Moreover, its overexpression leads to a decrease of both cellular and viral mRNAs, and causes a reduction on late viral protein synthesis. g5R is an early viral gene that is also important for the proper progression of the infection. g5Rp present different subcellular location during ASFV infection: at early times post infection, g5R mainly presents an ER pattern and interacts with several components of the cellular translation machinery, while at later times, this protein accumulates at the viral factories, where it co-localizes with Dcp1 and the cap structure and interacts with the ribosomes and the viral proteins pp220, p10 and p72. Taken together, and given that g5Rp possesses decapping activity *in vitro* (Parrish *et al.*, 2009) these results indicate that g5Rp

may acts as a viral regulator of both cellular and viral mRNA metabolism, being involved in impairing cellular protein synthesis and in ensuring viral temporal gene expression.

5.2 FUTURE PERSPECTIVES

Very little is known about how ASFV manipulates mRNA degradation and decay. To our knowledge this is the first experimental approach that tries to explain how this virus achieves this goal. However, several issues still remain elusive. Among them, the molecular mechanism used by g5Rp to distinguishes among different mRNAs or the possible strategies employed by the virus to regulate its activity. In this regard, obtaining an ASFVΔg5R by using new strategies, or, as achieved in vaccinia virus, an ASFV containing g5Rp mutated in its catalytic domain would also be interesting.

The fact that g5R gene seems to be essential to ASFV infection makes it a good candidate in order to obtain a vaccine, which has remain elusive, to date. ASFVΔg5R deletion mutant, or an ASFV encoding and inactive g5Rp mutant, may be able to trigger a protective host immune response, but will be unable to produce productive viral particles. In this regard, it has been described that widespread elimination of cellular mRNAs impairs anti-viral immune response, and deletion or inactivation of genes involved in mRNA degradation, such as D10 in vaccinia or muSOX in the murine gamma-herpesvirus 68, leads to a attenuation of the virulence (Liu *et al.*, 2014; Richner *et al.*, 2011). Interestingly, a recent study has demonstrated that the vaccinia double D9 and D10 mutant infection leads to a greater attenuation of the virulence than VACV point mutated D10 (Liu *et al.*, 2015). Therefore, and given that g5Rp is the only Nudix enzyme encoded to ASFV, a great attenuation of ASFV virulence might be expected if an ASFV mutant lacking active g5Rp could be generated in the future.

Conclusions

1- During ASFV infection, accumulation of cellular mRNA in the nucleus of infected cells and massive degradation of such messengers in the cytoplasm occurs. This phenomenon happens in parallel with the expression of viral genes.

2- ASFV infection causes the relocation of the cellular initiation translation factors eIF4G and 4E, as well as ribosomes, to the viral factories, where late mRNAs are also found.

3- During infection, the components of the cellular decapping machinery Dcp1 and Edc4 undergo rearrangement, leading to a decrease of P-Bodies. Furthermore, the infection causes the accumulation of the cap structure of mRNA in the cytoplasm of infected cells, especially around the viral factories.

4- ASFV genome encodes for a protein, g5Rp (pD250R in Ba71V strain), which has a Nudix hydrolase domain similar to that found in most of the cellular and viral decapping enzymes. g5R is an early gene whose transcript is maintained until late times of infection. At early stages of infection, g5Rp presents a pattern similar to the endoplasmic reticulum distribution and interacts with several components of the translational machinery, such as ribosomes or PABPC, while at later times, accumulates around the viral factories and interacts both with ribosomes and pp220, p10 and p72 viral proteins. On the periphery of these structures, g5Rp also co-localizes with Dcp1 and the cap structure.

5- g5Rp is able to bind polyadenylated RNA in cells stable expressing the protein. This interaction is mediated primarily by g5Rp N-terminal domain, which presents a basic channel similar to that found in other decapping enzymes. The point mutation of the Nudix domain conserved amino acids, although essential for catalysis *in vitro*, does not affect the g5R ability to bind RNA.

6- g5R protein interacts with both viral and cellular mRNA in the context of viral infection. Furthermore, overexpression of the viral protein causes a decrease in the levels of the two types of mRNAs, and affects late viral protein expression. Furthermore, g5R could be an essential gene for the proper progress of the infection, since it has not been possible to eliminate it from the viral genome by conventional methods.

.

Conclusiones

1- Durante la infección del VPPA se produce la acumulación de los ARN mensajeros celulares en el núcleo de las células infectadas, y la degradación masiva de dichos mensajeros en el citoplasma. Éste fenómeno se produce en paralelo a la expresión de los mensajeros virales.

2- La infección por VPPA provoca la relocalización de los factores celulares de iniciación de la traducción eIF4G y eIF4E, así como de los ribosomas, a las factorías virales, donde también se localizan los ARN mensajeros tardíos.

3- Durante la infección, los componentes de la maquinaria de decapping celular Dcp1 y Edc4 sufren una reorganización, lo que produce una dispersión de los cuerpos citoplasmáticos o P-Bodies. Asimismo, la infección causa la acumulación de la estructura cap de los ARN mensajeros en el citoplasma de las células infectadas, especialmente alrededor de las factorías virales.

4- El genoma del VPPA codifica para una proteína, g5Rp (pD250R en Ba71V), que posee un dominio Núdix hidrolasa similar al encontrado en enzimas de decapping celulares y virales. g5R es un gen temprano cuyo ARN mensajero se detecta durante todo el ciclo viral. A tiempos tempranos de la infección, g5Rp presenta un patrón de localización similar al del retículo endoplásmico e interacciona con distintos componentes de la maquinaria traduccional, como los ribosomas o PABPC, mientras que, a tiempos tardíos, se acumula alrededor de las factorías virales e interacciona tanto con los ribosomas como con las proteínas virales pp220, p10 y p72. En la periferia de éstas estructuras, g5Rp también co-localiza con Dcp1 y con la estructura cap.

5- g5Rp es capaz de unir ARN poliadenilado en células que expresan dicha proteína de manera estable. Ésta unión está mediada principalmente por el dominio N-terminal, que presenta un canal básico similar al encontrado en otras enzimas de decapping. La mutación puntual de los aminoácidos conservados en el dominio Núdix, aunque esenciales para la catálisis *in vitro*, no afectan a la capacidad de g5Rp para unir ARN.

6- La proteína g5R interacciona tanto con ARN mensajeros celulares como virales en el contexto de la infección. Asimismo, la sobreexpresión de ésta proteína provoca una disminución en los niveles de los dos tipos de ARN mensajeros, y afecta a la expresión de las proteínas virales tardías. Además, g5R podría ser un gen esencial para el adecuado progreso de la infección, ya que no ha sido posible su eliminación del genoma viral por métodos convencionales.

Bibliography

Abernathy, E., Clyde, K., Yeasmin, R., Krug, L. T., Burlingame, A., Coscoy, L. and Glaunsinger, B. (2014). Gammaherpesviral gene expression and virion composition are broadly controlled by accelerated mRNA degradation. *PLoS Pathog* **10**, e1003882.

Abernathy, E. and Glaunsinger, B. (2015). Emerging roles for RNA degradation in viral replication and antiviral defense. *Virology*.

Afonso, C. L., Piccone, M. E., Zaffuto, K. M., Neilan, J., Kutish, G. F., Lu, Z., Balinsky, C. A., Gibb, T. R., Bean, T. J., Zsak, L. and Rock, D. L. (2004). African swine fever virus multigene family 360 and 530 genes affect host interferon response. *J Virol* **78**, 1858-64.

Alcami, A., Carrascosa, A. L. and Vinuela, E. (1989a). The entry of African swine fever virus into Vero cells. *Virology* **171**, 68-75.

Alcami, A., Carrascosa, A. L. and Vinuela, E. (1989b). Saturable binding sites mediate the entry of African swine fever virus into Vero cells. *Virology* **168**, 393-8.

Almazan, F., Rodriguez, J. M., Andres, G., Perez, R., Vinuela, E. and Rodriguez, J. F. (1992). Transcriptional analysis of multigene family 110 of African swine fever virus. *J Virol* **66**, 6655-67.

Almazan, F., Rodriguez, J. M., Angulo, A., Vinuela, E. and Rodriguez, J. F. (1993). Transcriptional mapping of a late gene coding for the p12 attachment protein of African swine fever virus. *J Virol* **67**, 553-6.

Almendral, J. M., Almazan, F., Blasco, R. and Vinuela, E. (1990). Multigene families in African swine fever virus: family 110. *J Virol* **64**, 2064-72.

Andres, G., Alejo, A., Salas, J. and Salas, M. L. (2002a). African swine fever virus polyproteins pp220 and pp62 assemble into the core shell. *J Virol* **76**, 12473-82.

Andres, G., Garcia-Escudero, R., Salas, M. L. and Rodriguez, J. M. (2002b). Repression of African swine fever virus polyprotein pp220-encoding gene leads to the assembly of icosahedral core-less particles. *J Virol* **76**, 2654-66.

Andres, G., Garcia-Escudero, R., Simon-Mateo, C. and Vinuela, E. (1998). African swine fever virus is enveloped by a two-membraned collapsed cisterna derived from the endoplasmic reticulum. *J Virol* **72**, 8988-9001.

Andres, G., Simon-Mateo, C. and Vinuela, E. (1997). Assembly of African swine fever virus: role of polyprotein pp220. *J Virol* **71**, 2331-41.

Argilaguet, J. M., Perez-Martin, E., Gallardo, C., Salguero, F. J., Borrego, B., Lacasta, A., Accensi, F., Diaz, I., Nofrarias, M., Pujols, J., Blanco, E., Perez-Filgueira, M., Escribano, J. M. and Rodriguez, F. (2011). Enhancing DNA immunization by targeting ASFV antigens to SLA-II bearing cells. *Vaccine* **29**, 5379-85.

Arias, C., Walsh, D., Harbell, J., Wilson, A. C. and Mohr, I. (2009). Activation of host translational control pathways by a viral developmental switch. *PLoS Pathog* **5**, e1000334.

Ariumi, Y., Kuroki, M., Kushima, Y., Osugi, K., Hijikata, M., Maki, M., Ikeda, M. and Kato, N. (2011). Hepatitis C virus hijacks P-body and stress granule components around lipid droplets. *J Virol* **85**, 6882-92.

Arribas-Layton, M., Wu, D., Lykke-Andersen, J. and Song, H. (2013). Structural and functional control of the eukaryotic mRNA decapping machinery. *Biochim Biophys Acta* **1829**, 580-9.

Ballester, M., Rodriguez-Carino, C., Perez, M., Gallardo, C., Rodriguez, J. M., Salas, M. L. and Rodriguez, F. (2011). Disruption of nuclear organization during the initial phase of African swine fever virus infection. *J Virol* **85**, 8263-9.

Barber, G. N., Wambach, M., Wong, M. L., Dever, T. E., Hinnebusch, A. G. and Katze, M. G. (1993). Translational regulation by the interferon-induced double-stranded-RNA-activated 68-kDa protein kinase. *Proc Natl Acad Sci U S A* **90**, 4621-5.

Barnes, T., Kim, W. C., Mantha, A. K., Kim, S. E., Izumi, T., Mitra, S. and Lee, C. H. (2009). Identification of Apurinic/apyrimidinic endonuclease 1 (APE1) as the endoribonuclease that cleaves c-myc mRNA. *Nucleic Acids Res* **37**, 3946-58.

Baylis, S. A., Banham, A. H., Vydelingum, S., Dixon, L. K. and Smith, G. L. (1993). African swine fever virus encodes a serine protein kinase which is packaged into virions. *J Virol* **67**, 4549-56.

Beckham, C. J. and Parker, R. (2008). P bodies, stress granules, and viral life cycles. *Cell Host Microbe* **3**, 206-12.

Beelman, C. A., Stevens, A., Caponigro, G., LaGrandeur, T. E., Hatfield, L., Fortner, D. M. and Parker, R. (1996). An essential component of the decapping enzyme required for normal rates of mRNA turnover. *Nature* **382**, 642-6.

Bergman, N., Moraes, K. C., Anderson, J. R., Zaric, B., Kambach, C., Schneider, R. J., Wilusz, C. J. and Wilusz, J. (2007). Lsm proteins bind and stabilize RNAs containing 5' poly(A) tracts. *Nat Struct Mol Biol* **14**, 824-31.

Berlanga, J. J., Ventoso, I., Harding, H. P., Deng, J., Ron, D., Sonenberg, N., Carrasco, L. and de Haro, C. (2006). Antiviral effect of the mammalian translation initiation factor 2alpha kinase GCN2 against RNA viruses. *EMBO J* **25**, 1730-40.

Bessman, M. J., Frick, D. N. and O'Handley, S. F. (1996). The MutT proteins or "Nudix" hydrolases, a family of versatile, widely distributed, "housecleaning" enzymes. *J Biol Chem* **271**, 25059-62.

Bhandari, B. K., Feliers, D., Duraisamy, S., Stewart, J. L., Gingras, A. C., Abboud, H. E., Choudhury, G. G., Sonenberg, N. and Kasinath, B. S. (2001). Insulin regulation of protein translation repressor 4E-BP1, an eIF4E-binding protein, in renal epithelial cells. *Kidney Int* **59**, 866-75.

Blanchette, P., Kindsmuller, K., Groitl, P., Dallaire, F., Speiseder, T., Branton, P. E. and Dobner, T. (2008). Control of mRNA export by adenovirus E4orf6 and E1B55K proteins during productive infection requires E4orf6 ubiquitin ligase activity. *J Virol* **82**, 2642-51.

Blome, S., Gabriel, C. and Beer, M. (2013). Pathogenesis of African swine fever in domestic pigs and European wild boar. *Virus Res* **173**, 122-30.

Bochnig, P., Reuter, R., Bringmann, P. and Luhrmann, R. (1987). A monoclonal antibody against 2,2,7-trimethylguanosine that reacts with intact, class U, small nuclear ribonucleoproteins as well as with 7-methylguanosine-capped RNAs. *Eur J Biochem* **168**, 461-7.

Borca, M. V., Kutish, G. F., Afonso, C. L., Irusta, P., Carrillo, C., Brun, A., Sussman, M. and Rock, D. L. (1994). An African swine fever virus gene with similarity to the T-lymphocyte surface antigen CD2 mediates hemadsorption. *Virology* **199**, 463-8.

Borja, M. S., Piotukh, K., Freund, C. and Gross, J. D. (2011). Dcp1 links coactivators of mRNA decapping to Dcp2 by proline recognition. *RNA* **17**, 278-90.

Breese, S. S., Jr. and DeBoer, C. J. (1966). Electron microscope observations of African swine fever virus in tissue culture cells. *Virology* **28**, 420-8.

Brimacombe, R., Stiege, W., Kyriatsoulis, A. and Maly, P. (1988). Intra-RNA and RNA-protein cross-linking techniques in Escherichia coli ribosomes. *Methods Enzymol* **164**, 287-309.

Broyles, S. S. (2003). Vaccinia virus transcription. *J Gen Virol* **84**, 2293-303.

Buchan, J. R., Muhlrad, D. and Parker, R. (2008). P bodies promote stress granule assembly in Saccharomyces cerevisiae. *J Cell Biol* **183**, 441-55.

Buchkovich, N. J., Yu, Y., Zampieri, C. A. and Alwine, J. C. (2008). The TORrid affairs of viruses: effects of mammalian DNA viruses on the PI3K-Akt-mTOR signalling pathway. *Nat Rev Microbiol* **6**, 266-75.

Burger, K., Muhl, B., Kellner, M., Rohrmoser, M., Gruber-Eber, A., Windhager, L., Friedel, C. C., Dolken, L. and Eick, D. (2013). 4-thiouridine inhibits rRNA synthesis and causes a nucleolar stress response. *RNA Biol* **10**, 1623-30.

Burrage, T. G. (2013). African swine fever virus infection in Ornithodoros ticks. *Virus Res* **173**, 131-9.

Bushell, M., McKendrick, L., Janicke, R. U., Clemens, M. J. and Morley, S. J. (1999). Caspase-3 is necessary and sufficient for cleavage of protein synthesis eukaryotic initiation factor 4G during apoptosis. *FEBS Lett* **451**, 332-6.

Bushell, M. and Sarnow, P. (2002). Hijacking the translation apparatus by RNA viruses. *J Cell Biol* **158**, 395-9.

Caponigro, G. and Parker, R. (1995). Multiple functions for the poly(A)-binding protein in mRNA decapping and deadenylation in yeast. *Genes Dev* **9**, 2421-32.

Carrasco, L., de Lara, F. C., Martin de las Mulas, J., Gomez-Villamandos, J. C., Hervas, J., Wilkinson, P. J. and Sierra, M. A. (1996a). Virus association with lymphocytes in acute African swine fever. *Vet Res* **27**, 305-12.

Carrasco, L., Gomez-Villamandos, J. C., Bautista, M. J., Martin de las Mulas, J., Villeda, C. J., Wilkinson, P. J. and Sierra, M. A. (1996b). In vivo replication of African swine fever virus (Malawi '83) in neutrophils. *Vet Res* **27**, 55-62.

Carrascosa, A. L., Bustos, M. J., Galindo, I. and Vinuela, E. (1999). Virus-specific cell receptors are necessary, but not sufficient, to confer cell susceptibility to African swine fever virus. *Arch Virol* **144**, 1309-21.

Carrascosa, A. L., Sastre, I. and Vinuela, E. (1991). African swine fever virus attachment protein. *J Virol* **65**, 2283-9.

Carrascosa, J. L., Carazo, J. M., Carrascosa, A. L., Garcia, N., Santisteban, A. and Vinuela, E. (1984). General morphology and capsid fine structure of African swine fever virus particles. *Virology* **132**, 160-72.

Cartwright, J. L., Safrany, S. T., Dixon, L. K., Darzynkiewicz, E., Stepinski, J., Burke, R. and McLennan, A. G. (2002). The g5R (D250) gene of African swine fever virus encodes a Nudix hydrolase that preferentially degrades diphosphoinositol polyphosphates. *J Virol* **76**, 1415-21.

Castello, A., Alvarez, E. and Carrasco, L. (2006). Differential cleavage of eIF4GI and eIF4GII in mammalian cells. Effects on translation. *J Biol Chem* **281**, 33206-16.

Castello, A., Fischer, B., Eichelbaum, K., Horos, R., Beckmann, B. M., Strein, C., Davey, N. E., Humphreys, D. T., Preiss, T., Steinmetz, L. M., Krijgsveld, J. and Hentze, M. W. (2012). Insights into RNA biology from an atlas of mammalian mRNA-binding proteins. *Cell* **149**, 1393-406.

Castello, A., Izquierdo, J. M., Welnowska, E. and Carrasco, L. (2009a). RNA nuclear export is blocked by poliovirus 2A protease and is concomitant with nucleoporin cleavage. *J Cell Sci* **122**, 3799-809.

Castello, A., Quintas, A., Sanchez, E. G., Sabina, P., Nogal, M., Carrasco, L. and Revilla, Y. (2009b). Regulation of host translational machinery by African swine fever virus. *PLoS Pathog* **5**, e1000562.

Cohen, L. S., Mikhli, C., Jiao, X., Kiledjian, M., Kunkel, G. and Davis, R. E. (2005). Dcp2 Decaps m2,2,7GpppN-capped RNAs, and its activity is sequence and context dependent. *Mol Cell Biol* **25**, 8779-91.

Cohen, P. T. (2002). Protein phosphatase 1--targeted in many directions. *J Cell Sci* **115**, 241-56.

Coller, J. and Parker, R. (2005). General translational repression by activators of mRNA decapping. *Cell* **122**, 875-86.

Connor, J. H. and Lyles, D. S. (2002). Vesicular stomatitis virus infection alters the eIF4F translation initiation complex and causes dephosphorylation of the eIF4E binding protein 4E-BP1. *J Virol* **76**, 10177-87.

Costard, S., Mur, L., Lubroth, J., Sanchez-Vizcaino, J. M. and Pfeiffer, D. U. (2013). Epidemiology of African swine fever virus. *Virus Res* **173**, 191-7.

Cougot, N., Babajko, S. and Seraphin, B. (2004). Cytoplasmic foci are sites of mRNA decay in human cells. *J Cell Biol* **165**, 31-40.

Covarrubias, S., Gaglia, M. M., Kumar, G. R., Wong, W., Jackson, A. O. and Glaunsinger, B. A. (2011). Coordinated destruction of cellular messages in translation complexes by the gammaherpesvirus host shutoff factor and the mammalian exonuclease Xrn1. *PLoS Pathog* **7**, e1002339.

Cuesta, R., Xi, Q. and Schneider, R. J. (2004). Structural basis for competitive inhibition of eIF4G-Mnk1 interaction by the adenovirus 100-kilodalton protein. *J Virol* **78**, 7707-16.

Chacon, M. R., Almazan, F., Nogal, M. L., Vinuela, E. and Rodriguez, J. F. (1995). The African swine fever virus IAP homolog is a late structural polypeptide. *Virology* **214**, 670-4.

Chahar, H. S., Chen, S. and Manjunath, N. (2013). P-body components LSM1, GW182, DDX3, DDX6 and XRN1 are recruited to WNV replication sites and positively regulate viral replication. *Virology* **436**, 1-7.

Chang, C. T., Bercovich, N., Loh, B., Jonas, S. and Izaurralde, E. (2014). The activation of the decapping enzyme DCP2 by DCP1 occurs on the EDC4 scaffold and involves a conserved loop in DCP1. *Nucleic Acids Res* **42**, 5217-33.

Chen, C. Y. and Shyu, A. B. (2011). Mechanisms of deadenylation-dependent decay. *Wiley Interdiscip Rev RNA* **2**, 167-83.

Cheng, G., Feng, Z. and He, B. (2005). Herpes simplex virus 1 infection activates the endoplasmic reticulum resident kinase PERK and mediates eIF-2alpha dephosphorylation by the gamma(1)34.5 protein. *J Virol* **79**, 1379-88.

Decker, C. J. and Parker, R. (1993). A turnover pathway for both stable and unstable mRNAs in yeast: evidence for a requirement for deadenylation. *Genes Dev* **7**, 1632-43.

Decker, C. J. and Parker, R. (2012). P-bodies and stress granules: possible roles in the control of translation and mRNA degradation. *Cold Spring Harb Perspect Biol* **4**, a012286.

Decker, C. J., Teixeira, D. and Parker, R. (2007). Edc3p and a glutamine/asparagine-rich domain of Lsm4p function in processing body assembly in Saccharomyces cerevisiae. *J Cell Biol* **179**, 437-49.

Decroly, E., Ferron, F., Lescar, J. and Canard, B. (2012). Conventional and unconventional mechanisms for capping viral mRNA. *Nat Rev Microbiol* **10**, 51-65.

del Val, M. and Vinuela, E. (1987). Glycosylated components induced in African swine fever (ASF) virus-infected Vero cells. *Virus Res* **7**, 297-308.

Deshmukh, M. V., Jones, B. N., Quang-Dang, D. U., Flinders, J., Floor, S. N., Kim, C., Jemielity, J., Kalek, M., Darzynkiewicz, E. and Gross, J. D. (2008). mRNA decapping is promoted by an RNA-binding channel in Dcp2. *Mol Cell* **29**, 324-36.

Dixon, L. K., Abrams, C. C., Bowick, G., Goatley, L. C., Kay-Jackson, P. C., Chapman, D., Liverani, E., Nix, R., Silk, R. and Zhang, F. (2004). African swine fever virus proteins involved in evading host defence systems. *Vet Immunol Immunopathol* **100**, 117-34.

Dixon, L. K., Alonso, C., Escribano, J. M., Martins, C., Revilla, Y., Salas, M. L. and Takamatsu, H. (2012). Asfaviridae Virus Taxonomy: Ninth Report of the International Committee on Taxonomy of Viruses. *Elsevier*, 153-162.

Dixon, L. K., Bristow, C., Wilkinson, P. J. and Sumption, K. J. (1990). Identification of a variable region of the African swine fever virus genome that has undergone separate DNA rearrangements leading to expansion of minisatellite-like sequences. *J Mol Biol* **216**, 677-88.

Dixon, L. K., Chapman, D. A., Netherton, C. L. and Upton, C. (2013). African swine fever virus replication and genomics. *Virus Res* **173**, 3-14.

Donnelly, N., Gorman, A. M., Gupta, S. and Samali, A. (2013). The eIF2alpha kinases: their structures and functions. *Cell Mol Life Sci* **70**, 3493-511.

Dougherty, J. D., White, J. P. and Lloyd, R. E. (2011). Poliovirus-mediated disruption of cytoplasmic processing bodies. *J Virol* **85**, 64-75.

Dulbecco, R. and Freeman, G. (1959). Plaque production by the polyoma virus. *Virology* **8**, 396-7.

Dunckley, T. and Parker, R. (1999). The DCP2 protein is required for mRNA decapping in Saccharomyces cerevisiae and contains a functional MutT motif. *EMBO J* **18**, 5411-22.

Dykxhoorn, D. M. (2007). MicroRNAs in viral replication and pathogenesis. *DNA Cell Biol* **26**, 239-49.

Enjuanes, L., Carrascosa, A. L., Moreno, M. A. and Vinuela, E. (1976). Titration of African swine fever (ASF) virus. *J Gen Virol* **32**, 471-7.

Epifano, C., Krijnse-Locker, J., Salas, M. L., Rodriguez, J. M. and Salas, J. (2006). The African swine fever virus nonstructural protein pB602L is required for formation of the icosahedral capsid of the virus particle. *J Virol* **80**, 12260-70.

Esclatine, A., Taddeo, B. and Roizman, B. (2004). The UL41 protein of herpes simplex virus mediates selective stabilization or degradation of cellular mRNAs. *Proc Natl Acad Sci U S A* **101**, 18165-70.

Escribano, J. M., Galindo, I. and Alonso, C. (2013). Antibody-mediated neutralization of African swine fever virus: myths and facts. *Virus Res* **173**, 101-9.

Eulalio, A., Behm-Ansmant, I. and Izaurralde, E. (2007). P bodies: at the crossroads of post-transcriptional pathways. *Nat Rev Mol Cell Biol* **8**, 9-22.

Feederle, R., Bannert, H., Lips, H., Muller-Lantzsch, N. and Delecluse, H. J. (2009). The Epstein-Barr virus alkaline exonuclease BGLF5 serves pleiotropic functions in virus replication. *J Virol* **83**, 4952-62.

Feigenblum, D. and Schneider, R. J. (1993). Modification of eukaryotic initiation factor 4F during infection by influenza virus. *J Virol* **67**, 3027-35.

Feng, P., Everly, D. N., Jr. and Read, G. S. (2005). mRNA decay during herpes simplex virus (HSV) infections: protein-protein interactions involving the HSV virion host shutoff protein and translation factors eIF4H and eIF4A. *J Virol* **79**, 9651-64.

Fenger-Gron, M., Fillman, C., Norrild, B. and Lykke-Andersen, J. (2005). Multiple processing body factors and the ARE binding protein TTP activate mRNA decapping. *Mol Cell* **20**, 905-15.

Fischer, N. and Weis, K. (2002). The DEAD box protein Dhh1 stimulates the decapping enzyme Dcp1. *EMBO J* **21**, 2788-97.

Fromm, S. A., Truffault, V., Kamenz, J., Braun, J. E., Hoffmann, N. A., Izaurralde, E. and Sprangers, R. (2012). The structural basis of Edc3- and Scd6-mediated activation of the Dcp1:Dcp2 mRNA decapping complex. *EMBO J* **31**, 279-90.

Fromont-Racine, M., Mayes, A. E., Brunet-Simon, A., Rain, J. C., Colley, A., Dix, I., Decourty, L., Joly, N., Ricard, F., Beggs, J. D. and Legrain, P. (2000). Genome-wide protein interaction screens reveal functional networks involving Sm-like proteins. *Yeast* **17**, 95-110.

Fujimura, T. and Esteban, R. (2011). Cap-snatching mechanism in yeast L-A double-stranded RNA virus. *Proc Natl Acad Sci U S A* **108**, 17667-71.

Gabelli, S. B., Bianchet, M. A., Bessman, M. J. and Amzel, L. M. (2001). The structure of ADP-ribose pyrophosphatase reveals the structural basis for the versatility of the Nudix family. *Nat Struct Biol* **8**, 467-72.

Galindo, I., Almazan, F., Bustos, M. J., Vinuela, E. and Carrascosa, A. L. (2000). African swine fever virus EP153R open reading frame encodes a glycoprotein involved in the hemadsorption of infected cells. *Virology* **266**, 340-51.

Galindo, I., Cuesta-Geijo, M. A., Hlavova, K., Munoz-Moreno, R., Barrado-Gil, L., Dominguez, J. and Alonso, C. (2015). African swine fever virus infects macrophages, the natural host cells, via clathrin- and cholesterol-dependent endocytosis. *Virus Res* **200C**, 45-55.

Garcia-Escudero, R., Andres, G., Almazan, F. and Vinuela, E. (1998). Inducible gene expression from African swine fever virus recombinants: analysis of the major capsid protein p72. *J Virol* **72**, 3185-95.

Garcia-Escudero, R. and Vinuela, E. (2000). Structure of African swine fever virus late promoters: requirement of a TATA sequence at the initiation region. *J Virol* **74**, 8176-82.

Garcia, M. A., Meurs, E. F. and Esteban, M. (2007). The dsRNA protein kinase PKR: virus and cell control. *Biochimie* **89**, 799-811.

Garcia, R., Almazan, F., Rodriguez, J. M., Alonso, M., Vinuela, E. and Rodriguez, J. F. (1995). Vectors for the genetic manipulation of African swine fever virus. *J Biotechnol* **40**, 121-31.

Garneau, N. L., Wilusz, J. and Wilusz, C. J. (2007). The highways and byways of mRNA decay. *Nat Rev Mol Cell Biol* **8**, 113-26.

Geraldes, A. and Valdeira, M. L. (1985). Effect of chloroquine on African swine fever virus infection. *J Gen Virol* **66 (Pt 5)**, 1145-8.

Ghosh, A. and Lima, C. D. (2010). Enzymology of RNA cap synthesis. *Wiley Interdiscip Rev RNA* **1**, 152-72.

Ghosh, T., Peterson, B., Tomasevic, N. and Peculis, B. A. (2004). Xenopus U8 snoRNA binding protein is a conserved nuclear decapping enzyme. *Mol Cell* **13**, 817-28.

Glaunsinger, B., Chavez, L. and Ganem, D. (2005). The exonuclease and host shutoff functions of the SOX protein of Kaposi's sarcoma-associated herpesvirus are genetically separable. *J Virol* **79**, 7396-401.

Gomez-Puertas, P., Rodriguez, F., Oviedo, J. M., Brun, A., Alonso, C. and Escribano, J. M. (1998). The African swine fever virus proteins p54 and p30 are involved in two distinct steps of virus attachment and both contribute to the antibody-mediated protective immune response. *Virology* **243**, 461-71.

Gomez-Puertas, P., Rodriguez, F., Oviedo, J. M., Ramiro-Ibanez, F., Ruiz-Gonzalvo, F., Alonso, C. and Escribano, J. M. (1996). Neutralizing antibodies to different proteins of African swine fever virus inhibit both virus attachment and internalization. *J Virol* **70**, 5689-94.

Gomez-Villamandos, J. C., Bautista, M. J., Sanchez-Cordon, P. J. and Carrasco, L. (2013). Pathology of African swine fever: the role of monocyte-macrophage. *Virus Res* **173**, 140-9.

Granja, A. G., Nogal, M. L., Hurtado, C., Del Aguila, C., Carrascosa, A. L., Salas, M. L., Fresno, M. and Revilla, Y. (2006a). The viral protein A238L inhibits TNF-alpha expression through a CBP/p300 transcriptional coactivators pathway. *J Immunol* **176**, 451-62.

Granja, A. G., Nogal, M. L., Hurtado, C., Salas, J., Salas, M. L., Carrascosa, A. L. and Revilla, Y. (2004). Modulation of p53 cellular function and cell death by African swine fever virus. *J Virol* **78**, 7165-74.

Granja, A. G., Perkins, N. D. and Revilla, Y. (2008). A238L inhibits NF-ATc2, NF-kappa B, and c-Jun activation through a novel mechanism involving protein kinase C-theta-mediated up-regulation of the amino-terminal transactivation domain of p300. *J Immunol* **180**, 2429-42.

Granja, A. G., Sabina, P., Salas, M. L., Fresno, M. and Revilla, Y. (2006b). Regulation of inducible nitric oxide synthase expression by viral A238L-mediated inhibition of p65/RelA acetylation and p300 transactivation. *J Virol* **80**, 10487-96.

Granja, A. G., Sanchez, E. G., Sabina, P., Fresno, M. and Revilla, Y. (2009). African swine fever virus blocks the host cell antiviral inflammatory response through a direct inhibition of PKC-theta-mediated p300 transactivation. *J Virol* **83**, 969-80.

Greer, A. E., Hearing, P. and Ketner, G. (2011). The adenovirus E4 11 k protein binds and relocalizes the cytoplasmic P-body component Ddx6 to aggresomes. *Virology* **417**, 161-8.

Gregersen, L. H., Schueler, M., Munschauer, M., Mastrobuoni, G., Chen, W., Kempa, S., Dieterich, C. and Landthaler, M. (2014). MOV10 Is a 5' to 3' RNA helicase contributing to UPF1 mRNA target degradation by translocation along 3' UTRs. *Mol Cell* **54**, 573-85.

Guerra, S., Lopez-Fernandez, L. A., Pascual-Montano, A., Munoz, M., Harshman, K. and Esteban, M. (2003). Cellular gene expression survey of vaccinia virus infection of human HeLa cells. *J Virol* **77**, 6493-506.

Hafner, M., Landthaler, M., Burger, L., Khorshid, M., Hausser, J., Berninger, P., Rothballer, A., Ascano, M., Jr., Jungkamp, A. C., Munschauer, M., Ulrich, A., Wardle, G. S., Dewell, S., Zavolan, M. and Tuschl, T. (2010). Transcriptome-wide identification of RNA-binding protein and microRNA target sites by PAR-CLIP. *Cell* **141**, 129-41.

Hanahan, D. (1983). Studies on transformation of Escherichia coli with plasmids. *J Mol Biol* **166**, 557-80.

Heath, C. M., Windsor, M. and Wileman, T. (2001). Aggresomes resemble sites specialized for virus assembly. *J Cell Biol* **153**, 449-55.

Hebner, C. M., Wilson, R., Rader, J., Bidder, M. and Laimins, L. A. (2006). Human papillomaviruses target the double-stranded RNA protein kinase pathway. *J Gen Virol* **87**, 3183-93.

Hernaez, B. and Alonso, C. (2010). Dynamin- and clathrin-dependent endocytosis in African swine fever virus entry. *J Virol* **84**, 2100-9.

Huang, C., Lokugamage, K. G., Rozovics, J. M., Narayanan, K., Semler, B. L. and Makino, S. (2011). SARS coronavirus nsp1 protein induces template-dependent endonucleolytic cleavage of mRNAs: viral mRNAs are resistant to nsp1-induced RNA cleavage. *PLoS Pathog* **7**, e1002433.

Hurtado, C., Granja, A. G., Bustos, M. J., Nogal, M. L., Gonzalez de Buitrago, G., de Yebenes, V. G., Salas, M. L., Revilla, Y. and Carrascosa, A. L. (2004). The C-type lectin homologue gene (EP153R) of African swine fever virus inhibits apoptosis both in virus infection and in heterologous expression. *Virology* **326**, 160-70.

Iwasaki, S., Takeda, A., Motose, H. and Watanabe, Y. (2007). Characterization of Arabidopsis decapping proteins AtDCP1 and AtDCP2, which are essential for post-embryonic development. *FEBS Lett* **581**, 2455-9.

Jackson, R. J., Hellen, C. U. and Pestova, T. V. (2010). The mechanism of eukaryotic translation initiation and principles of its regulation. *Nat Rev Mol Cell Biol* **11**, 113-27.

Jagger, B. W., Wise, H. M., Kash, J. C., Walters, K. A., Wills, N. M., Xiao, Y. L., Dunfee, R. L., Schwartzman, L. M., Ozinsky, A., Bell, G. L., Dalton, R. M., Lo, A., Efstathiou, S., Atkins, J. F., Firth, A. E., Taubenberger, J. K. and Digard, P. (2012). An overlapping protein-coding region in influenza A virus segment 3 modulates the host response. *Science* **337**, 199-204.

Jonas, S. and Izaurralde, E. (2013). The role of disordered protein regions in the assembly of decapping complexes and RNP granules. *Genes Dev* **27**, 2628-41.

Katsafanas, G. C. and Moss, B. (2007). Colocalization of transcription and translation within cytoplasmic poxvirus factories coordinates viral expression and subjugates host functions. *Cell Host Microbe* **2**, 221-8.

Kedersha, N., Stoecklin, G., Ayodele, M., Yacono, P., Lykke-Andersen, J., Fritzler, M. J., Scheuner, D., Kaufman, R. J., Golan, D. E. and Anderson, P. (2005). Stress granules and processing bodies are dynamically linked sites of mRNP remodeling. *J Cell Biol* **169**, 871-84.

Khanna, R. and Kiledjian, M. (2004). Poly(A)-binding-protein-mediated regulation of hDcp2 decapping in vitro. *EMBO J* **23**, 1968-76.

Khaperskyy, D. A., Emara, M. M., Johnston, B. P., Anderson, P., Hatchette, T. F. and McCormick, C. (2014). Influenza a virus host shutoff disables antiviral stress-induced translation arrest. *PLoS Pathog* **10**, e1004217.

Kimball, S. R., Jefferson, L. S., Nguyen, H. V., Suryawan, A., Bush, J. A. and Davis, T. A. (2000). Feeding stimulates protein synthesis in muscle and liver of neonatal pigs through an mTOR-dependent process. *Am J Physiol Endocrinol Metab* **279**, E1080-7.

King, K., Chapman, D., Argilaguet, J. M., Fishbourne, E., Hutet, E., Cariolet, R., Hutchings, G., Oura, C. A., Netherton, C. L., Moffat, K., Taylor, G., Le Potier, M. F., Dixon, L. K. and Takamatsu, H. H. (2011). Protection of European domestic pigs from virulent African isolates of African swine fever virus by experimental immunisation. *Vaccine* **29**, 4593-600.

Kleiboeker, S. B. and Scoles, G. A. (2001). Pathogenesis of African swine fever virus in Ornithodoros ticks. *Anim Health Res Rev* **2**, 121-8.

Koonin, E. V. and Moss, B. (2010). Viruses know more than one way to don a cap. *Proc Natl Acad Sci U S A* **107**, 3283-4.

Kumar, G. R. and Glaunsinger, B. A. (2010). Nuclear import of cytoplasmic poly(A) binding protein restricts gene expression via hyperadenylation and nuclear retention of mRNA. *Mol Cell Biol* **30**, 4996-5008.

Kumar, G. R., Shum, L. and Glaunsinger, B. A. (2011). Importin alpha-mediated nuclear import of cytoplasmic poly(A) binding protein occurs as a direct consequence of cytoplasmic mRNA depletion. *Mol Cell Biol* **31**, 3113-25.

Kuznar, J., Salas, M. L. and Vinuela, E. (1980). DNA-dependent RNA polymerase in African swine fever virus. *Virology* **101**, 169-75.

Li, M. M., MacDonald, M. R. and Rice, C. M. (2015). To translate, or not to translate: viral and host mRNA regulation by interferon-stimulated genes. *Trends Cell Biol*.

Li, Y., Ho, E. S., Gunderson, S. I. and Kiledjian, M. (2009). Mutational analysis of a Dcp2-binding element reveals general enhancement of decapping by 5'-end stem-loop structures. *Nucleic Acids Res* **37**, 2227-37.

Li, Y., Song, M. and Kiledjian, M. (2011). Differential utilization of decapping enzymes in mammalian mRNA decay pathways. *RNA* **17**, 419-28.

Li, Y., Song, M. G. and Kiledjian, M. (2008). Transcript-specific decapping and regulated stability by the human Dcp2 decapping protein. *Mol Cell Biol* **28**, 939-48.

Lin, J., Abeygunawardana, C., Frick, D. N., Bessman, M. J. and Mildvan, A. S. (1996). The role of Glu 57 in the mechanism of the Escherichia coli MutT enzyme by mutagenesis and heteronuclear NMR. *Biochemistry* **35**, 6715-26.

Ling, S. H., Qamra, R. and Song, H. (2011). Structural and functional insights into eukaryotic mRNA decapping. *Wiley Interdiscip Rev RNA* **2**, 193-208.

Liu, S. W., Katsafanas, G. C., Liu, R., Wyatt, L. S. and Moss, B. (2015). Poxvirus Decapping Enzymes Enhance Virulence by Preventing the Accumulation of dsRNA and the Induction of Innate Antiviral Responses. *Cell Host Microbe* **17**, 320-31.

Liu, S. W., Wyatt, L. S., Orandle, M. S., Minai, M. and Moss, B. (2014). The D10 decapping enzyme of vaccinia virus contributes to decay of cellular and viral mRNAs and to virulence in mice. *J Virol* **88**, 202-11.

Lotan, R., Goler-Baron, V., Duek, L., Haimovich, G. and Choder, M. (2007). The Rpb7p subunit of yeast RNA polymerase II plays roles in the two major cytoplasmic mRNA decay mechanisms. *J Cell Biol* **178**, 1133-43.

Lubisi, B. A., Bastos, A. D., Dwarka, R. M. and Vosloo, W. (2007). Intra-genotypic resolution of African swine fever viruses from an East African domestic pig cycle: a combined p72-CVR approach. *Virus Genes* **35**, 729-35.

Lloyd, R. E. (2006). Translational control by viral proteinases. *Virus Res* **119**, 76-88.

Marissen, W. E. and Lloyd, R. E. (1998). Eukaryotic translation initiation factor 4G is targeted for proteolytic cleavage by caspase 3 during inhibition of translation in apoptotic cells. *Mol Cell Biol* **18**, 7565-74.

Martinez-Azorin, F., Remacha, M. and Ballesta, J. P. (2008). Functional characterization of ribosomal P1/P2 proteins in human cells. *Biochem J* **413**, 527-34.

Mas, A., Alves-Rodrigues, I., Noueiry, A., Ahlquist, P. and Diez, J. (2006). Host deadenylation-dependent mRNA decapping factors are required for a key step in brome mosaic virus RNA replication. *J Virol* **80**, 246-51.

Masternak, K. and Wittek, R. (1996). cis- and trans-acting elements involved in reactivation of vaccinia virus early transcription. *J Virol* **70**, 8737-46.

McLennan, A. G. (2006). The Nudix hydrolase superfamily. *Cell Mol Life Sci* **63**, 123-43.

McLennan, A. G. (2007). Decapitation: poxvirus makes RNA lose its head. *Trends Biochem Sci* **32**, 297-9.

McLennan, A. G. (2013). Substrate ambiguity among the nudix hydrolases: biologically significant, evolutionary remnant, or both? *Cell Mol Life Sci* **70**, 373-85.

Meyer, S., Temme, C. and Wahle, E. (2004). Messenger RNA turnover in eukaryotes: pathways and enzymes. *Crit Rev Biochem Mol Biol* **39**, 197-216.

Mildvan, A. S., Xia, Z., Azurmendi, H. F., Saraswat, V., Legler, P. M., Massiah, M. A., Gabelli, S. B., Bianchet, M. A., Kang, L. W. and Amzel, L. M. (2005). Structures and mechanisms of Nudix hydrolases. *Arch Biochem Biophys* **433**, 129-43.

Miller, J. N. and Pearce, D. A. (2014). Nonsense-mediated decay in genetic disease: friend or foe? *Mutat Res Rev Mutat Res* **762**, 52-64.

Montogomery, R. E. (1921). On a form of swine fever ocurring in British East Africa. *J Comp Pathol*, 59-131.

Morley, S. J. and Naegele, S. (2002). Phosphorylation of eukaryotic initiation factor (eIF) 4E is not required for de novo protein synthesis following recovery from hypertonic stress in human kidney cells. *J Biol Chem* **277**, 32855-9.

Mulumba-Mfumu, L. K., Goatley, L. C., Saegerman, C., Takamatsu, H. H. and Dixon, L. K. (2015). Immunization of African Indigenous Pigs with Attenuated Genotype I African Swine Fever Virus OURT88/3 Induces Protection Against Challenge with Virulent Strains of Genotype I. *Transbound Emerg Dis*.

Munoz, M., Freije, J. M., Salas, M. L., Vinuela, E. and Lopez-Otin, C. (1993). Structure and expression in E. coli of the gene coding for protein p10 of African swine fever virus. *Arch Virol* **130**, 93-107.

Nallagatla, S. R., Toroney, R. and Bevilacqua, P. C. (2008). A brilliant disguise for self RNA: 5'-end and internal modifications of primary transcripts suppress elements of innate immunity. *RNA Biol* **5**, 140-4.

Narayanan, K. and Makino, S. (2013). Interplay between viruses and host mRNA degradation. *Biochim Biophys Acta* **1829**, 732-41.

Nissan, T., Rajyaguru, P., She, M., Song, H. and Parker, R. (2010). Decapping activators in Saccharomyces cerevisiae act by multiple mechanisms. *Mol Cell* **39**, 773-83.

Nogal, M. L., Gonzalez de Buitrago, G., Rodriguez, C., Cubelos, B., Carrascosa, A. L., Salas, M. L. and Revilla, Y. (2001). African swine fever virus IAP homologue inhibits caspase activation and promotes cell survival in mammalian cells. *J Virol* **75**, 2535-43.

Nunes-Correia, I., Rodriguez, J. M., Eulalio, A., Carvalho, A. L., Citovsky, V., Simoes, S., Faro, C., Salas, M. L. and Pedroso de Lima, M. C. (2008). African swine fever virus p10 protein exhibits nuclear import capacity and accumulates in the nucleus during viral infection. *Vet Microbiol* **130**, 47-59.

Onisk, D. V., Borca, M. V., Kutish, G., Kramer, E., Irusta, P. and Rock, D. L. (1994). Passively transferred African swine fever virus antibodies protect swine against lethal infection. *Virology* **198**, 350-4.

Onomoto, K., Yoneyama, M., Fung, G., Kato, H. and Fujita, T. (2014). Antiviral innate immunity and stress granule responses. *Trends Immunol* **35**, 420-8.

Otsuka, Y., Kedersha, N. L. and Schoenberg, D. R. (2009). Identification of a cytoplasmic complex that adds a cap onto 5'-monophosphate RNA. *Mol Cell Biol* **29**, 2155-67.

Oura, C. A., Denyer, M. S., Takamatsu, H. and Parkhouse, R. M. (2005). In vivo depletion of CD8+ T lymphocytes abrogates protective immunity to African swine fever virus. *J Gen Virol* **86**, 2445-50.

Panda, S., Vedagiri, D., Viveka, T. S. and Harshan, K. H. (2014). A unique phosphorylation-dependent eIF4E assembly on 40S ribosomes co-ordinated by hepatitis C virus protein NS5A that activates internal ribosome entry site translation. *Biochem J* **462**, 291-302.

Park, N., Katikaneni, P., Skern, T. and Gustin, K. E. (2008). Differential targeting of nuclear pore complex proteins in poliovirus-infected cells. *J Virol* **82**, 1647-55.

Parker, R. and Song, H. (2004). The enzymes and control of eukaryotic mRNA turnover. *Nat Struct Mol Biol* **11**, 121-7.

Parrish, S., Hurchalla, M., Liu, S. W. and Moss, B. (2009). The African swine fever virus g5R protein possesses mRNA decapping activity. *Virology* **393**, 177-82.

Parrish, S. and Moss, B. (2006). Characterization of a vaccinia virus mutant with a deletion of the D10R gene encoding a putative negative regulator of gene expression. *J Virol* **80**, 553-61.

Parrish, S. and Moss, B. (2007). Characterization of a second vaccinia virus mRNA-decapping enzyme conserved in poxviruses. *J Virol* **81**, 12973-8.

Parrish, S., Resch, W. and Moss, B. (2007). Vaccinia virus D10 protein has mRNA decapping activity, providing a mechanism for control of host and viral gene expression. *Proc Natl Acad Sci U S A* **104**, 2139-44.

Pashev, I. G., Dimitrov, S. I. and Angelov, D. (1991). Crosslinking proteins to nucleic acids by ultraviolet laser irradiation. *Trends Biochem Sci* **16**, 323-6.

Pena, L., Yanez, R. J., Revilla, Y., Vinuela, E. and Salas, M. L. (1993). African swine fever virus guanylyltransferase. *Virology* **193**, 319-28.

Perdiguero, B. and Esteban, M. (2009). The interferon system and vaccinia virus evasion mechanisms. *J Interferon Cytokine Res* **29**, 581-98.

Piccirillo, C., Khanna, R. and Kiledjian, M. (2003). Functional characterization of the mammalian mRNA decapping enzyme hDcp2. *RNA* **9**, 1138-47.

Pichlmair, A., Schulz, O., Tan, C. P., Naslund, T. I., Liljestrom, P., Weber, F. and Reis e Sousa, C. (2006). RIG-I-mediated antiviral responses to single-stranded RNA bearing 5'-phosphates. *Science* **314**, 997-1001.

Powers, M. A., Forbes, D. J., Dahlberg, J. E. and Lund, E. (1997). The vertebrate GLFG nucleoporin, Nup98, is an essential component of multiple RNA export pathways. *J Cell Biol* **136**, 241-50.

Prados, F. J., Vinuela, E. and Alcami, A. (1993). Sequence and characterization of the major early phosphoprotein p32 of African swine fever virus. *J Virol* **67**, 2475-85.

Prevot, D., Darlix, J. L. and Ohlmann, T. (2003). Conducting the initiation of protein synthesis: the role of eIF4G. *Biol Cell* **95**, 141-56.

Proud, C. G. (2005). eIF2 and the control of cell physiology. *Semin Cell Dev Biol* **16**, 3-12.

Pyronnet, S. (2000). Phosphorylation of the cap-binding protein eIF4E by the MAPK-activated protein kinase Mnk1. *Biochem Pharmacol* **60**, 1237-43.

Pyronnet, S., Imataka, H., Gingras, A. C., Fukunaga, R., Hunter, T. and Sonenberg, N. (1999). Human eukaryotic translation initiation factor 4G (eIF4G) recruits mnk1 to phosphorylate eIF4E. *EMBO J* **18**, 270-9.

Quan, B., Seo, H. S., Blobel, G. and Ren, Y. (2014). Vesiculoviral matrix (M) protein occupies nucleic acid binding site at nucleoporin pair (Rae1 * Nup98). *Proc Natl Acad Sci U S A* **111**, 9127-32.

Ramiro-Ibanez, F., Ortega, A., Brun, A., Escribano, J. M. and Alonso, C. (1996). Apoptosis: a mechanism of cell killing and lymphoid organ impairment during acute African swine fever virus infection. *J Gen Virol* **77 (Pt 9)**, 2209-19.

Raught, B., Gingras, A. C., Gygi, S. P., Imataka, H., Morino, S., Gradi, A., Aebersold, R. and Sonenberg, N. (2000). Serum-stimulated, rapamycin-sensitive phosphorylation sites in the eukaryotic translation initiation factor 4GI. *EMBO J* **19**, 434-44.

Redrejo-Rodriguez, M., Garcia-Escudero, R., Yanez-Munoz, R. J., Salas, M. L. and Salas, J. (2006). African swine fever virus protein pE296R is a DNA repair apurinic/apyrimidinic endonuclease required for virus growth in swine macrophages. *J Virol* **80**, 4847-57.

Reid, D. W. and Nicchitta, C. V. (2015). Diversity and selectivity in mRNA translation on the endoplasmic reticulum. *Nat Rev Neurosci*.

Reineke, L. C. and Lloyd, R. E. (2013). Diversion of stress granules and P-bodies during viral infection. *Virology* **436**, 255-67.

Revilla, Y., Cebrian, A., Baixeras, E., Martinez, C., Vinuela, E. and Salas, M. L. (1997). Inhibition of apoptosis by the African swine fever virus Bcl-2 homologue: role of the BH1 domain. *Virology* **228**, 400-4.

Richner, J. M., Clyde, K., Pezda, A. C., Cheng, B. Y., Wang, T., Kumar, G. R., Covarrubias, S., Coscoy, L. and Glaunsinger, B. (2011). Global mRNA degradation during lytic gammaherpesvirus infection contributes to establishment of viral latency. *PLoS Pathog* **7**, e1002150.

Richter, J. D. and Sonenberg, N. (2005). Regulation of cap-dependent translation by eIF4E inhibitory proteins. *Nature* **433**, 477-80.

Rigby, R. E. and Rehwinkel, J. (2015). RNA degradation in antiviral immunity and autoimmunity. *Trends Immunol*.

Rivera, J., Abrams, C., Hernaez, B., Alcazar, A., Escribano, J. M., Dixon, L. and Alonso, C. (2007). The MyD116 African swine fever virus homologue interacts with the catalytic subunit of protein phosphatase 1 and activates its phosphatase activity. *J Virol* **81**, 2923-9.

Roberts, A. P., Doidge, R., Tarr, A. W. and Jopling, C. L. (2014). The P body protein LSm1 contributes to stimulation of hepatitis C virus translation, but not replication, by microRNA-122. *Nucleic Acids Res* **42**, 1257-69.

Rodriguez, J. M., Garcia-Escudero, R., Salas, M. L. and Andres, G. (2004). African swine fever virus structural protein p54 is essential for the recruitment of envelope precursors to assembly sites. *J Virol* **78**, 4299-1313.

Rodriguez, J. M. and Salas, M. L. (2013). African swine fever virus transcription. *Virus Res* **173**, 15-28.

Rodriguez, J. M., Salas, M. L. and Santaren, J. F. (2001). African swine fever virus-induced polypeptides in porcine alveolar macrophages and in Vero cells: two-dimensional gel analysis. *Proteomics* **1**, 1447-56.

Rodriguez, J. M., Salas, M. L. and Vinuela, E. (1996). Intermediate class of mRNAs in African swine fever virus. *J Virol* **70**, 8584-9.

Rodriguez, J. M., Yanez, R. J., Almazan, F., Vinuela, E. and Rodriguez, J. F. (1993). African swine fever virus encodes a CD2 homolog responsible for the adhesion of erythrocytes to infected cells. *J Virol* **67**, 5312-20.

Rojo, G., Chamorro, M., Salas, M. L., Vinuela, E., Cuezva, J. M. and Salas, J. (1998). Migration of mitochondria to viral assembly sites in African swine fever virus-infected cells. *J Virol* **72**, 7583-8.

Rojo, G., Garcia-Beato, R., Vinuela, E., Salas, M. L. and Salas, J. (1999). Replication of African swine fever virus DNA in infected cells. *Virology* **257**, 524-36.

Ross, J. (1995). mRNA stability in mammalian cells. *Microbiol Rev* **59**, 423-50.

Rothbauer, U., Zolghadr, K., Muyldermans, S., Schepers, A., Cardoso, M. C. and Leonhardt, H. (2008). A versatile nanotrap for biochemical and functional studies with fluorescent fusion proteins. *Mol Cell Proteomics* **7**, 282-9.

Rowe, M., Glaunsinger, B., van Leeuwen, D., Zuo, J., Sweetman, D., Ganem, D., Middeldorp, J., Wiertz, E. J. and Ressing, M. E. (2007). Host shutoff during productive Epstein-Barr virus infection is mediated by BGLF5 and may contribute to immune evasion. *Proc Natl Acad Sci U S A* **104**, 3366-71.

Rowlands, R. J., Michaud, V., Heath, L., Hutchings, G., Oura, C., Vosloo, W., Dwarka, R., Onashvili, T., Albina, E. and Dixon, L. K. (2008). African swine fever virus isolate, Georgia, 2007. *Emerg Infect Dis* **14**, 1870-4.

Royall, E., Doyle, N., Abdul-Wahab, A., Emmott, E., Morley, S. J., Goodfellow, I., Roberts, L. O. and Locker, N. (2015). Murine Norovirus 1 (MNV1) Replication Induces Translational Control of the Host by Regulating eIF4E Activity during Infection. *J Biol Chem* **290**, 4748-58.

Salas, J., Salas, M. L. and Vinuela, E. (1988). Effect of inhibitors of the host cell RNA polymerase II on African swine fever virus multiplication. *Virology* **164**, 280-3.

Salas, M. L. and Andres, G. (2013). African swine fever virus morphogenesis. *Virus Res* **173**, 29-41.

Salas, M. L., Kuznar, J. and Vinuela, E. (1981). Polyadenylation, methylation, and capping of the RNA synthesized in vitro by African swine fever virus. *Virology* **113**, 484-91.

Salas, M. L., Rey-Campos, J., Almendral, J. M., Talavera, A. and Vinuela, E. (1986). Transcription and translation maps of African swine fever virus. *Virology* **152**, 228-40.

Sanchez, E. G., Quintas, A., Nogal, M., Castello, A. and Revilla, Y. (2013). African swine fever virus controls the host transcription and cellular machinery of protein synthesis. *Virus Res* **173**, 58-75.

Sanchez, E. G., Quintas, A., Perez-Nunez, D., Nogal, M., Barroso, S., Carrascosa, A. L. and Revilla, Y. (2012). African swine fever virus uses macropinocytosis to enter host cells. *PLoS Pathog* **8**, e1002754.

Sandri-Goldin, R. M. (2011). The many roles of the highly interactive HSV protein ICP27, a key regulator of infection. *Future Microbiol* **6**, 1261-77.

Sanz, A., Garcia-Barreno, B., Nogal, M. L., Vinuela, E. and Enjuanes, L. (1985). Monoclonal antibodies specific for African swine fever virus proteins. *J Virol* **54**, 199-206.

Sanz, M. A., Castello, A. and Carrasco, L. (2007). Viral translation is coupled to transcription in Sindbis virus-infected cells. *J Virol* **81**, 7061-8.

Satterly, N., Tsai, P. L., van Deursen, J., Nussenzveig, D. R., Wang, Y., Faria, P. A., Levay, A., Levy, D. E. and Fontoura, B. M. (2007). Influenza virus targets the mRNA export machinery and the nuclear pore complex. *Proc Natl Acad Sci U S A* **104**, 1853-8.

Scheller, N., Mina, L. B., Galao, R. P., Chari, A., Gimenez-Barcons, M., Noueiry, A., Fischer, U., Meyerhans, A. and Diez, J. (2009). Translation and replication of hepatitis C virus genomic RNA depends on ancient cellular proteins that control mRNA fates. *Proc Natl Acad Sci U S A* **106**, 13517-22.

Schneider-Poetsch, T., Ju, J., Eyler, D. E., Dang, Y., Bhat, S., Merrick, W. C., Green, R., Shen, B. and Liu, J. O. (2010). Inhibition of eukaryotic translation elongation by cycloheximide and lactimidomycin. *Nat Chem Biol* **6**, 209-217.

Schneider, R. J. and Mohr, I. (2003). Translation initiation and viral tricks. *Trends Biochem Sci* **28**, 130-6.

Schwartz, D., Decker, C. J. and Parker, R. (2003). The enhancer of decapping proteins, Edc1p and Edc2p, bind RNA and stimulate the activity of the decapping enzyme. *RNA* **9**, 239-51.

Schwartz, D. C. and Parker, R. (1999). Mutations in translation initiation factors lead to increased rates of deadenylation and decapping of mRNAs in Saccharomyces cerevisiae. *Mol Cell Biol* **19**, 5247-56.

Schwartz, D. C. and Parker, R. (2000). mRNA decapping in yeast requires dissociation of the cap binding protein, eukaryotic translation initiation factor 4E. *Mol Cell Biol* **20**, 7933-42.

She, M., Decker, C. J., Chen, N., Tumati, S., Parker, R. and Song, H. (2006). Crystal structure and functional analysis of Dcp2p from Schizosaccharomyces pombe. *Nat Struct Mol Biol* **13**, 63-70.

She, M., Decker, C. J., Sundramurthy, K., Liu, Y., Chen, N., Parker, R. and Song, H. (2004). Crystal structure of Dcp1p and its functional implications in mRNA decapping. *Nat Struct Mol Biol* **11**, 249-56.

She, M., Decker, C. J., Svergun, D. I., Round, A., Chen, N., Muhlrad, D., Parker, R. and Song, H. (2008). Structural basis of dcp2 recognition and activation by dcp1. *Mol Cell* **29**, 337-49.

Sheth, U. and Parker, R. (2003). Decapping and decay of messenger RNA occur in cytoplasmic processing bodies. *Science* **300**, 805-8.

Shiflett, L. A. and Read, G. S. (2013). mRNA decay during herpes simplex virus (HSV) infections: mutations that affect translation of an mRNA influence the sites at which it is cleaved by the HSV virion host shutoff (Vhs) protein. *J Virol* **87**, 94-109.

Shors, T., Keck, J. G. and Moss, B. (1999). Down regulation of gene expression by the vaccinia virus D10 protein. *J Virol* **73**, 791-6.

Shu, M., Taddeo, B. and Roizman, B. (2013a). The nuclear-cytoplasmic shuttling of virion host shutoff RNase is enabled by pUL47 and an embedded nuclear export signal and defines the sites of degradation of AU-rich and stable cellular mRNAs. *J Virol* **87**, 13569-78.

Shu, M., Taddeo, B., Zhang, W. and Roizman, B. (2013b). Selective degradation of mRNAs by the HSV host shutoff RNase is regulated by the UL47 tegument protein. *Proc Natl Acad Sci U S A* **110**, E1669-75.

Simon-Mateo, C., Andres, G. and Vinuela, E. (1993). Polyprotein processing in African swine fever virus: a novel gene expression strategy for a DNA virus. *EMBO J* **12**, 2977-87.

Siwaszek, A., Ukleja, M. and Dziembowski, A. (2014). Proteins involved in the degradation of cytoplasmic mRNA in the major eukaryotic model systems. *RNA Biol* **11**, 1122-36.

Sonenberg, N. and Hinnebusch, A. G. (2009). Regulation of translation initiation in eukaryotes: mechanisms and biological targets. *Cell* **136**, 731-45.

Song, M. G., Bail, S. and Kiledjian, M. (2013). Multiple Nudix family proteins possess mRNA decapping activity. *RNA* **19**, 390-9.

Song, M. G., Li, Y. and Kiledjian, M. (2010). Multiple mRNA decapping enzymes in mammalian cells. *Mol Cell* **40**, 423-32.

Souliere, M. F., Perreault, J. P. and Bisaillon, M. (2009). Characterization of the vaccinia virus D10 decapping enzyme provides evidence for a two-metal-ion mechanism. *Biochem J* **420**, 27-35.

Souliere, M. F., Perreault, J. P. and Bisaillon, M. (2010). Insights into the molecular determinants involved in cap recognition by the vaccinia virus D10 decapping enzyme. *Nucleic Acids Res* **38**, 7599-610.

Steiger, M., Carr-Schmid, A., Schwartz, D. C., Kiledjian, M. and Parker, R. (2003). Analysis of recombinant yeast decapping enzyme. *RNA* **9**, 231-8.

Strein, C., Alleaume, A. M., Rothbauer, U., Hentze, M. W. and Castello, A. (2014). A versatile assay for RNA-binding proteins in living cells. *RNA* **20**, 721-31.

Studier, F. W. and Moffatt, B. A. (1986). Use of bacteriophage T7 RNA polymerase to direct selective high-level expression of cloned genes. *J Mol Biol* **189**, 113-30.

Suarez, C., Gutierrez-Berzal, J., Andres, G., Salas, M. L. and Rodriguez, J. M. (2010). African swine fever virus protein p17 is essential for the progression of viral membrane precursors toward icosahedral intermediates. *J Virol* **84**, 7484-99.

Taddeo, B., Sciortino, M. T., Zhang, W. and Roizman, B. (2007). Interaction of herpes simplex virus RNase with VP16 and VP22 is required for the accumulation of the protein but not for accumulation of mRNA. *Proc Natl Acad Sci U S A* **104**, 12163-8.

Taddeo, B., Zhang, W. and Roizman, B. (2013). The herpes simplex virus host shutoff RNase degrades cellular and viral mRNAs made before infection but not viral mRNA made after infection. *J Virol* **87**, 4516-22.

Taverniti, V. and Seraphin, B. (2015). Elimination of cap structures generated by mRNA decay involves the new scavenger mRNA decapping enzyme Aph1/FHIT together with DcpS. *Nucleic Acids Res* **43**, 482-92.

Taylor, M. J. and Peculis, B. A. (2008). Evolutionary conservation supports ancient origin for Nudt16, a nuclear-localized, RNA-binding, RNA-decapping enzyme. *Nucleic Acids Res* **36**, 6021-34.

Teixeira, D., Sheth, U., Valencia-Sanchez, M. A., Brengues, M. and Parker, R. (2005). Processing bodies require RNA for assembly and contain nontranslating mRNAs. *RNA* **11**, 371-82.

Tharun, S. and Parker, R. (2001). Targeting an mRNA for decapping: displacement of translation factors and association of the Lsm1p-7p complex on deadenylated yeast mRNAs. *Mol Cell* **8**, 1075-83.

Tjoelker, L. W., Seyfried, C. E., Eddy, R. L., Jr., Byers, M. G., Shows, T. B., Calderon, J., Schreiber, R. B. and Gray, P. W. (1994). Human, mouse, and rat calnexin cDNA cloning: identification of potential calcium binding motifs and gene localization to human chromosome 5. *Biochemistry* **33**, 3229-36.

Topisirovic, I., Svitkin, Y. V., Sonenberg, N. and Shatkin, A. J. (2011). Cap and cap-binding proteins in the control of gene expression. *Wiley Interdiscip Rev RNA* **2**, 277-98.

Tritschler, F., Eulalio, A., Truffault, V., Hartmann, M. D., Helms, S., Schmidt, S., Coles, M., Izaurralde, E. and Weichenrieder, O. (2007). A divergent Sm fold in EDC3 proteins mediates DCP1 binding and P-body targeting. *Mol Cell Biol* **27**, 8600-11.

Valdeira, M. L., Bernardes, C., Cruz, B. and Geraldes, A. (1998). Entry of African swine fever virus into Vero cells and uncoating. *Vet Microbiol* **60**, 131-40.

Valencia-Sanchez, M. A., Liu, J., Hannon, G. J. and Parker, R. (2006). Control of translation and mRNA degradation by miRNAs and siRNAs. *Genes Dev* **20**, 515-24.

van Dijk, E., Cougot, N., Meyer, S., Babajko, S., Wahle, E. and Seraphin, B. (2002). Human Dcp2: a catalytically active mRNA decapping enzyme located in specific cytoplasmic structures. *EMBO J* **21**, 6915-24.

Vilella, M. D., Remacha, M., Ortiz, B. L., Mendez, E. and Ballesta, J. P. (1991). Characterization of the yeast acidic ribosomal phosphoproteins using monoclonal antibodies. Proteins L44/L45 and L44' have different functional roles. *Eur J Biochem* **196**, 407-14.

Vinuela, E. (1985). African swine fever virus. *Curr Top Microbiol Immunol* **116**, 151-70.

von Kobbe, C., van Deursen, J. M., Rodrigues, J. P., Sitterlin, D., Bachi, A., Wu, X., Wilm, M., Carmo-Fonseca, M. and Izaurralde, E. (2000). Vesicular stomatitis virus matrix protein inhibits host cell gene expression by targeting the nucleoporin Nup98. *Mol Cell* **6**, 1243-52.

Walsh, D., Arias, C., Perez, C., Halladin, D., Escandon, M., Ueda, T., Watanabe-Fukunaga, R., Fukunaga, R. and Mohr, I. (2008). Eukaryotic translation initiation factor 4F architectural alterations accompany translation initiation factor redistribution in poxvirus-infected cells. *Mol Cell Biol* **28**, 2648-58.

Wang, Z., Jiao, X., Carr-Schmid, A. and Kiledjian, M. (2002). The hDcp2 protein is a mammalian mRNA decapping enzyme. *Proc Natl Acad Sci U S A* **99**, 12663-8.

Wang, Z. and Kiledjian, M. (2001). Functional link between the mammalian exosome and mRNA decapping. *Cell* **107**, 751-62.

Wardley, R. C., Norley, S. G., Wilkinson, P. J. and Williams, S. (1985). The role of antibody in protection against African swine fever virus. *Vet Immunol Immunopathol* **9**, 201-12.

Waterhouse, P. M., Wang, M. B. and Lough, T. (2001). Gene silencing as an adaptive defence against viruses. *Nature* **411**, 834-42.

Wek, R. C., Jiang, H. Y. and Anthony, T. G. (2006). Coping with stress: eIF2 kinases and translational control. *Biochem Soc Trans* **34**, 7-11.

Wells, S. E., Hillner, P. E., Vale, R. D. and Sachs, A. B. (1998). Circularization of mRNA by eukaryotic translation initiation factors. *Mol Cell* **2**, 135-40.

Whitlow, Z. W., Connor, J. H. and Lyles, D. S. (2008). New mRNAs are preferentially translated during vesicular stomatitis virus infection. *J Virol* **82**, 2286-94.

Wichroski, M. J., Robb, G. B. and Rana, T. M. (2006). Human retroviral host restriction factors APOBEC3G and APOBEC3F localize to mRNA processing bodies. *PLoS Pathog* **2**, e41.

Wilusz, C. J., Gao, M., Jones, C. L., Wilusz, J. and Peltz, S. W. (2001). Poly(A)-binding proteins regulate both mRNA deadenylation and decapping in yeast cytoplasmic extracts. *RNA* **7**, 1416-24.

Windsor, M., Hawes, P., Monaghan, P., Snapp, E., Salas, M. L., Rodriguez, J. M. and Wileman, T. (2012). Mechanism of collapse of endoplasmic reticulum cisternae during African swine fever virus infection. *Traffic* **13**, 30-42.

Yanez, R. J., Rodriguez, J. M., Nogal, M. L., Yuste, L., Enriquez, C., Rodriguez, J. F. and Vinuela, E. (1995). Analysis of the complete nucleotide sequence of African swine fever virus. *Virology* **208**, 249-78.

Yang, Z., Martens, C. A., Bruno, D. P., Porcella, S. F. and Moss, B. (2012). Pervasive initiation and 3'-end formation of poxvirus postreplicative RNAs. *J Biol Chem* **287**, 31050-60.

Yutin, N., Wolf, Y. I., Raoult, D. and Koonin, E. V. (2009). Eukaryotic large nucleo-cytoplasmic DNA viruses: clusters of orthologous genes and reconstruction of viral genome evolution. *Virol J* **6**, 223.

Zhang, F., Moon, A., Childs, K., Goodbourn, S. and Dixon, L. K. (2010). The African swine fever virus DP71L protein recruits the protein phosphatase 1 catalytic subunit to dephosphorylate eIF2alpha and inhibits CHOP induction but is dispensable for these activities during virus infection. *J Virol* **84**, 10681-9.